The role of laminin-2 in Schwann cell-neuron interactions.

Uziyel, Yael Sara

The role of laminin-2 in Schwann cell-axon interactions in the *dy/dy* mouse

Yael S. Uziyel

PhD Thesis

January 2001

MRC Centre for Developmental Neurobiology

GKT School of Biomedical Sciences-Guy's Campus

Kings College London

Abstract

Laminin-2 is a member of the laminin family of heterodimeric multidomain glycoproteins. This isoform is expressed in the endoneurial basal lamina surrounding axon-Schwann cell units and in the skeletal muscle basal lamina. The *dy/dy* mouse has a form of muscular dystrophy in which expression of the laminin α2 chain and consequently of the laminin-2 heterotrimer is substantially reduced. This mutant exhibits extensive abnormalities in peripheral nerves, principally abnormal Schwann cell ensheathment of axons and myelination. This suggests a vital role for laminin-2 in either the establishment or maintenance of Schwann cell-axon interactions. In this project I have examined various aspects of Schwann cell behaviour both *in vivo* and *in vitro* to determine the role of laminin-2 in Schwann cell-axon interactions.

Examination of laminin α2 chain expression in *dy/dy* mice showed differences in the extent of α2 chain down-regulation in myogenic and neural tissues. Immunohistochemistry and electron microscopy confirmed the abnormal interactions of Schwann cells and axons in *dy/*dy peripheral nerves. Transection of mutant sciatic nerves resulted in less extensive sprouting of axons into the distal stump and crush injuries to *dy/dy* nerves resulted in delayed and less extensive remyelination. Cryoculture using mutant nerve substrates showed significantly slower migration of normal Schwann cells on laminin-2-deficient substrates. Mutant dissociated Schwann cells showed an abnormal multipolar morphology. *dy/dy* Schwann cells were also found to migrate significantly faster from explants of mutant dorsal root ganglia. In addition mutant Schwann cells were a poor substrate for neurite branching in co-cultures with neurons.

The observations made on Schwann cell behaviour in *dy/dy* mice in this thesis suggest several roles for laminin-2. It promotes Schwann cell migration and neurite branching, facilitating axonal sprouting in regenerating nerves. Laminin-2 promotes Schwann cell differentiation into a bipolar myelin forming phenotype that ensheaths and interacts with axons, a pre-requisite for both myelination and remyelination. The multiple roles of laminin-2 in the peripheral nervous system support the theory that there is a major neurogenic as well as a myogenic component to this dystrophy.

Table of Contents

Declaration

The work described in this thesis was carried out in the MRC Centre for Developmental Neurobiology at King's College London, under the supervision of Dr James Cohen. The dissertation is a result of my own work and was carried out independently except for specific sections of chapters 3 and 4.

The sciatic nerve transection and sciatic nerve crushes described in chapter 4 were carried out by a project license holder, Professor Susan Standring. Intact and crushed sciatic nerves were embedded and prepared for semi-thin sectioning and electron microscopy by the electron microscopy unit at Guy's hospital, KCL. Electron micrographs of intact and crushed nerves were taken by Professor Susan Standring.

No part of this thesis has been submitted for any other qualification at this or any other university

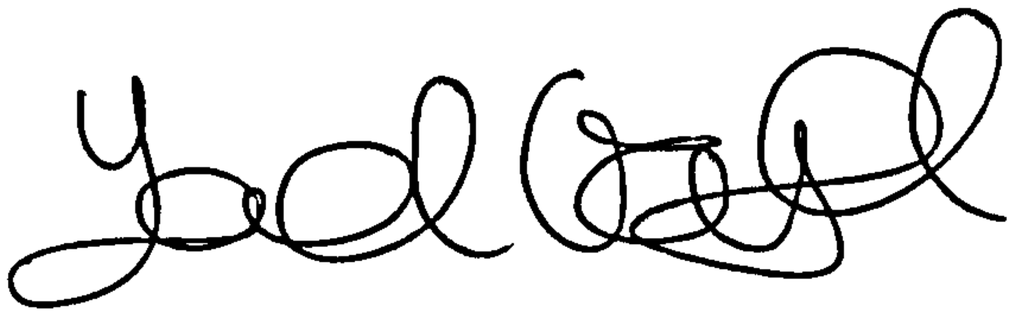

Yael Uziyel

Acknowledgements

I would like to thank Dr James Cohen for his guidance and encouragement through the course of my Phd and Professor Susan Standring for her help. Thanks also to Dr Caroline Sewry amd Dr Diane Watt at Imperial College for help in setting up the *dy/dy* mouse colony and for their help and guidance. I would also like to thank Phil and Sharon at the BSD at St. Thomas's for maintaining the *dy/dy* mouse colony. Thanks to Fiona, Derryck and Ken at the electron microscope unit at Guy's as well. I thank all the members of the lab, past and present in particular Dr Isabella Gavazzi and Dr Naima Reza for their help and friendship throughout the course of my studies.

Finally I would like to thank my parents, Izak and Freda and my sisters Keren and Liat for supporting me throughout, and their patience especially in these last few months.

List of Abbreviations

%	percentage
ARIA	acetylcholine receptor inducing activity
BDNF	brain derived neurotrophic factor
bFGF	basic fibroblast growth factor
bHLH	basic helix-loop-helix
BMP	bone morphogenetic protein
BrdU	5-Bromo-2'-deoxyuridine
BSF-2	modified Bottenstein and Sato's culture medium
°C	Centigrade
Caspr	contactin-associated protein
cDNA	complementary deoxyribonucleic acid
CHAPS	3-[3-cholamidopropyl imethylammonio]-1-propane-sulphonate
cm	centimetre
CMD	congenital muscular dystrophy
CMF	calcium- and magnesium-free Hanks buffered salt solution
CMFDA	5-chloromethylfluorescein diacetate
CMT	Charcot-Marie-Tooth
CNPase	2', 3'-cyclic nucleotide 3'-phosphodiesterase
CNS	central nervous system
CNTF	ciliary neurotrophic factor
CSPG	chondroitin sulphate protoeglycan
C-terminus	carboxy-terminus
CT-1	cardiotrophin-1
DABCO	1,4-diazobicyclo-(2,2,2)-octane
DAG	dystrophin-associated glycoprotein
DDW	double distilled water
Dhh	Desert hedgehog
DMD	Duchenne's muscular dystrophy
DMEM	Dulbecco's modified Eagle's medium

DNA	deoxyribonucleic acid
DRG	dorsal root ganglia
dy	*dystrophia muscularis*
E	embryonic day
E-cadherin	epithelial cadherin
ECM	extracellular matrix
EGF	epidermal growth factor
EHS	Engelbreth-Holm-Swarm
ERK	extracellular signal–regulated kinase
FAK	focal adhesion kinase
FCS	fetal calf serum
FGF	fibroblast growth factor
fig	figure
FITC	fluorescein isothiocyanate
GAP-43	growth-associated protein 43
GDNF	glial-derived neurotrophic factor
G	globular domain
GFAP	glial fibrillary acidic protein
GGF	glial growth factor
Grb2	growth receptor bound protein 2
HEPES	N-[2-Hydroxyethyl]piperazine-N'-[2-ethane-sulphonic acid]
HSPG	heparan sulphate proteoglycan
IGF	insulin-like growth factor
IgG	immunoglobulin G
IMS	industrial methylated spirit
kb	kilobase
kDa	kilo Dalton
LG4/5	laminin globular domain 4/5
LIF	leukaemia inhibitory factor
L-MAG	large myelin associated glycoprotein
L-periaxin	large periaxin
M	molar

MAG	myelin associated glycoprotein
mAmps	milliamps
MAP	mitogen-activated protein
MASH-1	mammalian achaete-scute homologue
MBP	myelin basic protein
MEM	Modified Eagle's Medium
mg	milligram
µg/ml	micrograms per millilitre
ml	millilitre
µl	microlitre
µm	micrometre
mm	millimetre
µm/hr	micrometres per hour
µM	micromolar
MMP	matrix metalloproteinases
MRI	magnetic resonance imaging
mRNA	messenger ribonucleic acid
m/sec	metres per second
n	number
N-cadherin	neural cadherin
N-CAM	neural cell adhesion molecule
NDF	neu differentiation factor
ng/ml	nanograms per millilitre
NrCAM	NgCAM-related cell adhesion molecule
NGF	nerve growth factor
NMJ	neuromuscular junction
NP-40	nonylphenoxy polyethoxy ethanol
N-terminus	amino-terminus
NT-3	neurotrophin-3
OCT	Optimum Cutting Temperature
P	postnatal day
p	probability

PBS	phospate buffered saline
PDGF-β	platelet derived growth factor
PGP 9.5	protein gene product 9.5
PI 3-kinase	phosphatidylinisitol 3-kinase
PLL	poly-L-lysine
PLP/DM20	proteolipid protein
PMP22	peripheral nerve myelin 22 kDa
PNA	peanut agglutinin
PNS	peripheral nervous system
PVDF	polyvinylidene difluoride
RGC	retinal ganglion cell
rpm	revolutions per minute
RT-PCR	reverse transcriptase polymerase chain reaction
SCIP	suppressed, cAMP-inducible POU-domain protein
SDS	sodium dodecyl sulphate
SDS-PAGE	sodium dodecyl sulphate-polyacrylamide gel electrophoresis
s.e.m.	standard error of the mean
Shh	Sonic hedgehog
SH2/ SH3	Src homology 2/ Src homology 3
S-MAG	small myelin associated glycoprotein
S-periaxin	small periaxin
TBS	triethanolamine buffered saline
TID	trypsin inhibitor DNAase
TEMED	N, N, N', N'-tetramethyl-ethylenediamine
TGF-β	transforming growth factor-β
TRITC	tetramethyl rhodamine isothiocyanate
V	volts

List of Tables and Figures

Tables

Figures

Chapter 1: General Introduction

In this chapter I set the scene for various aspects of the experiments carried out in this thesis. Firstly I have described the phenotype of the *dy/dy* mouse, a mouse with a spontaneous mutation resulting in a form of muscular dystrophy that affects both skeletal muscles and peripheral nerves. This mutation results in a down-regulation of laminin α2 chain expression in the basal laminae of skeletal muscle and of Schwann cells. I have described the expression and function of the laminin α2 chain-containing heterotrimer, laminin-2, and given a brief description of other laminin heterotrimers, particularly those that are also expressed in the nervous system. I have then described the two principal laminin receptor, the integrins and the dystrophin associated glycoproteins. This is followed by a description of how the peripheral nervous system is generated and in particular how Schwann cells arise from the neural crest. I have then detailed various aspects of Schwann cell maturation and myelination. Finally I have described the events involved in regeneration and remyelination in the peripheral nervous system following injury.

1.1: The *dy/dy* mouse

1.1.1: The dy/dy mouse suffers from muscular dystrophy

The *dystrophia muscularis* (*dy/dy*) mutation arose spontaneously and was described as a "myopathic mutation in mice", with similarities to human muscular dystrophy (Michelson et al., 1955). The pattern of transmission suggested that the mutation is passed on in an autosomally recessive manner. Mice suffering from this hereditary condition were substantially smaller than normal littermates throughout their life-spans and began to display an overt phenotype at three to four weeks of age.

Symptoms included occasional dragging of the hind-limbs and convulsive up and down nodding of the head. By about 8 weeks of age the muscular atrophy was more established and paralysis spread from the hind-limbs through to the axial and fore-limb musculature. These mice usually died by about 6 months of age of unknown causes, now known to be respiratory failure and were unable to breed (fig. 1.1).

In this initial characterisation of the *dy/dy* mouse, histopathological investigations revealed several abnormalities in the skeletal muscle but none were detectable at that time in both the central nervous system (CNS) and the peripheral nervous system (PNS). Fat cells were found between the muscle fibres and connective tissue hypertrophied and invaded the muscle. What appeared to be degenerating muscle fibres were found to be mixed with normal muscle fibres (Michelson et al., 1955). These degenerative changes included muscle fibre necrosis, myophagocytosis and small muscle fibres indicating the presence of regenerating foci (Ringelmann et al., 1999; Wewer and Engvall, 1996). Infiltration by mononuclear cells such as fibroblasts, myoblasts and inflammatory cells and an expanded interstitium (Michelson et al., 1955; Ringelmann et al., 1999; West and Murphy, 1960) have also been observed in the skeletal muscle of *dy/dy* mice.

Further investigation revealed other abnormalities in the skeletal muscle beyond the primary myopathy described above. An analysis of the number of motor units in *dy/dy* skeletal muscle revealed a decrease in motor units and in the twitch tension they generated compared to normal muscle fibres (Harris and Wilson, 1971). A decline in the number of nerve fibres innervating the mutant skeletal muscle and in particular in the number of myelinated nerve fibres was an early indication associated neural abnormalities. The twitch tension although reduced was within a

Figure 1.1: *dy/dy* mice are smaller than their unaffected littermates and suffer from hindlimb paralysis. A four week old Re129 *dy/dy* mouse and an unaffected littermate (ua). **(a)** The *dy/dy* mouse on the right (white arrow) appears much smaller than its unaffected littermate and can be seen to be dragging one of its hindlimbs (arrowhead). One or both of the eyes in many *dy/dy* mice may have thinning fur and scabs surrounding it (*). **(b)** When observed from the rear the *dy/dy* mouse can be seen to be suffering from hindlimb paralysis in both legs (arrowheads). *dy/dy* mice often develop a curvature of the spine (black arrow).

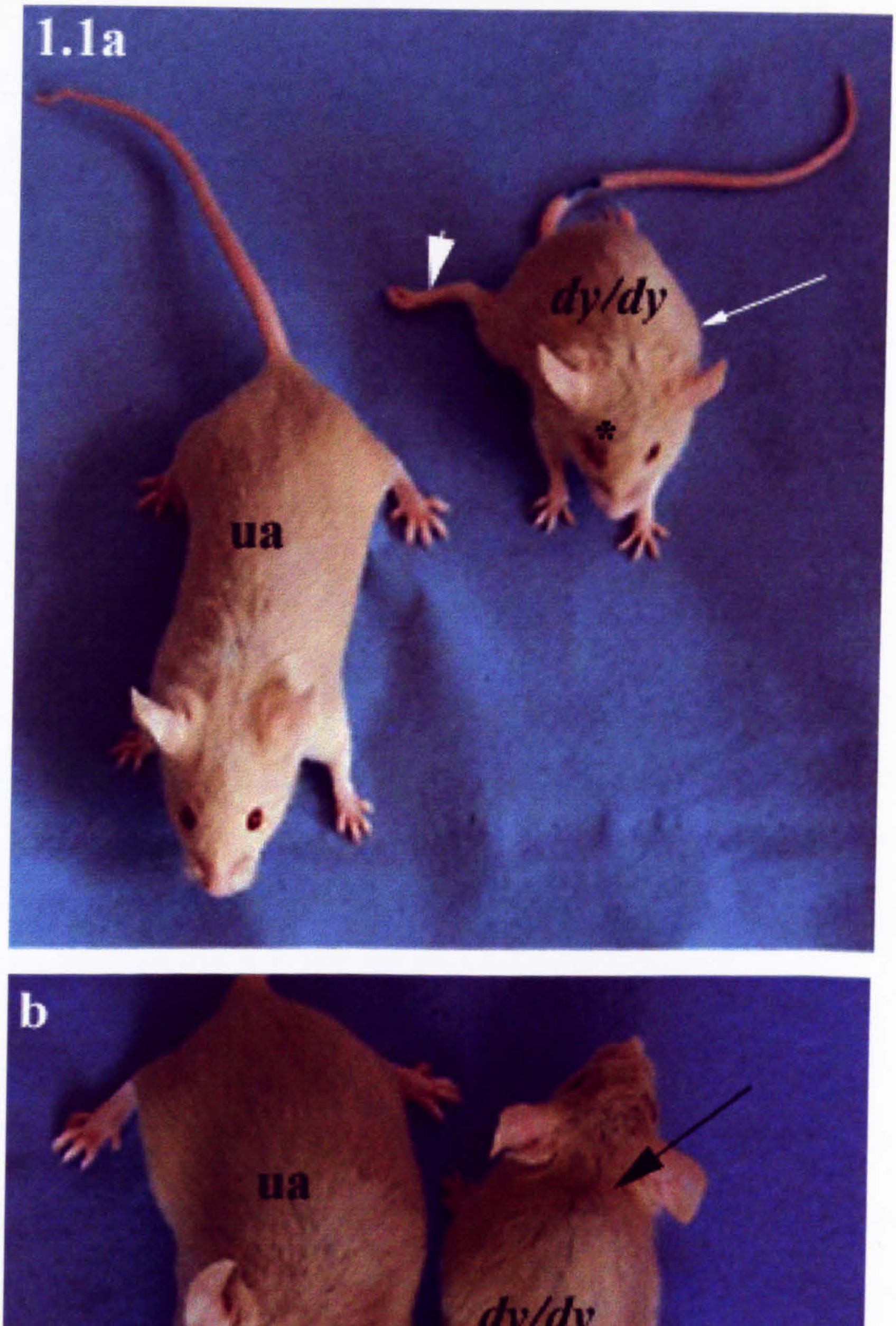
1.1a
dy/dy
ua
b
ua
dy/dy

normal range of amplitude, suggesting that these neural abnormalities were not necessarily secondary to skeletal muscle fibre loss (Harris and Wilson, 1971). It was proposed that a primary neuropathy, might be partially responsible for the myopathy observed in *dy/dy* skeletal muscle (Banker et al., 1979). Thus the neural abnormalities that I have described in detail in chapter *1.1.2*, may result in denervation of skeletal muscle and consequently in skeletal muscle atrophy.

Abnormalities detected at the neuromuscular junction (NMJ), could have been a consequence of the neural or skeletal muscle abnormalities or a combination of both. The post-synaptic area and membrane length was substantially reduced at the NMJ in *dy/dy* mice and Schwann cells abnormally extended processes into rather shallow synaptic clefts (Banker et al., 1979). The junctional folds in the post-synaptic terminal were poorly defined in the mutant NMJ with few secondary synaptic folds (Banker et al., 1979; Desaki et al., 1995; Law et al., 1983), a feature common in developing and regenerating muscle fibres. Choline acetyltransferase activity is reduced in *dy/dy* nerve fibres (Jablecki and Brimijoin, 1974).

1.1.2 The dy/dy mouse exhibits myelination abnormalities in the PNS

The preliminary finding that *dy/dy* mice had fewer myelinated fibres than normal mice was borne out by subsequent detailed investigations of its PNS (Bradley and Jenkison, 1973). Large areas of bare axons were found in lumbosacral dorsal and ventral roots and in areas of the sciatic nerve proximal to the spinal cord. These axons were not invested by Schwann cell cytoplasm or myelin (Bradley and Jenkison, 1973). *dy/dy* mice had approximately 10% of the normal number of myelinated axons in their spinal roots and about a third in proximal parts of the sciatic nerve (Bradley and Jenkison, 1973; Bray and Aguayo, 1975). It appeared

that amyelinated fibres became myelinated in more distal parts of the sciatic nerve. The nerves were described as being amyelinated as they resembled neither unmyelinated nor remyelinating regenerating nerve fibres.

The cranial nerves were also found to have the same abnormalities as the dorsal and ventral roots. There were closely packed, bare and amyelinated axons seen in all the cranial nerves from III to XII, although the abnormality was less pronounced in nerves V, VII and VIII (Biscoe et al., 1974). Both larger axons that would normally be myelinated and smaller axons that would normally remain unmyelinated were incompletely ensheathed or unensheathed by Schwann cells. Detailed analysis of the extent of the neural abnormality showed that in fact ventral and dorsal roots at all levels of the neuroaxis from cervical to sacral were amyelinated (Stirling, 1975a). Near the spinal cord entry and exit points of the dorsal and ventral roots, respectively, nerves appeared to be normally myelinated. The amyelination abnormality began in the roots within a short distance (≤1mm) of the spinal cord interface. Myelinated fibres became more frequent as the dorsal and ventral roots joined to make the mixed spinal nerve at the base of the dorsal root ganglia (DRG) (Stirling, 1975a).

The *dy/dy* mouse had focal deficiencies in Schwann cell numbers in the spinal roots but amyelination was also apparent in areas where Schwann cells were present. More distally in the peroneal nerve, there was in fact a substantial increase in the numbers of Schwann cells (Jaros and Bradley, 1979). In some parts of the ventral root, cells lacking a basal lamina and morphologically resembling oligodendrocytes were seen wrapping larger axons (Bray and Aguayo, 1975). The loose wrapping of axons by Schwann cells was reminiscent of foetal nerve ensheathment (Bradley and

Jenkison, 1973). Thus, groups of axons in developing nerves and small unmyelinated axons in mature nerves are usually bundled together within a Schwann cell and in mutant nerves large axons were often seen bundled together surrounded by a Schwann cell that failed to completely ensheath them and that lacked an intact basal lamina (Bray and Aguayo, 1975).

It was found that in myelinated fibres, particularly those distal to the spinal cord, the nodes of Ranvier were often abnormally wide, while myelin at the internodes was extremely thin. Closer inspection of the nodes of Ranvier revealed that there was also a retraction of Schwann cell cytoplasm and paranodal myelin in *dy/dy* mice at the nodes of Ranvier and in some cases complete detachment of the terminal myelin loops (Bradley et al., 1977). In addition it appears that the number of sodium channels at the node of Ranvier in *dy/dy* mice is reduced to levels comparable to those in normal internodes and unmyelinated fibres (Bradley and Jaros, 1979).

Similar neural abnormalities have been observed in another mutant with a mutation in the laminin α2, the less severely dystrophic dy^{2j}/dy^{2j} mouse (see chapter *1.1.6*). Amyelination was less extensive in these mice than in the *dy/dy* mice but was evident in cervical and lumbosacral dorsal and ventral roots and in cranial nerves V and VII to XII (Bradley and Jenkison, 1975). Both dorsal and ventral roots of dy^{2j}/dy^{2j} were amyelinated proximal to the spinal cord, becoming myelinated towards the DRG and amyelinated again in the mixed spinal nerves before becoming myelinated again in the distal peripheral nerves, a similar pattern to *dy/dy* mice (Bradley and Jenkison, 1975; Stirling, 1975a). As in the *dy/dy* mouse, groups of large naked axons were seen in the dy^{2j}/dy^{2j}, many in direct contact with the

endoneurium rather than ensheathed by Schwann cells. Those Schwann cells which did extend processes lacked basal lamina and did not completely ensheath the axons (Brown and Radich, 1979; Weinberg et al., 1975). Another feature rarely seen in normal nerves but observed with greater frequency in both *dy/dy* and dy^{2j}/dy^{2j} mice is polyaxonal myelination. Schwann cells were sometimes seen to extend processes to and myelinate more than one axon or to myelinate one in a group of axons that it ensheathed while the remainder in the group remained unmyelinated, whereas normally myelin forming Schwann cells form a one-to-one relationship with the axons they ensheath (Brown and Radich, 1979; Jaros and Bradley, 1979; Okada et al., 1977).

1.1.3: Abnormal conduction of impulses in mutant nerves

Conduction in larger myelinated axons occurs in a saltatory fashion from node to node, the structural abnormalities observed at the nodes of Ranvier of *dy/dy* mice may account for the reduced conduction velocity recorded in mutant mice. The conduction velocity in *dy/dy* dorsal and ventral roots was found to range from 0.1 to 2 m/sec compared to 10 to 100 m/sec in dorsal roots and 50 to 70 m/sec in ventral roots in normal mice (Biscoe et al., 1977). Although sciatic nerves are more heavily myelinated than spinal roots, conduction velocity is also reduced in *dy/dy* sciatic nerves by 25% (Huizar et al., 1975).

Impulses are usually directed towards the spinal cord in dorsal roots and away from it in ventral roots, but in *dy/dy* mice impulses have been recorded in both directions (Rasminsky, 1978). A large number of high amplitude spontaneous potentials are generated mid-root in unstimulated *dy/dy* nerve fibres (Carbonetto, 1977; Rasminsky, 1978). These ectopic impulses were almost always associated with

impulses passing by in neighbouring axons. The fact that many axons in *dy/dy* nerve fibres are bare with little or no Schwann cell or myelin ensheathment and are directly apposed suggests that as well as spontaneous potentials there is communication or "cross-talk" of impulses in these fibres (Rasminsky, 1978). It is known that the junction between myelinated and unmyelinated portions of axons in normal nerves can be hyperexcitable. Areas of amyelination in *dy/dy* mice may make these axons hyperexcitable too and thus more susceptible to spontaneous potentials and "cross-talk".

1.1.4: The dy/dy mouse has abnormal Schwann cell basal laminae

In a normal peripheral nerve, a myelin forming or non-myelin forming Schwann cell will completely ensheath an axon or group of axons so that they are not exposed to the endoneurium. The Schwann cells themselves are surrounded on their outer surface by a continuous endoneurial basal lamina (fig. 1.9). This was clearly not the case in *dy/dy* peripheral nerves; mutant myelinated fibres had a patchy deficiency of the basal lamina, which was thinner and discontinuous, leaving amyelinated axons bare without Schwann cell ensheathment or basal lamina coverage (Madrid et al., 1975). The basal lamina of other peripheral nerve cells such as perineurial and endothelial cells and of skeletal muscle fibres in *dy/dy* mice however appeared to be of normal thickness and continuous (Jaros and Bradley, 1979; Madrid et al., 1975). Although it was known at that time that Schwann cells were able to produce basal lamina (Church et al., 1973), the specific component of the endoneurial basal lamina that was deficient in *dy/dy* mice was not known.

1.1.5: The laminin α2 chain gene is the target for the mutation in the dy/dy mouse

With the discovery of the laminin family of extracellular matrix (ECM) molecules (see chapter *1.2*), it became possible to specifically determine the nature of the basal lamina deficiency in *dy/dy* mice. The laminin-2 (merosin in the old nomenclature; see fig. 1.2) heterotrimer was found to be expressed in both Schwann cell and skeletal muscle basal lamina (Leivo and Engvall, 1988). As Schwann cells and skeletal muscle fibres are the principal targets of the *dy/dy* mutation (Bradley and Jenkison, 1973; Michelson et al., 1955), laminin-2 appeared to be a good candidate as the molecule primarily responsible for the abnormalities in the *dy/dy* mouse.

Immunoflourescence and immunoblotting techniques were used to establish the expression of a variety of basal lamina components, including two of the chains that make up the laminin-2 heterotrimer, the α2 and β1 chains. Fibronectin, type IV collagen and the β1 chain were all normally expressed in *dy/dy* tissues, but there appeared to be minimal expression of the laminin α2 chain protein in the skeletal muscle, cardiac muscle and peripheral nerves of the *dy/dy* mice (Arahata, 1993). Moreover the *lama2* gene messenger ribonucleic acid (mRNA) encoding the α2 chain was barely detectable in *dy/dy* skeletal muscle. By using reverse transcriptase-polymerase chain reaction (RT-PCR), it was possible to determine that the small quantity of *lama2* mRNA expressed in *dy/dy* mice was however the same size as in unaffected mice. This implied that there was no major deletion in the α2 chain transcript in mutant mice.

Negligible expression of α2 chain protein in skeletal muscle, cardiac muscle and peripheral nerves was confirmed by other groups using a variety of antibodies in

immunofluorescence and immunoblotting (Sunada et al., 1994; Xu et al., 1994a). Densitometric analysis of immunoblots showed a reduction in the expression of the α2 chain in skeletal muscle of 94%, in cardiac muscle of 96% and in peripheral nerves of 97% (Sunada et al., 1994). Lowered levels of *lama2* mRNA were also detected in the cardiac muscle of *dy/dy* mice as well as in skeletal muscle (Xu et al., 1994a). Mapping of the *lama2* gene by analysis of the progeny of two genetic crosses, revealed that *lama2* was localised to the same region of mouse chromosome 10 as the *dy* locus. This region also showed conservative linkage to human chromosome 6q to which the human *lama2* gene has been mapped (Sunada et al., 1994).

1.1.6: Other mouse mutants in which the α2 chain gene is targeted

The nature of the mutation in the *lama2* gene that causes the muscular dystrophy in *dy/dy* mice has not yet been identified, but the dy^{2J}/dy^{2J} mouse and transgenic mice with targeted mutations of the laminin α2 chain have similar symptoms to the *dy/dy* mouse. In the less severely dystrophic dy^{2J}/dy^{2J} mouse, the laminin α2 chain is expressed in a truncated form (Sunada et al., 1995b; Xu et al., 1994b). There was a small decrease detected in the level of α2 chain expression in skeletal muscle in dy^{2J}/dy^{2J} mice and in the levels of *lama2* mRNA in cardiac and skeletal muscle but not as substantial as in *dy/dy* mice (Xu et al., 1994b). It was found that the truncation of the α2 chain was in the 300 to 325 kilo Dalton (kDa) N-terminus fragment of the α2 chain (Sunada et al., 1995b; Xu et al., 1994b). An antibody which detects the amino-terminus (N-terminus) fragment at 325 kDa in unaffected mice, showed that the truncated α2 chain was 270 kDa in skeletal muscle, 290 kDa in cardiac muscle and 300 kDa in peripheral nerves. Two similar mutations were

found in the dy^{2j}/dy^{2j} *lama2* gene, both of which resulted in deletions in potential N-glycosylation sites in domain VI of the α2 chain near the N-terminus (fig. 1.2). A single base G to A mutation in a splice donor site results in the expression of multiple mRNA variants, the largest of which is translated with a 55 amino acid deletion (Xu et al., 1994b). A 171 base in-frame deletion was also found, a glutamine to glutamic acid substitution at residue 91 resulted in a 57 amino acid deletion at residues 34 to 90 (Sunada et al., 1995b). The deletion of this region in dy^{2j}/dy^{2j} mice destabilises domain VI of the α2 chain and compromises its ability to form polymers with other laminin heterotrimers (Colognato and Yurchenco, 1999), resulting in a patchy basal lamina and in similar although less severe symptoms as the muscular dystrophy in *dy/dy* mice.

dy^{w}/dy^{w} and dy^{3k}/dy^{3k} mice are laminin α2 chain null mutants with targeted deletions and like *dy/dy* mice, they appeared normal at birth (Kuang et al., 1998b; Miyagoe et al., 1997). However within two or three weeks they were substantially smaller than controls and were exhibiting hind-limb paralysis. The complete absence of the α2 chain in these mice meant that the dystrophy was far more severe and progressed at a faster rate than in *dy/dy* mice and consequently the dy^{w}/dy^{w} and dy^{3k}/dy^{3k} mice usually died at one to two months of age.

1.1.7: Downstream effects of the α2 chain deficiency in dy/dy mice on the expression of other ECM molecules

Although the primary defects in *dy/dy* and dy^{2j}/dy^{2j} mice are almost both certainly caused by a mutation in the *lama2* gene, there also appears to be a downstream effect on the expression of other laminin chains, ECM molecules and laminin receptors in *dy/dy* mice. The laminin α4 chain is usually only found in

extrasynaptic basal lamina up to the first postnatal week, but is ectopically expressed in the endoneurial basal lamina of *dy/dy* mice and is also upregulated at the synaptic basal lamina. Although the functional consequence is unknown, it results in ectopic expression of the α4 chain-containing laminin-8 heterotrimer in the endoneurial basal lamina (Patton et al., 1997). The laminin α4 chain also seems to ectopically expressed in place of the α2 chain in the skeletal muscle of *dy/dy* mice, particularly in regenerating muscle fibres (Patton et al., 1999; Ringelmann et al., 1999; Sorokin et al., 2000). Expression of the laminin α5 chain in skeletal muscle is usually down-regulated postnatally but persists in *dy/dy* mice up to postnatal day (P) 7 (Patton et al., 1999; Ringelmann et al., 1999). The ectopic expression of the α4 chain in *dy/dy* tissues appears to be a specifically linked to the deficiency in the α2 chain, whereas the continued expression of the α5 chain is probably due to the presence of immature or regenerating muscle fibres in *dy/dy* skeletal muscle fibres (Ringelmann et al., 1999).

Fibronectin and tenascin-C are both ECM molecules that are normally expressed in the interstitium between skeletal muscle fibres of neonatal control mice. In mature fibres tenascin-C is restricted to the myotendenous junction and fibronectin to the myotendenous junction, between muscle fibres and surrounding blood vessels, however in *dy/dy* mice expression of both these molecules persists in the interstitium (Ringelmann et al., 1999). Like laminin α5 chain expression in *dy/dy* mice the increased expression of tenascin-C and fibronectin may be related to the presence of regenerating muscle fibres.

1.1.8: The dy/dy mouse is a model for human congenital muscular dystrophy

The *dy/dy* mouse was suggested as a model for human muscular dystrophies even before the cause of the dystrophy could be explained (Michelson et al., 1955). It has since become clear that there is indeed a type of human muscular dystrophy known as merosin (laminin-2) deficient congenital muscular dystrophy (CMD) in which a similar deficiency of the laminin α2 chain was identified soon after the α2 chain deficiency was characterised in the *dy/dy* mouse. It was found that a large proportion of the most severe cases of autosomal recessive CMD, with early onset of muscle weakness at birth or within a few months of birth, had a specific deficiency of the laminin α2 chain in their skeletal muscle (Tome et al., 1994). Splice site and nonsense mutations were identified in the same region of human chromosome 6q22-23 that the human *lama2* gene maps to (Helbling-Leclerc et al., 1995). This is a region which also shows conservative linkage to the portion of mouse chromosome 10 to which the murine *lama2* gene and the *dy/dy* locus have been mapped (Sunada et al., 1994).

Like *dy/dy* mice, humans with merosin deficient CMD also exhibit neural abnormalities. Histopathological data on PNS abnormalities in merosin-deficient CMD is limited, but a mild demyelinating neuropathy has been detected in patients with both severe and mild forms of merosin deficient CMD (Morandi et al., 1999). Motor nerve conduction velocity was correlated to α2 chain expression in a group of people with CMD. Only those with merosin deficient CMD where α2 chain expression was negligible, also had reduced motor nerve conduction velocity (Shorer et al., 1995) mirroring the decreased conduction velocity recorded in *dy/dy* mice (Biscoe et al., 1977; Huizar et al., 1975) and PNS amyelination in merosin-

deficient CMD could account for the deficit. Several groups have also reported white matter changes in the CNS of some subjects with merosin deficient CMD using magnetic resonance imaging (MRI). These do not appear to be degenerative and are not correlated to the clinical severity of the CMD (Caro et al., 1999; Herrmann et al., 1996; Morandi et al., 1999; Sunada et al., 1995a; Tan et al., 1997). The white matter changes are consistent with some deficit in myelination and autopsies have revealed spongy myelin and astrocytosis in some cases (Morandi et al., 1999). Changes in the MRIs of subjects with merosin deficient CMD also suggest that there may be some abnormalities of neuronal and oligodendrocyte migration in the CNS of these subjects (Sunada et al., 1995a).

Antibodies have detected differences in the extent of α2 chain expression in merosin-deficient DMD; in some cases there is only a minimal reduction in expression of the 80 kDa carboxy-terminus (C -terminus) fragment and a substantial reduction in the expression of the N-terminus 300 kDa fragment, others show partial expression of both or only of the 300 kDa fragment (Morandi et al., 1999; Sewry et al., 1997). Nonsense mutations and base pair deletions have been identified in the *lama2* gene of subjects with merosin deficient CMD that cause truncations in both the C-terminus and the N-terminus fragment (Guicheney et al., 1997).

In some cases of mild merosin deficient CMD, expression of the 80 kDa C-terminus fragment was normal whereas the 300 kDa N-terminus fragment was truncated and severely deficient (Allamand et al., 1997). This truncation was due to a one base substitution, resulting in a 63 amino acid deletion in domain IVa of the α2 chain in the N-terminus region. The dystrophy in dy^{2J}/dy^{2J} mice is also caused by

a mutation that truncates the region of the N-terminus of the α2 chain involved in polymerisation of the laminin-2 heterotrimer (Colognato and Yurchenco, 1999) and it may be that this is also the case in mild forms of merosin deficient CMD.

1.2: The laminins

1.2.1: Laminins are a family of heterotrimeric ECM molecules

Laminins are a rapidly expanding family of heterotrimeric glycoproteins that are major constituents of the basal lamina, combining with type IV collagen, fibronectin, tenascins and proteoglycans such as agrin to form an ECM. Sheets of this ECM are then arranged into a basal lamina between the cells and the connective tissue. Laminins have a variety of roles within the ECM, they polymerise with each other to form a network within the basal lamina and they also provide a structural link through receptor complexes between the cytoskeleton of the cells and the basal lamina. Laminin binding to these receptor complexes serves a dual purpose, as well as providing a structural link between the cell and the ECM, laminins act as cell signalling molecules through the same receptor complexes.

The first laminin heterotrimer to be isolated was from the ECM of Engelbreth-Holm-Swarm (EHS) tumour cells, now known as laminin-1 (Chung et al., 1979; Timpl et al., 1979). In this initial isolation of laminin, the protein was found to be made up of two components of approximately 440 kDa and 220 kDa. In a sodium dodecyl sulphate-polyacrylamide gel electrophoresis (SDS-PAGE) gel, the components when unreduced migrated through the gel with the characteristics of a molecule that contained two 220 kDa and a 440 kDa component (Timpl et al., 1979). An antibody raised against the laminin protein isolated from the matrix

showed that it was also expressed in the basal lamina of tissues such as skin, kidney and placenta.

The heterotrimeric structure of laminins was verified by electron micrography, which showed, in rotary shadowing, a cross-shaped structure made up of three short arms and one long arm (Engel et al., 1981) (fig.1.2). Two globular domains were visible at the end of each of the short arms and a larger structure at the end of the long arm. It became clear that the laminin-1 heterotrimer was composed of three distinct glycosylated chains, an A chain of 450 kDa, a B1 chain of 240 kDa and a B2 chain of 230 kDa (Cooper et al., 1981), encoded by distinct but homologous genes (Martin and Timpl, 1987). The three short arms of the laminin cross were composed of the N-terminus regions of the A, B1 and B2 chains, which then aligned to form the long arm cross-linked by an α helix to form a coiled-coil (fig. 1.2). Substantial homology was found between the N-terminus of A, B1 and B2 chains (Sasaki et al., 1988). This included globular domains IV and VI, made up of approximately 250 residues, plus a globular domain IVa in the A chain and the rod-like domains III and V composed of consecutive epidermal growth factor-like (EGF) cys-rich repeats of about 50 residues. At the C-terminus, the B1 and B2 chains form a disulphide bridge and the A chain extends to form the globular G-domain (Ott et al., 1982; Paulsson et al., 1985; Timpl, 1989).

A structural role was soon assigned to laminin-1, normally situated between type IV collagen and the cell in the basal lamina. It promoted the attachment of epithelial cells both as an isolated substrate and when bound to type IV collagen (Terranova et al., 1980). It was soon shown that laminin is expressed very early in development, at the morula stage even before the formation of the blastocyst (Leivo

et al., 1980), suggesting that it may be an important signalling and adhesive molecule during embryogenesis.

The A, B1 and B2 chains were the first of many laminin chains to be identified. In recent years, a new nomenclature has been introduced for laminins such that in the laminin-1 heterotrimer the heavy A chain is known as the α1 chain, the B1 chain as β1 and the B2 chain as γ1. The A, B1 and B2 laminin isoforms that have been subsequently found have the same nomenclature and are identified as α, β and γ chains, numbered according to the order in which they have been discovered (Burgeson et al., 1994). There are now twelve known laminin heterotrimers; each composed of one α, one β and one γ chain. Currently five α, three β and three γ chains have been identified (Colognato and Yurchenco, 2000) (table 1.1).

1.2.2: A new laminin: The α2 chain and laminin-2 heterotrimer

Following the identification of laminin-1, it was to be some years before other laminin chains and heterotrimers were identified and the true diversity of laminin expression and function fully realised. The first one to follow laminin-1 was merosin, now known as laminin-2, composed of the α2, β1 and γ1 chains. Antibodies prepared against placental extracts recognised an ECM-associated protein that, unlike laminin-1, showed a very restricted pattern of expression. Whereas laminin-1 appeared to be expressed in most epithelial and endothelial cells, expression of laminin-2 was more restricted to placental trophoblasts, the basal lamina of skeletal muscle, the Schwann cell basal lamina and in heart (Leivo et al., 1989; Schuler and Sorokin, 1995). A 65 kDa fragment of an 80 kDa precursor, most probably the C-terminus fragment of the α2 chain, was detected which was immunologically distinct from other ECM components such as laminin-

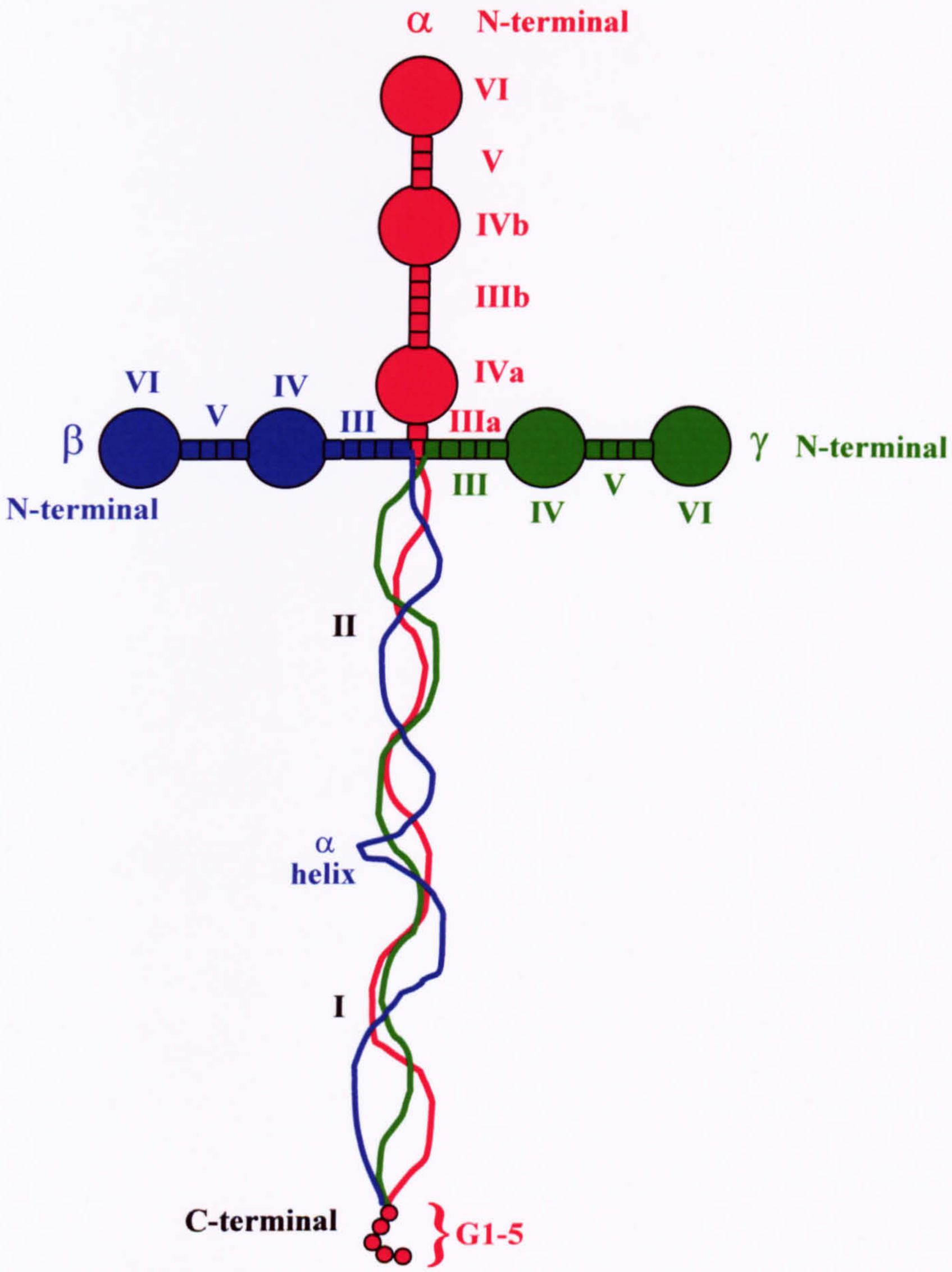

Figure 1.2: The laminin heterotrimer. laminin heterotrimers are composed of an α (red), β (blue) and γ chain (green), generally forming a cruciform sha -pe. The N-terminal of each chain forms a short arm and the C-terminals are joined together by an α helix to form a coiled coil. Some α chains are trunca -ted and do not have a short arm. The short arms contain 2 globular domains (large circles) in the β and γ chains known as domains IV and VI and 2 rod-like domains composed of cysteine-rich repeats known as domains III and V (squares). Full-length α chains have 3 globular domains, IVa, IVb and VI, and three rod-like domains, IIIa, IIIb and V, in the short arm. Domains I and II are located in the coiled-coil of the long arms of the laminin chains, bound by an α helix in the β chain. The C-terminal of the α chain has a receptor-binding domain, made up of 5 globular repeats (small circles) known as the G domain.

Table 1.1: Summary of laminin heterotrimers and their expression

Laminin heterotrimer	Components	Expression
Laminin-1	α1β1γ1	Early embryogenesis, in the morula, developing kidney
Laminin-2	α2β1γ1	Endoneurial basal lamina in peripheral nerves, skeletal and cardiac muscles, placenta, capillaries, brain
Laminin-3	α1β2γ1	NMJ, immature glomerulus, perineurium
Laminin-4	α2β2γ1	NMJ- the primary cleft and junctional folds
Laminin-5	α3Aβ3γ2	Skin and other epithelial cells
Laminin-6	α3Aβ1γ1	Skin and other epithelial cells
Laminin-7	α3Aβ2γ1	Skin and other epithelial cells
Laminin-8	α4β1γ1	Mesenchymal cells: blood vessels, lung, muscle, NMJ in Schwann cell basal lamina; expression may be lost in adulthood
Laminin-9	α4β2γ1	Primary cleft and perineurial basal lamina
Laminin-10	α5β1γ1	Developmental expression at synaptic basal lamina and in skeletal muscle, kidney and blood vessels

→ continued on next page

Table 1.1 continued

Laminin-11	$\alpha5\beta2\gamma1$	NMJ- primary cleft and junctional folds and perineurial basal lamina
Laminin-12	$\alpha2\beta1\gamma3$	Placenta, peripheral nerves; restricted expression at the dermal-epidermal junction?

1, type IV collagen and fibronectin (Leivo and Engvall, 1988). These initial immunological surveys failed to detect laminin-2 expression in developing mouse embryos. Since it was only detectable in new-born mice, it was concluded that laminin-2 may have a limited role in early developmental processes (Leivo and Engvall, 1988). More recently laminin-2 chains have been detected as early as embryonic (E) day 11.5 in mouse embryos (Lentz et al., 1997) (discussed below).

Laminin isolated from mouse hearts was found to contain a 300 kDa polypeptide that was not antigenically related to any of the laminin-1 chains but an unreduced fraction contained epitopes also found on laminin-1, suggesting that the new laminin was bound to one of the laminin-1 chains (Paulsson and Saladin, 1989). The amino acid sequence of laminin-2 was deduced and was found to share a 40% sequence identity with the C-terminus region of the α1 chain (Ehrig et al., 1990). Thus a peptide had been characterised which had sequence homology with the α1 chain, which was similar in size and which was found to be covalently bound to the β1 and γ1 chains in the centre of a cruciform structure (Ehrig et al., 1990; Paulsson et al., 1991).

1.2.3: The lama2 gene

The human *lama2* gene was found to encode a full-length α chain with a primary structure closely resembling that of the α1 chain. The overall homology was 46.6%, highest in the short arm especially in domain VI, less so in the long arm domains I and II (Vuolteenaho et al., 1994). This is also true of the murine *lama2* gene, located on chromosome 10; it encodes an α2 chain with an overall 45.9% homology to the murine α1 chain. Again the highest degree of homology, 77.3%, is found at the N-terminus with only 30.3% homology in the C-terminus long arm

domain (Bernier et al., 1995). The high degree of homology in the short arm may be linked to its role in the self-assembly of the laminin heterotrimers although there is evidence that the C-terminus long arm domains may also be involved (Utani et al., 1995; Yurchenco et al., 1992; Yurchenco and Schittny, 1990). The internal repeats of the α2 chain G-domain share a 30 to 50% homology with those of the α1 chain. As this is a receptor binding domain for both integrins and for the dystrophin-associated glycoproteins (DAG), this differences in the G-domain may reflect differences in receptor-ligand interactions in the two chains (Vuolteenaho et al., 1994).

The human *lama2* gene has 64 exons, which makes it approximately three times larger than the *lamb1* and *lamc1* genes encoding the smaller β1 and γ1 genes. It encodes a 9500 nucleotide transcript and a 3110 residue α2 chain (Zhang et al., 1996). α2 chain mRNA has now been detected during embryogenesis in mice from E11.5 onwards and in neonates (Lentz et al., 1997; Miner et al., 1997). Expression in developing mice as well as in mature mice was found in cells of mesenchymal origin rather than epithelial or endothelial cells, such as cardiac muscle, skeletal muscle, lung, skin, liver and kidney, but also in neural crest derivatives such as Schwann cells. This early expression is consistent with a role for laminin-2 (and laminin-4) in the formation and maintenance of tissues such as skeletal muscle and peripheral nerves (Bernier et al., 1995; Vuolteenaho et al., 1994).

1.2.4: Formation of the laminin-2 heterotrimer

The first step in the formation of the laminin-2 heterotrimer appears to be mediated by the C-terminus long arm domains where the triple stranded coiled-coil is formed. Deletion mapping detected two neighbouring sites on the β1 chain and 2

adjacent sites on the γ1 chain which involved in trimerisation (Utani et al., 1994). The α2 chain contained one site for trimerisation directed by charged amino acid residues. Stabilisation of the coiled-coil structure was found to be mediated by iosleucine residues in the α2 and γ1 chains (Nomizu et al., 1994). A specific 25 amino acid sequence in the C-terminus of the α2 chain was found to be particularly important in the electrostatic interactions between the α2, β1 and γ1 chains and also contained an α-helical structure vital in the initiation of trimerisation (Utani et al., 1995). Spectroscopy showed that the α2 and γ1 chains subsequently undergo conformational changes with a drastic increase in the α-helix content particularly at the extreme C-terminus. Proper folding of the α2 chain at the C-terminus end ensured the stability of the newly formed heterotrimer.

1.2.5: Polymerisation of laminin-2

While the C-terminus is vital for trimerisation, the N-terminus of each of the α, β and γ chains mediate the self or co-polymerisation of laminin heterotrimers in full length trimers such as laminins-1, 2 and 4, in a temperature, concentration and calcium-dependent manner (Cheng et al., 1997; Yurchenco and Cheng, 1993). Laminin heterotrimers such as laminins-5 and 6, truncated in the N-terminus, are not able to co-polymerise with full-length laminins, stressing the importance of the N-terminus domain. Moreover it has recently been shown that the dy^{2J}/dy^{2J} mouse, which suffers from a deletion in the N-terminus domain VI of the α2 chain is not able to polymerise the laminin-2 or laminin-4 heterotrimer very efficiently (Colognato and Yurchenco, 1999). Receptor interactions may also play a vital role in the polymerisation of laminin heterotrimers. The α1 and α2 laminin chains both bind to dystroglycan and integrin α7β1 receptors in their C-terminus domain. In

muscle cells laminin-1, 2 and 4 heterotrimers showed preferential self-polymerisation when bound to either of these two receptors. Polymerised laminin is then able to induce the reorganisation of these receptors into a reciprocal network as a consequence of the rearrangement of cytoskeletal components, actin reorganisation and tyrosine phosphorylation (Colognato et al., 1999).

Laminin polymers interact with proteoglycans such as perlecan and with the type IV collagen polymer through bridges formed by entactin/nidogen which binds laminins in the centre of the heterotrimer (Timpl and Brown, 1996; Yurchenco and Schittny, 1990) to complete the supramolecular architecture of the ECM (fig. 1.3). Laminins are expressed in the basal lamina in early development and adulthood and since the initial discovery of laminins-1 and 2, many more laminin chains and heterotrimers have been detected, a brief introduction to these follows (Table 1.1).

1.2.6: Expression and function of other laminin chains

Soon after the discovery of laminin-2, a basal lamina protein specific to the NMJ was discovered (Hunter et al., 1989b). The S-laminin heterotrimer is known as laminin-3 and the S-laminin chain as the β2 chain. The β2 chain was enriched at synaptic sites in muscle and also found to a lesser extent in peripheral nerves in perineurial but not endoneurial basal lamina, in the glomerular basal lamina in kidney and in arterial basal lamina. In fact the β2 chain was detected in locations where the basal lamina was apposed on both sides by a cellular membrane (Hunter et al., 1989b).

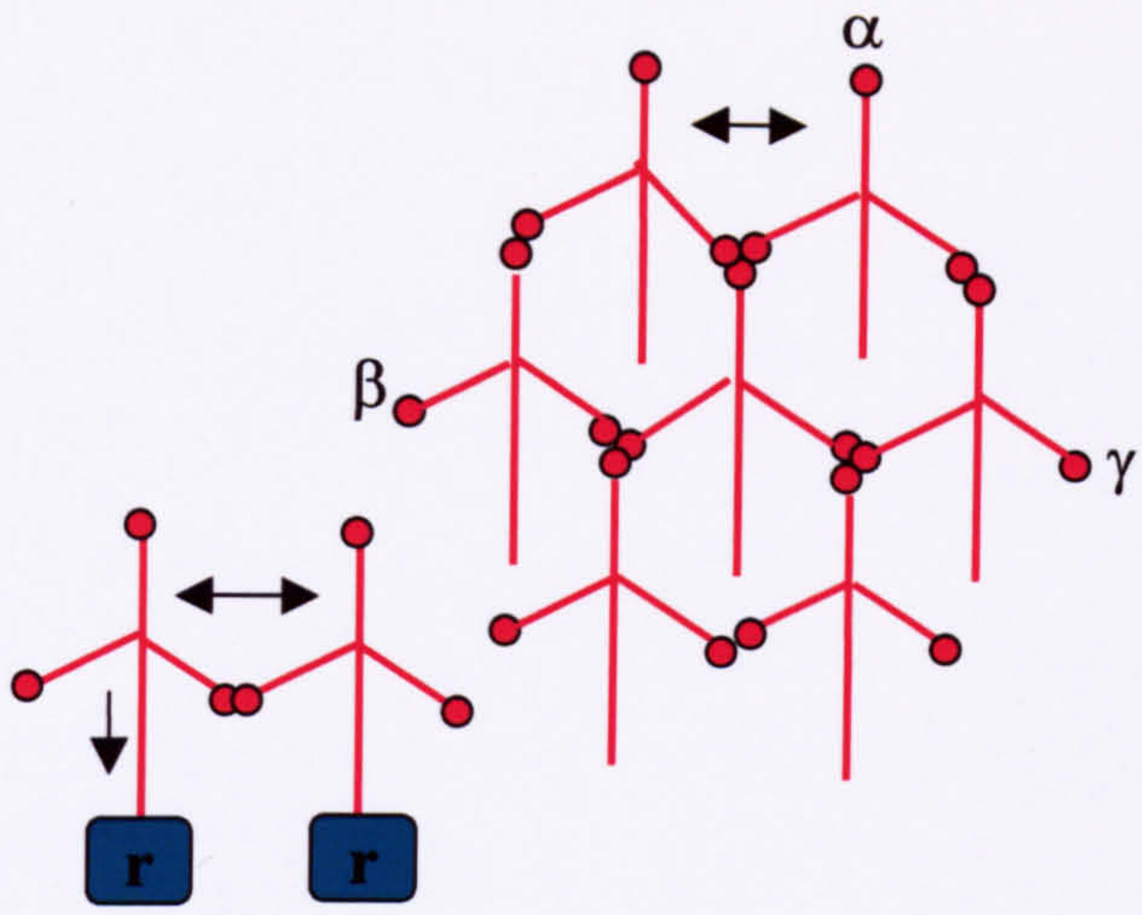

Figure 1.3: Laminin self-polymerisation: Laminin heterotrimers self-polymerise through interactions (double arrow) between α, β and γ chains in their globular N-terminal domains (red circles). Receptor (r) interactions (arrow) enhances laminin self-polymerisation.
Modified from Cheng et al. (1997) and Colognato and Yurchenco (2000).

The location of β2 at the neuromuscular junction indicated that it may exert an influence on neurons and in fact β2 substrates were found to be selectively adhesive for embryonic motorneurons rather than for sensory neurons (Hunter et al., 1989b). Targeted deletion of the β2 chain resulted in mice with abnormal NMJs; the number of active zones containing synaptic vesicles and the number of junctional folds was reduced and Schwann cells extended processes into the synapse (Noakes et al., 1995). The *lamb2* gene was found to be located on mouse chromosome 9 and encoded a cysteine-rich protein with N-glycosylation sites showing homology with the α1, γ1 chains and particularly the β1 chain (Hunter et al., 1989a; Porter et al., 1993). The β2 chain is currently known to be incorporated in several laminin heterotrimers, in laminin-4 (α2β2γ1) (Engvall et al., 1990), laminin-7 (α3Aβ2γ1), laminin-9 (α4β2γ1) and laminin-11 (α5β2γ1); all except laminin-7 can be detected at the synaptic basal lamina (fig.1.4).

Laminins-5, 6 and 7 have been detected at the dermal-epidermal junction in epithelia in hemidesmosome-like anchoring filaments. Laminin-5 (α3Aβ3γ2; also known as kalinin or epiligrin) was isolated from keratinocytes and contained similarly sized non-identical chains of 165 to 170 kDa, 145 to 155 kDa and of 135 to 140 kDa (Carter et al., 1991; Rousselle et al., 1991). Laminin-5 was found to exert an adhesive effect on keratinocytes and facilitated the attachment of growing keratinocytes in culture, a property that corresponds with its expression *in vivo*. These adhesive properties appear to be mediated by the α6β1 and α3β1 integrin receptors (Carter et al., 1991; Marinkovich et al., 1992a; Rousselle and Aumailley, 1994; Rousselle et al., 1991).

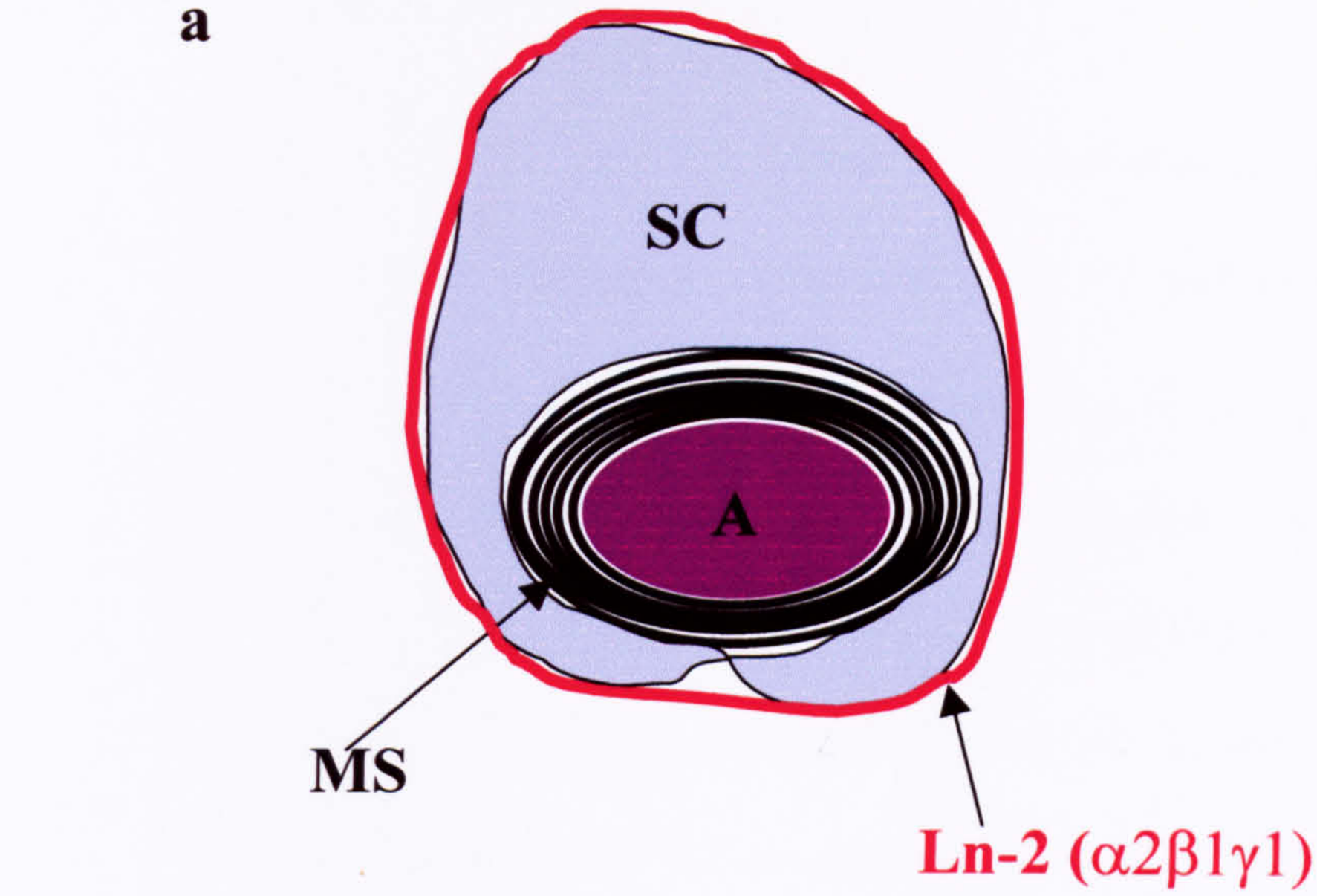

Figure 1.4: Expression of laminin chains and heterotrimers in the PNS. (a) A myelinated axon; the axon(A) is surrounded by a myelin sheath (MS) produced by the Schwann cell (SC) that is ensheathing it. Individual nerve-Schwann cell units in the PNS are surrounded by an endoneurial basal lamina in which the major non-collagenous constit -uent is laminin-2 (Ln-2). **(b)** At the NMJ, the nerve is surrounded by a terminal Schwann cell and a variety of laminin heterotrimers are present. Laminins-2 and 8 are expressed in the Schwann cell basal la -ina, although expression of the latter may be lost in adulthood. The laminin-2 heterotrimer is also expressed in the basal lamina of the skeletal muscle around the NMJ. Laminins-4, 9, and 11 are expressed in the primary cleft of the synapse and laminins-4 and 11 are also to be found in the junctional folds.
Modified from Patton et al. (1997).

Immunochemical investigation of laminin-6 (α3Aβ1γ1; K-laminin) revealed that it contained two chains that were common to laminin-1, the β1 and γ1 chains and another α chain that was common to laminin-5 (Marinkovich et al., 1992b). The laminin-7 (α3Aβ2γ1) heterotrimer was also found to be expressed in the dermal-epidermal junction and in amniotic fluid (Champliaud et al., 1996). It was proposed that laminin-5 complexes with either laminin-6 or 7 at the dermal-epidermal junction through interactions in the novel truncated α chain that is common to all three (Champliaud et al., 1996).

The *lama3* gene encoding the α3A chain produces two distinct transcripts of different sizes. It has a truncated N-terminus region that undergoes proteolytic processing (Ryan et al., 1994). The *lama3B* transcript encoded a longer chain with more EGF repeats and a globular domain similar to a α1 chain globular domain but with only two rather than three globular domains (Miner et al., 1997; Ryan et al., 1994). Laminin-5 also contained a novel β chain, the β3 chain (Pulkkinen et al., 1995) and a novel γ2 chain (Pulkkinen et al., 1994). The *lamb3* gene is compact relative to other β chains and was found to encode a β3 chain that is truncated with only one globular domain instead of two at the N-terminus of the short arm (Colognato and Yurchenco, 2000; Pulkkinen et al., 1995). The *lamc2* gene encoded two transcripts of the γ2 chain that are highly homologous to the γ1 chain (Airenne et al., 1996).

Another truncated laminin α chain was identified that was expressed in heart, pancreas, lung and muscle and other mesenchymal tissues. The α4 chain has a long arm sequence similar to those found in other α chains but is truncated at the N-terminus and contains only a few EGF repeats in domain IIIa and no globular

domains (Iivanainen et al., 1995; Richards et al., 1996; Richards et al., 1994). The human *lama4* gene is located on chromosome 6q21 close to the *lama2* gene on chromosome 6q22 (Richards et al., 1994). This may account for the specific upregulation of the α4 chain in place of the α2 chain in *dy/dy* mice and in humans with merosin-deficient CMD. The α4 chain has currently been allocated to two laminin heterotrimers, laminin-8 (α4β1γ1) expressed in the endoneurial basal lamina during development but down-regulated neonatally and in the basal lamina of blood vessels, lung and skeletal muscle fibres (Miner et al., 1997). Laminin-9 (α4β2γ1) is expressed at the synaptic basal lamina and particularly in the primary synaptic cleft and in the perineurial basal lamina surrounding axon fascicles (Miner et al., 1997).

The laminin-10 (α5β1γ1) and laminin-11 (α5β2γ1) heterotrimers both contain the novel α5 chain (Miner et al., 1997). The *lama5* gene encodes a full length α chain that is somewhat longer in the N-terminus region due to a greater number of EGF repeats in domain V (Miner et al., 1997). Laminin-10 is expressed during development at the synaptic basal lamina and in skeletal muscle (Miner et al., 1997; Patton et al., 1997; Ringelmann et al., 1999) and in hematopoietic cells and kidney (Gu et al., 1999; Miner et al., 1997). The laminin-11 heterotrimer is a β2 chain-containing laminin and is therefore largely restricted to synaptic basal lamina in the primary cleft and junctional folds (fig. 1.4), but can also be found in perineurial basal lamina (Miner et al., 1997; Patton et al., 1997). The presence of the α5 chain appears to be important as a stop signal for Schwann cells in the formation of the NMJ (Patton et al., 1998).

Recently a further laminin heterotrimer has been characterised which incorporates a

new γ chain. The laminin-12 heterotrimer (α2β1γ3) contains the γ3 chain (Koch et al., 1999) which appears to be a full-length γ chain containing all the expected domains (Iivanainen et al., 1999; Koch et al., 1999). The γ3 chain is expressed in heart, in skin at the point of nerve penetration at the dermal-epidermal junction and on the apical surface of the lung and a variety of reproductive tissues. The γ3 chain is not found in structurally defined basal laminae, suggesting that laminin-12 may be involved in the formation and maintenance of ciliated processes in these cells. The most important of the three known γ chains is the γ1 chain encoded by the *lamc1* gene. The wide expression of this chain in all but two of the twelve known heterotrimers, laminins-5 and 12, both of which show limited patterns of expression, results in severe consequences if it is deleted. Targeted deletion of the γ1 chain in mice using homologous recombination results in fatality at E5.5 in homozygous mutant embryos due to their failure to produce a proper basal lamina (Smyth et al., 1999). Instead, extracellular deposits of type IV collagen and perlecan were found. Although small amounts of the α1 chain and the glycoprotein nidogen/elastin were detected, it was insufficient in the absence of almost all the laminin heterotrimers to assemble the ECM necessary for formation of the basal lamina. The early death of homozygous embryos indicated that a basal lamina is vital from the time of endoderm differentiation.

1.2.7: The role of laminins in the developing nervous system

The functional significance of these laminins *in vivo* has become clearer recently with the characterisation by the Sanes laboratory of the spatio-temporal pattern of expression of laminin chain genes in the pathways and targets of the developing nervous system (Lentz et al., 1997) and with the development of transgenic mice

with targeted deletions in a number of laminin chain genes. It appears that while laminin chain genes are highly expressed in the developing PNS, expression in the CNS is limited. In E11.5 mouse embryos, in situ hybridisation showed wide expression of β1 and γ1 chain mRNA. Expression of α1, α2 and α4 chain mRNA was restricted to the spinal cord meninges and to non-neural cells around the DRG, the α4 chain mRNA was also expressed in unidentified cells along peripheral nerves (Lentz et al., 1997).

Laminin chain mRNA expression was detected in target tissues for sensory and motor axons, such as skin and muscle. There was wide expression of β1 and γ1 chain mRNA in limb-buds in both skin and muscle at E13, although expression of the β1 chain mRNA was more diffuse in muscle. Expression of α2 and α4 chain mRNA was restricted to muscle and the α5 chain mRNA to skin at this stage (Lentz et al., 1997). α3, β3 and γ2 chain mRNA is widely expressed in skin at this stage as well as in adulthood where they form the laminin-5 heterotrimer expressed at the dermal-epidermal junction. By E15.5 high expression of α2, α4, β1 and γ1 chain mRNA can be detected in the DRG, although whether or not expression of these chains is neuronal or not is unclear. α4 and α2 chain containing laminins such as laminin-2 and 8 are expressed in dorsal and ventral roots and along peripheral axonal pathways at a time during development when sensory and motor axon outgrowth and Schwann cell migration occurs.

The NMJ is a specialised structure that occurs where motor axons synapse on their target tissues, the skeletal muscle fibres, and begins to form at around E13 to E14 in mice. There is restricted expression of laminin chains here, whereas the α2, α4, α5, β1 and γ1 chains appear to be widely expressed in both synaptic and extrasynaptic

regions of the developing peripheral nerves, the β2 chain is exclusively expressed in synaptic basal lamina throughout (Patton et al., 1997). Expression of these laminin chains changes with maturation such that α4 chain expression is lost from extrasynaptic sites and expression of the β1 chain is lost from synaptic basal lamina. Thus it appears that while laminins-2, 8 and 10 may be expressed early on in the formation of the NMJ, only laminins-4, 9 and 11 are retained.

Laminins expressed at the NMJ have a specialised function that has been demonstrated in both *in vitro* assays and in targeted deletions of the *lamb2* gene. Although the number of NMJs appeared to be normal in mice lacking the β2 chain, the morphology differed substantially. In the mutants both the post and pre-synaptic terminus were relatively unbranched. The active sites where synaptic vesicles are concentrated were sparse and the synaptic vesicles themselves were scattered throughout the nerve terminus. Finally Schwann cells extended processes into the synaptic cleft instead of simply capping the nerve terminus (Noakes et al., 1995). Targeted deletion of the β2 chain gene also results in the loss of α5 chain expression and consequently the loss of laminin-11 in synaptic basal lamina. This laminin heterotrimer appears to have a particularly important role in the formation of the NMJ. Whereas other laminin heterotrimers that motor axons may encounter during development, such as laminins-2, 4 and 8 promote neurite outgrowth laminin-11 was found to be inhibitory. When embryonic motor neurons encountered laminin-11 *in vitro* their processes were short and bore large flattened growth cones (Cho et al., 1998). Moreover Schwann cells do not adhere well to a laminin-11 substrate and are inhibited from extending processes on it (Cho et al., 1998; Patton et al., 1998). Thus laminin-11 stops the motor axons during

development and prevents the Schwann cells from entering into the synaptic cleft. The expression of a *lama2* transgene in the skeletal muscle of mice with targeted deletions in the *lama2* gene does not obliterate all the symptoms. The persistence of lameness in the hind-limbs is linked to the loss of laminin-2 expression in the PNS (Kuang et al., 1998b), which results in a variety of Schwann cell ensheathment and myelination abnormalities in all mice deficient in laminin-2 (Bradley and Jenkison, 1973). It has long been known that an intact basal lamina is necessary for maintaining Schwann cell-axon interactions and promoting myelination (Bunge and Bunge, 1978; Bunge et al., 1986). As laminin-2 is produced by Schwann cells (Hsiao et al., 1993) and is the major laminin heterotrimer expressed extrasynaptically in the PNS (Patton et al., 1997), it clearly has a vital role to play in these processes.

Laminin-2's role in maintaining the integrity of the PNS has been demonstrated recently by its link to peripheral neuropathy in leprosy. The Myobacterium leprae bacteria responsible for causing leprosy were known to target Schwann cells but their mode of action was unknown. A 21 kDa protein on the Myobacterium leprae bacteria has been found to bind specifically to the C-terminus of the α2 chain in the G-domain (Shimoji et al., 1999). This then serves as a bridge for the bacteria to bind to the laminin receptors expressed in the Schwann cells such as the α6β4 integrin and the dystroglycan receptor. Thus the link between the ECM and the Schwann cell cytoskeleton that is vital for maintaining peripheral nerves is disrupted (Rambukkana et al., 1997; Rambukkana et al., 1998).

1.2.8: Laminins-1 and 2 in skeletal muscle development

Both laminins-1 and 2 can affect the behaviour of myoblasts *in vitro*, suggesting that both may be involved in myogenesis. Myoblasts are certainly capable of synthesising the laminin α2 chain (Vilquin et al., 1999; Vilquin et al., 1996). While laminin-1 promotes myoblast proliferation and fusion and the formation of myotubes, expression is downregulated as the myoblasts differentiate, this may explain why there is no need for laminin-1 expression in mature muscle fibres. Laminin-2 is expressed in myoblasts as laminin-1 expression is downregulated and myoblasts begin to differentiate. Although both laminin-1 and laminin-2 were able to induce fusion of myoblasts in cell lines, only laminin-2 was found to promote stability in the myotubes that were formed (Vachon et al., 1996).

When expression of the *lama2* gene was disrupted in embryonic stem cells, they were still capable of generating a variety of muscle cell types *in vitro* such as myotubes of skeletal muscle, smooth muscle cells and cardiomyocytes. As soon as they differentiated into a mature, contracting phenotype these α2 chain-deficient myotubes began to detach and degenerate (Kuang et al., 1998a). Like *dy/dy* mice, the deficiency in laminin-2 causes muscle fibres to degenerate within ten days of birth in mice with targeted deletions in the *lama2* gene, probably as a result of apoptotic cell death (Miyagoe et al., 1997). Skeletal muscle fibres in mice which do not express the laminin α2 chain also show poor regenerative properties which can be corrected with the expression of a human *lama2* transgene in skeletal muscle (Kuang et al., 1999). All of these findings are consistent with a role for laminin-2 in the basal lamina of mature skeletal muscle fibres in maintaining the stability of muscle fibres, preventing them from degenerating and helping them to acquire and

maintain their mature phenotype.

1.3: Laminin receptors

1.3.1: The integrin receptor family

Integrins are a large family of heterodimeric cell surface receptors which bind a variety of ECM molecules, including the laminins. The integrin heterodimers are composed of one of at least 16 α subunits and 8 β subunits that make up over twenty distinct subunit combinations (Hynes, 1992; Rosales et al., 1995). Most cells will express more than one integrin receptor throughout the course of their development and most integrins act as receptors for more than one ECM molecule. All integrin subunits have a large extracellular ligand binding domain and a small cytoplasmic domain except for the β4 subunit, which has a rather large cytoplasmic domain. The N-terminus of α and β subunits in the extracellular domain contains the ligand binding domain (Arnaout, 1990; D'Souza et al., 1994; Loftus et al., 1990; Smith and Cheresh, 1990; Wardlaw et al., 1990). Binding to this region of the integrin receptor is thought to be promoted by the presence of three to five divalent cations (Plow et al., 2000).

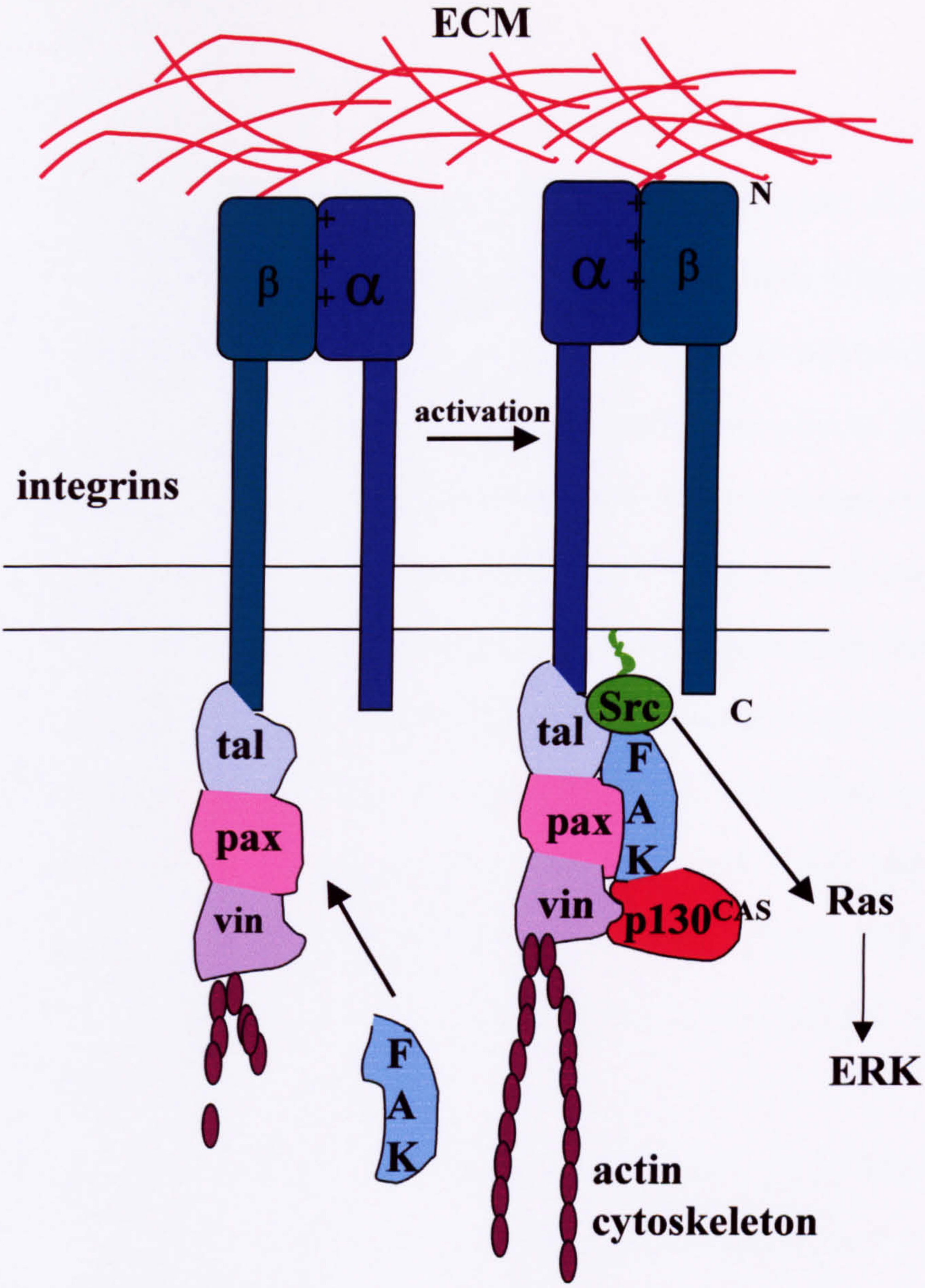

Figure 1.5: The integrin receptor complex: The extracellular matrix (ECM) binds to the integrin receptor subunits in their large extracellular N-terminus(N) domains. There are usually three to five divalent cations (+) in the N-terminus region which may be associated with ligand binding. Cytoskeletal proteins such as talin (tal), paxillin (pax) and vinculin (vin) bind to the short C-terminus (C) domain of the β integrin subunit. As the receptor binds to the ECM protein tyrosine kinases such as the focal adhesion kinase (FAK) pathway are activated and autophosphorylated, creating binding sites for Src kinases. The Src kinases phosphorylate focal adhesion kinases such as paxillin which have signalling as well as structural functions and the docking protein $p130^{CAS}$. Src phosphporylation may result in activation of the Ras-ERK (extracellular signal-related kinase) cascade. Receptor activation also induces assembly of actin filaments in the cytoskeleton and aggregation of ECM molecules and of their integrin receptors.
Modified from Giancotti and Ruoslahti (1999).

When the integrin receptor is bound to ECM molecules, the cytoplasmic domain of the integrin subunits will associate with cytoskeletal proteins and signalling complexes, promoting the assembly of actin filaments and resulting in aggregates of ECM molecules and cytoskeletal proteins on either side of the cell membrane (Giancotti and Ruoslahti, 1999). The binding of ECM molecules to integrin receptors provides both a structural link between the basal lamina and also activates signal transduction through the cytoskeletal proteins to which it binds (fig.1.5). Integrins mediate signal transduction through activation of protein tyrosine kinases, when integrin receptors were clustered they induced phosphorylation of a complex of proteins termed pp130 (Kornberg et al., 1991), now known as the focal adhesion complex. Most integrins activate the focal adhesion kinase (FAK) pathway (Parsons, 1996). The FAK pathway may interact either directly with the cytoplasmic tail of the integrin β subunit or through cytoskeletal proteins such as talin and paxillin.

The Src family of kinases, Src, Fyn, and Yes are thought to play a role in both FAK and Shc pathways. FAK activation creates a binding site for the Src homology 2 (SH2) domains of Src and Fyn resulting in phosphorylation of cytoskeletal focal adhesion proteins such as paxillin by Src kinases (Schaller et al., 1995; Schaller and Parsons, 1994; Schlaepfer and Hunter, 1996a; Schlaepfer and Hunter, 1996b). Both the FAK and Shc pathway may then activate the Ras-extracellular signal–regulated kinase (ERK) class of mitogen-activated protein (MAP) kinases and downstream signalling cascades.

1.3.2: Laminin-integrin interactions

Laminins in particular bind to a wide variety of integrins in different tissues and possess several binding domains for them. Most laminin-receptor binding interactions occur in the C-terminus domain of the long arm of laminin chains but some have also been identified in the short arm N-terminus domains. Although many integrins are recognised by a variety of ECM molecules, α6 integrins are largely specific for the laminins. The α6β1 integrin binds to the laminin α2 chain in its C-terminus end in domain I and in the G-domain (Delwel et al., 1993; Hall et al., 1990) as does the α6β4 integrin (Rambukkana et al., 1997; Spinardi et al., 1995). The α3β1 and α7β1 integrins also act as receptors for α2 chain containing laminins and bind the heterotrimer in the C-terminus domain I and G-domain region (Cohen et al., 2000; Delwel et al., 1994; Gehlsen et al., 1989; Kramer et al., 1991; Schober et al., 2000; Yao et al., 1996). The α1β1 and α2β1 integrin receptors bind to laminins in the short arm N-terminus domains (Hall et al., 1990; Tomaselli et al., 1990). Specific binding sites, which promote cell adhesion and neurite extension, have been found for these two receptors in domain VI of the laminin α2 chain (Colognato et al., 1997).

1.3.3: Integrins in the developing nervous system

Laminin-integrin interactions are thought to mediate several processes in the development and maintenance of the nervous system and in skeletal muscle. The α1β1 integrin is not widely expressed in adult tissues but is expressed transiently in both the CNS and PNS during early development; between E3 and E5 in the quail CNS and in the PNS from E3 when laminin-1 expression is first detected in neural crest cells regrouping into prospective DRGs (Duband et al., 1992). The α1β1

integrin receptor appears to promote neural crest cell migration when bound to laminin-1 *in vitro* (Desban and Duband, 1997). Laminin-1 binding to the α1β1 integrin receptor has different effects on neural crest cell spreading depending on whether it is bound to the laminin heterotrimer in the N-terminus domain which induces poor spreading or in the C-terminus domain which induces flattening and spreading of the neural crest cells (Desban and Duband, 1997).

PNS expression of the α1β1 dimer was strong at E4 to 4.5 up to E9 to10 in quail spinal sensory ganglia where sensory axons were extending neurites and in ciliary ganglia from E3.5 to E10 (Duband et al., 1992). Corresponding expression of the β1 integrin subunit has also been detected on ciliary ganglion neurons concurrent with laminin-1 expression (Weaver et al., 1995). In fact several β1 integrins were detected on the surface of the cell bodies of ciliary ganglion neurons from E4 to 8, but only the α3β1 and the α6β1 and not the α1β1 integrins mediated neurite outgrowth on laminin-1 *in vitro*. The same β1 integrins are expressed on the surface of DRG neurons and exhibit differential selectivity in promoting neurite outgrowth on laminins-1 and 2. Neurite extension on laminin-2 is more efficient on the α3β1 integrin receptor and on laminin-1 the α1β1 integrin receptor is preferred (Tomaselli et al., 1993). The neurite promoting properties of integrins are clearly dependent on the neuronal cell type and the laminin isoform to which it is bound.

1.3.4: Integrins and glial cells

Integrin binding is also involved in mediating the response of glial cells in both the CNS and PNS to ECM molecules. The β1 and β4 integrins are major Schwann cell laminin receptors, both are expressed by Schwann cells in human foetuses from about the eleventh to the twenty-second week but are down-regulated subsequently

(Jaakkola et al., 1993). The β1 integrin receptor subunit can be expressed by Schwann cells in the absence of axonal contact, (Einheber et al., 1993). In fact the α1β1 integrin is expressed mostly on mature non-myelin-forming Schwann cells and is only upregulated when axonal contact is lost following injury in non-myelin-forming Schwann cells (Stewart et al., 1997). β1 integrins are able to promote laminin-1 and 2-mediated Schwann cell migration *in vitro*, a necessary prerequisite to myelination in developing and regenerating nerves (Milner et al., 1997). Schwann cell migration is also promoted on another ECM substrate, fibronectin, through interactions with αv integrins. It is likely that laminin-mediated Schwann cell migration occurs through interactions with the α6β1 integrin, which is most highly expressed in undifferentiated Schwann cells before they begin to myelinate (Fernandez-Valle et al., 1994). The attachment of Schwann cells to the ECM preceding myelination is probably also mediated by the α6β1 receptor as blocking the activity of the β1 subunit inhibits myelination as the Schwann cells are most likely unable to attach to the ECM (Fernandez-Valle et al., 1994). Once the Schwann cells have attached to the ECM and are able to ensheath and myelinate the axon, expression of the α6β1 dimer is down-regulated and it is not normally expressed in myelinating Schwann cells. Myelination in the CNS by oligodendrocytes may also be regulated by laminin-integrin interactions. Blocking the activity of the α6β1 integrin receptor on oligodendrocytes, affects their ability to terminally differentiate and to form myelin membranes on a laminin-2 substrate *in vitro* (Buttery and ffrench-Constant, 1999).

The β4 integrin is expressed by Schwann cells only when in contact with axons and particularly upon myelination, when expression of the α6β1 integrin receptor is

downregulated (Einheber et al., 1993; Feltri et al., 1994; Fernandez-Valle et al., 1994). Thus the peak of β4 integrin expression occurs in late development and early adulthood, concurrent with the time of myelination. β4 integrin mRNA expression reaches it peak following the peak of myelin gene mRNA expression. It is downregulated again following injury to peripheral nerves and the loss of axonal contact and reinduced by contact with regenerating axons (Feltri et al., 1994). Expression of the α6β4 receptor is localised mostly to the outer plasma membrane of Schwann cells and to the Schmidt-Lanterman clefts/incisures (Einheber et al., 1993).

Integrin receptors have also been detected at the NMJ and may regulate its formation. The α1 integrin subunit has been detected at the NMJ in presynaptic cells such as Schwann cells and at nerve terminals (Martin et al., 1996). The α3β1 integrin, which is a laminin-binding integrin, is concentrated in the active zones where synaptic vesicles are gathered and released in the NMJ (Cohen et al., 2000). The α5β1 integrin, which is known to act predominately as a fibronectin receptor (Lefcort et al., 1992) is highly expressed in terminal Schwann cells at the NMJ (Cohen et al., 2000). This particular α5β1 integrin receptor is usually only expressed in neurites and Schwann cells along the axon during development and regeneration. The expression of these integrin receptors probably mediates the specific way in which terminal Schwann cells respond to laminins in the basal lamina of the NMJ. Terminal Schwann cells do not adhere very well to the synaptic basal lamina, preventing Schwann cell process extension into the NMJ. This may occur if the integrin receptors expressed there lack a cognate ligand, a laminin isoform with which they can interact.

1.3.5: Integrins in skeletal muscle

The α1 integrin is expressed in the myotomes in quail at E4 as the myoblasts begin to separate from the myotome, migrate and differentiate. Expression is maintained in skeletal muscle up to E11 when the myotubes have fused and become differentiated (Duband et al., 1992). Myoblast proliferation and differentiation up to myotube fusion are processes which are promoted by both laminins-1 and 2 (Vachon et al., 1996). One of the major laminin receptors in skeletal muscle is the α7β1 integrin receptor. The ability of laminins-1, 2 and 4 to promote adhesion and migration appears to be mediated *in vitro* by all three isoforms of the α7 integrin, α7A, α7B and α7C, in HEK293 and MCF-7 cell lines (Schober et al., 2000; Yao et al., 1996). All of these isoforms are capable of combining with the β1 integrin subunit to form a receptor that binds well to laminins-1, 2 and 4.

In adult mice α7A integrin mRNA was detected exclusively on skeletal muscle whereas α7B integrin mRNA showed a less restricted pattern of expression, in cardiac muscle, in brain and skeletal muscle (Collo et al., 1993). α7A mRNA was expressed postnatally once myoblasts had begun to differentiate and fuse and exclusively at the synapse and may therefore be involved in stabilising these structures (Martin et al., 1996). Proliferating skeletal muscle myoblasts exclusively expressed α7B integrin mRNA but although it was detected in developing skeletal muscle, it also appeared to be restricted to the synapse within a couple of weeks of birth. The α7C integrin subunit is the only one which appears to be expressed throughout skeletal muscle in both synaptic and extrasynaptic sites both during development and in adult skeletal muscle (Martin et al., 1996). The spatio-temporal expression patterns of these different isoforms of the α7 integrin subunit, suggests

different roles in the development and maintenance of skeletal muscle and the synapse. Mutations that cause a deficiency of α7 integrins result in congenital myopathy and indicates that this receptor is probably predominant in skeletal muscle (Hayashi et al., 1998).

1.3.6: Integrin receptor expression is regulated by laminins

Neurite outgrowth from embryonic chick DRG neurons is promoted by laminin-1 *in vitro* through interactions with the α6β1 integrin receptor. When the amount of laminin-1 on the substrate was lowered ten-fold, there was an increase in the adhesion of these DRG neurons and in neurite outgrowth from them (Condic and Letourneau, 1997). This was due to a compensatory four to fivefold increase in the number of neuronal α6β1 integrin receptors. However α6 mRNA and protein was decreased, suggesting that the increase in the number of receptors on the cell surface was due to post-translational regulation, i.e. activation, of α6 integrin induced by low levels of laminin-1.

Laminin regulation of integrin receptor levels has also been observed *in vivo*. In *dy/dy* mice and humans with merosin-deficient CMD, there is decreased expression of the α7β1 integrin receptor in skeletal muscle. This is not seen in mice and humans where the muscular dystrophy is caused by a deficiency of the cytoskeletal protein dystrophin (Hodges et al., 1997; Vachon et al., 1997). Thus the decrease in the levels of α2 chain-containing laminins in skeletal muscle leads to regulation of α7β1 integrin levels at both the gene expression and post-transcriptional levels. Moreover this regulation appears to selectively affect the levels of the α7A and β1D transcripts in particular. These are exclusively expressed in differentiated muscle in which laminin-2 promotes stability (Hodges et al., 1997; Vachon et al.,

1996; Vachon et al., 1997). Mice with targeted deletions of the synapse-specific laminin β2 chain also exhibit secondary changes in the distribution of integrins at the NMJ. Of the two synapse-specific α7 integrin isoforms, only the α7B isoform was lost (Martin et al., 1996). Integrin expression may also affect expression of laminins; embryoid bodies are normally capable of depositing a basal lamina incorporating laminin-1, but when embryoid bodies were derived from β1 integrin null embryonic stem cells, there was no basal lamina deposition. The lack of β1 integrin expression resulted in laminin α1 chain synthesis being terminated, without which a basal lamina could not be assembled (Aumailley et al., 2000).

1.3.7: Laminin-integrin binding and growth factors

Activated integrin receptors bound to ECM molecules such as the laminins are able to form complexes with growth factors and their receptors through shared signalling pathways resulting in optimal activation of these growth factors. Thus activation of the EGF receptor results in the phosphorylation of tyrosine residues on the β4 subunit of the α6β4 integrin when bound to laminin-5 (Mainiero et al., 1996). However this does not result in activation of the Shc pathway and instead EGF signals may suppress signalling in activated α6β4 integrin receptors. Ligand-bound clusters of integrin receptors are able to stimulate fibroblast growth factor (FGF) receptor aggregation (Plopper et al., 1995) and phosphorylation of platelet derived growth factor-β (PDGF) receptors (Sundberg and Rubin, 1996). The synergism between ligand-bound integrins and growth factors is linked to downstream signalling mechanisms, thus EGF, PDGF and basic FGF (bFGF) all activate the ERK pathway in ligand-bound and aggregated integrins (Miyamoto et al., 1996). Aggregation and phosphorylation of the receptors for all these growth

factors was in turn stimulated by the presence of ligand-bound integrins. Thus binding of laminin and other ECM molecules to integrin receptors not only provides a structural link between the basal lamina and cytoskeleton but also results in the activation of complex signalling pathways.

1.3.8: The dystrophin-associated glycoprotein receptor complex

The DAG receptor also binds ECM molecules, but its distribution, ligand specificity and function is far more restricted than that of the integrins. The first major component of this transmembrane complex to be identified was dystrophin in smooth and skeletal muscle. This was identified as the 400 kDa protein product of the gene that is mutated in Duchenne's muscular dystrophy (DMD) (Hoffman et al., 1987). Dystrophin had a 240 amino acid N-terminus domain that showed homology to the actin-binding domain of α-actinin, followed by a spectrin-like rod shaped domain with a triple helical structure, a cysteine-rich domain with α-actinin homology and finally a unique 420 kDa C-terminus domain (Koenig et al., 1988). Dystrophin was found to associate to a transmembrane complex in skeletal muscle that included a 50 kDa and 156 kDa component (Ohlendieck et al., 1991b). The large 156 kDa component formed the extracellular part of the complex and bound to the transmembrane 43 kDa component, which in turn bound a variety of intracellular cytoskeletal proteins (Ervasti and Campbell, 1991). Both components are encoded by the same gene, a 5.8 kilobase (kb) mRNA transcript was detected in skeletal muscle, cardiac muscle, lung and brain (Ibraghimov-Beskrovnaya et al., 1992). The transcript encoded a 97 kDa precursor protein that underwent post-translational modification, the N-terminus region of this precursor was processed into the extracellular 156 kDa component known as α-dystroglycan and the C-

terminus into the 43 kDa transmembrane component known as β-dystroglycan. The 156 kDa protein was found to be processed into a lower molecular weight protein in non-muscle tissues such as lung and brain of approximately 120 kDa (Gee et al., 1993; Ibraghimov-Beskrovnaya et al., 1992). The differences in molecular weight could be due to differential glycosylation of the extracellular component in various tissues (fig. 1.6).

1.3.9: Different cytoskeletal proteins are associated with the DAG receptor complex in different tissues

The composition of the DAG receptor complex differs from tissue to tissue, especially in the variety of cytoskeletal proteins associated with it. β-dystroglycan associates with several transmembrane and cytoskeletal proteins in skeletal muscle. The sarcoglycan complex is composed of α, β, γ and δ-sarcoglycan, four transmembrane proteins of between 35 to 50 kDa that are associated with β-dystroglycan (Durbeej et al., 1998; Ervasti and Campbell, 1991; Hemler, 1999). Dystrophin binds to β-dystroglycan and is also bound to the actin cytoskeleton and syntrophins in skeletal muscle. The syntrophins are 58-60 kDa proteins (Froehner et al., 1987), that associate with dystrophin (Ahn and Kunkel, 1995; Suzuki et al., 1995).

The composition of the DAG receptor complex in skeletal muscle at the NMJ differs from that in extrasynaptic skeletal muscle. An autosomal transcript was cloned from skeletal muscle encoded a 427 kDa cytoskeletal protein, utrophin, that had a high homology to dystrophin (Love et al., 1989) and was restricted to the NMJ in skeletal muscle (Ohlendieck et al., 1991a). Utrophin is associated with the same transmembrane and cytoskeletal proteins as dystrophin including the

sarcoglycans and actin (Matsumura et al., 1992). Rapsyn is a transmembrane protein associated with acetylcholine receptors, which is thought to provide a link between these receptors and the DAG receptor complex by binding to β-dystroglycan at the NMJ (Apel et al., 1995; Cartaud et al., 1998; Qu et al., 1996).

The DAG receptor complex has also been detected in peripheral nerves in a thin sheet surrounding the outermost layer of the myelin sheath (Matsumura et al., 1993). The α-dystroglycan protein could not be detected at the nodes of Ranvier, where myelin is not found, thus it appears that in peripheral nerve the DAG receptor complex is exclusively associated with the myelin sheath (Yamada et al., 1994). Utrophin, a 120 kDa α-dystroglycan, β-dystroglycan, a 59 kDa and a 35 kDa protein and Dp116 (a 116 kDa product of the gene that encodes dystrophin) but not the sarcoglycan complex were all co-localised in the peripheral nerve (fig. 1.6).

The DAG receptor complex varies in its composition but has now been detected in skeletal muscle, smooth muscle, cardiac muscle, at the NMJ, in the PNS, the CNS, the digestive system, respiratory system, skin, in basal epithelia such as kidney and in the reproductive system (Durbeej et al., 1998). Moreover expression of the DAG receptor complex has been detected during development as early as E5.5, in Reichert's membrane and in the basement membrane between the visceral endoderm and the ectoderm (Williamson et al., 1997; Yotsumoto et al., 1996). Homozygous mice with a null allele of the *Dag-1* gene encoding dystroglycan have a disrupted Reichert's membrane.

Figure 1.6: The DAG receptor complex in Schwann cells: (a) The transmembrane and extracellular components of the DAG (dystrophin associated glycoproteins) receptor complex, β-dystroglycan and α-dystroglycan have been detected on the Schwann cell outer membrane. The cytoskeletal proteins that bind to β-dystroglycan are found in the Schwann cell cytoplasm, between the Schwann cell outer membrane and the compacted myelin sheath surrounding the axon (A). **(b)** Laminin-2 in the basal lamina surrounding the axon- Schwann cell units binds to the extracellular component of the DAG receptor complex, α-dystroglycan (α-DG), through the fourth and fifth G-domain repeats in the C-terminal of the laminin α2 chain (α2LG4/5). α-Dystroglycan binds to β-dystroglycan (β-DG), which is a transmembrane protein found in the Schwann cell outer membrane. Dp116 and utrophin are cytoskeletal proteins that bind to β-dystroglycan in its intracellular domain in the Schwann cell cytoplasm. Downstream binding of utrophin and Dp116 to other cytoskeletal proteins and actin has not been well characterised for the DAG receptor complex in peripheral nerves.

Modified from Yamada et al. (1996) and Hemler (1999).

Figure 1.6 : The DAG receptor complex in Schwann cells

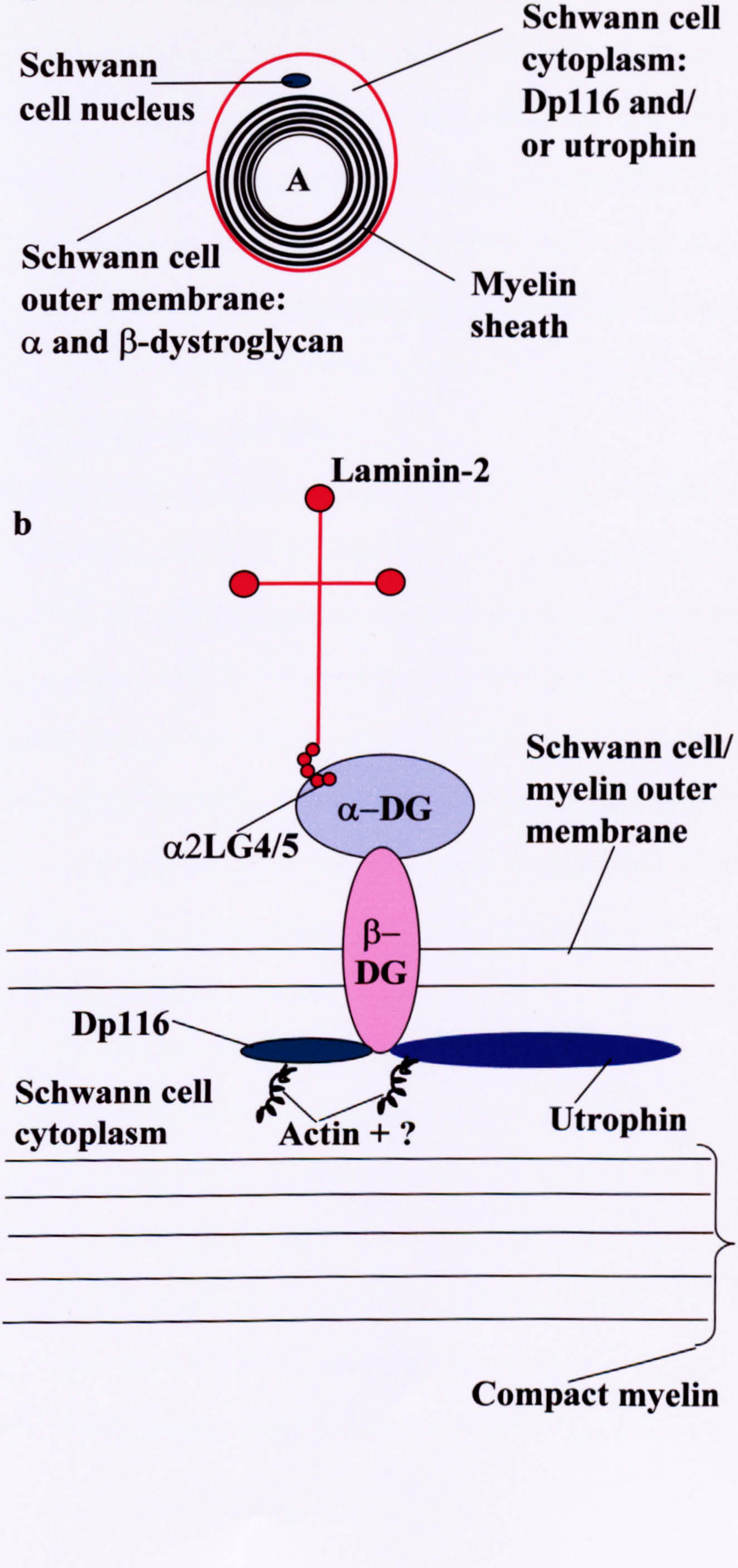

1.3.10: The DAG receptor complex binds laminin-1 and 2 in the ECM

Laminin-1 but not fibronectin was found to bind to the 156 kDa component of the DAG receptor complex (Ibraghimov-Beskrovnaya et al., 1992). This was also the case with the 120 kDa α-dystroglycan produced in non-muscle tissue, which bound laminin-1 with equal affinity and specificity as the 156 kDa α-dystroglycan (Gee et al., 1993). The expression of the DAG receptor complex in skeletal muscle and in peripheral nerves where the laminin-2 heterotrimer is the principal laminin isoform suggested that it too might bind α-dystroglycan.

Purified skeletal muscle DAG receptor complex was overlaid with ^{125}I-laminin-2 and shown to specifically bind this laminin isoform in a Ca^{2+}-dependent manner (Sunada et al., 1994). As with skeletal muscle, the 120 kDa peripheral nerve isoform of α-dystroglycan showed a Ca^{2+}-dependent binding affinity for laminin-2 (Yamada et al., 1994). *In vivo*, the principle ligand for α-dystroglycan is most likely to be laminin-2; The ECM is anchored to the Schwann cell cytoplasm by binding of the α-dystroglycan receptor by laminin-2 in the ECM, the α-dystroglycan is in turn bound to β-dystroglycan in the transmembrane domain. β-dystroglycan binds through its C-terminus cytoplasmic domain to either Dp116 or utrophin in the abaxonal Schwann cell cytoplasm (Saito et al., 1999; Yamada et al., 1996).

The binding region of the 120 kDa α-dystroglycan was determined to be in the heparin-binding region of the laminin-1 heterotrimer in the C-terminus G-domain (Gee et al., 1993). In fact heparin inhibits the binding of both laminin-1 and laminin-2 to the 156 kDa α-dystroglycan (Pall et al., 1996), consistent with a similar binding domain for the different α-dystroglycan isoforms on both the laminin α1 and α2 chains. Analysis of the crystal structure of the G-domain of the

laminin α2 chain reveals binding sites for α-dystroglycan in the fourth and fifth G-domains (LG4 and LG5, nearest to the laminin α2 chain C-terminus) (Hohenester et al., 1999; Tisi et al., 2000). A calcium ion was detected at the tip of both the α2LG4 and LG5 domains, consistent with the Ca^{2+}-dependent manner of laminin-binding to α-dystroglycan.

The DAG receptor complex clearly acts as a structural link between the basal lamina and the cytoskeleton, but its role in signal transduction is not clear. However among the cytoskeletal proteins that β-dystroglycan is able to bind to is growth receptor bound protein 2 (Grb2), an adapter protein that binds through its Src homology 3 (SH3) domains to the C-terminus of β-dystroglycan (Yang et al., 1995). The N-terminus SH3 domains of Grb2 shows a particularly strong affinity for the cytoplasmic tail of β-dystroglycan (Russo et al., 2000). As with the integrins, the SH3 domains are involved in signal transduction and cytoskeletal organisation and these domains in Grb2 are able to activate Ras signalling through receptor tyrosine kinases (Lowenstein et al., 1992). In addition the SH2 domains of Grb2 are able to associate with both EGF and PDGF receptors.

It is not clear whether the DAG receptor complex or integrins are more prominent in the pathology of the *dy/dy* mouse or humans with merosin-deficient CMD. Blocking the interaction of laminin-2 with α-dystroglycan in differentiated mouse myotubes disrupts the ability of laminin-2 to stabilise differentiated skeletal muscle (Vachon et al., 1996). A dystrophic phenotype is induced in these myoblast cultures, with reduced myotube size and loss of contractile activity (Brown et al., 1999). However expression of the DAG receptor complex is not affected in humans with merosin-deficient CMD even though expression of the α7β1 integrin receptor

is (Vachon et al., 1997). The interaction of laminin-2 with α-dystroglycan in Schwann cells may play an important role in myelination. The *Myobacterium leprae* bacteria responsible for causing leprosy bind to the laminin α2 chain in the G-domain blocking the sole binding sites for α-dystroglycan on laminins and results in peripheral neuropathy (Rambukkana et al., 1998).

1.4: Formation of the peripheral nervous system

1.4.1: Generation of the neural crest

Prospective neural crest cells lie on the border of the neural plate and the neuroepithelium, the prospective epithelium (fig. 1.7). Neural crest cells do not appear to be a segregated population; both neural tube and neural crest cells are derived from this region, consistent with a common lineage for some PNS and CNS cells (Bronner-Fraser and Fraser, 1989; Bronner-Fraser and Fraser, 1988). Inductive interactions between the neuroepithelium and the neural plate results in "dorsalisation" of the neural tube prior to the emergence of neural crest cells. The ability of non-neural ectoderm/neuroepithelium to generate signals that result in dorsalisation of the neural tube and generation of the neural crest is determined by the developmental stage of the non-neural ectoderm and the neural plate.

Slug can be induced in the neural plate of both stage 4 and stage 8 to 10 chick embryos but *Wnt-1* and *Wnt-3a* can only be induced in stage 8-10 neural plate. Thus early inductive interactions are capable of inducing neural crest only whereas later signals can generate both neural crest cells and dorsalised cells (Dickinson et al., 1995; Selleck and Bronner-Fraser, 1996). The inductive signalling properties of the neuroepithelium may be mediated by members of the bone morphogenetic

protein (BMP) family such as BMP-4 or BMP-7 and both are expressed in the neuroepithelium (Liem et al., 1995).

1.4.2: The PNS is generated from the neural crest

Neural crest cells migrate from the neural plate in a rostro-caudal wave and go on to form a wide range of neural and non-neural cells. Iontophoretic labelling of individual cells in dorsal neural tube also showed that these cells had multiple derivatives. As well as being able to generate both neural tube and neural crest cells, individual clones were able to generate sensory and sympathetic neurons, Schwann cells, melanocytes (Bronner-Fraser and Fraser, 1989; Bronner-Fraser and Fraser, 1988). Neural crest cells can also generate smooth muscle and bone as well as enteric neurons. The multipotent nature of neural crest cells appears to become restricted with age, thus when neuroepithelium confronts early neural plate (stages 4 to 5) both melanocytes and sympathoadrenal cells are generated but when placed next to later neural plate tissue only melanocytes are generated (Selleck and Bronner-Fraser, 1995). These fates are also determined by the factors encountered along the paths of migrating neural crest cells (see overleaf). There is however some recent evidence that suggests that the fate of neural crest cells may be determined before they begin to migrate. Neuronal cells *in vitro* derived from early neural crest cells expressed *Delta1* that encodes a Notch receptor (Wakamatsu et al., 2000). Notch suppresses neurogenesis, but lateral inhibition upon contact with Notch antagonists such as Numb suppresses the anti-neurogenic effects of Notch. Early expression of ligands such as Notch in specific neural crest cells may determine which neural crest cells differentiate into glial and which into neuronal cells before they encounter environmental cues during migration.

Figure 1.7: Neural crest cell development: (a) The blastula undergoes gastrulation through involution of a group of cells from the involuting marginal zone at the blastopore, these cells go on to form the mesoderm, one of the primary germ layers, the endoderm consists of the innermost layer of cells. The blastocoel is formed at the point where the cells have involuted at the blastopore to from the mesoderm and have induced the overlying ectodermal cells to form a layer of neurogenic cells known as the neural plate.

(b) Prospective neural crest cells arise from the border between the neuroepithelium and the neural plate. **(c)** The neural plate folds at the border of the neuroepithelium and forms a tube. The cells at the neural folds will become neural crest cells, while the tube formed by fusion at the neural folds will become the neural tube. The neuronal and glial cells whose cell bodies lie within the CNS arise from the neural tube, while the majority of neuronal and glial cells within the PNS will arise from neural crest cells. Cells in the mesoderm underlying the neural tube condense to form a rod-like structure known as the notochord. **(d)** The neural tube fuses and separates from the epithelium, the neural crest cells which arise from the point of fusion and from the dorsal neural tube begin to migrate away, following two main pathways. The neural tube is surrounded by a mesodermally-derived somite on either side, from which the sclerotome, myotome and dermatome arise. Neural crest cells migrate firstly through a ventral pathway (VP) in the anterior half of the sclerotome, these neural crest cells will form the DRG cells, sympathetic ganglion cells and adrenal medulla cells. A second wave of neural crest cell migration follows a dorsolateral pathway (DLP), above the somites and these cells will become melanocytes.

Figure 1.7: Neural crest cell development

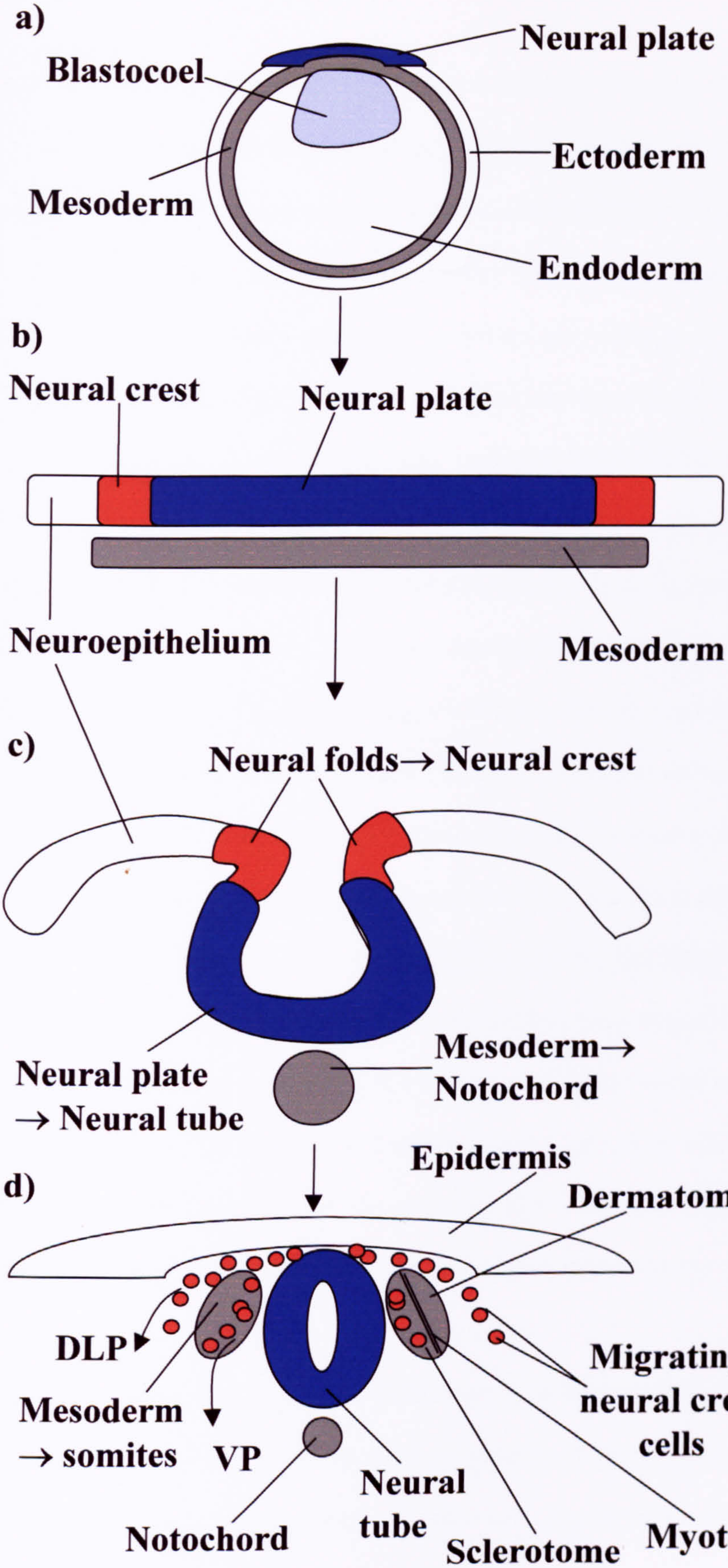

In the trunk, migrating neural crest cells follow two main pathways, the first is a ventral pathway through the somites which generates DRG and sympathetic ganglion cells and adrenal cells, the second dorsolateral pathway over the top of the somites follows later and generates melanocytes (Selleck and Bronner-Fraser, 2000). Furthermore neural crest migration pathways are defined by inhibitory mechanisms in the trunk which restricts migration to the rostral half of the sclerotome. The eph family of ligands may mediate these inhibitory signals, Ephrin-B1 and Ephrin-B2 are expressed in the caudal half of the somite avoided by both neural crest cells and motor axons. Both neural crest cells and motor axons express receptors for these ligands, predominantly EphB2 in neural crest (Wang and Anderson, 1997). *Sema III (Collapsin-1)*, a member of the semaphorin family, is expressed in areas surrounding neural crest migration pathways and neural crest cells express the neuropillin receptor for it. *In vitro* experiments show that neural crest cells avoid collapsin-1 and undergo changes similar to neuronal growth cone collapse in the presence of collapsin-1 (Eickholt et al., 1999). The ECM molecule F-spondin may also exert an inhibitory guiding influence on neural crest cell migration and is expressed in regions of the somite avoided by neural crest cells (Debby-Brafman et al., 1999). F-spondin overexpression inhibited migration of neural crest cells into normally permissive substrates and antibody blockade of F-spondin activity allowed migration of neural crest cells along normally inhibitory pathways.

The fate of neural crest cells is thought to be defined by factors encountered along their migratory pathway (fig. 1.7). BMPs-2 and 4 appear to be the primary inducers of autonomic derivatives of neural crest cells and both are expressed in regions

where autonomic nerves are generated (Bitgood and McMahon, 1995; Lyons et al., 1995; Shah et al., 1996). BMP-2 can induce the expression of the basic helix-loop-helix (bHLH) protein mammalian achaete-scute homologue (MASH-1) (Shah et al., 1996) required for the differentiation of autonomic neurons (Sommer et al., 1995). BMP-2 can also induce the expression of *Phox 2b*, a homeobox gene that induces the expression of the ret receptor and thus allows transduction of the glial-derived neurotrophic factor (GDNF), which is necessary for the production of sympathetic and enteric neurons (Durbec et al., 1996; Pattyn et al., 1999).

The signals that induce neural crest-derived sensory neurons may also involve another group of bHLH proteins, the neurogenins. Expression of neurogenin leads to the expression of neuroD, a transcription factor required for neuronal differentiation. Two chick neurogenin genes, *c-ngn-1* and *c-ngn-2*, have been detected in a subset of early migrating neural crest cells next to the neural tube at around stage 16 to 17 and is followed by expression of *neuroD* (Perez et al., 1999). *C-ngn-2* is expressed from stage 18 to 24 in the DRG, whereas *c-ngn-1* is expressed in the DRG at slightly later stages from stage 27 to 31. Expression of *c-ngn-1* spreads to the periphery of the DRG where neuronal precursors and non-neuronal cells are located and is lost from the differentiating neurons of the DRG. Both *c-ngn-1* and *c-ngn-2* are also expressed in ventral and dorsal regions of the neural tube. Ectopic expression of mouse *ngn-1* in chick embryos biased neural crest cells towards the DRG and can induce the expression of neuronal markers specific to sensory neurons in the dermamyotome (Perez et al., 1999).

Some neural crest clones treated with BMP-2 and 4, which are members of the transforming growth factor-β (TGF-β) superfamily, can also become smooth

muscle cells. Addition of TGF-βs1, 2 and 3 increased the proportion of smooth muscle cells and expression of TGF-βs *in vivo* is consistent with an instructive role for them in the generation of smooth muscle from neural crest cells (Shah et al., 1996). Presumptive melanocytes appear to express a bHLH transcription factor, Mitf that may instruct their fate as melanocytes (Opdecamp et al., 1997).

Schwann cells in the trunk are largely generated from the neural crest along with other glial cells such as the satellite cells. Glial growth factor (GGF; neuregulin), a member of the TGF-α superfamily (Marchionni et al., 1993), was known to be mitogenic for Schwann cells (Lemke and Brockes, 1984) but was found to have an effect earlier in the lineage, suppressing neurogenesis while promoting glial differentiation in neural crest cells (Shah et al., 1994). When colonies of neural crest cells were grown in recombinant GGF-2, neurogenesis was almost completely abolished and the majority of cells expressed a marker of immature Schwann cells, glial fibrillary acidic protein (GFAP). In addition the recombinant GGF-2 was able to inhibit the expression of MASH-1 necessary for neurogenesis. While the neurogenic BMP-2 and the smooth muscle cell inducer TGF-β1 are codominant, in neural crest cell cultures the ability of GGF-2 to inhibit neurogenesis, by downregulating MASH-1 expression, occurs only when BMP-2 expression is low (Shah and Anderson, 1997). In addition neural crest cells require 48 to 96 hours to respond to GGF-2 and commit to a glial fate and only about 24 hours to respond to TGF-β1 (Shah and Anderson, 1997). *In vivo* glial cells are generated later than neurons, this may be due to the slow response to GGFs of neural crest cells and to the fact that they are only able to inhibit neurogenesis once expression of BMP-2 has fallen, perhaps after neurogenesis is largely complete. Thus neural crest cells

will respond first to the neurogenic signals of BMP-2 rather than the gliogenic signals of GGFs, negative feedback signals from transient Notch activation dominates BMP-2 signalling and prevents all neural crest cells following the neurogenic pathway (Morrison et al., 2000).

1.4.3: Outgrowth of sensory and motor axons

Ventrally migrating neural crest cells aggregate in the anterior half of the sclerotomes to form the DRG (Bronner-Fraser, 1993; Keynes and Stern, 1984). DRG neurons are bipolar, with growth cones extending in two opposite directions within the anterior half of the sclerotome. There are several possible candidate repulsion molecules expressed in the posterior half of the sclerotome, which may determine the pathway of sensory axon outgrowth within the anterior half of the sclerotome. These molecules include those that are thought to restrict motor axon outgrowth and neural crest migration to the anterior sclerotome, such as the eph transmembrane ligands, Ephrin-B1 and Ephrin-B2 (Wang and Anderson, 1997) and collapsin-1, which can cause DRG growth cone collapse (Luo et al., 1993) as well as PNA (peanut agglutinin) (Davies et al., 1990). However explants of posterior half-sclerotomes do not exert significant long-distance repulsion of DRG axons growing from stage 28 DRGs or from stage 17 to 19 anterior half-sclerotomes containing DRGs (Keynes et al., 1997). The linear guidance cues that dictate the bipolar direction of growth cone extension may be sufficient to restrict sensory axon outgrowth to the anterior half of the sclerotomes.

One growth cone extends dorsomedially from the DRGs towards the dorsal root entry zone and CNS, while the other extends in a ventrolateral direction between the dermamyotome and notochord. Growth cones extending along the ventrolateral

pathway unite with motor axons to form the mixed spinal nerves of the PNS. It seems likely that the prominent mode of sensory axon guidance is through surround repulsion by molecules in surrounding structures both medially and laterally, such that the sensory axons follow the path of least resistance. Axonal outgrowth from DRG explants is repelled rather than inhibited in the presence of explants of tissue lateral to the DRGs, such as dermamyotome and surface ectoderm. This is also true when DRG explants are cocultured with explants of tissue medial to the DRGs, notochord exerts strong repulsion on sensory axons and the floor plate of the neural tube is also weakly repulsive (Keynes et al., 1997). To determine whether sensory axons extending dorsomedially towards the dorsal root entry zone, were guided by chemoattractants, DRG explants were cocultured with explants of the alar plate, the dorsal half of the neural tube. It was found that the alar plate did not act as a chemoattractant for sensory axons, but DRG explants sandwiched between explants of dermamyotome and notochord were able to direct bipolar extension of axons from the DRG (Keynes et al., 1997). Thus surround repulsion from the notochord and dermamyotome may be sufficient to direct sensory axon outgrowth in both directions *in vivo*. The molecules involved in this surround repulsion are not yet defined but it is known that neither chondroitin sulphate proteoglycans (CSPG) nor Sonic hedgehog (Shh) are involved.

The same environmental cues as migrating neural crest cells encounter are found along the path of the growing motor neuron and help to guide its growth towards its target tissues, skeletal muscles. The Eph transmembrane ligands Ephrin-B1 and Ephrin-B2 are expressed in the posterior sclerotome while motor axons express the EphB2 receptor that recognises these ligands (Henkemeyer et al., 1994; Wang and

Anderson, 1997). This interaction may contribute to the avoidance of the posterior sclerotome by motor axons during the first part of their outgrowth towards the limbs. Semaphorins are chemorepellents that have been detected in the ventral region of the developing spinal cord and may mediate guidance of both motor and sensory axons by repelling them towards the periphery. Sema III was initially shown to cause growth cone collapse of sensory axons in the NGF-responsive sub-population (Kolodkin et al., 1993; Messersmith et al., 1995). The neuropilin-1 and neuropilin-2 receptors mediate the chemorepellent activity of class 3 semaphorins, these two receptors mediate guidance and fasciculation of distinct but overlapping populations of CNS and PNS projections, such as cranial and spinal nerves (Giger et al., 2000).

1.5: Schwann cells

1.5.1: Schwann cell precursors generated from migrating neural crest cells are dependent on axonal signalling

Migrating neural crest cells as discussed above are induced to become glial cells through the suppression of neurogenic signalling by BMP-2 and the induction of gliogenesis by GGFs (Morrison et al., 2000; Shah and Anderson, 1997; Shah et al., 1994). These Schwann cell precursors can be detected in mice at E12 to 13 and in rats at E14 to 15. They have distinct properties which distinguish them from immature Schwann cells that are generated at E15 in mouse and E17 in rat and from mature non-myelin-forming and myelin-forming Schwann cells (Dong et al., 1999; Jessen et al., 1994). At this stage of development Schwann cell precursors are dependent on axonal contact for their survival, but Schwann cell signalling to the

axons at this precursor stage and at later stages is also vital for the formation of the PNS. In the PNS of E14 rats, Schwann cell precursors were spread across the surface of axons, separating them from surrounding tissue, but not associated with basal lamina. The precursors were also found between the axons, spreading thin cytoplasmic sheets that contacted each other and separated the axons (Jessen et al., 1994).

The first property that differentiated these Schwann cell precursors from more mature Schwann cells, was their inability to survive *in vitro* in the absence of axonal contact. Thus precursor cells from E14 rats were unable to survive when plated at moderate to high density in neuron-free cultures. When neuron-conditioned medium was added to Schwann cell precursors in neuron-free cultures they were able to survive, this confirmed that Schwann cell precursor survival was dependent on axonal signalling (Jessen et al., 1994). The number of Schwann cell precursors that died by apoptotic cell death in the absence of neurons, or neuron-conditioned medium, decreased with age such that by E16 some rat Schwann cell precursors were able to survive under these conditions and by E17 all the plated cells survived. Mouse Schwann cell precursors had similar properties, at E13 90% of Schwann cell precursors died *in vitro* when cultured in the absence of neurons, but by E15, 90% of the mouse cells were able to survive under the same conditions (Dong et al., 1999). Thus by E17 in rats and E15 in mice, the precursors have differentiated into immature Schwann cells that are no longer reliant on axonal signals for survival and have their own autocrine survival loops, mediated by a variety of growth factors (Meier et al., 1999).

A combination of a variety of FGFs and insulin-like growth factors-1 or 2 (IGF)

can rescue rat Schwann cell precursors in the short term from the apoptotic cell death that they undergo when axonal contact is lost, but without being mitogenic (Gavrilovic et al., 1995). In adult Schwann cells bFGF and IGF-1 are both mitogenic (Schumacher et al., 1993; Stewart et al., 1991). In cultures of E12 mouse Schwann cell precursors without neurons, FGF-2 was found to be mitogenic. However the total number of Schwann cells remained constant, indicating that while some Schwann cell precursors were proliferating, others were unable to survive in the long term in the absence of axonal contact (Dong et al., 1999).

Schwann cell precursors were found to differ from Schwann cells in several distinct ways during the period that they were dependent on axons for survival. Schwann cell precursors in both rats and mice tended to cluster and presented a flattened multipolar morphology, whereas E18 and new-born rat Schwann cells were very similar to each other and adopted a gradually more elongated bi- or tripolar morphology (Dong et al., 1999; Jessen et al., 1994). Like neural crest cells, Schwann cell precursors are highly motile, significantly more so than Schwann cells (Jessen et al., 1994). During the time that Schwann cell precursors are dependent on axonal survival they do not express the cytoplasmic Ca^{2+}-binding protein, S100, commonly used as a marker for Schwann cells. Schwann cell precursors in both mice and rats also failed to express the O4 lipid antigen, which is expressed in all immature, myelin forming and non-myelin forming Schwann cells (Dong et al., 1999; Jessen et al., 1994; Jessen and Mirsky, 1991).

Despite the lack of S100 immunoreactivity in Schwann cell precursors the expression of other molecules, such as growth-associated protein 43 (GAP-43), indicated that these cells were a distinct population and not neural crest cells

(Jessen et al., 1994). Almost all Schwann cell precursors in culture express other proteins besides GAP-43 that have been associated with more mature Schwann cells, particularly immature Schwann cells and mature non-myelin forming Schwann cells. Laminin-1 immunoreactivity has been observed in Schwann cells at all stages of development and in both myelin forming and non-myelin forming Schwann cells. Other proteins such as cell adhesion molecules neural cell adhesion molecule (N-CAM) and L1 and the low affinity neurotrophin receptor (p75) are expressed on Schwann cell precursors, immature Schwann cells and non-myelin forming Schwann cells, but not myelin forming Schwann cells (Dong et al., 1999; Jessen et al., 1994). GFAP is expressed a little later and can be detected in immature and non-myelin forming Schwann cells (Jessen and Mirsky, 1991; Jessen et al., 1990).

1.5.2: Neuregulins regulate the survival of Schwann cell precursors

Although growth factors such as the FGFs and IGFs are able to promote survival of Schwann cell precursors in the short term and their conversion to Schwann cells (Dong et al., 1999; Jessen et al., 1994), these are not the neuronally-derived signals that directly regulate the survival of Schwann cell precursors. The strongest candidates for this appear to be the neuregulins. Neu differentiation factor (NDF) is one of the products of the neuregulin gene; the mRNA encodes a group of alternatively spliced EGF-related peptides, such as acetylcholine receptor inducing activity (ARIA) and heregulin, as well as GGFs and NDFs (Falls et al., 1993; Lemke, 1996; Marchionni et al., 1993). NDF mRNA is highly expressed in both sensory and motor neurons but not in glia (Marchionni et al., 1993; Meyer and Birchmeier, 1994; Orr-Urtreger et al., 1993). Neuregulin signalling is mediated by a

family of receptor protein tyrosine kinases, ErbB2, ErbB3 and ErbB4, all of which have been detected in Schwann cells (Levi et al., 1995).

The addition of NDF-β to Schwann cell precursors in culture produces much the same effects as addition of neuron-conditioned medium. The EGF-like domains of NDF-β are sufficient to promote the long-term survival of E14 rat Schwann cell precursors. Blocking the activity of NDFs in neuron-conditioned medium with a soluble protein that contained the NDF-β binding site of the ErbB4 receptor resulted in the abolition of the survival activity of neuron-conditioned medium (Dong et al., 1995; Jessen et al., 1994). Deoxyribonucleic acid (DNA) synthesis in Schwann cell precursors exposed to NDF-β indicated that it can act as a mitogen and is able to promote proliferation too (Dong et al., 1995). Moreover Schwann cell precursors in defined medium exposed to NDF-β undergo the transition from precursor to immature Schwann cell at the same rate as *in vivo*.

Schwann cell precursors fail to develop in neuregulin$^{-/-}$ mice in adequate numbers and there is a subsequent lack of mature Schwann cells (Meyer and Birchmeier, 1995). Targeted mutations in the genes encoding the neuregulin receptors have produced ErbB3$^{-/-}$ null mutants in which both Schwann cell precursors and Schwann cells are absent. This receptor may therefore be involved in both the neuregulin-mediated conversion of neural crest cells to Schwann cell precursors and of precursors to Schwann cells (Riethmacher et al., 1997). In ErbB2 mutants, Schwann cell precursors are present in the DRGs but fail to differentiate and migrate out of the DRGs (Morris et al., 1999).

Neuregulins continue to be expressed by axons and the ErbB2 and ErbB3 receptors are also expressed in mature Schwann cells. Neuregulins may regulate early

postnatal survival of Schwann cells, when numbers are controlled so as to ensure that the one-to-one relationship between axons and myelin forming Schwann cells is attained. Apoptosis of Schwann cells during normal development and following axotomy *in vivo* and of early postnatal Schwann cells in serum-free medium can be inhibited with the addition of exogenous neuregulin/NDF-β, mediated by an ErbB2/ErbB3 receptor heterodimer (Grinspan et al., 1996; Syroid et al., 1996). Terminal Schwann cells rely on neuregulins for survival following neonatal denervation (Trachtenberg and Thompson, 1996). Thus Schwann cell numbers in early postnatal nerves are regulated by apoptotic cell death caused by competition between ErbB2/ErbB3-expressing Schwann cells for neuronally-derived neuregulins (Grinspan et al., 1996; Nakao et al., 1997; Syroid et al., 1996; Trachtenberg and Thompson, 1996).

1.5.3: Autocrine survival loops in developing Schwann cells

Upon conversion from Schwann cell precursors to immature Schwann cells at E15 in mice and E17 in rats, growth factors ensure that the Schwann cells are able to block apoptosis without being entirely dependent on the neuronally-derived signals. Both rat E18 and new-born Schwann cells, but not E14 precursors, survived in purified cultures in a density-dependent manner. Schwann cell death can be rescued in low-density cultures by the addition of conditioned medium from dense cultures of Schwann cells, indicating that Schwann cells were secreting factors that ensured their own survival. Several growth factors were tested to determine which mimicked the properties of Schwann cell conditioned medium. Of those tested, only IGFs, neurotrophin-3 (NT-3) and PDGF-BB were capable of enhancing Schwann cell survival in low-density cultures. In combination, they mimicked the

properties of Schwann cell conditioned medium through activation of the MAP kinase pathway. Moreover blocking antibodies to these growth factors inhibited the ability of Schwann cell-conditioned medium to rescue low-density cultures (Meier et al., 1999). It seems likely that these growth factors are involved in mediating autocrine survival loops both *in vitro* and *in vivo* as Schwann cells express both the ligands and their receptors (Eccleston et al., 1990; Meier et al., 1999).

Other growth factors may also be involved in regulating aspects of Schwann cell behaviour throughout development. Schwann cell precursors, immature Schwann cells and mature non-myelin forming Schwann cells all express the low affinity neurotrophin receptor, p75 (Jessen et al., 1994; Jessen and Mirsky, 1991). Expression of NGF (nerve growth factor) is also elevated in Schwann cells during development; the expression of both the p75 receptor and NGF indicates that Schwann cell activity may be regulated by NGF signalling. Schwann cell migration along growing axons is a vital part of the development of the PNS and NGF may be involved in this process. Addition of NGF enhances Schwann cell migration from DRG explants on denervated sciatic nerve substrates that, like Schwann cell precursors and immature Schwann cells, are rich in the p75 receptor. Antibodies to both NGF and the p75 receptor partially inhibit Schwann cell migration from these explants (Anton et al., 1994b). Thus NGF may be one of several factors that mediates Schwann cell migration during development.

1.5.4: Transcription factors in developing Schwann cells

As Schwann cells mature and begin to interact with axons, they express a variety of transcription factors that are thought to regulate the prospective Schwann cell phenotypes. The final stages of Schwann cell development occur during late

embryogenesis and in the first few postnatal weeks. Immature Schwann cells develop either into non-myelin-forming Schwann cells, similar in molecular phenotype to immature Schwann cells (Jessen and Mirsky, 1991) or they begin to express myelin proteins and differentiate into myelin forming Schwann cells (fig. 1.8). As such they express different sets of transcription factors that are thought to regulate their differentiation.

The transcription factors expressed in immature and non-myelin-forming Schwann cells are also expressed in myelin forming denervated Schwann cells as they dedifferentiate to the immature Schwann cell phenotype (Mirsky and Jessen, 1996) and are thought to suppress the expression of myelin genes. An inverse relationship was observed between expression of the *Pax3* gene (expressed from the precursor stage onwards and in mature myelin-forming Schwann cells) and expression of the myelin protein myelin basic protein (MBP) in developing and regenerating sciatic nerves and *in vitro* (Kioussi et al., 1995). Schwann cells exposed to *Pax3 in vitro* expressed molecular markers for immature and non-myelin forming Schwann cells and repressed endogenous expression of MBP.

Krox-24/egr1 is a zinc finger transcription factor expressed in immature and non-myelin forming Schwann cells. An increase in the expression of *Krox-24/egr1* in cultured Schwann cells leads to a corresponding increase in the level of the p75 receptor that is expressed on immature and non-myelin forming Schwann cells (Nikam et al., 1995). In fact, *Krox-24/egr1* binds to the p75 promoter and a direct interaction is necessary between the gene encoding the *p75* and the *Krox-24/egr1* gene in order for the receptor to be expressed in Schwann cells.

Figure 1.8: Schwann cell differentiation and myelination: (a) The Schwann cell (SC) precursor is generated from neural crest cells at E12 to13 in mice and E14 to 15 in rats. The precursor is multipolar and extends processes between the axons, but does not ensheath them. **(b)** Immature Schwann cells are generated from Schwann cell precursors at E15 in mice and E17 in rats. They adopt a bi- or tripolar morphology and are able to survive without neuronal contact. **(c)** Immature Schwann cells form a basal lamina and ensheath individual axons of more than 1 μm in diameter shortly before birth. Differentiation towards the premyelinating phenotype is initiated before differentiation towards the non-myelin forming phenotype. **(d)** Immature Schwann cells differentiate towards the non-myelin forming phenotype in the early postnatal period. These Schwann cells have several small diameter axons embedded in grooves. The Schwann cell plasma membrane becomes apposed at the mesaxon and axons are enveloped by Schwann cell cytoplasm, the Schwann cell is then surrounded by the endoneurial basal lamina. **(e)** During myelination the mesaxon of the Schwann cell rotates around the axon, enveloping it in concentric circles of Schwann cell cytoplasm. Differentiation towards the myelin and non-myelin forming phenotypes is reversible upon loss of axonal contact. **(f)** A myelinated axon in transverse section. The inner leaflets of the apposing Schwann cell plasma membranes fuse to form the major dense lines and Schwann cell cytoplasm is extruded. Concentric layers of plasma membrane surrounding the axon constitute the myelin sheath. The axon, myelin sheath and Schwann cell cytoplasm are surrounded by endoneurial basal lamina. **(g)** Myelinated axon in longitudinal section. Each segment of axon surrounded by a Schwann cell is termed an internode. The unmyelinated segments between internodes aid saltatory conduction and are known as the nodes of Ranvier. Schwann cell cytoplasm is not completely excluded from the myelin sheaths and can be found at the paranodal loops and the Schmidt-Lanterman clefts.

a) SC precursor
b) Immature SC
Axon
Nucleus
Axon
c) Pre-myelinating SC
Basal lamina
Axon
Mesaxon
d) Non-myelin forming SC
Basal lamina
e) Myelin-forming SC
Axon
Myelin: major dense line
mesaxon
f) Myelin-forming SC
g) Myelin-forming SC
Schmidt-Lanterman cleft
Endoneurial basal lamina
Axon
Mesaxon
Node of Ranvier
Myelin
Paranodal loops

Suppressed, cAMP-inducible POU-domain protein (SCIP; also known as Oct-6 or Tst-1) is a POU domain transcription factor expressed in developing Schwann cells as well as in CNS glia. The expression pattern of SCIP and the phenotype of SCIP null mutant mice, in which Schwann cells show a transient delay in differentiation at the premyelinating stage, suggested a role in premyelinating Schwann cells. SCIP is therefore involved, but not essential, in the transition of Schwann cells from the premyelinating to the myelinating phenotype (Arroyo et al., 1998; Jaegle et al., 1996). SCIP mRNA and protein can be detected from about E14 in rat in Schwann cell precursors and expression increases as the Schwann cells mature, peaking at P1 but still detectable at P12 in myelin forming Schwann cells (Blanchard et al., 1996; Jaegle et al., 1996; Monuki et al., 1990; Monuki et al., 1989). The expression of this transcription factor is regulated by axonal contact, thus axotomy leads to a sharp fall in SCIP mRNA levels followed by upregulation during regeneration (Scherer et al., 1994a). However SCIP is barely detectable in mature myelin forming Schwann cells once myelination is complete although non-myelin forming Schwann cells continue to express SCIP in adulthood (Blanchard et al., 1996; Zorick and Lemke, 1996). SCIP also represses the transcription of the P_0 myelin gene promoter by binding to it through its POU domain and an N-terminus domain (Monuki et al., 1993). Thus SCIP may regulate terminal differentiation of Schwann cells into a myelin-forming phenotype by repressing the activity of myelin genes.

Krox-20/Egr2 encodes a zinc finger transcription factor, which has several roles in the developing nervous system. The phenotype of *krox-20*$^{-/-}$ mice, in which Schwann cells form a one-to-one association and begin to ensheath axons that

would normally be myelinated but do not actually myelinate, suggests that *krox-20* is either directly or indirectly involved in the final stages of differentiation of myelin forming Schwann cells. *Krox-20*$^{-/-}$ mice express only the early myelin marker, myelin associated glycoprotein (MAG), and do not express later myelin proteins such as P_0 and MBP (Topilko et al., 1994). *Krox-20* was detected in Schwann cells 24 to 36 hours after *SCIP* expression, as Schwann cells underwent the transition from precursor to immature Schwann cell, but expression of the *krox-20* gene was restricted to myelin forming Schwann cells only, where it continued to be expressed postnatally (Zorick et al., 1996). *Krox-20* expression is induced by axonal contact, thus in co-cultures only those Schwann cells that were in direct contact with neurons showed induction of *krox-20* expression (Murphy et al., 1996). The exclusive expression of *krox-20* on myelin forming Schwann cells suggests that it may activate myelin gene expression in these Schwann cells. Myelin gene promoters do not contain any binding sites for *krox-20*, which suggests that intermediate genes may be involved (Topilko et al., 1994). One such gene may be *SCIP*; in *krox-20*$^{-/-}$ mice expression of the SCIP transcription factor is sustained rather than transient (Zorick et al., 1999).

1.5.5: Neuronal development and Schwann cell signalling

Recent work has shown that there is a mutual aspect of the dependence of neurons and Schwann cells for their survival and differentiation. Targeted deletions of the ErbB3 neuregulin receptor have revealed the extent to which neuronal development is dependent on the trophic support of Schwann cells. *ErbB3*$^{-/-}$ mice lack Schwann cell precursors and Schwann cells, and although DRG neuronal development is normal at E12.5, by E14.5 there was a 70% reduction and by E18.5 an 82%

reduction in the number of neurons. The vast majority of apoptotic cells were identified as post-mitotic sensory neurons (Riethmacher et al., 1997). Similarly the number of motor neurons in the ventral horn was normal in E12.5 *ErbB3*$^{-/-}$ mice, but by E18.5 79% had died. The neuronal degeneration observed was far more severe than in any mutants lacking neurotrophins or neurotrophin receptors. Loss of trophic support from developing Schwann cells was responsible for the widespread loss of neurons.

Targeted deletion of another neuregulin receptor, ErbB2, suggests that Schwann cells not only provide trophic support to developing neurons but also regulate axon guidance (Morris et al., 1999; Woldeyesus et al., 1999). By rescuing the cardiac defect of *ErbB2*$^{-/-}$ mice, they can survive till birth, allowing axon pathways to form. The *ErbB2*$^{-/-}$ mutants, with the cardiac defect rescued, do have Schwann cell precursors, but these do not migrate properly and do not mature such that Schwann cells are completely absent in their peripheral nerves. There is a severe reduction of both motor and sensory neurons in *ErbB2*$^{-/-}$ mice, with 70% fewer motor neurons in the spinal cord of mutants by E18.5 (Morris et al., 1999; Woldeyesus et al., 1999). Surviving axons were severely defasciculated and their projections to their target tissues was aberrant and disorganised. Although acetylcholine receptors were present, their morphology and dispersal was abnormal. Addition of exogenous Schwann cells to an *in vitro* neurite outgrowth assay enhanced neurite outgrowth in mutant DRG neurons in contact with the exogenous Schwann cells (Morris et al., 1999). This was consistent with a loss of Schwann cell trophic support as the cause of the neuronal degeneration and defasciculation in *ErbB2*$^{-/-}$ mice.

Growth factors expressed by Schwann cells may regulate neuronal survival and

guidance and include brain derived neurotrophic factor (BDNF), leukaemia inhibitory factor (LIF), NT3, ciliary neurotrophic factor (CNTF) and GDNF (Davies, 1998). CNTF can prevent the degeneration of motor neurons in mice with motor neuronopathy and *cntf*$^{-/-}$ mice lose approximately 20% of their motor neurons. However this growth factor is expressed only in mature Schwann cells in intact Schwann cell-axon units, suggesting that CNTF may have a limited developmental role (Friedman et al., 1992; Masu et al., 1993; Sendtner et al., 1992). GDNF is widely expressed during development and has been detected in Schwann cell precursors (Wright and Snider, 1996). Moreover it is a potent survival factor for motor neurons, preventing the degeneration of motor neurons that have been deprived of target-derived trophic support due to axotomy (Henderson et al., 1994). Loss of GDNF expression results in a 20 to 30% reduction in the number of motorneurons, as well as loss of some sensory and enteric neurons (Moore et al., 1996; Sanchez et al., 1996). Motor neurons express receptors for both GDNF and for cardiotrophin-1 (CT-1; a growth factor expressed in myotubes) and are receptive to synergistic trophic and tropic support from both Schwann cell derived and target-derived growth factors.

Sensory neurons may rely on other growth factors for survival. NT-3 is secreted by developing Schwann cells and is part of the autocrine survival loop of immature Schwann cells (Meier et al., 1999). Antibody neutralisation of NT-3 activity during gangliogenesis results in a 30% reduction in the number of sensory neurons, consistent with a role for Schwann cell-derived NT-3 contributing to the survival of sensory neurons (Gaese et al., 1994). Thus it appears that growth factors support the survival of different subpopulations of sensory and motor neurons. However

neither sensory nor motor neurons are solely dependent on any single growth factor, most neurons are probably dependent on the synergistic activity of several Schwann cell-derived growth factors and on growth factors derived from target tissues such as skeletal muscle.

Laminins are known to have neurite-promoting properties (Anton et al., 1994a; Cho et al., 1998; Cohen and Johnson, 1991; Engvall et al., 1992) and Schwann cells are a rich source of laminin-2 in particular (Hsiao et al., 1993). This is consistent with a role for Schwann cell-derived laminins as contributory factors in axon growth and guidance during development. Immature and non-myelin forming Schwann cells express the cell adhesion molecule L1 (Jessen and Mirsky, 1991). Antibody blockade of L1 in co-cultures of retinal explants on Schwann cell monolayers results in a 95% inhibition of neurite outgrowth from the explants (Kleitman et al., 1988). Its role in axonal guidance may be linked to its ability to influence growth cone behaviour and actin distribution (Burden-Gulley et al., 1997). Growth cone filopodial contact with Schwann cells is sufficient to induce veil extension in sensory neurons *in vitro*. This Schwann cell-mediated veil extension can be inhibited with antibodies to neural cadherin (N-cadherin) a cell adhesion molecule expressed on Schwann cells (Letourneau et al., 1991; Letourneau et al., 1990; Polinsky et al., 2000). Stabilisation of this veil extension by continued Schwann cell-filopodial contact results in the advancement of the growth cone (Polinsky et al., 2000). Thus Schwann cell-mediated signalling through cell adhesion molecules may aid growth cone advancement in developing neurons.

1.5.6: Schwann cells and basal lamina formation

Periphernal nerves contain three layers of basal lamina, which serve to strengthen the nerve fibre and contain ECM molecules that are capable of regulating the behaviour of cells such as neurons and Schwann cells in the nerve fibre. The first layer, the endoneurium, surrounds axon-Schwann cell units (fig. 1.4, 1.9). The second perineurial layer surrounds axon bundles and the third outer layer directly outside of the perineurium is the epineurium. Although Schwann cells are capable of synthesising some basal lamina components such as laminin (Hsiao et al., 1993), elaboration of basal lamina requires the presence of other components of the nerve fibre. E15 Schwann cells were co-cultured with E15 DRG neurons to determine the influence of neuronal contact on basal lamina assembly. Schwann cells grown in the absence of neurons or not in direct contact with them in co-cultures, deposited only short segments of basal lamina that were neither continuous nor adherent (Clark and Bunge, 1989).

Although the basal lamina formed in Schwann cell-neuron co-cultures already contains laminins, type IV collagen and heparan sulphate proteoglycan (HSPG), the addition of fibroblasts increases the deposition of basal lamina (Obremski et al., 1993a; Obremski et al., 1993b). Fibroblasts are mesenchymal cells found in the epineurium, perineurium and in endoneurium and enhance basal lamina deposition by augmenting the deposition of basal lamina components such as laminins-1 and 2 and type IV collagen. Schwann cells produce some of the components necessary for endoneurial basal lamina formation but Schwann cell-derived signalling to mesenchymal tissue is also involved in controlling basal lamina deposition in the PNS. Desert hedgehog (Dhh) is expressed in mouse Schwann cell precursors from

E11.5 and in Schwann cells up to P10 and its Patched receptor in mesenchymal tissue surrounding the nerve from E15.5, at the time that the perineurium begins to form (Bitgood and McMahon, 1995; Mirsky et al., 1999). *Dhh*$^{-/-}$ mice had extensive abnormalities in perineurial basal lamina formation in particular but also in the epineurial and endoneurial basal lamina (Parmantier et al., 1999). The epineuria and perineuria of *Dhh*$^{-/-}$ mice were less compacted; contained fewer layers and the basal lamina was patchy and disorganised. The basal lamina in return regulates Schwann cell ensheathment and myelination. Basal lamina formation *in vitro* leads to Schwann cell differentiation, elongation and finally ensheathment of axons (Carey et al., 1986; Obremski and Bunge, 1995; Obremski et al., 1993b). The extent of Schwann cell ensheathment is correlated to the condition of the basal lamina, the addition of fibroblasts to Schwann cell-neuron co-cultures resulted in a continuous basal lamina and consequently more complete ensheathment of neurites (Obremski et al., 1993a). The presence of basal lamina induced differentiation of Schwann cells in co-culture with neurons into functional Schwann cell phenotypes that ensheathed the neurites and was a prerequisite for myelination in long-term cultures (Eldridge et al., 1989; Eldridge et al., 1987).

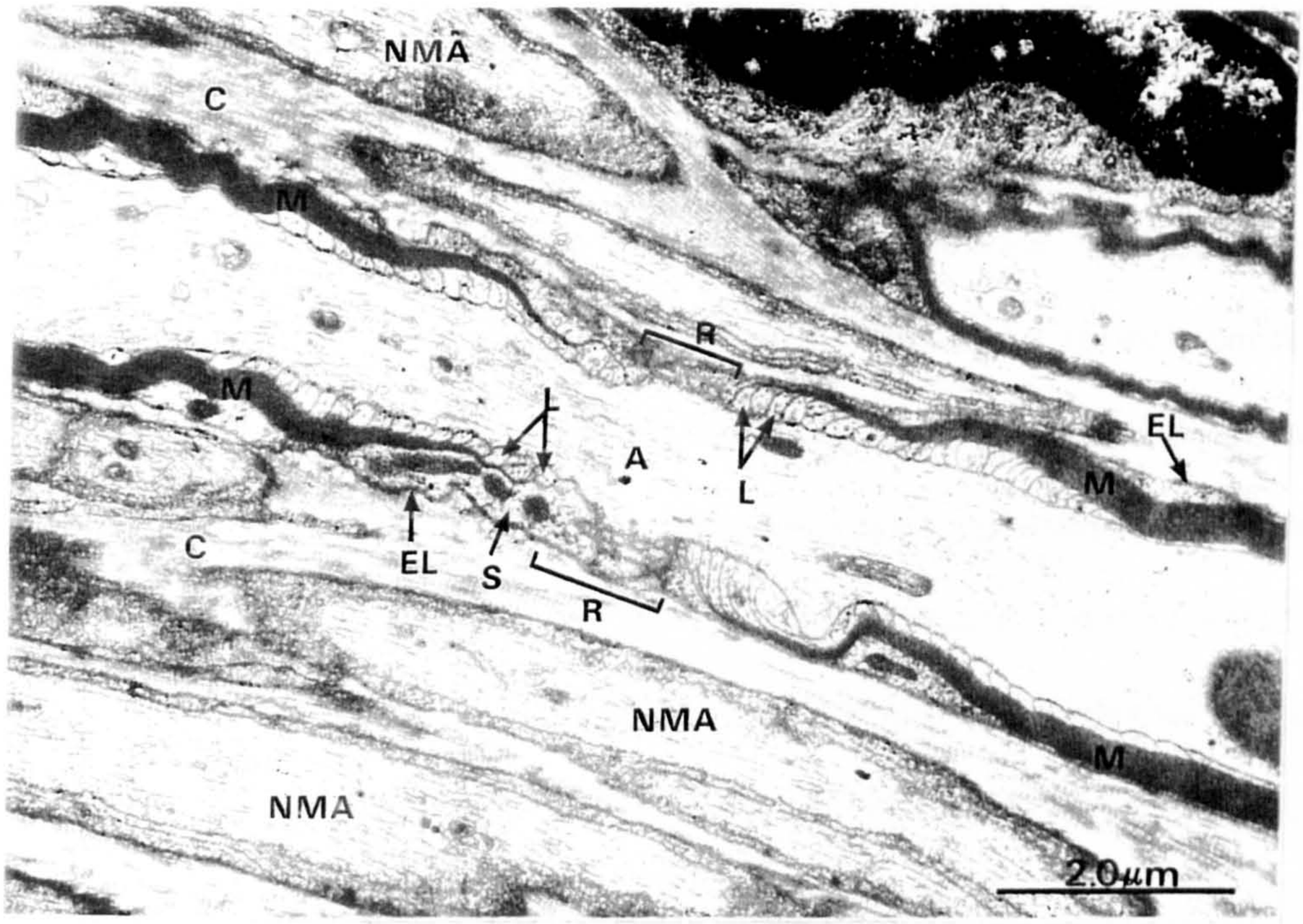

Figure 1.9: Electron micrograph of a peripheral nerve. The nerve fibre contains both non-myelinated axons (NMA) and myelinated axons (A). The compacted myelin sheath (M) produced by each Schwann cell in a myelinated axon terminates in paranodal loops (L) that contain Schwann cell cytoplasm. These paranodal loops border the nodes of Ranvier (R). The Schwann cell cytoplasm (S) surrounds the myelin sheath and extends over the paranodal loops and nodes of Ranvier. Schwann cell cytoplasm can also be seen between non-myelinated axons. Schwann cells are surrounded by an endoneurial basal lamina (EL) and collagen (C) fibrils are found in the surrounding endoneurium. Scale bar = 2 μm. Magnification x14000.

Taken from Wheater's Functional Histology by B. Young and J. W. Heath. Fourth edition (2000): p125.

1.5.7: Schwann cell ensheathment; myelin forming, non-myelin forming and terminal Schwann cells

As Schwann cells mature their relationship with axons changes (fig. 1.8). Schwann cell precursors extend multiple flattened processes between bundles of axons but do not actually ensheath them. As they differentiate into immature Schwann cells they loose their multipolar morphology and groups of bi- or tripolar Schwann cells ensheath axon bundles. Just before birth, Schwann cells begin to differentiate towards their final mature phenotype (Jessen and Mirsky, 1999; Mirsky and Jessen, 1996; Scherer, 1997). Small diameter axons are ensheathed by non-myelin forming Schwann cells. The small diameter axon will become embedded in one of several channels in the non-myelin forming Schwann cell. The plasma membranes at the opening of each channel become apposed and the axon is surrounded by Schwann cell cytoplasm, providing it with physical protection.

Myelin forming Schwann cells ensheath larger diameter axons of 0.7μm or more (Webster, 1971; Windebank et al., 1985). Immature Schwann cells differentiate into myelin gene-expressing premyelinating Schwann cells that form a one to one relationship with axons. Terminally differentiated myelin forming Schwann cells ensheath the axon; the mesaxon of the Schwann cell rotates around the axon and completely envelopes it in concentric layers of Schwann cell cytoplasm beginning the process of myelination (fig. 1.8). Phosphatidylinisitol (PI) 3-kinase may also be involved in signalling pathways between axons and myelin forming Schwann cells during myelination. Inhibition of PI 3-kinase blocks the initial interaction between axons and Schwann cells and consequently prevents terminal differentiation, elongation and myelination by myelin forming Schwann cells (Maurel and Salzer,

2000). Myelin sheaths were shorter and the rate of accumulation of myelin proteins was decreased in Schwann cell-neuron cocultures where PI 3-kinase activity was blocked, although maintenance of mature myelin sheaths was not affected. This recent work highlights the importance of axonal contact for the final stages of Schwann cell differentiation preceding myelination.

Terminal Schwann cells differ phenotypically from both myelin forming and non-myelin forming Schwann cells. They are located exclusively at the NMJ where they cover the terminal arborisations of the motor nerves, but do not extend into the synaptic cleft. They do not myelinate, but unlike non-myelin forming Schwann cells elsewhere they do not normally express GAP-43 (Woolf et al., 1992). Upregulation of GAP-43 expression after nerve transection occurs within a day and is far more rapid in terminal Schwann cells than in myelin-forming Schwann cells that can take several weeks to upregulate GAP-43 (Curtis et al., 1992). The rapid upregulation of GAP-43 may be linked to the rapid extension of processes by terminal Schwann cells following denervation of motor endplates. These processes extend to neighbouring innervated endplates, providing a guide for axons to sprout from the innervated to the denervated endplates to form new nerve terminals (Son and Thompson, 1995a; Son and Thompson, 1995b).

1.5.8: Myelination

As myelin-forming Schwann cells envelope the axons, the Schwann cell cytoplasm becomes extruded and the inner leaflets of the plasma membranes become fused to form the major dense lines. The close apposition of the outer leaflets of the Schwann cell plasma membranes forms the intraperiod lines. Some cytoplasm can be detected at the Schmidt-Lanterman clefts providing a cytoplasmic channel

between the narrow band of Schwann cell cytoplasm adjacent to the axon and the bulk of the cytoplasm surrounding the outside of the myelin sheath. Schwann cell cytoplasm is also present in the paranodal loops that border the nodes of Ranvier, but in general the extrusion of the cytoplasm leaves a lipid-rich myelin sheath surrounding the axons. The segment of nerve ensheathed and myelinated by each myelin forming Schwann cell is known as an internode. A small gap remains between each internode, a specialised structure known as the node of Ranvier (fig. 1.9).

The myelin sheath is composed of a mixture of lipids such as cholestorols, galactolipids and phospholipids, glycoproteins, basic proteins and other proteins. P_0, a 28 kDa integral membrane glycoprotein, makes up about 50 to 70% of the protein composition of myelin and is expressed exclusively in the PNS (Greenfield et al., 1973; Kitamura et al., 1976; Roomi et al., 1978; Smith and Curtis, 1979; Wiggins et al., 1975). P_0 is a member of the immunoglobulin (Ig) superfamily and the extracellular N-terminus shows structural similarities to some cell adhesion molecules (Lemke et al., 1988). The N-terminus may contribute to the formation of the myelin intraperiod line by hydrophobic and electrostatic interactions. The C-terminus cytoplasmic domain is basic and may promote the formation of the major dense line through interactions with acidic lipids in the plasma membrane (Garbay et al., 2000). Thus P_0 is involved in the compaction of the myelin sheath particularly through homophilic interactions in its extracellular domain (Filbin et al., 1990).

Recent evidence shows that P_0 mRNA is detectable in rats in a population of migrating neural crest cells at E11, with preferential localisation to those neural

crest cells neighbouring motor axons growing from the neural tube, which are likely to be prospective Schwann cells (Lee et al., 1997). P_0 mRNA was also detectable in Schwann cell precursors at E14 and just prior to myelination in both prospective myelin forming and non-myelin forming Schwann cells. Expression of P_0 is elevated postnatally in actively myelinating Schwann cells, before decreasing to basal levels after myelination is complete. The basal levels of P_0 protein and mRNA in non-myelin forming Schwann cells neonatally is down-regulated and is undetectable in mature non-myelin forming Schwann cells (Lee et al., 1997). Transection of unmyelinated nerve fibres and loss of axonal contact restores basal P_0 expression in non-myelin forming Schwann cells, consistent with a P_0-inhibitory signal in mature unmyelinated nerve fibres.

Peripheral nerve myelin 22 kDa (PMP22) is a small myelin glycoprotein of 22 kDa that includes complex glycosylation sites and constitutes 2 to 5% of myelin (Kitamura et al., 1976; Pareek et al., 1993). The PMP22 protein contains four transmembrane domains (Manfioletti et al., 1990; Suter et al., 1992a) that resemble domains in proteolipid protein (PLP) /DM20, and in the connexin subunits of gap junctions (Lemke, 1993). PMP22 may serve a similar function in PNS myelin as P_0, as it contains carbohydrate residues that mediate adhesion (Pareek et al., 1993; Snipes et al., 1992). PMP22 is not restricted to the PNS and has been detected at low levels in the lung, brain and gut (Hagedorn et al., 1999; Parmantier et al., 1995). Mutations in the PMP22 gene result in a variety of peripheral neuropathies such as those seen in Trembler and Trembler-J mice caused by mutations in one of the transmembrane domains (Suter et al., 1992a; Suter et al., 1992b). These mice suffer from hypomyelination and persistent Schwann cell proliferation. Similar

point mutations in the PMP22 gene have also been linked to CMT 1A (Charcot-Marie-Tooth) disease in humans in which there is a severe deficiency of myelin (Naef and Suter, 1998; Valentijn et al., 1992). Mutations in the PMP22 gene result in arrest of Schwann cell differentiation at the premyelinating stage (Sereda et al., 1996). Thus PMP22 may play a role in the development of Schwann cells and their transition to myelin forming Schwann cells as well as maintaining a compact myelin sheath.

MAG is a glycosylated myelin protein that is expressed in both the PNS and CNS. There are two isoforms of the MAG protein, small MAG (S-MAG) is the 67 kDa isoform that is predominant in Schwann cells and large MAG (L-MAG) is the 72 kDa isoform that is more widely expressed in the CNS (Frail and Braun, 1984; Trapp et al., 1989). MAG is a member of the Ig superfamily and has a large N-terminus extracellular domain that includes five Ig-like domains and, a short transmembrane domain and either a 46 (S-MAG) or 90 (L-MAG) amino acid C-terminus cytoplasmic domain (Salzer et al., 1987). Expression of MAG is limited in the PNS and it constitutes only 0.1% of total myelin protein (Figlewicz et al., 1981). It is located on the paranodal loops, both externally and internally at the mesaxon and at the Schmidt-Lanterman clefts (Martini and Schachner, 1988; Sternberger et al., 1979; Trapp et al., 1989; Trapp and Quarles, 1984; Trapp and Quarles, 1982; Trapp et al., 1984b). The role of MAG in intermembrane spacing prevents the exclusion of the Schwann cell cytoplasm at the Schmidt-Lanterman clefts. MAG is also capable of regulating neurite outgrowth in an inhibitory manner (McKerracher et al., 1994; Mukhopadhyay et al., 1994). MAG can also mediate myelin-axonal signalling, recent evidence suggests that MAG may regulate the

calibre of myelinated axons ensuring that they are viable for myelination. Mice with a null mutation in the MAG gene have reduced axonal calibres and reduced spacing between neurofilaments (Yin et al., 1998).

MBP's are a group of small highly basic proteins (about 25% of the residues), the four that have been detected in the PNS are 14, 17, 18.5 and 21.5 kDa and all are generated from a single gene by alternative splicing of the primary transcript (de Ferra et al., 1985; Gilbert et al., 1982; Greenfield et al., 1980; Mentaberry et al., 1986; Takahashi et al., 1985). The MBP proteins make up about 5 to 15% of the proteins found in myelin (Benjamins and Morell, 1978) and are thought to play a similar role to the P_0 protein, in maintaining the integrity of the major dense lines and in compaction of the myelin sheath. The localisation of MBP to the major dense lines, is consistent with this role (Omlin et al., 1982). Loss of both P_0 and MBP expression results in absence of major dense lines and uncompacted myelin. Loss of only P_0 results in only partial compaction of the myelin sheath and loss of MBP only, in shiverer mice, results in normal compaction in the PNS but no compaction of CNS myelin (Martini et al., 1995; Privat et al., 1979). Thus MBP can partially compensate for the loss of P_0 in the PNS, but as P_0 is exclusively expressed in the PNS it can only compensate for the loss of MBP expression in the PNS, leaving CNS myelin uncompacted.

The PLP myelin protein is a 30 kDa protein that constitutes 50% of CNS myelin where it is thought to play a role in maintaining the intraperiod line, probably by promoting the apposition of the outer leaflets of the plasma membrane (Boison et al., 1995; Duncan et al., 1987). The gene encoding PLP also produces DM20 through alternative splicing. Loss of PLP/DM20 expression in the CNS results in a

variety of phenotypes such as compacted myelin with axonal swelling and degeneration (Griffiths et al., 1998), in other cases there is widespread hypomyelination and oligodendrocyte death (Griffiths et al., 1995). PLP has four transmembrane domains and a large extracellular domain, DM20 is identical except for the loss of 35 amino acids (Nave et al., 1987). PLP/DM20 constitutes only about 1% of myelin proteins in the PNS; its localisation and role here are not yet clearly defined. Some have argued that they are expressed in the Schwann cell cytoplasm outside of the myelin sheath (Griffiths et al., 1989; Puckett et al., 1987). More recently PLP/DM20 has been detected in the compact myelin sheath, incorporated into the Schwann cell plasma membrane (Agrawal and Agrawal, 1991; Garbern et al., 1997). Individuals with null mutations in which PLP is not expressed rather than misexpressed show PNS abnormalities such as demyelinating peripheral neuropathy consistent with a role for PLP/DM20 in the development and maintenance of the myelin sheath in the PNS (Garbern et al., 1997).

P_2 is a basic 14.8 kDa myelin protein that is found only in the cytoplasmic side of compact myelin membranes (Hahn et al., 1987; London, 1971; Trapp et al., 1984a). The level of P_2 expression varies from species to species and may be as little as 1% of PNS myelin proteins in mice and rats or as much as 12 % in human and bovine nerves (Garbay et al., 2000; Greenfield et al., 1982). It is thought that P_2 is involved in fatty acid uptake and transport and its role as a lipid carrier suggests that it may be involved in myelin assembly and maintenance. CNPase (2', 3'-cyclic nucleotide 3'-phosphodiesterase) constitutes only 0.5% of total PNS myelin proteins (Uyemura et al., 1972). A single gene encodes both CNPase1, a 46 kDa protein, and CNPase2, a 48 kDa protein (Douglas and Thompson, 1993; Gravel et al.,

1994). CNPase is a cytoplasmic myelin protein that has been detected at the paranodal loops, the outer mesaxon and in the Schmidt-Lanterman clefts (Trapp et al., 1988a; Yoshino et al., 1985). Its exact physiological function is unclear, but CNPase interacts with oligodendrocyte membranes and with the actin cytoskeleton and may therefore be able to modulate glial cell morphology (De Angelis and Braun, 1996; Gravel et al., 1996).

1.5.9: The node of Ranvier

Specialised proteins are expressed at the nodes of Ranvier that may be involved in its formation or stabilisation. Epithelial cadherin (E-cadherin) is an adhesive glycoprotein in Schwann cells and is expressed only in uncompacted myelin, at the Schmidt-Lanterman clefts and in the paranodal loops (Fannon et al., 1995). The cytoplasmic C-terminus domain of E-cadherin forms complexes with cytoskeletal proteins such as F-actin to regulate the architecture of the Schwann cell cytoplasmic network at the paranodes and Schmidt-Lanterman clefts.

Periaxin is a myelin protein expressed exclusively by myelin forming Schwann cells at the paranodal (periaxonal) loops of the nodes of Ranvier and constitutes 5% of myelin proteins (Gillespie et al., 1994). Large periaxin (L-periaxin) is a 147 kDa protein expressed in the plasma membrane of myelinating Schwann cells at the paranodes while the 16 kDa small periaxin (S-periaxin) is expressed diffusely throughout the paranodal cytoplasm (Dytrych et al., 1998; Gillespie et al., 1994). Periaxin expression is first detected before other myelin proteins at the Schwann cell membrane apposing the axon as the Schwann cells and peaks postnatally during active myelination, when expression of periaxin becomes concentrated to the Schwann cell membrane apposing the basal lamina (Scherer et al., 1995).

Periaxin expression is also increased during active remyelination following injury. Contactin-associated protein (Caspr; also known as paranodin) is a neurexin family integral membrane protein of 190 kDa expressed by neurons. Although initially expressed throughout the axon, Caspr becomes concentrated at the paranodal loops of mature myelinated fibres (Einheber et al., 1997). Caspr1 is connected with the axonal cytoskeletal by proteins such as spectrin binding to protein 4.1. A large extracellular domain binds contactin, regulating the colocalisation of contactin and Caspr1 to the paranodal loops (Menegoz et al., 1997; Peles et al., 1997; Rios et al., 2000). The 155 kDa isoform of neurofascin is a glial component of the paranodal loops that also binds Caspr1 (Tait et al., 2000). The complex of contactin, Caspr1, protein 4.1 and neurofascin mediates interactions between the paranodal loops of the Schwann cell and the axonal cytoskeleton at the nodes of Ranvier.

The juxtaparanode, located under the compact myelin sheath neighbouring the paranode, is rich in K^+ channels. Caspr2, is colocalised with delayed rectifier K^+ channels in the juxtaparanodal region (Poliak et al., 1999). Caspr2 associates through a PDZ-binding domain in the cytoplasmic C-terminus region with the Kv1.1, Kv1.2 and Kvβ2 channel subunits by binding to the C-terminus domain of the K^+ channels' α subunits (Poliak et al., 1999). Clusters of Na^+ channels at the nodes of Ranvier are anchored by ankyrin G, an axonal cytoskeletal protein with a 480 kDa and a 270 kDa unit. Thus Casprs and associated proteins such as contactin and neurofascins mediate specialisation of both the nodal, paranodal and juxtaparanodal regions of myelinated axons.

1.6: Peripheral nerve regeneration

1.6.1: Wallerian degeneration

Wallerian degeneration describes the processes following crush or transection injury to nerves. The regenerative process itself involves recapitulation of many developmental processes in peripheral nerves. Upon injury to the nerve the axons in the distal stump that have become isolated from the neuronal cell body begin to disintegrate within 24 hours, this is followed by fragmentation of the myelin sheath. In the PNS early invasion by macrophages facilitates regeneration by clearing the debris (Beuche and Friede, 1984; Franzen et al., 1998). Schwann cells persist in degenerating nerves and help to clear the debris created by axonolysis and myelinolysis over a period of weeks along with the macrophages and possibly fibroblasts (Weinberg and Spencer, 1978). Mice in which macrophage recruitment is delayed undergo very slow Wallerian degeneration but are still able to regenerate (Lunn et al., 1989), as Schwann cells are also able to clear the myelin debris (Fernandez-Valle et al., 1995).

1.6.2: The bands of Büngner

Schwann cells align themselves along the endoneurial basal lamina tubes known as bands of Büngner that remain intact following crush injury. Fibroblasts and perineurial cells also invade the bands of Büngner, which serve as guides for axons between the proximal and distal stumps in regenerating nerves (Anderson et al., 1991; Hall, 1986b; Hall, 1989; Weinberg and Spencer, 1978; Williams et al., 1983). The bands of Büngner are more likely to remain aligned following crush injury and this is probably why regeneration following crush is usually more successful than following transection. These Schwann cell lined basal lamina tubes are the

exclusive conduits for successful axonal regeneration *in vivo* (Nathaniel and Pease, 1963) and the presence of both the basal lamina and Schwann cells is vital for axonal regeneration in the PNS.

Expression of laminin chains, such as the α1, α2, β1 and γ1 chains, is upregulated in Schwann cells when axonal contact is lost (Doyu et al., 1993; Masaki et al., 2000; Tona et al., 1993). The ability of regenerating axons in the bands of Büngner to interact with laminin-2 is particularly important in mediating neurite outgrowth during regeneration. Antibody blockade of laminin-2 activity is more inhibitory to neurite outgrowth on denervated nerve substrates than on intact nerve substrates (Agius and Cochard, 1998; Anton et al., 1994a). Other ECM molecules such as fibronectin and chondroitin sulphate are also upregulated following peripheral nerve injury (Tona et al., 1993; Vogelezang et al., 1999). The levels of protein and mRNA of F-spondin, an ECM molecule normally expressed by Schwann cells when sensory and motor neurons are projecting to their peripheral targets, is upregulated in Schwann cells distal to the site of injury (Burstyn-Cohen et al., 1998; Klar et al., 1992). Moreover antibody blockade of F-spondin in axotomised nerves inhibits neurite outgrowth. However the bands of Büngner alone are not sufficient for axonal regeneration, many of the ECM molecules upregulated in the basal lamina of regenerating nerves are in fact produced by Schwann cells. Axons extending from the proximal stump in regenerating nerves are always accompanied by migrating Schwann cells, without which axonal regeneration is substantially delayed and less widespread (Feneley et al., 1991; Hall, 1986a; Rodriguez et al., 2000).

1.6.3: Schwann cell migration and proliferation

Both myelin forming and non-myelin forming Schwann cells enter a proliferative stage within a couple of days of axonal and myelin fragmentation following injury and loss of axonal contact (Clemence et al., 1989). This proliferative stage closely follows macrophage infiltration and these cells may induce mitogenic activity in Schwann cells. Lysosomal processing of myelin membranes by macrophages induces the production of a mitogenic factor for Schwann cells by the macrophages (Baichwal et al., 1988). However Schwann cells involved in clearing the myelin debris are able to proliferatè without the presence of macrophages and their mitogenic factors (Fernandez-Valle et al., 1995). The proliferative activity of Schwann cells in regenerating nerves suggests that these Schwann cells may not be terminally differentiated. Loss of axonal contact in degenerating nerves leads to dedifferentiaton of Schwann cells and alters the phenotype of terminally differentiated Schwann cells to one similar to that of non-myelin forming or immature Schwann cells (Mirsky and Jessen, 1996). Expression of myelin proteins and of mRNA for proteins such as P_0, MBP and MAG is substantially reduced in these Schwann cells (Lemke and Chao, 1988; Trapp et al., 1988b; Willison et al., 1988).

Fluid conditioned by cells in regenerating nerves contains biologically active factors that promote Schwann cell adhesion, migration and proliferation (Le Beau et al., 1988). Thus cells in regenerating nerves differentiate into a state in which they produce factors conducive to a vital aspect of regeneration. Adhesion may be mediated by laminins and other ECM molecules produced by Schwann cells as well as by upregulated levels of N-cadherin, NCAM and L1 in Schwann cells that have

dedifferentiated to an immature/ non-myelin forming phenotype (Fu and Gordon, 1997). Expression levels of some growth factors such as NGF, CNTF and IGFs that are normally expressed in developing Schwann cells are also elevated following injury to the nerve (Fu and Gordon, 1997; Lemke and Chao, 1988). CNTF is a survival factor for motor neurons and its elevated expression during regeneration probably helps to support the survival of motor axons as they sprout towards their peripheral targets. IGFs act as autocrine survival factors for immature Schwann cells and elevated expression of this growth factor probably helps to support the survival of Schwann cells that have dedifferentiated upon loss of axonal contact after injury.

Nerve injury also results in induction of expression of the low affinity p75 neurotrophin receptor in Schwann cells in the bands of Büngner distal to the lesion and in Schwann cells proximally at the actual site of the lesion (Funakoshi et al., 1993; Taniuchi et al., 1986; Taniuchi et al., 1988). This receptor is normally only expressed by Schwann cell precursors, immature and non-myelin forming Schwann cells (Jessen et al., 1994; Jessen and Mirsky, 1991), but Schwann cells dedifferentiate in regenerating nerves and consequently re-express the receptor. Moreover once axons had regenerated into the area of p75 positive Schwann cells and had established contacts with the Schwann cells, expression of the receptor was down-regulated (Taniuchi et al., 1988). *In vitro* NGF promotes Schwann cell migration, a prerequisite for successful axonal regeneration (Anton et al., 1994b), but it is not known whether NGF-mediated Schwann cell migration is a major factor in regeneration *in vivo*. mRNA for the high affinity NGF receptor, TrkA, was not detectable in any part of both intact nerves and in lesioned nerves over a 3 week

time period (Funakoshi et al., 1993), suggesting that any NGF-mediated promotion of neurite outgrowth and Schwann cell migration is mediated by the p75 receptor. Schwann cell survival in the distal nerve stumps is substantially higher 24 hours after axotomy in mice lacking the p75 receptor than in wild type mice, consistent with NGF-mediated activation of p75 receptors in regulating Schwann cell apoptosis (Syroid et al., 2000). This difference in apoptotic Schwann cell death in p75 deficient mice is developmentally regulated and occurs only postnatally and in regenerating nerves and was not observed in E15 immature Schwann cells. Schwann cell numbers and proliferation may also be regulated during Wallerian degeneration by interactions of neuregulins with their ErbB2 receptors. The ErbB2 and ErbB3 receptors are expressed in mature Schwann cells and phosphorylation and activation of the ErbB2 receptor occurs in Schwann cells during Wallerian degeneration at a time corresponding to Schwann cell proliferative activity (Kwon et al., 1997). Moreover addition of exogenous neuregulins can inhibit Schwann cell apoptosis *in vivo* following axotomy (Grinspan et al., 1996; Syroid et al., 1996). Control of Schwann cell numbers in regenerating nerves is a necessary prerequisite to remyelination. Myelin forming Schwann cells need to re-establish contact with individual axons before induction of myelin genes and myelination can proceed.

1.7: Aims of the project

The *dy/dy* mouse exhibits myelination abnormalities and is severely deficient in laminin-2. This project aimed to use this mutant mouse to test the hypothesis that laminin-2 regulates several aspects of Schwann cell behaviour and interactions between Schwann cells and axons, including regulation of Schwann cell morphology and myelination. I have investigated the ultrastructure of intact mutant nerves and investigated the expression of laminin-2 in myogenic and neural tissues of the *dy/dy* mouse. I have used sciatic nerve transection and crush injuries to determine the role of laminin-2 in axon sprouting and remyelination *in vivo* during regeneration. I have used cryoculture to determine the extent to which laminin-2 acts as a substrate for Schwann cell migration. Explant cultures of mutant DRGs determined the role of laminin-2 in regulating the intrinsic motility of Schwann cells and cultures of dissociated Schwann cells were used to investigate the role of laminin-2 in several aspects of Schwann cell behaviour, particularly morphology. Finally Schwann cell-neuron co-cultures were used to investigate what role Schwann cell-mediated laminin-2 expression plays in neurite outgrowth. These techniques helped to clarify the role of laminin-2 in regulating Schwann cell behaviour.

Chapter 2: Materials and Methods

Table 2.1: Antibodies: Table showing primary antibodies used for immunohistochemical, immunocytochemical and immunoblotting analysis:

Antibody	Antigen	Host animal	Source
Clone 4H8-2	Laminin α2 chain 300 kDa fragment	Rat	Alexis
Clone 403	Laminin α2 chain G1-3 domain	Rabbit	Gift of L. Sorokin
Paulsson α2 chain	Laminin α2 chain 300 kDa fragment	Rabbit	Gift of M. Paulsson
EHS-laminin	Laminin-1 heterotrimer	Rabbit	Sigma
PGP 9.5	Protein gene product 9.5 (PGP 9.5)	Rabbit	Biogenesis
Clone 2H3	155 kDa Neurofilament protein	Mouse	Developmental Studies Hybridoma Bank
S100	S100 Schwann cell cytoplasmic protein	Rabbit	Dako
GAP-43	GAP-43	Rabbit	Gift of G. Wilkin

2.1: Animals

Heterozygous 129/ReJ *dy/dy* mice from Jackson Laboratories (USA) were bred using brother/sister matings. Each litter usually had a penetrance of 1 in 3 to 1 in 4 mutant mice Homozygous dystrophic mice were distinguishable from their heterozygous and homozygous unaffected littermates at 2-3 weeks of age. At this point they were distinguishably smaller in size and had begun to exhibit hind-limb paralysis, which manifested itself as dragging of the hindlimbs. In addition dystrophic mice often had convulsions of the head and arched backs. The eye area of dystrophic mice was usually scabby and the eyes often only half-open. *dy/dy* mice normally die of respiratory failure by 6 months of age, but I did not maintain them beyond 3 months of age at which point they are severely dystrophic. Homozygous and heterozygous unaffected mice were indistinguishable. Animals were killed at 0.5-2 months of age by asphyxiation in CO_2.

2.2: Immunohistochemistry of sections

2.2.1: Fresh frozen sections

The sciatic nerves, cardiac muscle and thigh skeletal muscles were removed from 4 severely ataxic P45-55 *dy/dy* mice and four of their unaffected littermates for immunohistochemistry. The tissues were immediately embedded in Optimum Cutting Temperature compound (OCT; BDH-Merck, UK) and snap frozen in liquid nitrogen. Cryosections 7-8 μm thick were cut on a Bright OTF/AS/D cryostat (UK) and 4-6 sections were collected onto each polysine pre-treated slide (BDH-Merck). Sections were allowed to dry onto the slides and then immunostained immediately. Fresh-frozen sections of skeletal and cardiac muscle and of sciatic nerve in the

longitudinal plane were first immunostained with a rat monoclonal antibody raised against laminin α2 chain isolated from mouse heart (clone 4H8-2; Alexis, UK) diluted 1:100 in antibody diluent. Section were alternatively stained with a rabbit polyclonal antibody to mouse α2 chain G1-3 domain (clone 403; gift of Dr L Sorokin, University of Erlangen-Nürnberg, Erlangen, Germany) diluted 1:200 in antibody diluent. Antibody diluent was made up of 10% MEM (Modified Eagle's Medium; Gibco Brl, UK), 1.35% 1M N-[2-Hydroxyethyl]piperazine-N'-[2-ethane-sulphonic acid] (HEPES; Sigma, UK), 10% fetal calf serum (FCS), 0.1% sodium azide (Sigma) and 1.35% of a 7.5% sodium bicarbonate solution (Gibco Brl). Incubation with the primary antibody was for 1-2 hours at room temperature (all antibody staining was carried out at room temperature). The antibody was then removed and the slides were rinsed in three 10 minute washes of phospate buffered saline (PBS; Sigma), followed by a rinse in double distilled water (DDW). Sections were then fixed for 15 minutes in 4% paraformaldehyde (TAAB, UK) and rinsed in PBS and DDW as above. The 4H8-2 rat monoclonal antibody was visualised with a tetramethyl rhodamine isothiocyanate (TRITC) -conjugated goat anti-rat IgG (Jackson Immunoresearch Laboratories Inc., USA) diluted 1:100. The clone 403 rabbit anti-α2 chain antibody was visualised with a Cy3-conjugated goat anti-rabbit IgG (1:100; Amersham, UK). Sections were incubated in both these conjugate for 45 minutes. The conjugates were removed and the slides washed in PBS and DDW as above.

For double immunostaining of laminin α2 chain with laminin-1, sections were then incubated with a rabbit polyclonal antibody to EHS-laminin (1:100; Sigma; UK) for 1-2 hours. The rabbit anti-EHS-laminin antibody was rinsed off with PBS and

DDW as above and the sections incubated in donkey anti-rabbit IgG (1:100; Amersham) for 45 minutes, washed in PBS and DDW and visualised by incubating the sections in Streptavidin fluorescein (1:100; Amersham) for 45 minutes. The slides were rinsed in PBS and DDW and post-fixed for 3 minutes in methanol (BDH-Merck) at –20 °C. The slides were rinsed in PBS and DDW and the coverslips mounted in glycerol (BDH-Merck) containing 2.5% 1,4-diazobicyclo-(2,2,2)-octane (DABCO; Sigma) to inhibit fading of fluorescence. Immunofluorescence was observed using a Zeiss Axioskop microscope equipped with epifluorescence optics (Germany) and digitised images taken under a x20 and a x40 objective using a Spot 2 cooled CCD camera (Diagnostic Instruments, Sterling Heights, MI, USA).

2.2.2: Fixed tissues (transected nerves)

Transected *dy/dy* and unaffected sciatic nerves (see chapter *2.4.1*) were removed two weeks after injury and immediately placed in 4% paraformaldehyde for 4 hours at room +4°C. The paraformaldehyde was removed and the nerves washed in three rinses of PBS. The nerves were then left in 1M sucrose (BDH-Merck) in PBS solution overnight or until the nerves had sunk to the bottom of the solution. After three rinses in PBS, the nerves were embedded in OCT and the distal to proximal orientation noted. The sciatic nerves were then snap frozen at -70°C in liquid nitrogen. 7-8 μm thick sections were cut in the longitudinal plane on a Bright cryostat and 4 sections were collected onto each polysine pre-treated slide in the same proximal to distal orientation.

Sections were incubated in one of two axonal markers; a rabbit polyclonal antibody to PGP 9.5 (1:400; Biogenesis, UK) or a mouse monoclonal antibody to the 155-

kDa neurofilament (clone 2H3; 1:2000; Developmental Studies Hybridoma Bank, USA). Sections were incubated in primary antibody for 1-2 hours at room temperature. The antibodies were removed and the slides washed in three, ten minute, washes of PBS and one, ten minute, wash of DDW. The PGP 9.5 antibody was visualised with a Cy3-conjugated goat anti-rabbit IgG (1:100) and the 2H3 antibody was visualised with a Cy3-conjugated goat anti-mouse IgG (1:100; Amersham). Sections were incubated in conjugates for 45 minutes and the slides were then rinsed in PBS and DDW as above. Sections were post-fixed for 3 minutes in methanol at –20 °C and rinsed in PBS and DDW. Coverslips were mounted in glycerol containing DABCO. Immunofluorescence was observed using a Zeiss Axioskop microscope and digitised images taken under a x40 objective using a Spot 2 cooled CCD camera.

2.2.3: Polyester wax embedded tissues

Sciatic nerves were removed from 11 severely ataxic P45-55 *dy/dy* mice and 13 of their unaffected littermates. The sciatic nerves were left in 4% paraformaldehyde overnight and then placed in PBS for 24 hours. The sciatic nerves were then dehydrated in graded concentrations of industrial methylated spirit (IMS; BDH-Merck) as below:

% IMS	**Time** (minutes)
50	45
70	45
90	45
100	30
100	30

The sciatic nerves were then infiltrated with graded concentrations of polyester wax (400 polyethylene glycol distearate; Aldrich, UK) at 40°C as described below:

Ratio: **100%IMS:wax**	**Time** (hours)
50:50	1
25:75	1
100% wax	1
100% wax	1

The nerves were then embedded in 100% polyester wax in preparation for sectioning on a microtome. 7-8 μm thick sections were cut on a microtome using Teflon-coated glass knives. Ribbons of sections were cut, a drop of 5% gelatin was placed on an uncoated glass slide (BDH-Merck) and 4 sections from the ribbon were then placed on the gelatin to mount them on the slides. The sections were allowed to dry onto the slides and then could be stored at +4°C until needed.

Sections had to undergo dewaxing before immunostaining could be carried out. Sections were left to equilibrate for 30 minutes at room temperature and then dewaxed in graded concentrations of IMS, DDW and PBS as described below:

Solution	**Time** (minutes)
100% IMS	5
100% IMS	3
90% IMS	3
70% IMS	3
50% IMS	3
DDW	3
PBS	3

Sections were incubated in a rabbit polyclonal antibody to the Schwann cell cytoplasmic protein, S100 (1:400; DAKO, UK) for 1-2 hours at room temperature. The antibody was washed off with three ten-minute rinses of PBS, followed by a rinse in DDW. The sections were then incubated in fluorescein isothiocyanate (FITC) -conjugated goat anti-rabbit IgG (1:100; Sigma) for 45 minutes to visualise S100 immunoreactivity. The slides were washed as above and the sections double immunostained with an axonal marker. Sections were incubated in clone 2H3 mouse monoclonal antibody to the 155-kDa neurofilament protein (1:2000) for 1-2 hours at room temperature. Slides were then washed in PBS and DDW as above and incubated with a Cy3-conjugated goat anti-mouse IgG for 45 minutes (1:100). The slides were then rinsed in PBS and DDW and the sections post-fixed in methanol at -20°C for 3 minutes. Sections were rinsed in PBS and DDW and coverslips mounted in DABCO in glycerol.

2.2.3.1: Analysis of Schwann cell morphology and numbers

Polyester wax embedded sections of sciatic nerves from 11 *dy/dy* mice and 13 unaffected littermates that had been double immunostained with S100 and 2H3 were viewed using a Zeiss Axioskop microscope equipped with epifluorescence optics under a x20 and a x40 objective. Digitised images were taken a using a Spot 2 cooled CCD camera. These images were analysed for Schwann cell morphology and numbers. S100 immunoreactive Schwann cells were classified as either round or ellipsoid (elongated) in morphology and the number of each was counted on each section. The number of round and ellipsoid Schwann cells were expressed as a percentage for each nerve analysed and the average percentage of each in *dy/dy* and unaffected sciatic nerves calculated. Digitised images were also used to calculate the total number of S100 immunoreactive Schwann cells per mm. All the Schwann cells in each digitised image were counted and the length of nerve in which they were contained was calculated using the Optimas image analysis programme (Optimas v.6, Media Cybernetics, Silver Spring, MD, USA). The Student's *t*-test (0.05% significance level) was used to compare the number of Schwann cells per unit of length of nerve. Statistical analysis was carried out using Microsoft Excel (v.6, USA) in all experiments.

2.3: Western Blotting

2.3.1: Preparation of SDS-PAGE gels

Samples were subjected to electrophoresis on a denaturing 5% SDS-PAGE gel with a 4% stacking gel (Laemmli, 1970). Briefly, a 30 ml solution of resolving gel was made up using 5 ml of a 30% acrylamide solution (Ultrapure Protogel; National

Diagnostics, Atlanta, GA., USA), 7.5 ml resolving gel buffer (1.5M Trizma Hydrochloride, pH8.8; Sigma), 300 µl of 10% sodium dodecyl sulphate (SDS; BDH-Merck), 150 µl of 10% (Sigma), 15 µl of N, N, N', N'-tetramethyl-ethylenediamine (TEMED; Biorad) and made up to 30ml with 17 ml DDW. A 15 ml solution of 4% stacking gel was made up with 2 ml of 30% acrylamide, 3.75 ml of stacking gel buffer (0.5M Trizma Hydrochloride; pH 6.8), 150 µl of 10% SDS, 7.5 µl of TEMED, 150 µl of ammonium persulphate and 9 ml of DDW.

2.3.2: Preparation of Samples

Skeletal muscle, dorsal roots and sciatic nerves were removed from 6 severely ataxic P30-P50 *dy/dy* mice and 5 unaffected littermates and frozen in liquid nitrogen. Tissues were homogenised in 50-300 µl of lysis buffer, depending on the quantity of the tissue. The lysis buffer contained 0.05M Trizma Hydrochloride (pH 6.8), 4M urea (BDH-Merck), 1% SDS, 0.1% each of PMSF phenylmethylsulphonyl fluoride (PMSF; Sigma), 3-[3-cholamidopropyl imethylammonio]-1-propane-sulphonate (CHAPS; Sigma), nonylphenoxy polyethoxy ethanol (NP-40; Sigma) and Triton X100 (Sigma).

The total amount of protein was determined using BCA Protein Assay Reagent (Pierce, Ill, USA) and each sample made up to a protein concentration of 2 mg/ml with lysis buffer. Laminin-2 (human placental merosin; Gibco Brl) standards were diluted to a concentration of 0.25 mg/ml in lysis buffer. Before use tissue homogenates and standards were mixed at a ratio of 2:1 tissue homogenate: x3 treatment buffer (0.75 M Trizma Hydrochloride, 30% glycerol, 15% mercapthanol [Biorad], 15% SDS and bromophenol blue [Sigma]) and denatured at 100°C for 3 minutes. 20 µl of each sample and the standard were loaded onto each gel 5% gel

along with a molecular weight marker (Rainbow marker; Amersham). Samples were run through the stacking gel at 60V and through to the end of the resolving gel at 100V. Once the dye front had reached the bottom of the gel, proteins were transferred for immunoblotting.

2.3.3: Immunoblotting

Gels were blotted onto millipore polyvinylidene difluoride (PVDF; Sigma) membranes at 300 mAmps for 2 hours. Membranes were then blocked for 1 hour in blocking buffer made up from 5% powdered milk (Marvel; UK) in TBS (triethanolamine buffered saline; 0.15M sodium chloride [BDH-Merck] and 0.05M Trizma Hydrochloride). Membranes were incubated overnight at room temperature in either a rabbit polyclonal antibody against the 300 kDa fragment of laminin α2 isolated from mouse heart (1:100; gift of Dr M Paulsson, University of Cologne, Cologne, Germany) (Paulsson and Saladin, 1989) or a rabbit polyclonal antibody against EHS-laminin (1:100; Sigma); both antibodies were diluted in blocking buffer. The primary antibody was removed and membranes were washed three times in 10 minute washes of TBS. Membranes were incubated for 2 hours in peroxidase-conjugated goat anti-rabbit IgG (1:500 in blocking buffer; Sigma). Membranes were washed in TBS as above and the immunostaining visualised with 0.6% 4-chloro-1-napthol (Sigma). Immunoblots were photographed and black and white photographs were taken and scanned and imported as Adobe Photoshop 5.5 files.

2.4: Sciatic nerve lesions

2.4.1: Sciatic nerve transection

Three severely ataxic *dy/dy* mice aged 6 weeks and three unaffected littermates were anaesthetised with a mixture of Hypnorm (fentanyl citrate and fluanisone) and Hypnovel (midazolam). Under a dissecting microscope the left sciatic nerve was exposed and transected at midthigh using a pair of fine scissors. The wounds were closed and the animals allowed to recover for a period of 2 weeks. At this time the mice were killed by asphyxiation in CO_2 and a 1cm length of transected nerve removed and fixed in 4% paraformaldehyde. Cryosections of transected nerve were immunostained with axonal markers (see chapter *2.2.2*) to determine the extent of axonal sprouting.

2.4.2: Sciatic nerve crush injury

Eleven severely ataxic *dy/dy* mice and 4 unaffected littermates were anaesthetised as in *2.4.1*.Under a dissecting microscope, the left sciatic nerve was exposed and crushed at midthigh with a pair of fine forceps. The wounds were closed and the mice allowed to recover for periods of 2, 4 and 6 weeks. At these post-operative times mice were killed by asphyxiation in CO_2 and a 1cm length of crushed sciatic nerve was removed from each mouse. Contralateral nerves were also removed from some *dy/dy* mice for investigation of the ultrastructure of intact *dy/dy* sciatic nerve. Lesioned and intact sciatic nerves were processed for semi-thin sectioning and electron microscopy.

2.4.3: Preparation of tissues for semi-thin sectioning and electron microscopy

One centimetre lengths of intact and crushed nerves were removed from *dy/dy* and unaffected mice and stretched lightly across a small piece of card and immersion-

fixed in 2.5% gluteraldehyde in PBS for 4 hours at +4°C. Specimens were washed in PBS and post-fixed in 1% OsO_4 for 90 minutes at +4°C and then dehydrated through graded ethanol and embedded in TAAB resin. Each nerve was cut into 2mm blocks in a proximodistal sequence before embedding for sectioning. Intact nerves were prepared for longitudinal sectioning, lesioned nerves were embedded for transverse sectioning such that the site of the crush was consistently within block 2.

2.4.4: Semi-thin sectioning and quantitative assessment of remyelination

One micrometre thick semi-thin sections were cut from each block and stained with 1% toluidine blue to screen appropriate sections for qualitative electron microscopic analysis and for quantitative light microscopy. The total number of myelinated axons in transverse sections of each proximal and distal nerve stump in unaffected and *dy/dy* mice was counted approximately 0.4cm from the crush site. Myelinated axons were counted using a x100 objective on a Zeiss Axioskop microscope and the average numbers of myelinated axons in these sites at each time point compared. Student's *t*-tests (5% significance level) were used to compare remyelination at the 2 week time point only.

2.4.5: Electron microscopy

Ultra-thin sections of intact nerves were cut in the longitudinal plane and of each distal stump in lesioned nerves, approximately 0.2-0.4 cm distal to the crush site, in the transverse plane. The ultra-thin sections were collected onto copper grids and contrasted with uranyl acetate and lead citrate. Ultra-thin sections were viewed with a Hitachi H-7000 transmission electron microscope.

2.5: Schwann cell migration assays

2.5.1: Cryoculture

The cryoculture technique has been used previously to assay neurite outgrowth and Schwann cell migration *in vitro* (Anton et al., 1995; Anton et al., 1994a; Anton et al., 1994b; Shewan et al., 1995). Cryosections of peripheral nerve were used as substrates for Schwann cell migration in *in vitro* studies. This technique provides a physiologically relevant substrate for studying the factors involved in Schwann cell migration but without the added complexity of interactions with other cell types and with trophic factors. Thus ECM molecules and cell surface molecules are included in the substrate while diffusable factors are excluded.

2.5.2: Homologous cryoculture assay

Intact sciatic nerves were removed from adult Wistar rats that had been killed by asphyxiation in CO_2 and immediately mounted onto slices of rat liver and fresh-frozen in liquid nitrogen. Cryostat sections of rat sciatic nerve, 7-8 μm thick, were cut in the longitudinal plane and collected onto each sterile poly-L-lysine-coated (PLL; 2 mg/ml; Sigma) 13mm diameter round glass coverslip (BDH-Merck). Briefly, coverslips were prepared by placing coverslips in a 10 cm diameter petri dish (Nunc; UK) and washing with sterile DDW, coverslips were then incubated in 20 ml of sterile PLL solution for 2 hours at room temperature. The PLL was drained off and the coverslips allowed to dry under sterile conditions in a tissue culture hood. Coverslips containing 3-4 cryostat sections were stored at -70°C in preparation for cryoculture.

Intact DRG explants were prepared from P3 Wistar rats. The DRGs were removed and placed in warmed Ham's F-12 medium (Gibco) and trimmed free of attached

roots under a dissecting microscope. Trimmed DRGs were incubated with 2 ml of 0.025% trypsin (Sigma) in calcium- and magnesium-free Hanks buffered salt solution (CMF; Gibco Brl) containing 50 µl of 1.25% collagenase (Sigma) for 20 minutes. They were next washed in Ham's F-12 medium and then incubated in trypsin inhibitor DNAase (TID) for 20 minutes. Briefly, TID was prepared with 50 µg/ml of DNAse (Type I; Sigma), 250 µg/ml of soybean trypsin inhibitor (Type II; Sigma), 3 mg/ml bovine serum albumin (BSA; Sigma) and 0.038% magnesium sulphate (BDH-Merck). The DRGs were washed again in Ham's F-12 medium and then explanted onto cryosections. Coverslips containing rat sciatic nerve cryosections were placed at the base of a well in a 4-well culture plate (Nunc) and a DRG placed carefully on each section under a dissecting microscope, taking care not to disrupt the nerve section. DRG explants were allowed to stick to the nerve sections by incubating in a small amount (less than 50 µl) of Dulbecco's modified Eagle's medium (DMEM; Gibco Brl) containing 10% FCS and 100 ng/ml of NGF (Promega, UK). Once the explant had stuck to the cryosection the culture medium was topped up to 500 µl. Cultures were maintained for either 24 (n = 74), 40 (n =120) or 65 (n = 99) hours in a humidified CO_2 incubator (Jouan; UK) at 37°C in 7.5% CO_2 before labelling (*2.5.4)*.

2.5.3: Heterologous cryoculture: Rat DRG explants on mouse sciatic nerve cryosections

Intact sciatic nerves were removed from severely ataxic P45-P55 *dy/dy* mice and their unaffected littermates and mounted onto slices of rat liver and frozen in liquid nitrogen. Seven to 8 µm thick cryosections of nerve were cut and collected as in *2.5.2*. P3 rat DRG explants were prepared and plated onto *dy/dy* (n = 71; proximal,

n = 20; distal, n = 51) and unaffected (n = 51; proximal, n = 37, distal, n = 49) mouse sciatic nerve cryosections as above (chapter *2.5.2*). DRG explants were incubated for 40 hours before labelling (chapter *2.5.5*) in an incubator at 37°C in a humidified atmosphere with 7.5% CO_2 in 500 µl DMEM containing 10% FCS and 100 ng/ml of NGF.

To assess the effect of laminin-2 on Schwann cell migration on *dy/dy* sciatic nerve substrates, heterologous cryocultures were carried out on laminin-2 pre-treated nerve sections. *dy/dy* (n = 6) and unaffected (n = 7) sciatic nerve cryosections were prepared as above, but in each experiment half of the coverslips containing sections of unaffected (n = 5) or *dy/dy* (n = 14) sciatic nerve were preincubated with 10 µg/ml of human placental merosin (laminin-2) in culture medium for 2 hours prior to plating of the explant. Rat E19 DRG explants were used in these experiments; these were prepared using the same method as in *2.5.2* but incubation time in 0.025% trypsin and in TID was shortened to 15 minutes each. E19 DRGs were plated onto laminin-2 preincubated and untreated *dy/dy* and unaffected sciatic nerve cryosections as above and cultures were incubated in DMEM containing 10% FCS and 100 ng/ml of NGF in an incubator at 37°C in a humidified atmosphere with 7.5% CO_2 in 500 µl for 40 hours before labelling.

2.5.4: Migration of dy/dy Schwann cells

Intact DRG were prepared from ataxic P16-P20 *dy/dy* (n = 7) mice and their unaffected (n = 8) littermates and prepared as in *2.5.2* except that incubation time in 0.025% trypsin and in CMF containing 50µl of 1.25% collagenase and in TID was increased to 30 minutes each. 13 mm diameter round coverslips that had been precoated in PLL and then incubated in 10 µg/ml of laminin-1 (EHS-laminin;

Sigma) were placed in a 4-well plate and one DRG explant was positioned in the centre of each laminin-1 preincubated coverslip. Cultures were then incubated for 40 hours in DMEM culture medium with 10% FCS containing 100 ng/ml of NGF in an incubator at 37°C in a humidified atmosphere with 7.5% CO_2.

2.5.5: Analysis and Quantification of Schwann cell migration

In order to analyse Schwann cell migration from DRG explants the cell tracker dye, 5-chloromethylfluorescein diacetate (CMFDA; Molecular Probes, Eugene, OR, USA) was used. CMFDA is membrane permeable and is taken up by living cells where cytoplasmic esterases cleave the acetate groups to produce a fluorescent product. The CMFDA was added to cultures at 4 μM and incubation continued for 45 minutes. Explants were then washed three times in Ham's F-12 medium and fixed in 4% paraformaldehyde.

Both DRG neurons extending neurites and migrating Schwann cells take up CMFDA in explant cultures and cryocultures but it labels Schwann cells with much greater intensity than neurites. Schwann cells are also distinguishable from CMFDA-labelled neurites by morphology. To further distinguish between the two, some explant cultures and cryocultures were double-labelled with an antibody to GAP-43 a marker for growing neurites after paraformaldehyde fixation. Cells in the cultures were first permeabilised by incubation with methanol at -20°C for 3 minutes, rinsed in PBS and incubated with a rabbit polyclonal antibody to GAP-43 (1:1000; gift of Dr G Wilkin, Imperial College, London, UK) at room temperature for 1-2 hours. The primary antibody was rinsed off in three washes of PBS and the coverslips incubated in Cy3-conjugated goat anti-rabbit IgG (1:100) for 45 minutes and then rinsed in three washes of PBS. CMFDA-labelled and CMFDA/GAP-43

double-labelled explants were mounted in DABCO in glycerol.

CMFDA-labelled cells were analysed using a Zeiss Axioskop microscope equipped with epifluorescence optics using x10, x20 and x40 objectives. Digitised images were captured with a Spot 2 cooled CCD camera. The distance migrated by Schwann cells was determined as the distance from the centre of the DRG explant to the leading edge of migrating Schwann cells. Measurements were taken using Optimas v.6. Statistical analysis was carried out using Microsoft Excel; the correlation coefficient was calculated for the distances migrated at the three time points in the homologous cryoculture system. Student's *t*-tests were used to compare migration from P3 rat DRG explants on *dy/dy* and unaffected mouse sciatic nerve substrates (1% significance level), from E19 rat DRG explants on laminin-2 treated and untreated mutant and unaffected substrates (5% significance level) and to compare migration of P16-20 *dy/dy* and unaffected Schwann cells (0.1% significance level).

2.6: Sciatic nerve cultures containing dissociated Schwann cells

2.6.1: Sciatic nerve dissociation

Sciatic nerve cell cultures consisting largely of Schwann cells were prepared from the sciatic nerves of ataxic P16-20 *dy/dy* mice and their unaffected littermates using a method adapted from the chapter on Schwann cell culture (p223) by Louise Morgan in "Neural Cell Culture" (edited by J. Cohen and G. P. Wilkin, 1995, OUP). Sciatic nerves were dissected out from near the vertebral column to their point of bifurcation in the hind-limbs and then cut approximately in half such that each unit length of sciatic nerve was 1 cm. Dissected sciatic nerves were placed in

cold MEM buffered with 25 mM HEPES. The nerves were then cleaned of any attached muscle or fat and desheathed, using a pair of forceps to pull away the epineurial sheath. The nerves were then chopped into 1 mm pieces and incubated at 37°C for 45 minutes in an enzyme solution containing 1.25 mg/ml trypsin and 2 mg/ml collagenase in CMF (250 µl per cm of nerve). The nerves were subsequently triturated in TID (125 µl per cm of nerve) 15-20 times (through a P-1000 Gilson pipette tip) to prepare a single cell suspension.

The cell suspension was centrifuged for 5 minutes at 500 rpm (revolutions per minute). The supernatant was removed and the cell pellet resuspended in DMEM with 10% FCS (about 100 µl of culture medium per cm of nerve) containing 5 µg/ml of insulin (Sigma) and 1 mM of glutamine (Gibco Brl). 100 µl of cell suspension was plated onto each PLL-precoated 13mm round coverslip that had been incubated at 37°C for at least 2 hours in 10 µg/ml of either laminin-1, laminin-2 or fibronectin (Sigma) in a 4-well culture plate. When cells had adhered to the coverslip at around 1-2 hours after plating, the medium in each well was topped up to 500 µl. Cultures were maintained for a period of 2 hours to 40 hours in a humidified CO_2 incubator at 37 °C containing 7.5% CO_2 before fixation and immunostaining. At least 4 animals were used for each time point and each substratum (see figs. 6.2, 6.4, 6.7).

2.6.2: Immunocytochemistry, analysis and quantification of dissociated Schwann cells

Dissociated Schwann cells were examined *in vitro* at 3 time points before fixation. Live cultures were observed at 3, 16 and 40 hours after plating using a Nikon DIAPHOT-TMD inverted microscope (Japan) with a x20 and a x40 objective.

Digitised images were captured at these time points using a CCD camera (Model FA87; Grundig, Germany).

Cultures of sciatic nerve containing Schwann cells were fixed and immunostained at 3 and 40 hour timepoints using the rabbit polyclonal antibody against the S100 (1:400) Schwann cell cytoplasmic protein. Cultures were fixed at room temperature in 4% paraformaldehyde for 15 minutes and then rinsed 3 times in PBS followed by permeabilisation for 3 minutes in methanol at -20°C and further washes in PBS. Coverslips were then incubated for 1-2 hours in the primary antibody at room temperature. After rinsing in PBS cultures were incubated in Cy3-conjugated goat anti-rabbit IgG (1:100) for 30-45 minutes and rinsed. For double immunostaining of Schwann cells for S100 and the laminin α2 chain, cultures were first incubated, unfixed, for 1 hour at room temperature in rat monoclonal antibody against laminin α2 (1:100; clone 4H8-2), then washed in prewarmed MEM medium before fixation for 15 minutes in 4% paraformaldehyde followed by rinsing in PBS and permeabilisation in methanol at -20°C for 3 minutes. S100 staining was then carried out as above, the S100 staining was then visualised with Cy3-conjugated goat anti-rabbit IgG as above and the α2 chain staining by incubation with biotinylated anti-rat IgG (1:100; Sigma) for 30-45 minutes followed by incubation in Streptavidin flourescein (1:100) for 30-45 minutes. Cultures were mounted in DABCO in glycerol.

Fluorescence immunostained Schwann cells were viewed under a x20 and x40 objective on a Zeiss Axioskop microscope equipped with epifluorescence and digitised images taken using a Spot 2 cooled CCD camera. The numbers of S100 immunopositive Schwann cells on laminin-1, laminin-2 and fibronectin substrates

in cultures fixed at 3 hours and 40 hours after plating was counted manually and the numbers of *dy/dy* and unaffected Schwann cells compared using Student's *t*-tests (5% significance level at 3 hours and 0.5% significance level at 40 hours). Numbers of bipolar (2 or less processes) or multipolar (more than 2 processes) were also counted manually in cultures of *dy/dy* and unaffected Schwann cells on laminin-1 and laminin-2 substrates at 40 hours. The percentage of multipolar cells was calculated in each culture and Student's *t*-tests were used to compare the numbers of *dy/dy* and unaffected multipolar Schwann cells (0.1% significance level) and the numbers of multipolar *dy/dy* Schwann cells on laminin-1 and laminin-2 substrates (5% significance level).

2.7: Schwann cell-neuron co-cultures

2.7.1: Preparation of dissociated Schwann cells as a culture substratum

Dissociated suspensions of sciatic nerve cells were prepared as described above from P16-20 *dy/dy* mice and their unaffected littermates (chapter *2.6.1*), but pellets of unaffected and or *dy/dy* sciatic nerve cells were resuspended to a final concentration of 30,000 in modified Bottenstein and Sato's culture medium (BSF-2; 100 µg/ml transferrin [Sigma], 3 mg/ml BSA, 2% FCS, 6 µg/ml progesterone [Sigma], 16 µg/ml each of putrescine [Sigma] and sodium selenite [Sigma] and 100 µg/ml insulin all in 94% Ham's F-12 medium) supplemented with 1mM glutamine. These cell suspensions were plated onto laminin-1/PLL pre-coated 13 mm round glass coverslips, prepared as described above, in a 4-well culture plate. Cultures were maintained in a humidified incubator containing 5% CO_2, at 37°C for 48 hours until confluent, before the addition of dissociated DRG neurons.

2.7.2: Dissociated DRG neurons

DRG neurons were prepared from the DRGs of 4-6 week old *dy/dy* mice and their unaffected littermates (Gavazzi et al., 1999). DRGs were removed and attached roots trimmed in Ham's F-12 medium. DRGs underwent enzymic dissociation in 0.0125% collagenase in BSF-2 for 1.5 hours in a humidified CO_2 incubator at 37°C containing 5% CO_2. The DRGs were removed from solution by means of a broken glass pasteur pipette and washed by being placed in a 20 ml Universal tube (Sterilin, UK) with 10 ml of Ham's F-12 such that the DRGs sunk to the bottom of the tube. Most of this solution was then removed carefully, leaving a moist plaque of DRGs at the bottom of the tube. Using a cut Gilson P-1000 pipette tip the DRGs were mechanically triturated 10-15 times in 500 µl of BSF-2. The top layer of the suspension was removed and floated gently over 2 ml of 15% BSA in a 10 ml conical centrifuge tube (Sterilin). A further 500 µl of BSF-2 was added to the remainder of the DRG plaque in the Universal tube and DRGs were again mechanically triturated 10-15 times through a P-1000 Gilson pipette tip. The remainder of the suspension was added to the cell suspension floating over the BSA in the centrifuge tube. The cell suspension was spun at 600 rpm for 7 minutes. The supernatant was removed carefully and the pelleted neurons resuspended in 100 µl of TID. The suspensions of *dy/dy* or unaffected DRG neurons were then diluted to a final concentration of 2-2,500 cells/ ml in BSF-2 containing 100 ng/ml NGF and 1mM glutamine before plating on pre-established confluent cultures of *dy/dy* or unaffected Schwann cells. In each experiment half of the Schwann cell cultures were pre-incubated for 2 hours in culture medium supplemented with 10 µg/ml of laminin-2 before the addition of neurons. Co-cultures were maintained for a further

18-20 hours in a humidified CO_2 incubator at 37°C containing 5% CO_2 before fixation and immunostaining. At least 26 DRG neurons were assessed under each condition (see fig. 7.2).

2.7.2: Immunocytochemistry and quantification of Schwann cell-neuron co-cultures

Schwann cell-neuron co-cultures were labelled with an antibody to GAP-43, and antigen expressed in growing neurites. Co-cultures were firstly fixed at room temperature in 4% paraformaldehyde for 15 minutes, followed by rinses in PBS and permeabilisation with methanol at -20°C for 3 minutes and further rinses in PBS. Co-cultures were then incubated in a rabbit polyclonal antibody to GAP-43 (1:1000) for 1-2 hours, followed by rinsing in PBS. The primary antibody was then visualised by incubating the cultures in Cy3-conjugated goat anti-rabbit IgG (1:100) for 30-45 minutes followed by further rinses in PBS. Coverslips were then mounted in DABCO in glycerol.

Fluorescence immunostained co-cultures were viewed on a Zeiss Axioskop microscope equipped with epifluorescence and digitised images taken using a Spot 2 cooled CCD camera under a x20 objective. Digitised images were taken only of DRG neurons in co-cultures that were observed to be growing in direct contact with recognisable Schwann cells. The number of processes projecting from the cell bodies of the DRG neurons and the number of process endings were counted from digitised images. The branching frequency and thus branching complexity was computed as the ratio of processes stemming from their cell bodies to the number of process endings (Butt et al., 1994). Student's *t*-tests were used to compare branching complexity of DRG neurons on laminin-2-treated and untreated *dy/dy* and unaffected Schwann cells at the 1% and 5% significance levels.

Chapter 3: The *dy/dy* mouse: Morphological abnormalities in sciatic nerves and expression of laminin α2 protein in myogenic and non-myogenic tissues

3.1: Introduction

The *dy/dy* mutation is a spontaneous mutation, resulting in an inherited myopathy in mice. In the earliest description by Michelson and colleagues in 1955, clear signs of atrophy and degeneration of skeletal muscle fibres were identified but no neural abnormalities were reported. Using electron microscopy, Bradley and Jenkison (1973) first identified extensive abnormalities in the PNS. *dy/dy* peripheral nerves contained large areas of bare, "amyelinated" axons, directly apposed and unensheathed by Schwann cells or myelin and displayed abnormally elongated nodes of Ranvier. Dorsal and ventral roots, cranial nerves and portions of sciatic nerve proximal to the spinal cord were all affected (Biscoe et al., 1974; Bradley et al., 1977; Bradley and Jenkison, 1973).

The primary defect in these mice was first characterised as a "genetic deficiency of the basal lamina" in skeletal muscle and peripheral nerves by Madrid and colleagues (1975). Myelinated fibres appeared to have a patchy basal lamina and amyelinated fibres were completely devoid of basal lamina. These neural abnormalities were shown to result in slowed conduction velocities, abnormal, spontaneous propagation of impulses mid-axon and "cross-talk" of impulses between apposing naked axons (Carbonetto, 1977; Rasminsky, 1978). In the first part of this chapter I have described further detailed electron microscopy that we have carried out to determine the ultrastructure of *dy/dy* peripheral nerves and a novel immunohistochemical analysis, revealing more details of the abnormal axon-

Schwann cell relationships.

Detailed molecular characterisation of the defect in *dy/dy* mouse basal lamina was first described by Arahata and colleagues (1993), who showed a severe reduction in both the laminin α2 chain protein and in mRNA transcripts of the *lama2* gene in skeletal muscle, peripheral nerves and cardiac muscle (Arahata, 1993; Sunada et al., 1994; Xu et al., 1994a). These previous investigations into laminin α2 chain protein expression in *dy/dy* mice, used a variety of polyclonal antibodies raised against different fragments of the laminin α2 chain. These included antibodies raised against recombinant peptides, affinity purified antibodies against both the 300 kDa N-terminus domain and the C-terminus G-domain of the laminin α2 chain and against G-domain synthetic peptides (Ehrig et al., 1990; Paulsson et al., 1991; Sunada et al., 1994; Xu et al., 1994a; Xu et al., 1994b). However none of these studies used antibodies against native mouse laminin α2 chain. So to further analyse the cause of the histological abnormalities seen in *dy/dy* peripheral nerves in relation to patterns of laminin α2 chain expression in muscle and neural tissue, I used antibodies to the native protein to re-assess the expression of the laminin α2 chain in *dy/dy* mice. I have employed two different antibodies, one a rabbit polyclonal antibody for immunohistochemistry and the other a rat monoclonal antibody for immunoblotting, both raised against mouse whole heart merosin rather than synthetic peptides (Paulsson and Saladin, 1989; Schuler and Sorokin, 1995). Our use of novel antibodies raised against native α2 antigens, revealed strikingly different expression patterns of the laminin α2 chain in *dy/dy* skeletal muscle to those published previously (Sewry et al., 1998).

3.2: Results

3.2.1: The interaction of Schwann cells with axons is disturbed in *dy/dy* sciatic nerves

3.2.1.1: Ultrastructure

Electron micrographs of *dy/dy* sciatic nerves sectioned in the longitudinal plane (fig. 3.1) showed the abnormalities characteristic of the mutant PNS initially observed by Bradley and Jenkison (1973). Patches of amyelinated sciatic nerve were observed where myelinated fibres had lost their myelin sheath (fig. 3.1a). Many axons with patchy myelin sheaths were not fully ensheathed by Schwann cells and some unmyelinated axons completely lacked any contact or ensheathment by Schwann cells. Naked axons were thus often directly apposed with no separation by Schwann cell cytoplasm. These bundles of naked axons are also found apposed to axons that are partially myelinated (fig. 3.1b). The nodes of Ranvier, normally short gaps of less than 1μm (Rios et al., 2000) in Schwann cell ensheathment and myelination, that allow for saltatory conduction of action potentials were often abnormally long in *dy/dy* sciatic nerves (fig. 3.1c) (Bradley et al., 1977). The endoneurial basal lamina is frequently patchy and fails to completely surround Schwann cells ensheathing the axons (fig. 3.1c).

Figure 3.1: Intact *dy/dy* sciatic nerves show abnormalities of Schwann cell ensheathment and myelination. Electron micrographs of longitudinal sections of intact *dy/dy* sciatic nerves. **(a)** The axon (A) is incompletely ensheathed by a Schwann cell (SC) and partially myelinated (thin arrow), but the myelin sheath (MS) does not ensheath the whole axon. The lack of membrane loops where the myelin sheath terminates distinguishes this portion of the axon as being amyelinated rather than containing a node of Ranvier. **(b)** In this portion of nerve there is a partially myelinated axon (thin arrows), apposed by a group of naked axons (thick arrow) which are not ensheathed by Schwann cells. **(c)** The axon is myelinated but has an elongated node of Ranvier clearly seen by the paranodal membrane loops (PL) formed by the expansion of the myelin sheath (thin arrows). The endoneurial basal lamina in this region is patchy (arrowhead). Some axons are not properly ensheathed by Schwann cells and are directly apposed (thick arrow). Magnification: (a, b) x7500, (c) x22500. Scale bar: (a, b) = 2.4 μm, (c) = 7.2 μm.

Sciatic nerves processed and prepared for electron microscopy by the Electron Microscopy unit at Guy's hospital and photographed by Professor Susan Standring.

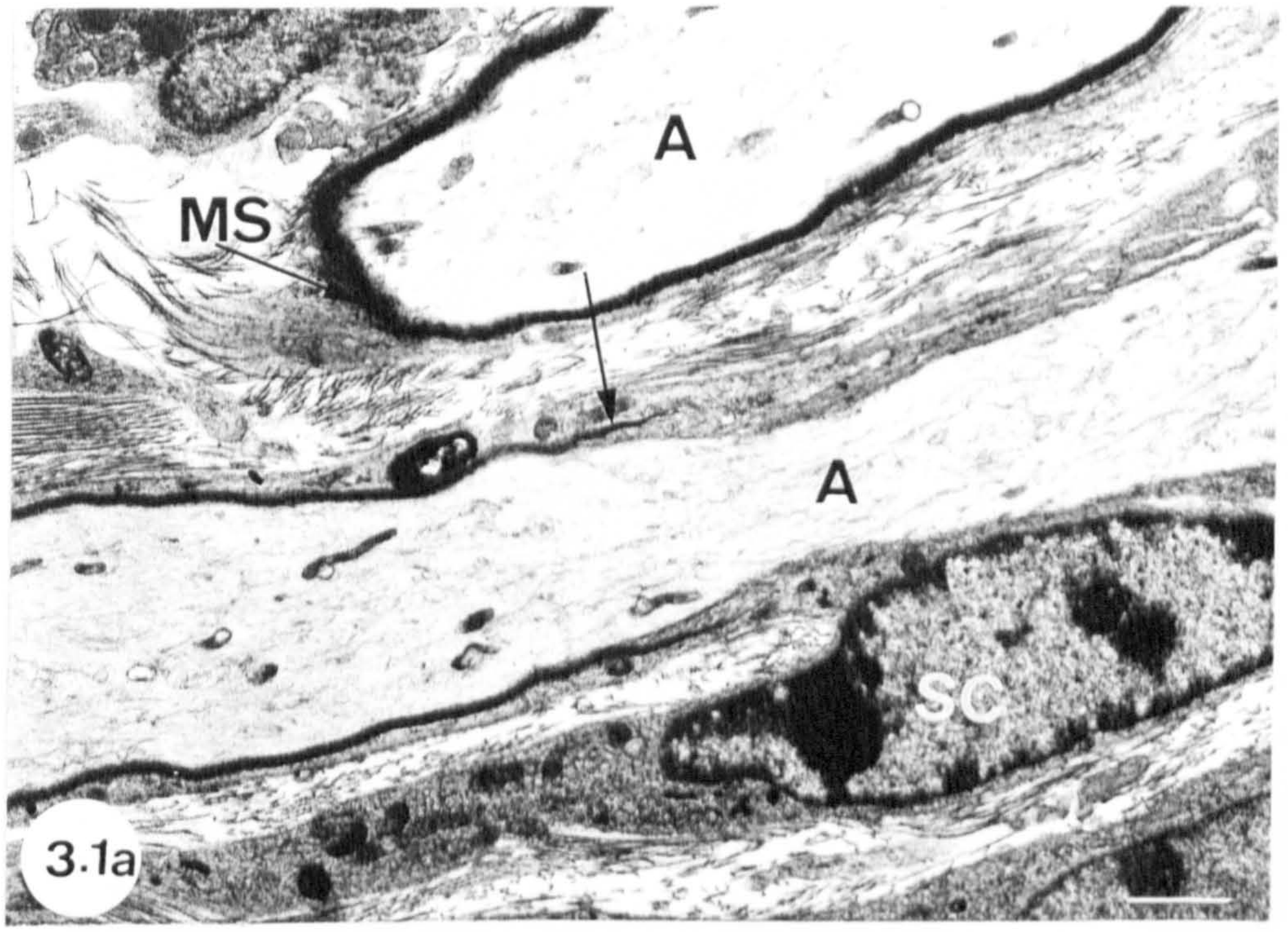
A
MS
A
SC
3.1a

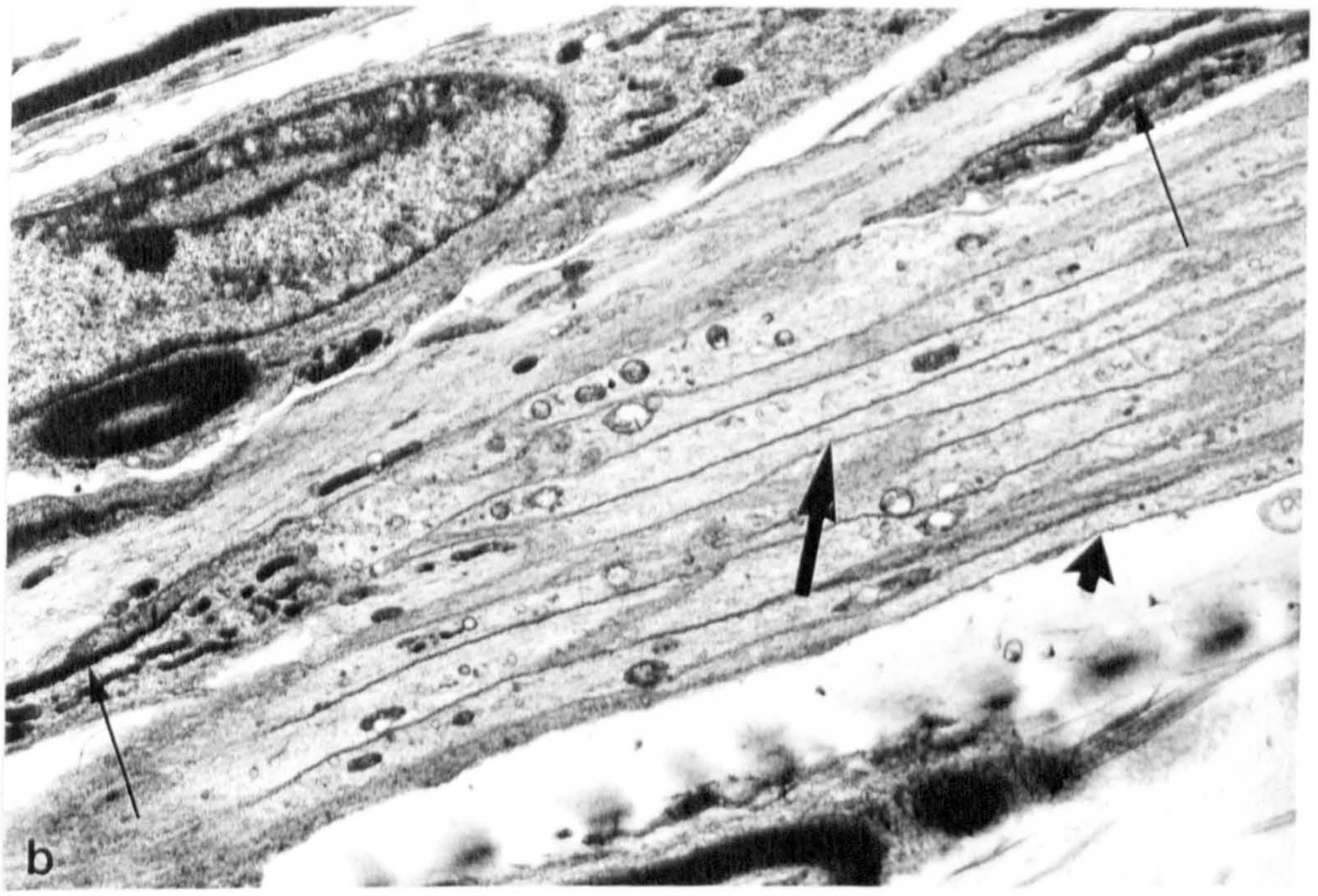
b


PL
C

3.2.1.2: Immunohistochemistry

Immunohistochemical analysis of *dy/dy* mice also showed abnormalities in both axonal and Schwann cell morphology in the PNS. Sciatic nerves from severely ataxic P45-P55 *dy/dy* mice were immunostained with an antibody against S100, a Schwann cell cytoplasmic protein. Quantification showed that a significantly greater ($p<0.0005$) number of Schwann cells per unit length of nerve were to be found in *dy/dy* compared to unaffected nerves (table 3.1; fig. 3.2 c, d). Thus in longitudinal sections of unaffected sciatic nerve, there were 20.28 ± 1.44 (mean ± s.e.m., n = 13) S100-positive Schwann cells per mm of nerve compared with 30.57 ± 1.99 (n = 11) Schwann cells per mm of *dy/dy* nerve.

In addition, Schwann cells in *dy/dy* sciatic nerves often displayed a different morphology to those in unaffected nerves and an apparently looser association with axons. Double-staining with antibodies to both S100 and 2H3, an antibody against high molecular weight neurofilament, showed that in unaffected nerves Schwann cells were generally ellipsoid in shape and appeared to be closely aligned with axons as indicated by the neurofilament staining (fig. 3.2a, c, e). In contrast, the Schwann cells in *dy/dy* sciatic nerves appeared rounder and exhibited a looser association with 2H3-labelled axons (fig. 3.2b, d, f). A semi-quantitative analysis showed that 46.3% of *dy/dy* Schwann cells were ellipsoid whereas 81.4% of unaffected Schwann cells were ellipsoid. Moreover neurofilament staining appeared to be less extensive in mutant nerves (fig. 3.2a, b); this difference was more apparent in the sciatic nerves of older *dy/dy* mice (data not shown).

Figure 3.2: *dy/dy* sciatic nerve shows morphological differences to unaffected nerves. Polyester wax embedded unaffected (ua) (a, c, e) and *dy/dy* (b, d, f) sciatic nerves were cut into 8 μm thick sections and double-labelled with antibodies to the Schwann cell cytoplasmic protein, S100 (green) and with 2H3 against the 165 KDa neurofilament protein (red) and observed at a magnification of x40 (a-d) and x100 (e and f). **(a)** In unaffected nerves immunostaining with the 2H3 antibody showed that the nerve contained many long, straight neurofilaments (arrowhead) and the axons neatly aligned. **(b)** Neurofilament staining in *dy/dy* sciatic nerves is patchy (arrowhead) and less extensive and the axons do not appear to be neatly aligned with each other. **(c)** Schwann cells in unaffected sciatic nerves are usually ellipsoid in shape (arrow). **(d)** In *dy/dy* nerves there are far more Schwann cells and in addition a substantial proportion of them are rounded rather than ellipsoid (arrow). **(e, f)** Double-staining shows that the largely ellipsoid Schwann cells in unaffected nerves all seem to be closely aligned with axons (arrow) and in *dy/dy* nerves many of the rounded Schwann cells are not aligned with axons (arrow). Scale bar = 100 μm (a-d), 40 μm (e, f).

ua

dy/dy

3.2a

b

2H3

c

d

S100

e

f

merge
high
power

Table 3.1: Quantification of Schwann cell numbers per unit length in unaffected and *dy/dy* sciatic nerves. Sections of sciatic nerve were immunostained with an antibody to the cytoplasmic protein S100. The number of S100 immunoreactive cells were counted in digitised fluorescent images of unaffected (n = 13) and *dy/dy* (n = 11) sciatic nerves and the length of nerve in which these cells were contained was calculated to determine the number of Schwann cells per mm of nerve. The difference in the number of S100 immunoreactive cells was highly significant ($p<0.0005$).

	Unaffected sciatic nerves	*dy/dy* sciatic nerves
Average number of Schwann cells/mm	20.28	30.57
Number of nerves analysed (n)	13	11
Standard deviation (±)	6.62	5.20
Standard error of the mean (±)	1.44	1.99

3.2.2 Immunoblotting of *dy/dy* mouse tissues shows a differential expression pattern of the laminin α2 chain in peripheral nerve, cardiac muscle and skeletal muscle

Immunoblotting of tissue extracts with the antibody to EHS-laminin/laminin-1 revealed intense staining at approximately 400 kDa equivalent to that of the α1 chain, staining at a 220 kDa band indicated the presence of the β1 chain. The human placental merosin standard used is not a pure source of laminin-2 and contains detectable levels of the laminin α1 chain. There was comparable staining intensity for the α1 chain, and for the β1 chain in skeletal muscle and in neural tissues of *dy/dy* and unaffected mice (figs 3.3b, 3.4b, 3.5b). Thus the β1 chain that is also normally constituents of the laminin-2 heterotrimer, is not down-regulated in *dy/dy* tissue.

Immunoblotting of the same samples with an antibody specific to the laminin α2 chain (Paulsson and Saladin, 1989) however, showed differences in the expression of this constituent of the laminin-2 heterotrimer. The antibody used recognises a 300 kDa proteolytic fragment of the laminin α2 chain protein. As expected, samples of dorsal roots, sciatic nerve, cardiac and skeletal muscle from unaffected mice showed strong expression of the laminin α2 chain with a sharp, intensely stained band at 300 kDa. A few bands at approximately 220 kDa and below probably represent degradation products (Paulsson et al., 1991), as the antibody does not detect the β1 and γ1 chains in laminin-2 standards (figs. 3.3a, 3.4a, 3.5a).

The *dy/dy* mice analysed for expression of the laminin α2 chain were used only when they had begun to show advanced symptoms typical of *dy/dy* mice. Thus all mice classified as mutants in this study displayed advanced hind-limb paralysis. In

previous reports, using different antibodies, negligible levels of laminin α2 protein were detected by Western blotting in either peripheral nerves or skeletal muscles from *dy/dy* mice (Arahata, 1993; Sunada et al., 1994; Xu et al., 1994a). In contrast, in our experiments expression of the 300 kDa α2 chain band by *dy/dy* mouse tissues in western blots was substantially reduced only in nerve tissue. In *dy/dy* skeletal muscle, a strong 300 kDa band was clearly visible (fig. 3.6a) and almost as intense as the level in skeletal muscle from unaffected mice (the limited availability of the non-commercial antibody used for immunoblotting meant α2 chain expression in cardiac muscle could only be analysed immunohistochemically; see below). In contrast, sciatic nerves and dorsal roots in *dy/dy* mice appeared not to express significant quantities of the laminin α2 chain. Staining at 300 kDa in the peripheral nerves of *dy/dy* mice appeared to be negligible (fig. 3.4a, 3.5a), suggesting a complete absence or severe deficiency of the laminin α2 chain, in agreement with previous studies using different antibodies.

Figure 3.3: The laminin α2 chain is weakly expressed in the sciatic nerves of *dy/dy* mice. 2mg/ml of homogenised unpurified sciatic nerve proteins from *dy/dy* and unaffected (ua) mice were run on 5% SDS-PAGE gels, blotted onto PVDF membranes and stained with either a rabbit polyclonal antibody to the laminin α2 chain (a) or a rabbit polyclonal antibody against laminin-1 (b). **(a)** A 300 kDa α2 chain was clearly seen in lanes containing the human placental merosin standard (m) and unaffected sciatic nerve, as well as a degradation product at 220 kDa. In *dy/dy* sciatic nerves the staining intensity of the α2 chain is greatly reduced and the chain is barely detectable. **(b)** The α1 and β1 chains were detected at 400 and 220 kDa respectively with a degradation product with a lower molecular weight than 220 kDa. There is no decrease in the expression of these chains in *dy/dy* sciatic nerves. (r = rainbow marker, A = 220 kDa marker on rainbow marker, B = 97.4 kDa marker on rainbow marker, green arrow = origin, blue arrow = dye front, * = degradation products).

3.3: Sciatic nerve
a: anti-laminin α2 chain

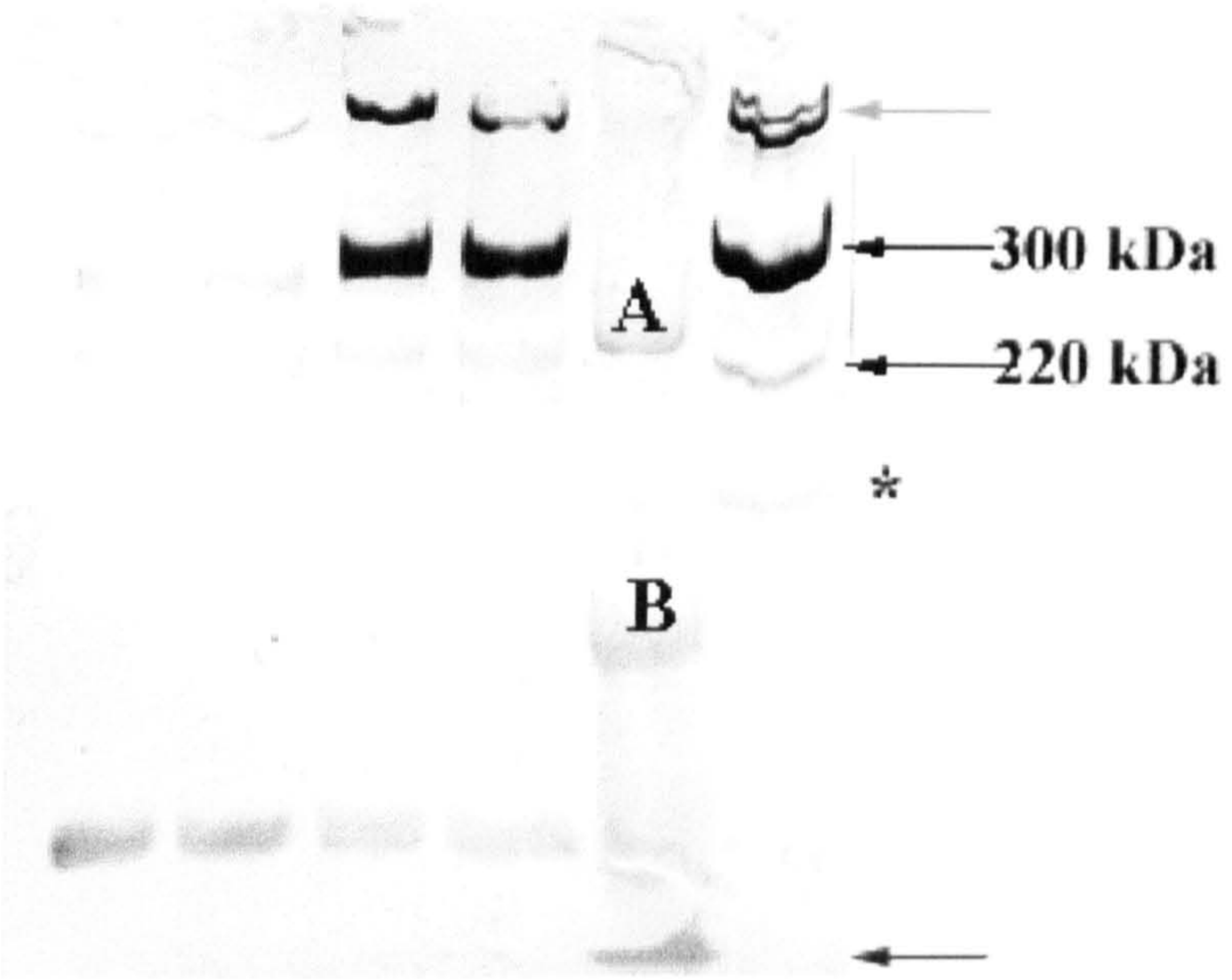

b: anti-laminin-1

Figure 3.4: The laminin α2 chain is weakly expressed in the dorsal roots of *dy/dy* mice. 2mg/ml of homogenised unpurified dorsal root proteins from *dy/dy* and unaffected (ua) mice were run on 5% SDS-PAGE gels, blotted onto PVDF membranes and stained with either a rabbit polyclonal antibody to the laminin α2 chain (a) or a rabbit polyclonal antibody against laminin-1 (b). **(a)** There was strong expression of a 300 kDa α2 chain band in the lanes containing the dorsal roots of unaffected mice and in the lane containing the human placental merosin standard (m), as well as the degradation product at 220 kDa. In lanes containing *dy/dy* dorsal roots, expression of the laminin α2 chain was negligible. **(b)** The α1and β1 chains can be seen at 400 and 220 kDa respectively. The staining intensity is comparable in lanes containing the human placental merosin standard. (r = rainbow marker [molecular weights as before], green arrow = origin, blue arrow = dye front, * = degradation products).

3.4: Dorsal roots

a: anti-laminin α2 chain

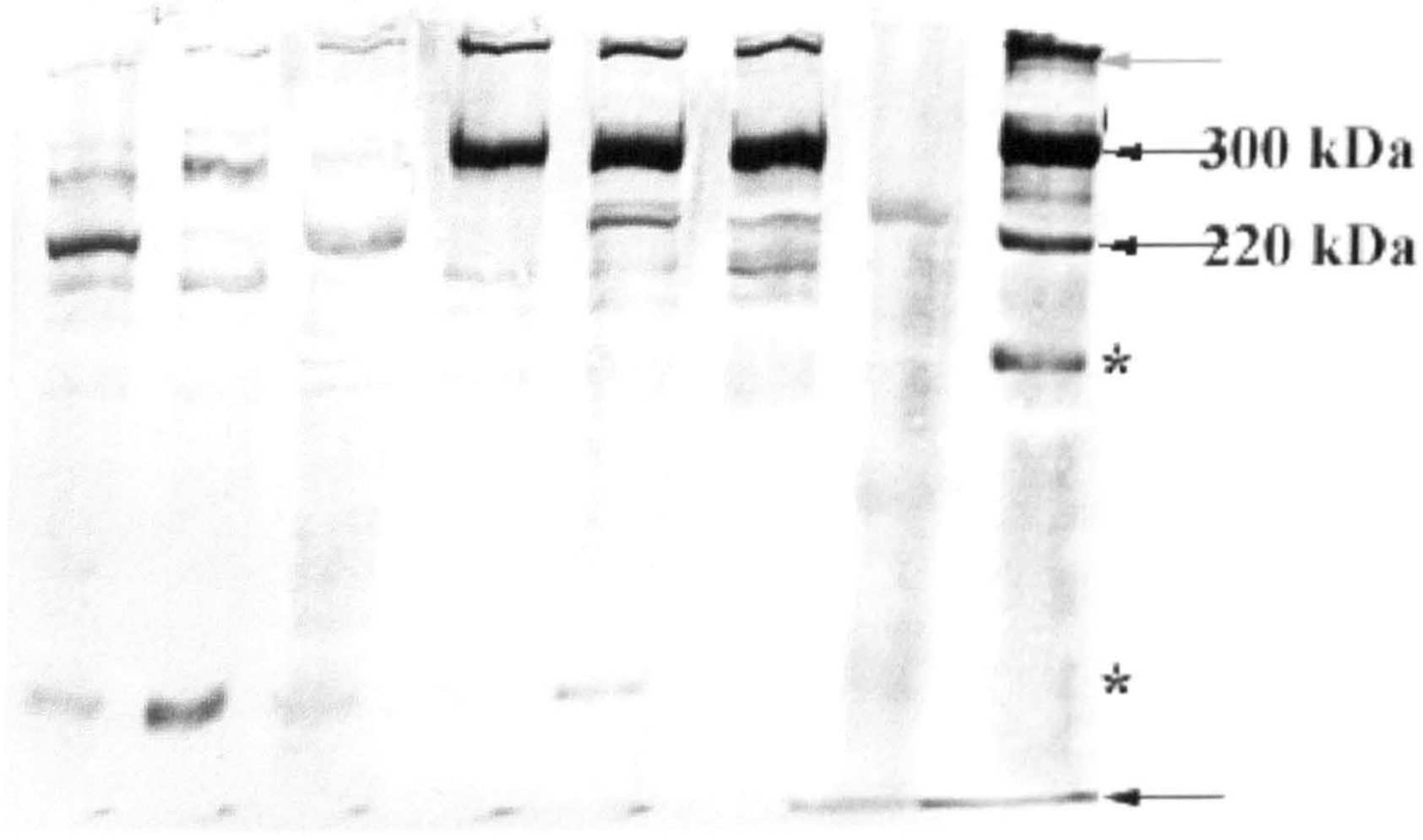

b: anti-laminin-1

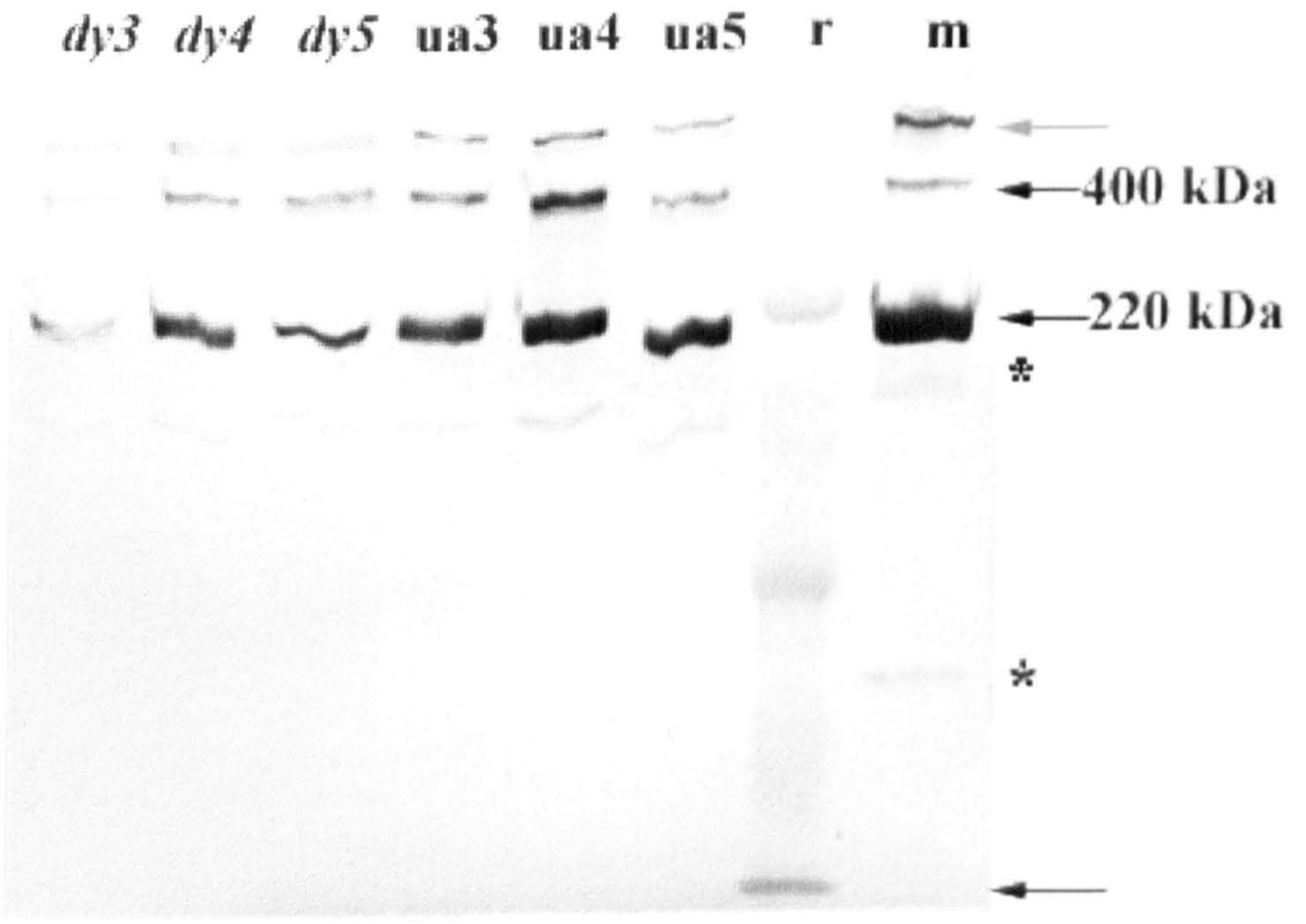

Figure 3.5: The laminin α2 chain is strongly expressed in *dy/dy* skeletal muscle. 2mg/ml of unpurified homogenised skeletal muscle proteins from unaffected (ua) and *dy/dy* mice were run on 5% SDS-PAGE gels, blotted with PVDF membranes and stained with either a rabbit polyclonal antibody against the laminin α2 chain (a) or a rabbit polyclonal antibody against laminin-1 (b). **(a)** There is strong expression of the α2 chain at 300 kDa and a degradation product at 220 kDa in both unaffected and *dy/dy* skeletal muscles and in the human placental merosin standard (m). There does not seem to be a substantial decrease in the staining intensity of the α2 chain bands in the skeletal muscle of *dy/dy* mice as there is in peripheral nerves. **(b)** The α1 and β1 chains are equally well expressed at 400 and 220 kDa, respectively, in the skeletal muscle of *dy/dy* and unaffected mice. (r = rainbow marker [molecular weights as before], green arrow = origin, blue arrow = dye front, * = degradation products).

3.5: Skeletal muscle

a: anti-laminin α2 chain

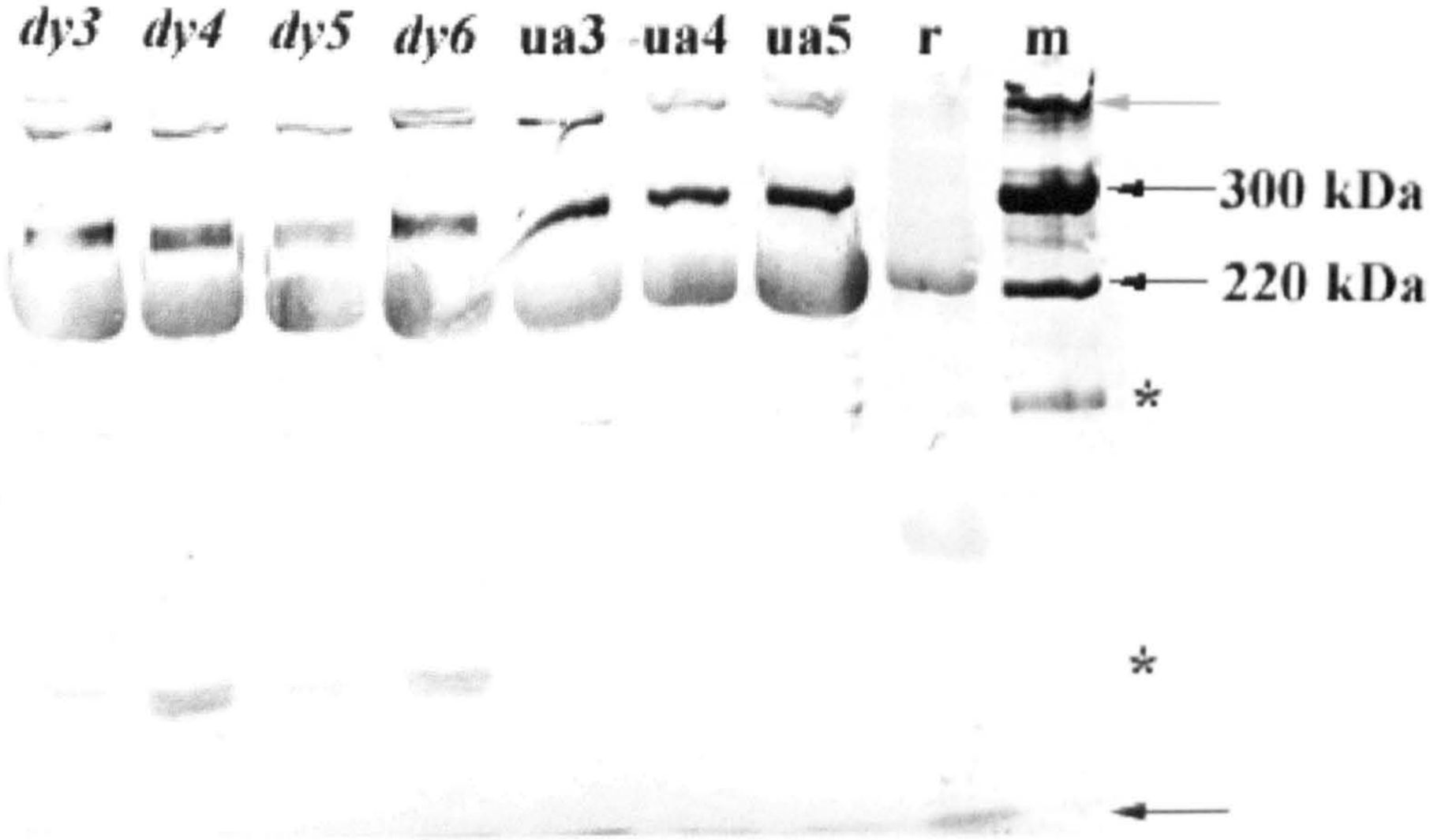

b: anti-laminin-1

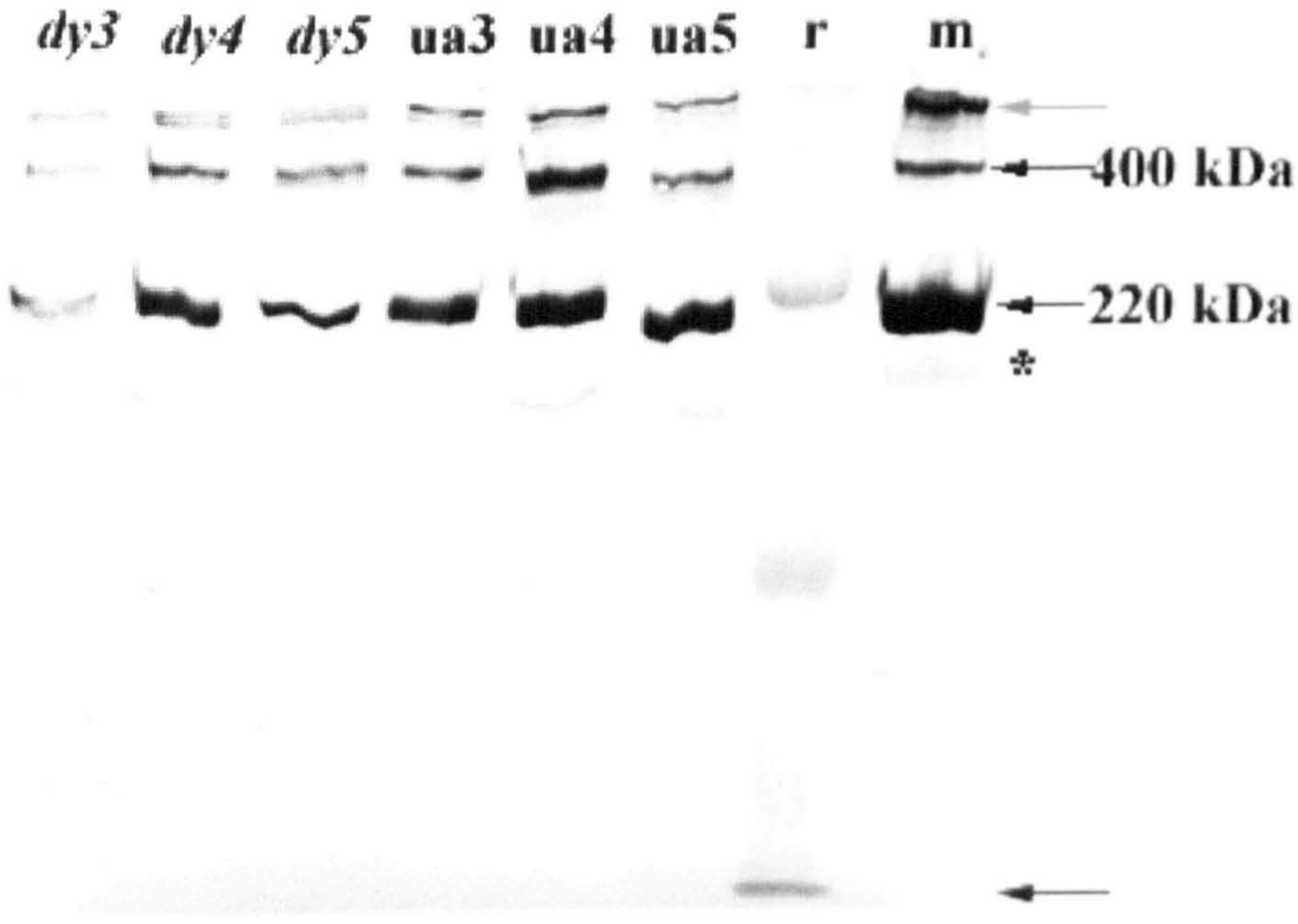

3.2.3: Immunohistochemical analysis also shows differential expression of the laminin α2 chain in *dy/dy* peripheral nerves, cardiac muscle and skeletal muscle

The rat monoclonal antibody 4H8 used for immunohistochemical analysis, like the rabbit polyclonal antibody used above, was raised against mouse heart laminin and recognises a 300 kDa fragment of the laminin α2 chain (Schuler and Sorokin, 1995). Skeletal and cardiac muscle and sciatic nerve from both *dy/dy* and unaffected mice, stained with an antibody against EHS-laminin (fig. 3.6c, d, 3.7c, d, 3.8c, d), are all strongly immunopositive, indicating that the β1 and γ1 chain are present at comparable levels in mutant and unaffected tissue. However, staining with the α2 chain-specific antibody (4H8-2) showed that whilst levels of α2 were expressed at negligible levels in *dy/dy* peripheral nerves (fig. 3.6a, b), the intensity of immunostaining in skeletal muscle was comparable in both mutants and controls and was not substantially reduced in *dy/dy* cardiac muscle (fig. 3.7a, b, 3.8a, b). Wherever the laminin α2 chain was expressed, it co-localised with EHS-laminin immunoreactivity (fig. 3.6e, f, 3.7e, f, 3.8e, f).

Another antibody to laminin α2 chain, (clone 403; gift of L. Sorokin) was obtained to try and clarify the results of these experiments. This antibody was raised in rabbit against the C-terminus G1-3 domain of mouse laminin α2 chain. However, it was found that in skeletal and cardiac muscle and in sciatic nerve, immunoreactivity was of comparable intensity in all tissues from unaffected (fig. 3.6g, 3.7g, 3.8g) and *dy/dy* (fig. 3.6h, 3.7h, 3.8h) mice. Thus two principal antibodies used for the detection of the α2 chain in immunoblotting and in immunohistochemistry, corresponded in their ability to detect significant expression of the laminin α2 chain

in *dy/dy* skeletal and cardiac muscle but not in peripheral nerves.

Figure 3.6: Laminin α2 chain immunoreactivity is not detected in *dy/dy* sciatic nerve with clone 4H8 monoclonal antibody. Fresh frozen, 8 μm cryosections of sciatic nerve from unaffected (ua) (a, c, e) and *dy/dy* (b, d, f) mice were double immunostained with antibodies to the laminin α2 chain (α2; clone 4H8) and to EHS-laminin (ln1) and visualised with fluorescein and rhodamine conjugates, respectively, at x40 magnification. Sections were also immunostained with an antibody to the laminin α2 chain, clone 403, and visualised with a rhodamine conjugate (g, h). **(a)** The endoneurium in the sciatic nerves of unaffected (ua) mice appears to express high levels of the laminin α2 chain (arrowhead). **(b)** The endoneurium in the sciatic nerves of *dy/dy* mice appears to be completely devoid of the laminin α2 chain and no immunoreactivity could be detected. **(c)** The endoneurium of unaffected sciatic nerves was strongly immunoreactive for EHS-laminin (arrow), consistent with expression of all or some of α1, β1 and γ1 chains. **(d)** The endoneurium in *dy/dy* sciatic nerves is also strongly immunoreactive for EHS-laminin (arrow). Although the staining intensity is comparable to that seen in unaffected nerves, the pattern of staining is less organised than in unaffected nerves where clear bands of endoneurium are visible. **(e)** Double-staining shows that in unaffected nerves the laminin α2 chain co-localises with all or some of α1, β1 and γ1 chains. **(f)** Double-labelling of *dy/dy* sciatic nerve shows only EHS-laminin immunoreactivity with no co-localisation with the laminin α2 chain. **(g)** The endoneurial basal lamina of sciatic nerves in unaffected mice is strongly immunoreactive (arrowhead) with the clone 403 antibody against the mouse G-domain of the mouse laminin α2 chain. **(h)** The endoneurial basal lamina of *dy/dy* sciatic nerves (arrowhead) is also strongly immunoreactive with the 403 antibody. Scale bar = 50 μm.

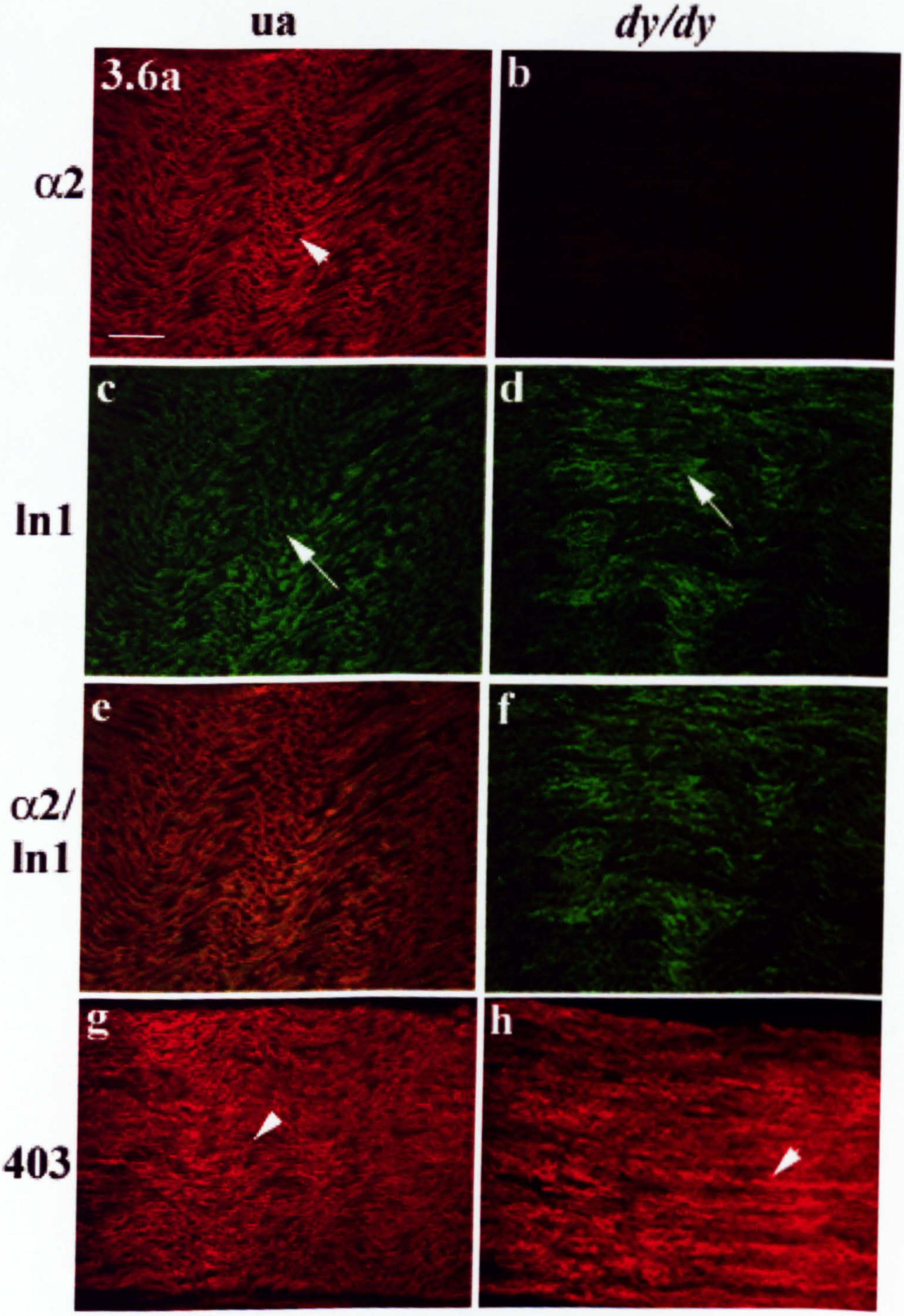
ua
dy/dy
3.6a
b
α2
c
d
ln1
e
f
α2/
ln1
g
h
403

Figure 3.7: Laminin α2 chain immunoreactivity is detected at low levels in the cardiac muscle of *dy/dy* mice with 4H8 antibody. Fresh frozen, 8 μm cryosections of cardiac muscle from unaffected (ua) (a, c, e) and *dy/dy* (b, d, f) mice were double immunostained with antibodies to the laminin α2 chain (α2; clone 4H8) and to EHS-laminin (ln1) and visualised with fluorescein and rhodamine conjugates, respectively, at x40 magnification. Sections were also immunostained with an antibody to the laminin α2 chain, clone 403, and visualised with a rhodamine conjugate (g, h). **(a)** Laminin α2 chain is strongly expressed (arrowhead) in the basal lamina surrounding cardiac muscle fibres in unaffected mice. **(b)** In the cardiac muscle of *dy/dy* laminin α2 chain immunoreactivity is very weak (arrowhead). **(c)** Immunoreactivity for the α1/β1/γ1 chains recognised by the antibody against EHS-laminin is strong in cardiac muscle from unaffected mice (arrow). **(d)** The cardiac muscle of *dy/dy* mice is immunoreactive for the α1/β1/γ1 chains but staining intensity is weaker than in the cardiac muscle of unaffected mice (arrow). **(e)** The laminin α2 chain co-localises with the α1/β1/γ1 chains in the cardiac muscle of unaffected mice. **(f)** Although immunoreactivity is substantially weaker for both the anti-EHS-laminin and the anti-laminin α2 chain antibodies, co-localisation is still observed in the cardiac muscle of *dy/dy* mice. **(g)** Strong immunoreactivity is observed in the basal lamina of cardiac muscle (arrowhead) stained with clone 403 antibody against the G-domain of the mouse laminin α2 chain in unaffected mice. **(h)** *dy/dy* cardiac muscle basal lamina is also strongly immunoreactive with the clone 403 antibody (arrowhead). Scale bar = 50 μm.

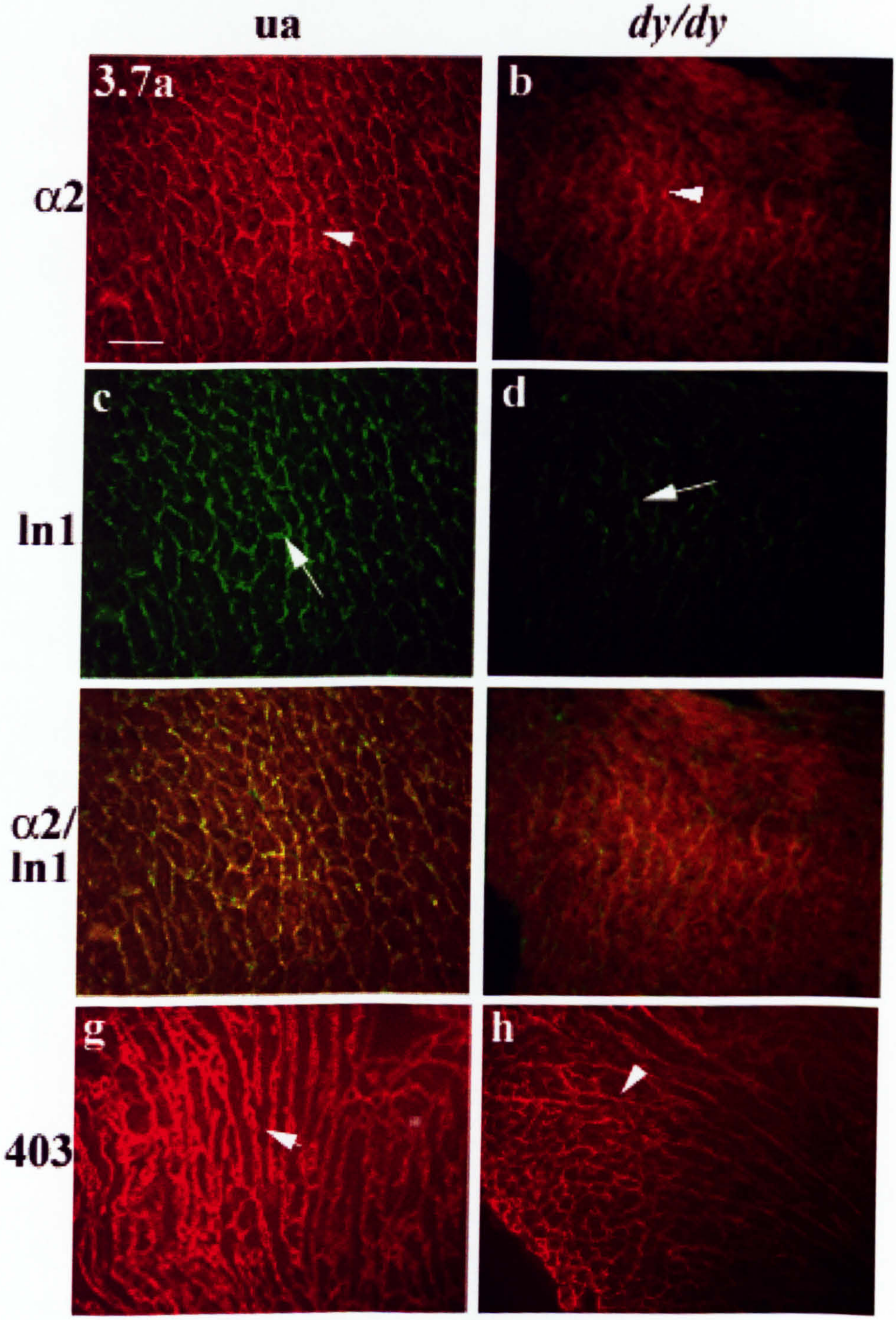
ua
dy/dy
3.7a
b
α2
c
d
ln1
α2/
ln1
g
h
403

Figure 3.8: Laminin α2 chain immunoreactivity is slightly reduced in the skeletal muscle of the *dy/dy* mouse with 4H8 antibody. Fresh frozen, 8 μm cryosections of skeletal muscle from unaffected (ua) (a, c, e) and *dy/dy* (b, d, f) mice were double immunostained with antibodies to the laminin α2 chain (α2; clone 4H8) and to EHS-laminin (ln1) and visualised with fluorescein and rhodamine conjugates, respectively, at x40 magnification. Sections were also immunostained with an antibody to the laminin α2 chain, clone 403, and visualised with a rhodamine conjugate (g, h). **(a)** The skeletal muscle basal lamina of unaffected mice is strongly immunoreactive for the laminin α2 chain (arrowhead). **(b)** Although the staining intensity appears slightly weaker than in unaffected mice, the skeletal muscle basal lamina of *dy/dy* mice is still quite strongly immunoreactive for the laminin α2 chain (arrowhead) and there does not appear to be a very substantial reduction in expression. **(c)** The skeletal muscle basal lamina is strongly immunoreactive for the α1/β1/γ1 chains (arrows) in unaffected mice. **(d)** The skeletal muscle basal lamina of *dy/dy* mice appears to be strongly immunoreactive for the laminin α1/β1/γ1 chains (arrow). **(e)** Expression of the laminin α1/β1/γ1 chains co-localises with laminin α2 chain expression in the skeletal muscle basal lamina of unaffected mice. **(f)** The laminin α2 chain and α1/β1/γ1 chains also co-localise in the skeletal muscle basal lamina of *dy/dy* mice. **(g)** The skeletal muscle basal lamina of unaffected mice is strongly immunoreactive (arrowhead) with the clone 403 antibody against the G-domain of mouse laminin α2 chain. **(h)** The 403 antibody is also strongly immunoreactive in the basal lamina of the skeletal muscle (arrowhead) of *dy/dy* mice. Scale bar = 50 μm.

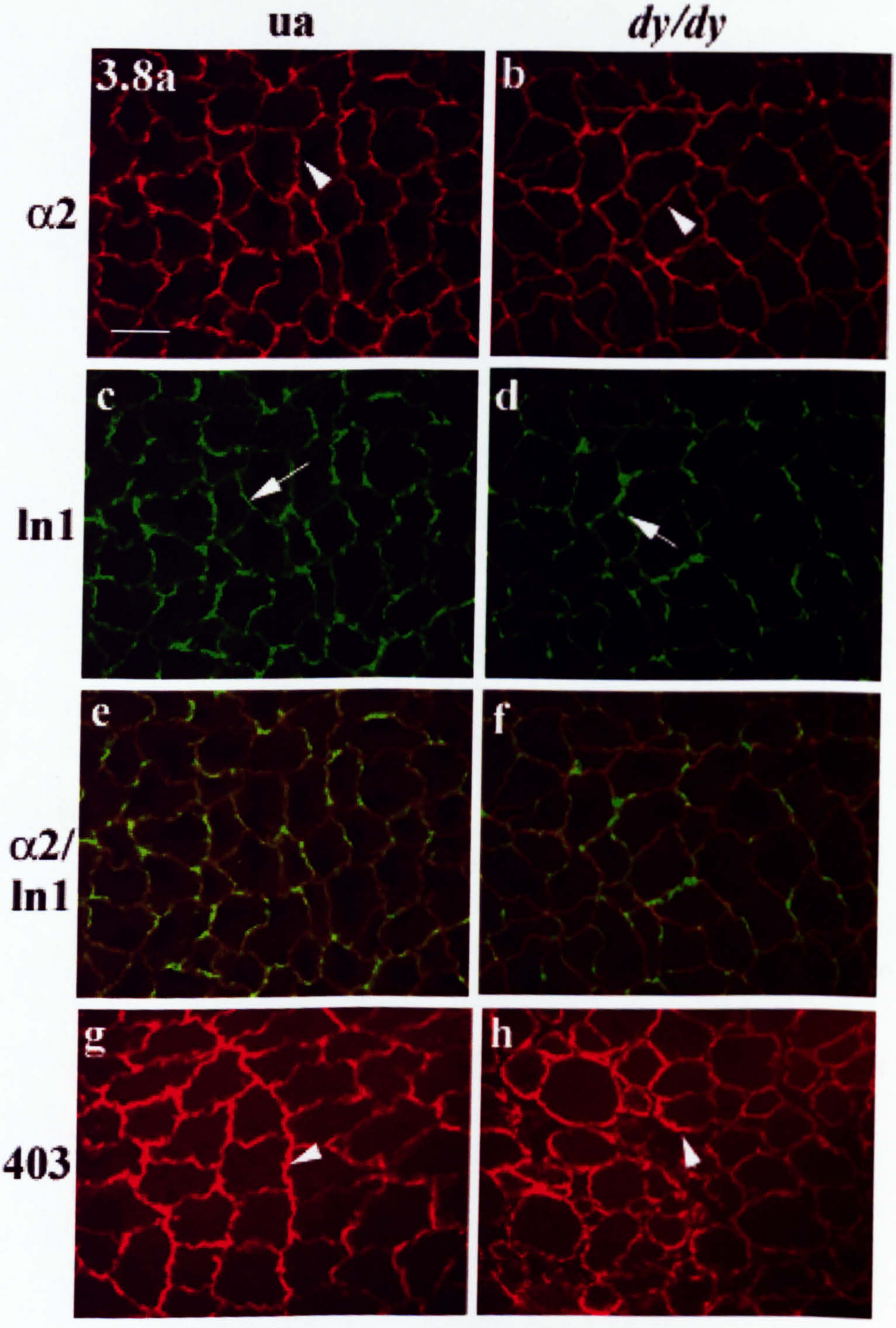
ua
dy/dy
3.8a
b
α2
c
d
ln1
e
f
α2/
ln1
g
h
403

3.3: Discussion

3.3.1: Morphological differences in the peripheral nerves of *dy/dy* mice

The laminin α2 chain affected in *dy/dy* mice and in humans with merosin-deficient CMD is pleiotropic, being expressed in both myogenic and neural tissues. In contrast, the mutation in humans with DMD and in *mdx* mice, affects the gene that encodes dystrophin, a component of the DAG receptor complex. Dystrophin is widely expressed in muscle, but another cytoskeletal protein, utrophin, serves the same function in Schwann cells (Hoffman et al., 1987; Ohlendieck and Campbell, 1991). This mutation results in a dystrophy that is primarily myogenic, without extensive neural abnormalities and is a less severe dystrophy than in *dy/dy* mice or humans with merosin-deficient CMD.

Thus the discovery of neural abnormalities in *dy/dy* mice raised the possibility that these may contribute to severity of the dystrophy (Banker et al., 1979). Schwann cells have a major role in axonal guidance and survival as evidenced in mutant mice with targeted deletions of the ErbB2 or ErbB3 neuregulin receptors which are deficient in Schwann cells and suffer from apoptotic death of neurons and defasciculation (Morris et al., 1999; Riethmacher et al., 1997; Woldeyesus et al., 1999). Schwann cells are also involved in the development and regeneration of NMJs (Love and Thompson, 1998; Son and Thompson, 1995a; Son and Thompson, 1995b; Son et al., 1996; Trachtenberg and Thompson, 1997; Trachtenberg and Thompson, 1996). Schwann cell abnormalities, for instance invasion of the synaptic cleft by Schwann cell processes in mice lacking the laminin-11 heterotrimer (Patton et al., 1998), result in loss of synapses and consequent loss of neuromuscular transmission. It is therefore possible that the neural abnormalities in *dy/dy* mice also

affect the ability of nerves to innervate and conduct impulses to skeletal muscles. The main neural target of the mutation in *dy/dy* mice are the Schwann cells and the data in this chapter provides additional evidence for a major neurogenic component to the resulting dystrophy.

Previous ultrastructural studies had shown that patchy endoneurial basal lamina, hypomyelination and abnormally wide nodes of Ranvier were common in the spinal roots and peripheral nerves of *dy/dy* mice (Bradley et al., 1977; Bradley and Jenkison, 1973; Bradley and Jenkison, 1975; Madrid et al., 1975). Our electron microscopical studies confirmed these abnormalities in the intact sciatic nerves of the *dy/dy* mouse. Immunohistochemical studies further showed that the deficiency in the laminin α2 chain was associated with substantial changes in the organisation of *dy/dy* sciatic nerves.

Thus S100 positive cells were significantly more numerous in *dy/dy* sciatic nerves as shown by a 56% increase in the number of immunoreactive cells per unit length of nerve (see table 3.1). Also, whilst the vast majority of Schwann cells in unaffected nerves appeared to have the ellipsoid morphology characteristic of Schwann cells that have associated with and elongated along axons, in *dy/dy* nerves almost half the Schwann cells were rounded in shape. Furthermore double immunostaining of Schwann cells and axons showed a lack of close alignment in *dy/dy* nerves. Analysis of ultrastructure (fig. 3.1) confirmed that *dy/dy* Schwann cells often only loosely contacted axons. This failure to elongate and align with the axon would lead to the more rounded morphology of *dy/dy* Schwann cells, since it would expose less Schwann cell surface membrane to axons. In addition electron micrographs showed that some *dy/dy* Schwann cells extended processes to several

axons, which would account for the abnormal morphology revealed in S100 immunohistochemistry of *dy/dy* nerves. The extension of multiple processes could contribute to the apparent increase in the density of S100 positive cells in *dy/dy* sciatic nerves. These rounded and densely packed areas of S100 immunoreactivity in *dy/dy* nerves may in some cases represent Schwann cell processes.

Several *in vitro* studies have shown that the deposition of basal lamina leads to changes in Schwann cell morphology linked to their terminal differentiation and axonal ensheathment. In cultures with neurons, addition of exogenous basal lamina led to longitudinal spreading of the Schwann cells along the nerve fibres. This was a basal lamina and not a nerve-dependent phenomen, as the removal of neurons from the culture did not prevent the Schwann cells from elongating (Carey et al., 1986). Similarly, in co-cultures with fibroblasts, elaboration of the basal lamina results in the elongation of the Schwann cells and alignment with respect to each other (Obremski et al., 1993b). The patchy basal lamina observed in *dy/dy* nerves is probably insufficient to support this differentiation and elongation of Schwann cells and may account for the morphology of S100 positive cells in mutant nerves.

Thus for those Schwann cells that are able to differentiate in *dy/dy* nerves, contact with basal lamina is essential for normal Schwann cell-axon interactions. When suspended nerve fascicles were grown *in vitro* in the absence of basal lamina, clusters of Schwann cells extended processes to more than one axon (Bunge and Bunge, 1978). Few Schwann cells actually ensheathed the axons and there was no myelin formation, abnormalities reminiscent of those found in *dy/dy* mice. Addition of ECM constituents resulted in Schwann cell ensheathment of both small and large diameter axons and myelination of the latter (Bunge and Bunge, 1978).

Furthermore control of Schwann cell differentiation and basal lamina formation can be triggered by ascorbic acid in co-cultures of axons and Schwann cells, suggesting that myelination could be regulated by the ability of Schwann cells to form basal lamina (Eldridge et al., 1989; Eldridge et al., 1987).

The endoneurial basal lamina in *dy/dy* nerves may be insufficient for normal development of Schwann cells and myelination of axons on two counts; firstly its scarcity means that few Schwann cells are in intimate contact with the basal lamina and secondly the composition of the basal lamina that is present is abnormal. The endoneurial basal lamina in adult *dy/dy* nerves contains abnormally high levels of laminin α4 chain, which is not normally found there (Patton et al., 1997). The α4 chain could, in principle, heterotrimerise in the endoneurial basal lamina with the β1 and γ1 chains normally associated with the α2 chain, but evidently this cannot compensate structurally or functionally for the absence of laminin α2 chain in the mutant. Thus ectopic upregulation of the α4 chain in *dy/dy* endoneurium is unable to fully compensate for laminin α2 chain in inducing Schwann cell ensheathment and myelination in the mutant nerves.

I have observed abnormalities of Schwann cell ensheathment and morphology in the sciatic nerves of *dy/dy* mice, which may disrupt the ability of nerves innervating skeletal muscles to transmit impulses. Abnormalities have also been observed at the NMJ in *dy/dy* mice, which may interfere with synaptic transmission. The post-synaptic area per nerve terminal, post-synaptic membrane length and the post-synaptic area per nerve terminal area are all significantly less in *dy/dy* mice. The junctional folds were less complex and Schwann cell cytoplasm was seen to extend into the synaptic cleft (Banker et al., 1979; Desaki et al., 1995; Law et al., 1983).

This latter abnormality has been more recently observed in transgenic mice lacking the laminin-11 heterotrimer ($\alpha5\beta2\gamma1$) which like laminin-4 ($\alpha2\beta2\gamma1$) is normally expressed in synaptic basal lamina (Patton et al., 1998). This is consistent with a role for specific laminin chains in controlling Schwann cell process extension. However these abnormalities at the NMJ do not appear to be severe enough to significantly affect neuromuscular transmission in *dy/dy* mice as defined by spontaneous transmitter release rather than evoked transmitter release. The failure rate for neuromuscular transmission in *dy/dy* mice of 2% was equivalent to that seen in normal mice (Carbonetto, 1977). Conduction velocity is however lower in *dy/dy* nerves (Rasminsky et al., 1978). This lowered conduction velocity arises as a result of two of the neural abnormalities that we have observed. Firstly, large axons that are normally myelinated throughout their lengths to aid conduction are either not myelinated or have long amyelinated patches (fig. 3.1a, b). Secondly, the widened nodes of Ranvier in myelinated mutant nerves (fig. 3.1c) compromise the saltatory conduction that occurs from node to node. An abnormally high frequency of giant spontaneous potentials has been noted in *dy/dy* peripheral nerves and ectopic generation of impulses also arises mid-nerve due to "cross-talk" between apposing, naked axons unsheathed by Schwann cells (fig. 3.1b) (Carbonetto, 1977; Rasminsky, 1978). If conduction to the muscle is compromised or the axon itself degenerates, the muscle fibre would become functionally denervated and may begin to atrophy. Denervation of *dy/dy* skeletal muscle produces certain mechanical changes on muscle weight, contraction time and twitch and tetanus relaxations that suggest that some mechanical alterations seen in *dy/dy* skeletal muscle arise neurogenically (Zeman and Sandow, 1979).

Early observations on axoplasmic flow of proteins determined that slow axonal transport is decreased and fast axonal transport was increased in the nerves of *dy/dy* mice (Bradley and Jaros, 1973; Komiya and Austin, 1974). However this is not necessarily indicative of axonal degeneration and may simply be due to a higher turnover of protein in *dy/dy* peripheral nerves. The rate of axonal transport of choline acetyltransferase activity is reduced in *dy/dy* sciatic nerves (Jablecki and Brimijoin, 1974). This may indicate a reduction in the activity of motorneurons in *dy/dy* mice as a result of either axonal degeneration or of muscle necrosis.

Nicotinic receptors in both *dy/dy* and *mdx* mouse skeletal muscle show reduced sensitivity to the agonistic effects of acetylcholine; in dystrophic muscle synaptic transmission may be altered as a result of phosphorylation of one of the nicotinic receptor subunits. However spontaneous opening of nicotinic receptors without impulse conduction is a common feature of *dy/dy* but not *mdx* mouse skeletal muscle and is suggestive of an inability to downregulate the activity of this receptor (Franco-Obregon and Lansman, 1995). The fact that spontaneous activity is unique to *dy/dy* mice suggests that the pathogenesis in *dy/dy* skeletal muscle differs from that of *mdx* skeletal muscle. Severe neuronal abnormalities in *dy/dy* mice may result in more profound alterations in activity at the NMJ compared to *mdx* mice. The spontaneous activity is a feature characteristic of undifferentiated myoblasts, which may be present in *dy/dy* skeletal muscle either as a result of retarded development or due to regeneration of focal lesions in *dy/dy* skeletal muscle (Ringelmann et al., 1999). These focal lesions may be either a direct consequence of the dystrophy in the muscles or due to denervation as a result of the neural abnormalities in *dy/dy* mice.

Mice with targeted deletions in which the ErbB2 neuregulin receptor is deficient, are able to form acetylcholine receptors at the NMJ, probably due to activation of alternate ErbB3 and ErbB4 receptors (Lin et al., 2000; Woldeyesus et al., 1999). However an absence of Schwann cells means that the unensheathed motor axons innervating skeletal muscles degenerate and defasciculate, generating both pre and post-synaptic abnormalities. The motor nerve terminals are not ensheathed by Schwann cells at all in *ErbB2*$^{-/-}$ mice and post-synaptically there is a deficiency or absence of junctional folds (Lin et al., 2000). Poor junctional folding is also seen at the NMJ of *dy/dy* mice and is a feature of developing and regenerating muscle fibres (Banker et al., 1979; Desaki et al., 1995; Law et al., 1983). Thus neuromuscular and skeletal muscle abnormalities could be generated purely as a result of motor axon degeneration caused by lack of Schwann cell ensheathment.

With the recent construction of several different lines of laminin α2 null mutant mice, it has been possible to further test the neurogenic aspect of α2-chain-deficient dystrophies (Kuang et al., 1998b; Miyagoe et al., 1997). In these null mutants it was evident that laminin-2 was necessary for the repair and maintenance of skeletal muscle (Kuang et al., 1998a; Kuang et al., 1998b; Kuang et al., 1999). However insertion of a human laminin α2 chain transgene under a muscle-specific creatine kinase promoter improved muscle morphology and integrity but the mice were still left with the progressive lameness of the hind-limbs consistent with a major neurogenic contribution in the dystrophy (Kuang et al., 1998b). It is clear therefore, that both neurogenic and myogenic pathology contribute to the dystrophy in α2-deficient mice.

3.3.2: Differential expression of the laminin α2 chain in skeletal muscle and neural tissue suggests the existence of tissue-specific variants of the α2 chain

When the basal lamina deficiency in *dy/dy* mice was initially identified, it appeared that expression of the laminin α2 chain protein was negligible in skeletal and cardiac muscles and peripheral nerves. Moreover these early studies also found that levels of *lama2* gene mRNA were also substantially reduced and barely detectable in some cases in skeletal and cardiac muscles (Arahata, 1993; Sunada et al., 1994; Xu et al., 1994a). In this chapter I have shown that in fact, myogenic *dy/dy* tissues continue to express laminin α2 chain, while expression in neural tissue is negligible (Sewry et al., 1998) and this has been confirmed recently both immunohistochemically and at the mRNA level (Ringelmann et al., 1999; Sorokin et al., 2000). These findings suggest that a laminin α2 chain variant exists.

We found that laminin α2 chain immunoreactive protein expression was negligible in the peripheral nerves of *dy/dy* mice, but was detected at low levels in cardiac muscle and at apparently close to normal levels in skeletal muscle. In this study, I used a rabbit polyclonal antibody for immunoblotting (Paulsson and Saladin, 1989) and a rat monoclonal antibody for immunostaining (Schuler and Sorokin, 1995), both raised against mouse heart laminin; both recognise the 300 kDa N-terminus fragment of the laminin α2 chain. In the first study to attribute the cause of the muscular dystrophy in *dy/dy* mice to a deficiency of the laminin α2 chain (Arahata, 1993), rabbit polyclonal antibodies against the C-terminus segment of the human α2 chain and against the N-terminus segment of mouse α2 chain were used. Immunoblotting and immunohistochemistry both showed that laminin α2 chain immunoreactivity was negligible in cardiac and skeletal muscle and peripheral

nerves. In addition, electron microscopy showed that the skeletal muscle basal laminae were thinner and discontinuous in *dy/dy* mice (Arahata, 1993). Other previous studies used antibodies raised against the C-terminus and N-terminus fragments of the laminin α2 chain, synthetic peptides and recombinant proteins, and also showed a substantial deficiency of the laminin α2 chain protein in mutant skeletal and cardiac muscle and peripheral nerves (Sunada et al., 1994; Xu et al., 1994a).

My study concurs with previous work in showing that laminin α2 chain protein expression is severely deficient or absent in *dy/dy* peripheral nerves but provides conflicting evidence that laminin α2 chain protein may be expressed at substantial levels in myogenic tissues of *dy/dy* mice (Sewry et al., 1998). The differences between laminin α2 chain immunoreactive protein expression in *dy/dy* myogenic tissue in this study compared to previous work could simply reflect a variation in the epitopes recognised by the different antibodies used. This is unlikely however, as my study used two different antibodies, albeit both raised against α2 chain protein of mouse heart laminin. Furthermore two recently published studies have also shown that the laminin α2 chain protein is detectable in *dy/dy* myogenic tissues such as skeletal and cardiac muscle but not in non-myogenic tissues such as peripheral nerves and lung (Ringelmann et al., 1999; Sorokin et al., 2000). One of the antibodies used in these two published studies is the 4H8 antibody that I have used to analyse α2 chain protein expression immunohistochemically. It is possible that mouse heart laminin, against which these antibodies were raised, contains a variant form of the laminin α2 chain protein. Antibodies raised against heart laminin may recognise epitopes that do not exist on the primary variant of the

laminin α2 chain that was found to be deficient in both the myogenic and non-myogenic tissues of *dy/dy* mice. Thus the antibodies used in my experiments appear to recognise variant laminin α2 chain, which is expressed in all tissues in unaffected mice and is substantially down-regulated in all except myogenic tissues in *dy/dy* mice.

The idea that a variant of the laminin α2 chain exists in mice is supported by the recent identification of a variant laminin α2 chain in patients with the human equivalent of the *dy/dy* muscular dystrophy, merosin-deficient CMD (Pegoraro et al., 1998; Pegoraro et al., 2000). A mutation in exon 31 of the *lama2* gene resulted in an expressed variant of the laminin α2 chain that may fail to assemble a laminin-2 heterotrimer. The inability of this variant α2 chain to incorporate a heterotrimer means that any basal laminae in these patients that would normally express the α2 chain are not formed properly. Immunostaining and immunoblotting by myself and in previous studies show that both variants of the α2 chain are expressed in unaffected and *dy/dy* mice (Arahata, 1993; Ringelmann et al., 1999; Sewry et al., 1998; Sorokin et al., 2000; Sunada et al., 1994; Xu et al., 1994a), rather than as a consequence of mutations in the *lama2* chain gene as in seen in subjects with CMD by Pegoraro and her colleagues (2000). There is at least one example of a laminin α chain with expressed variants. The *lama3* gene has been shown to encode more than one isoform of the laminin α3 chain. Initially a shorter, truncated isoform, laminin α3A was identified (Aberdam et al., 1994; Rousselle et al., 1991), a longer isoform, the laminin α3B also exists (Miner et al., 1997). This raises the possibility that other laminin chains such as the α2 chain may have more than one variant in normal tissues.

dy/dy mice may seem at odds with earlier observations that showed a marked reduction in the *lama2* mRNA encoding the protein. The *lama2* gene mRNA was not detectable in skeletal muscle by Northern blotting in affected mice, however amplification of the mRNA signal with RT-PCR showed that detectable levels of *lama2* mRNA were expressed in skeletal and cardiac muscle but at significantly reduced levels (Arahata, 1993; Xu et al., 1994a). Also Ringelmann and colleagues (1999) have recently reported that reduced but clearly detectable *lama2* mRNA expression in *dy/dy* skeletal muscle but not in non-myogenic tissues using Northern blot analysis, without the benefit of RT-PCR amplification. The cDNA probes used in these studies detected different sequences in the *lama2* mRNA, Xu and colleagues (1994) used probes that recognised 3' sequences in what would translate to the N-terminus domain of the protein whereas Ringelmann and colleagues (1999) used cDNA probes that recognised sequences in the 5' region. These findings indicate that the particular sequence of *lama2* mRNA may be more stable in the myogenic than non-myogenic tissues of *dy/dy* mice or that more is generated than in non-myogenic tissues. Although there is no conclusive evidence, an alternative explanation for continued high-level expression of α2 chain protein and mRNA in myogenic tissues of *dy/dy* mice is that differentially spliced variants of the α2 chain exist.

Despite the finding that a possible variant of the laminin α2 chain is expressed at clearly detectable levels in the skeletal muscles of *dy/dy* mice they still suffer from a severe myopathy and the skeletal muscle basal laminae are discontinuous (Arahata, 1993). Neurogenic myopathy in *dy/dy* and merosin-deficient CMD skeletal muscle as a result of neural abnormalities may heighten the severity of the

myogenic myopathy compared to other muscular dystrophies where the PNS remains largely unaffected. The antibodies I have used may also detect an alternative variant that is expressed but functionally ineffective in *dy/dy* myogenic tissues. Although the *dy/dy* locus is known to map to the same region of mouse chromosome 10 as the *lama2* gene (Sunada et al., 1994), the exact site of the mutation is unknown and the locus may encompass more than one site in the α2 chain. This could result in the absence of one isoform in non-myogenic tissues but continued low-level expression in myogenic tissues.

The mutation in dy^{2j}/dy^{2j} mouse and in some humans with merosin-deficient CMD, leads to the production of an altered but still detectable laminin α2 chain that is unable to heterotrimerise in skeletal muscle (Colognato and Yurchenco, 1999; Pegoraro et al., 1998; Pegoraro et al., 2000). It is possible that the variant I have detected fails to heterotrimerise and so the basal laminae of myogenic tissues in *dy/dy* mice are abnormal despite detectable expression of a laminin α2 chain. If so, then processing skeletal muscle in a native gel without denaturing the heterotrimer may reveal whether the α2 chain variant in *dy/dy* myogenic tissue is incorporated into a heterotrimer. In fact in this chapter I have shown that an antibody against the G1 to G3 C-terminus domains of the laminin α2 chain detects expression of this α2 chain fragment in skeletal and cardiac muscle and sciatic nerves. Thus in skeletal and cardiac muscle an α2 chain isoform may be expressed that is truncated rather than deleted but which is not able to incorporate into a basal lamina.

Chapter 4: The response of *dy/dy* sciatic nerves to injury

4.1: Introduction

It is thought that many of the processes involved in the development of the peripheral nervous system are recapitulated during regeneration following injury to the nerve. The absence of laminin-2 in the PNS of *dy/dy* mice results in the extensive abnormalities that have been described in chapter 3. To investigate how and why these may arise and to understand the role of laminin-2 in aspects of regeneration in the PNS, *dy/dy* mice underwent crush or transection of the sciatic nerve.

By transecting the sciatic nerves of *dy/dy* and unaffected mice and leaving a 0.5mm gap between the severed ends, it was possible to investigate the importance of laminin-2 *in vivo* in regulating the ability of axons to sprout across this gap to the distal stump. The bands of Büngner are endoneurial basal lamina tubes that are aligned with migrating Schwann cells and form between the distal and proximal stumps of regenerating nerves to provide a conduit for axons (Anderson et al., 1991; Hall, 1986b; Hall, 1989; Williams et al., 1983). Transection of the nerve severs the endoneurial basal lamina tubes that form the bands of Büngner. Thus regeneration following transection requires the formation of new basal lamina tubes, an obstacle to regeneration in unaffected transected nerves but an even greater challenge for laminin-2-deficient mice. Axonal sprouting into the distal stump was observed in transected *dy/dy* nerves, but appeared to be less extensive than in unaffected nerves.

Crushing rather than transecting peripheral nerves leaves the endoneurial basal lamina tubes largely intact and therefore presents less of a challenge for

regenerating axons. *dy/dy* sciatic nerves were crushed to investigate the initiation and maintenance of Schwann cell interactions with axons that had sprouted into the distal stump. In a previous study partial and complete crush to the severely hypomyelinated dorsal roots of *dy/dy* mice resulted in increased numbers of Schwann cells and more extensive myelination within 1 month of injury (Stirling, 1975b). Another previous study investigated longer-term regeneration in spinal roots and peroneal nerves of *dy/dy* mice 6 weeks following crush injury, which appeared to result in increased Schwann cell basal lamina coverage (Bray et al., 1983). I found that Schwann cell ensheathment of axons following crush was abnormal and incomplete in *dy/dy* nerves and that remyelination was both delayed and less extensive when it did occur.

4.2: Results

4.2.1: Axonal regeneration occurs following transection of *dy/dy* sciatic nerve, but is less extensive than in unaffected nerves

The sciatic nerves of *dy/dy* and unaffected mice were transected, leaving a small gap of less than 0.5 mm between the severed ends of the nerve to investigate the consequences of a severe reduction in laminin α2 chain on axonal regeneration *in vivo*. Previous experiments have shown that laminin-2 promotes neurite outgrowth *in vitro* (Engvall et al., 1992) and that blocking laminin-2/4 activity has an inhibitory affect on neurite outgrowth in regenerating nerves both *in vitro* and *in vivo* (Agius and Cochard, 1998; Anton et al., 1994a). If the basal lamina tubes, the bands of Büngner were unable to re-form in *dy/dy* mice, this might prohibit axonal regeneration.

Regenerating sciatic nerves were removed 2 weeks post-transection such that each length of nerve contained the lesion site and approximately 0.5 cm of nerve from either side of the lesion site. 7-8 μm thick sections of regenerating nerve were stained with antibodies against two axonal markers, a 165 KDa intermediate neurofilament protein (2H3) and PGP 9.5. The proximal stumps of transected nerves in *dy/dy* and unaffected mice were immunopositive for both 2H3 (not shown) and PGP 9.5 (fig. 4.1a, b), although staining appeared to be patchier in the *dy/dy* mice. The difference in axonal staining between the proximal stumps of transected *dy/dy* and control nerves was equivalent to that seen between mature intact *dy/dy* and control nerves (fig. 3.2).

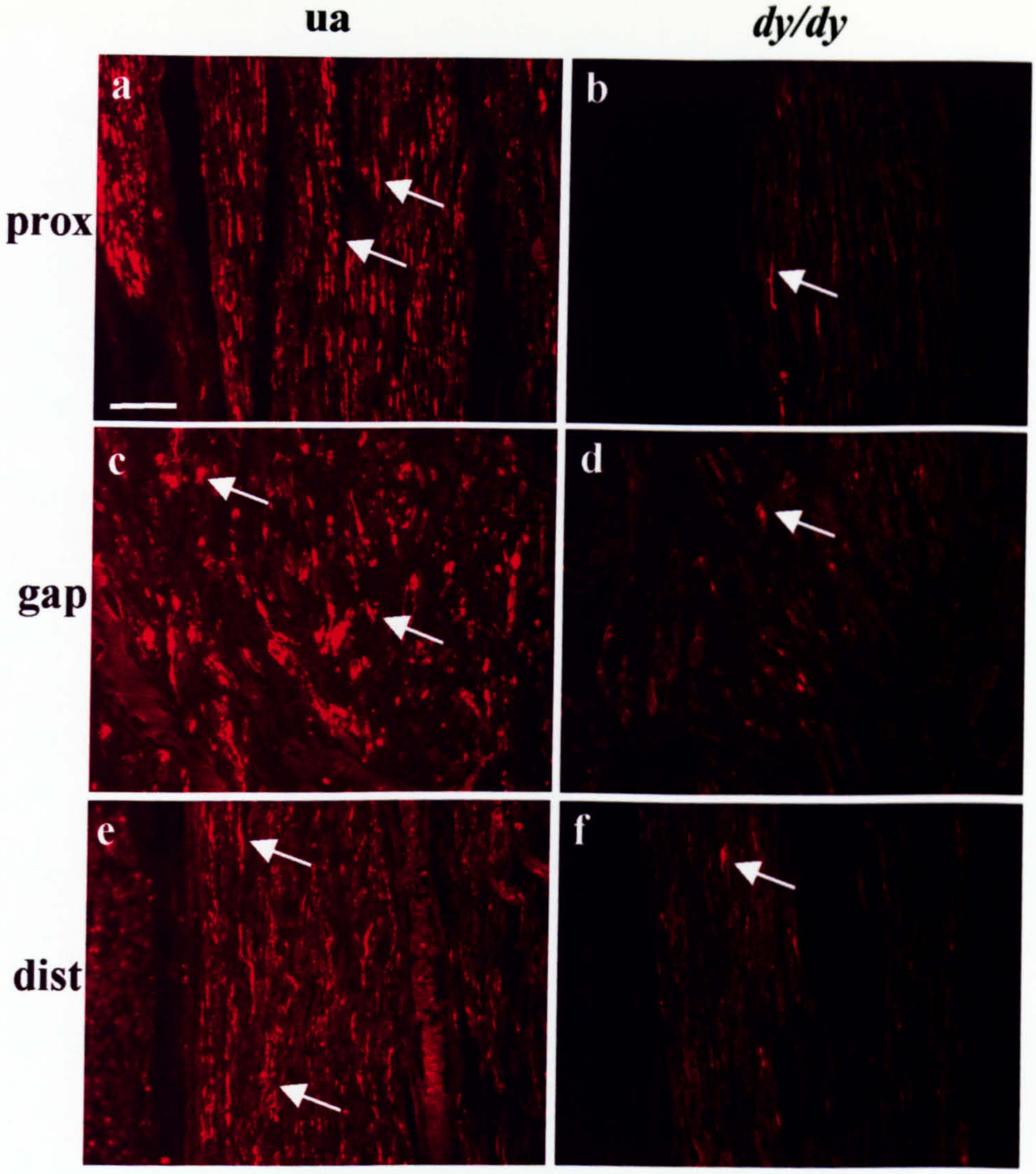

Figure 4.1: Very few axons grow into the distal stump in *dy/dy* sciatic nerves following transection. Sciatic nerves of unaffected (ua) and *dy/dy* mice were transected, removed two weeks post-transection, fixed and immunostained with an antibody against PGP 9.5, an axonal marker (arrows). **(a)** The proximal (prox) stump in unaffected nerves appears to be full of PGP 9.5 immunoreactive axons. **(b)** There were few immunoreactive axons (arrow) in the proximal stump of tran -sected *dy/dy* sciatic nerves. **(c)** In unaffected nerves there is substantial growth of axons through the gap left by the transection. **(d)** There are very few axons in the gap between the two cut ends of the transected *dy/dy* sciatic nerves. **(e)** There is widespread axonal outgrowth into the distal stump of the transected sciatic ner -ves of unaffected mice. **(f)** Axonal outgrowth into the distal stump of transected *dy/dy* sciatic nerves is still sparse two weeks post-lesion. Scale bar = 50 μm.

By two weeks post-transection, it was possible to see macroscopically that the gap between the severed ends of the nerve in both *dy/dy* and control nerves had been bridged and the lesion site was marked by a swollen, discoloured area. The lesion site was immunoreactive for both PGP 9.5 and 2H3 in unaffected and mutant transected nerves although immunoreactivity for these axonal markers appeared far less extensive in transected *dy/dy* nerves (fig 4.1c, d). The immunoreactivity indicated that a few axons were able to sprout through the lesion site in *dy/dy* nerves. By two weeks post-transection immnuonreactivity was also detectable in the distal stump of transected mutant and unaffected nerves. Although there was extensive axonal sprouting into the distal stump in the transected nerves of unaffected mice only a very limited amount of axonal immunoreactivity was detectable in transected *dy/dy* nerves (fig. 4.1e, f).

4.2.2: Remyelination is delayed, aberrant and less extensive in the sciatic nerves of *dy/dy* mice following crush injury

Transection of *dy/dy* sciatic nerves showed that some axons are capable of sprouting into the distal stump, even when there is a severe deficiency of laminin-2. To investigate what role laminin-2 has in other regenerative and by implication developmental processes sciatic nerve crushes were carried out. Axonal sprouting into the distal stump is usually more successful following crush and therefore presents a better model for establishing the role of laminin-2 in mediating interactions between axons and Schwann cells.

Figure 4.2: 1 week post-crush the distal stumps of both unaffected and *dy/dy* sciatic nerves have undergone Wallerian degeneration. Light micrographs of toluidine blue-stained 1 μm transverse resin sections 1 week post-crush. **(a)** In the proximal stump of unaffected nerves the myelinated axons remain intact. **(b)** The proximal stumps of crushed *dy/dy* sciatic nerves also remain intact, but there appear to be fewer myelinated axons. **(c)** 0.4 cm distal to the crush the unaffected nerve has undergone Wallerian degeneration and there are no myelinated axons. **(d)** The nerve 0.4 cm distal to the crush in *dy/dy* mice also undergoes what appears to be normal Wallerian degeneration. Magnification x40. Scale bar = 40 μm.

Sciatic nerves were crushed by Professor Susan Standring, processed, stained and sectioned into semi-thin sections by the Electron Microscopy unit at Guy's hospital and photographed by Yael Uziyel.

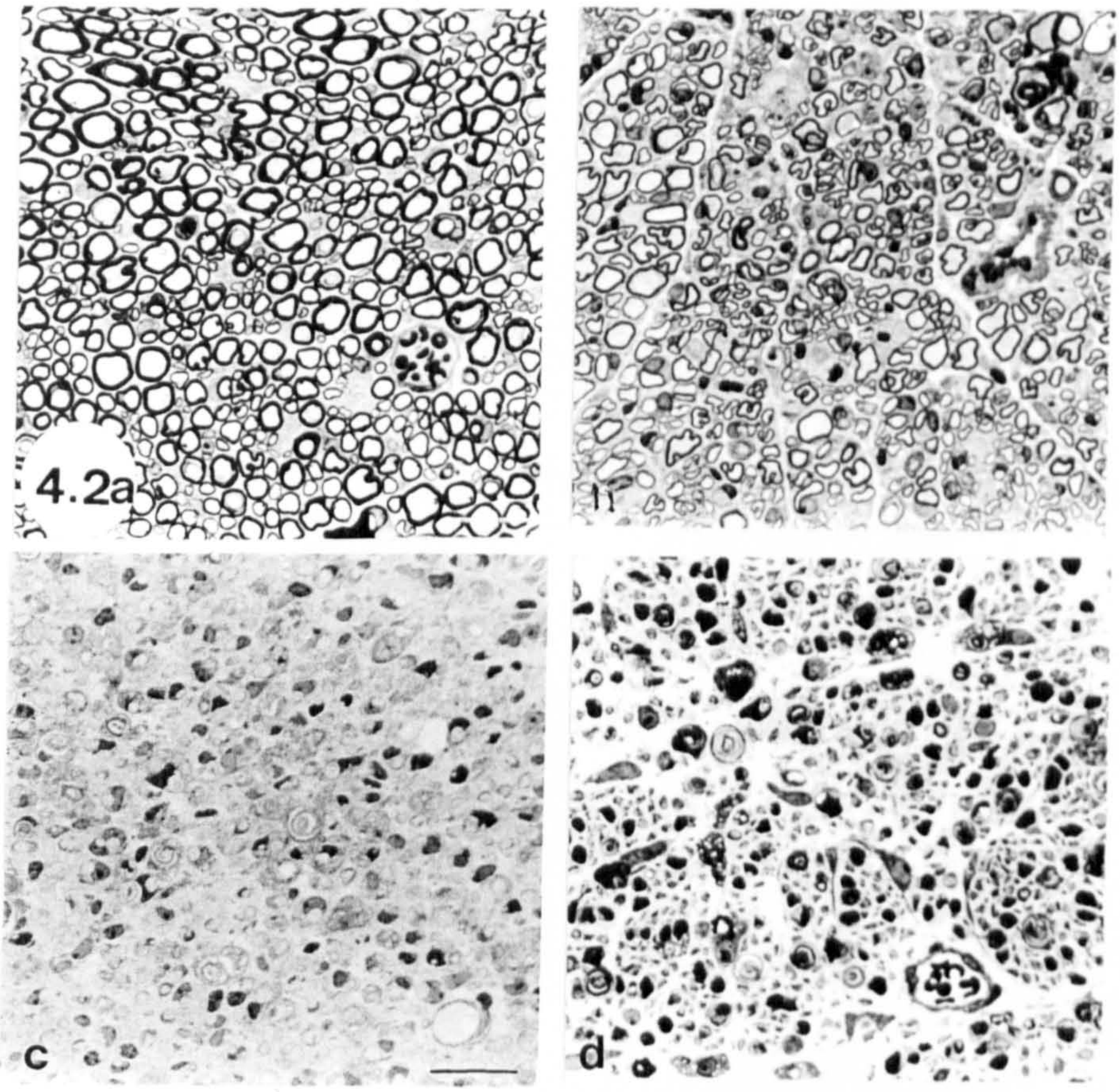
4.2a
c
d

As expected one week post-crush the proximal stump of *dy/dy* and unaffected nerves appeared to be intact and there was no sign of axonal degeneration (fig. 4.2a, b). Wallerian degeneration was evident in the distal stumps of both *dy/dy* and unaffected crushed sciatic nerves, which had a similar appearance (fig. 4.2c, d), both were undergoing axonolysis and myelinolysis with degeneration of axons and myelin. Differences in regeneration between *dy/dy* and control nerves became apparent however two weeks post crush. Significantly fewer axons were myelinated in the distal stump of crushed *dy/dy* nerves than in control nerves (fig. 4.3a, $p<0.05$; fig. 4.4). Quantification of toluidine-blue stained semi-thin sections at 2 weeks showed that axons in approximately 14.9% of the bands of Büngner in *dy/dy* mice were thinly remyelinated whereas in unaffected mice approximately 63.6% of axons in the bands of Büngner contained myelinated axons. Electron micrographs revealed severe abnormalities in the distal stumps of *dy/dy* nerves. The endoneurial basal lamina surrounding axon-Schwann cell units was patchy; bundles of axons were often incompletely ensheathed by Schwann cell processes and were directly in contact with the basal lamina (fig. 4.5). In some cases axons shared Schwann cells or several Schwann cells would surround an axon and there were few axons that were completely ensheathed by one Schwann cell and encased in basal lamina as seen in normal remyelinating nerves.

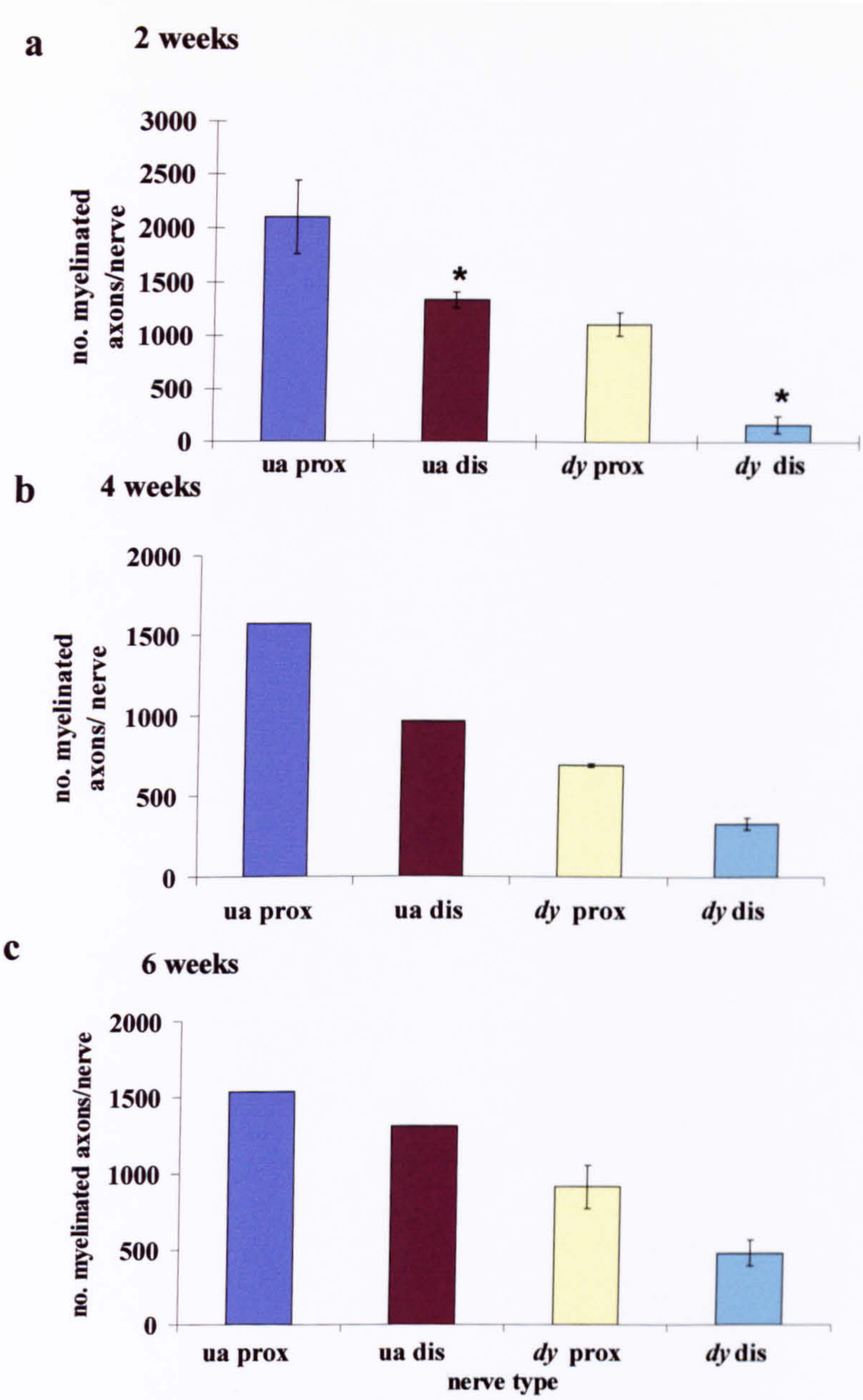

Figure 4.3: Remyelination following sciatic nerve crush is delayed and less extensive in the distal stump of *dy/dy* mice. The number of myelinated axons was quantified in the proximal (prox) and distal (dis) stumps of crushed *dy/dy* and unaffected (ua) sciatic nerves at 2, 4 and 6 weeks post-crush. **(a)** At two weeks post-crush, there is a significant (*, $p<0.05$) difference in the number of myelinated axons in the distal stump of unaffected and *dy/dy* mice (ua =1, *dy/dy* = 3). The proportion of myelin axons in the distal stump relative to the proximal stump is 14.9% in *dy/dy* nerves and 63.6% in unaffected nerves. **(b)** At 4 weeks there is an increase in the proportion of myelinated axons in the distal stump of *dy/dy* sciatic nerves to 47.9%, but this is still substantially less than in unaffected nerves at 61.3% (ua = 1, *dy/dy* = 2). **(c)** At 6 weeks post-crush remyelination is almost complete in unaffected nerves (85.1%), but in the distal stump of *dy/dy* nerves the proportion of myelinated axons (52.7%) was not substantially more than at 4 weeks (ua = 1, *dy/dy* = 2). Mean ± s.e.m.

Figure 4.4: Semi-thin sections of *dy/dy* sciatic nerves show that remyelination appears to be delayed 2 weeks post-crush. Light micrographs of toluidine blue-stained 1 μm resin sections of the distal stumps of sciatic nerves 0.4 cm distal to the crush. **(a)** In a transverse section of unaffected nerve, there are many myelinated axons visible. **(b)** Typically, there are no myelinated axons visible in transverse sections of *dy/dy* sciatic nerve. **(c)** Myelinated axons (thin arrow) are clearly visible in longitudinal sections of unaffected nerves 2 weeks post-crush. **(d)** Although Schwann cells are present (thin arrow), there is little evidence of remyelination in longitudinal sections of *dy/dy* sciatic nerve. Magnification x40. Scale bar = 40 μm.

Sciatic nerves were crushed by Professor Susan Standring, processed, stained and sectioned into semi-thin sections by the Electron Microscopy unit at Guy's hospital and photographed by Yael Uziyel.

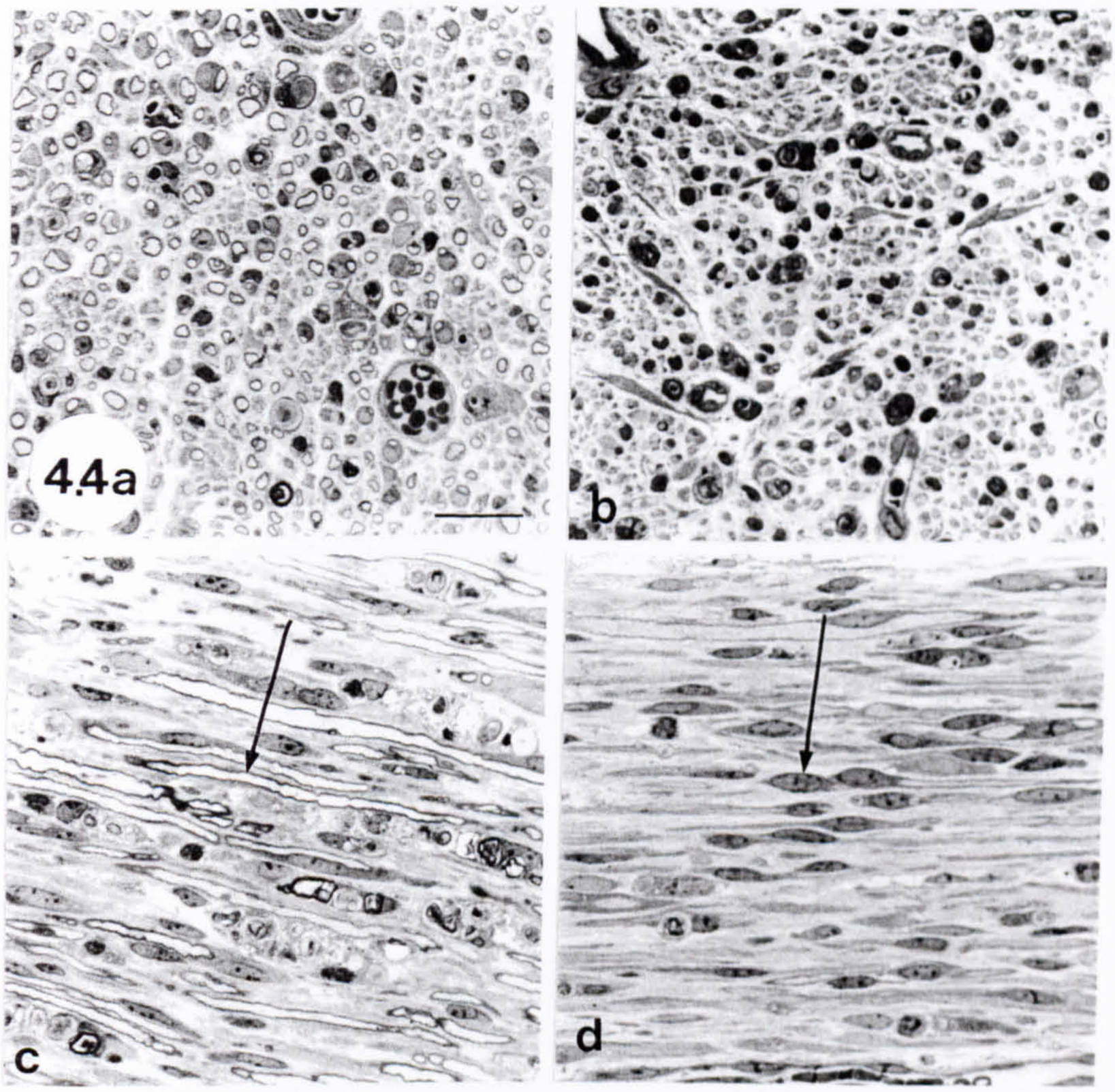
4.4a
b
c
d

Figure 4.5: Electron micrographs show that 2 weeks post-crush, remyelination in the distal stump of *dy/dy* sciatic nerves is delayed and abnormal. Electron micrographs of transverse sections of distal stumps of sciatic nerves 0.4 cm to crush, 2 weeks post-crush. **(a)** In unaffected nerves remyelination is widespread (thin arrows) and individual myelinated axons are each completely ensheathed by one Schwann cell (thick arrow). **(b)** In *dy/dy* nerves, the regenerating axons are not remyelinated and the associations between the axons and Schwann cells are abnormal. Schwann cells extend processes that surround but do not completely ensheath several axons and many axons are in direct contact with the basal lamina (thick arrows). **(c)** In *dy/dy* nerves, the axon has a very thin, uncompacted myelin sheath (thin arrow), but the Schwann cell ensheathing it also extends processes towards neighbouring unmyelinated axons (thick arrows). The basal lamina in these regenerating nerves is patchy (arrowhead). **(d)** Axons that are remyelinated in *dy/dy* sciatic nerves have a very thin myelin sheath, which usually remains uncompacted (thin arrows). **(e)** In regenerating *dy/dy* sciatic nerves, the basal lamina is patchy (arrowhead) and many large diameter axons are barely or incompletely ensheathed by Schwann cells (thick arrows). Magnification: (a, b) x6250, (c) x12500, (d) x15000, (e) x17500. Scale bar: (a, b) = 2 μm, (c) = 4μm, (d) = 4.8 μm, (e) = 5.6 μm.

Sciatic nerves were crushed by Professor Susan Standring, processed for electron microscopy by the Electron Microscopy unit at Guy's hospital and photographed by Professor Susan Standring.

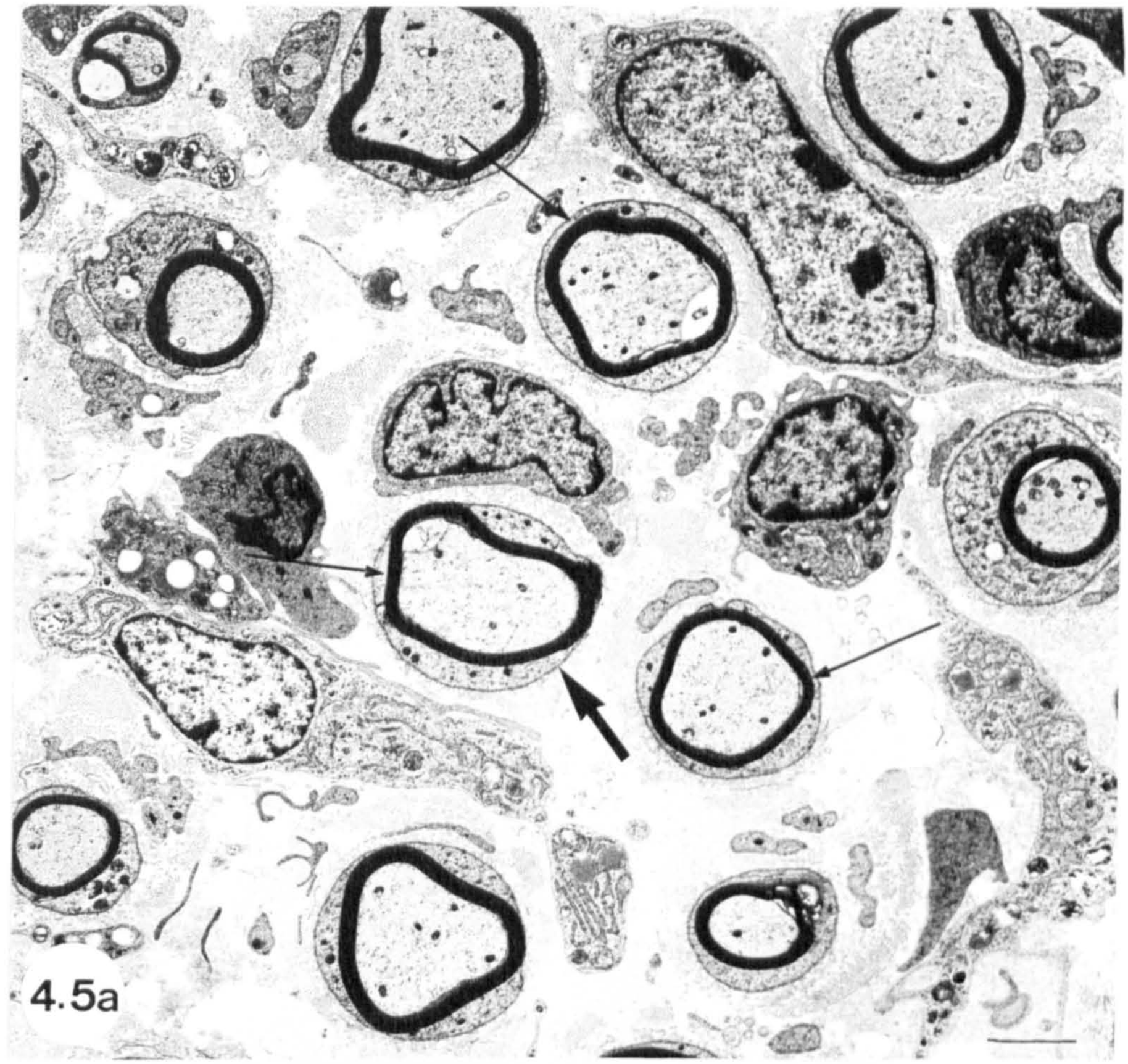
4.5a

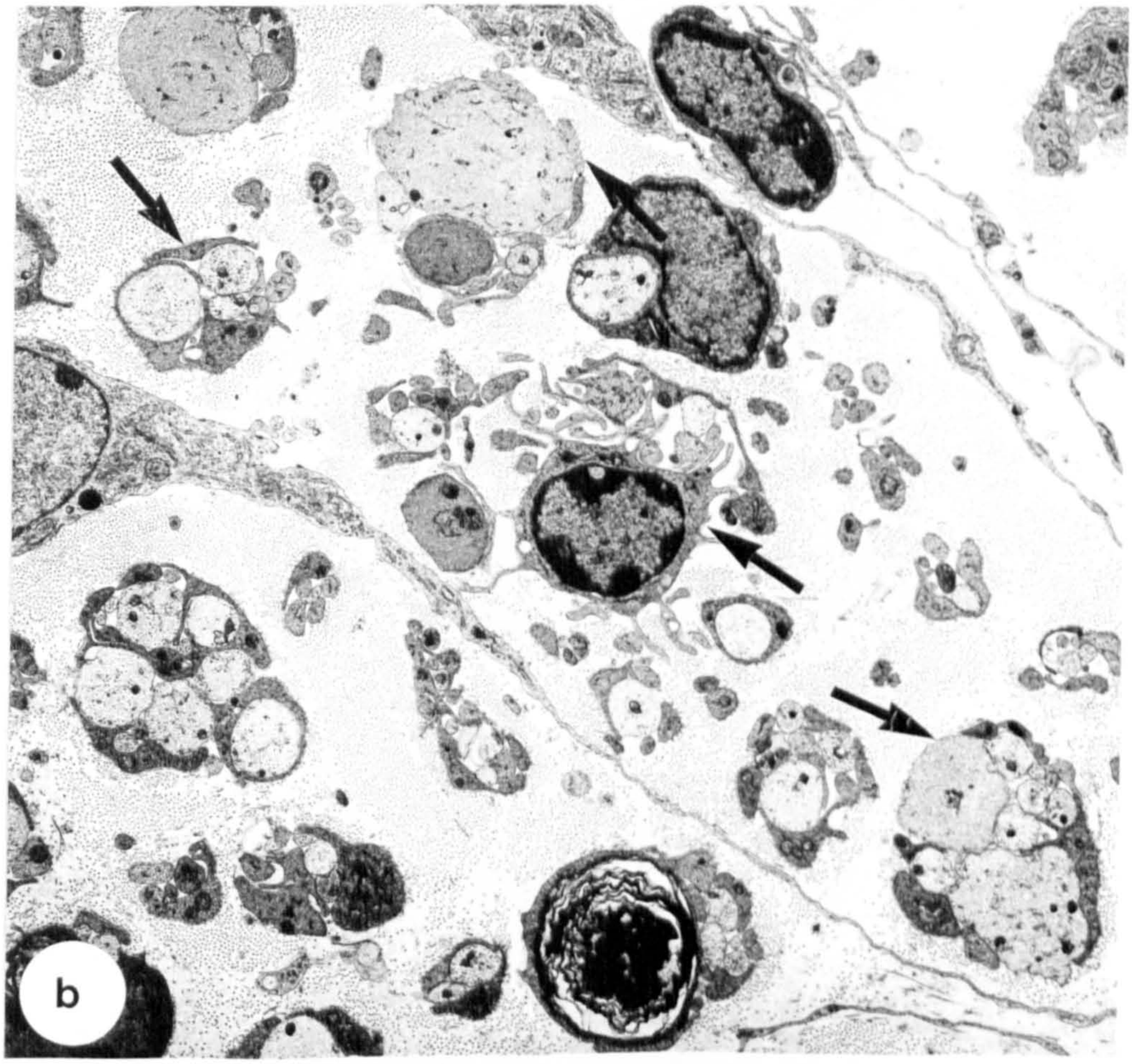
b

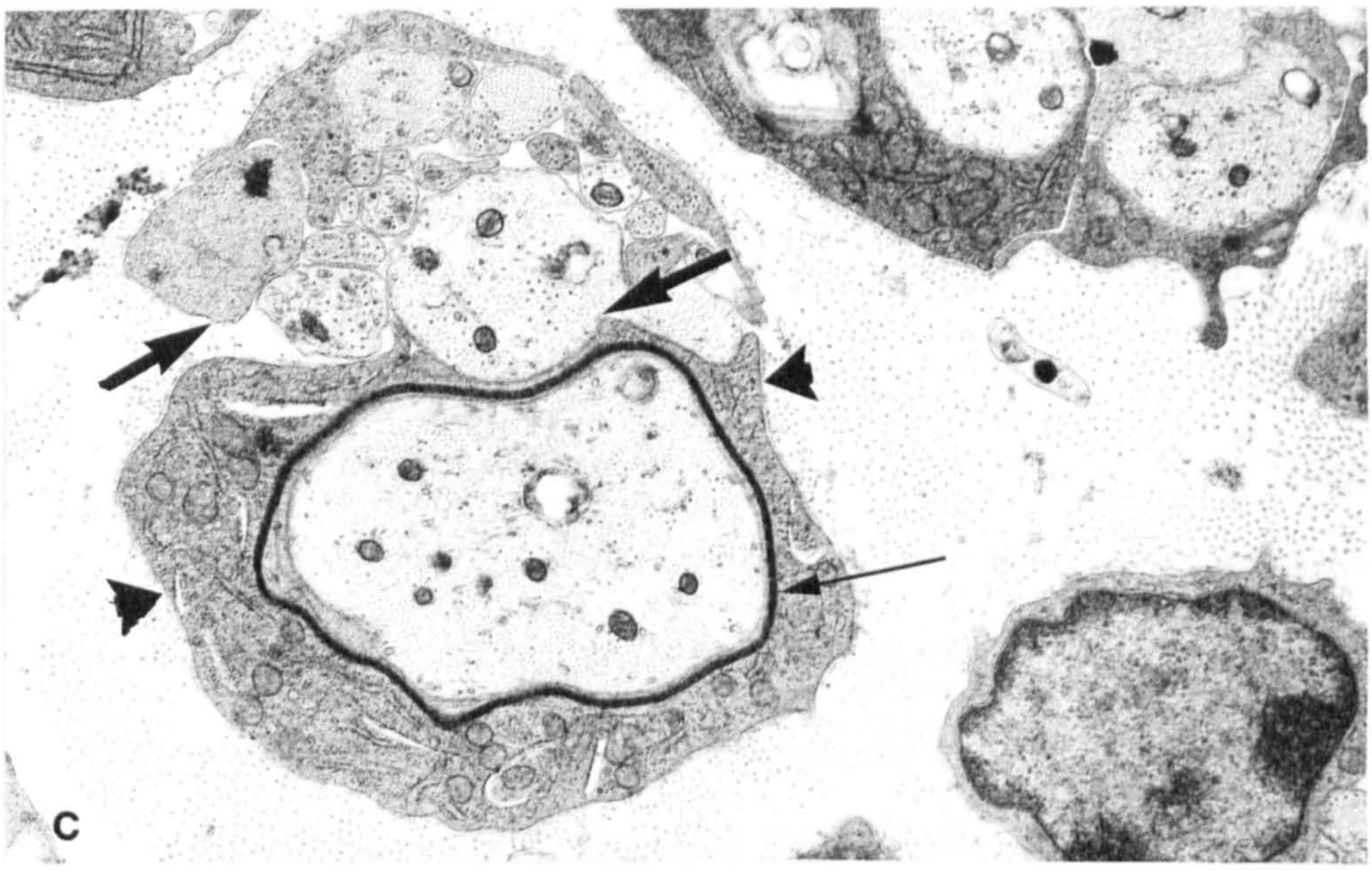
C

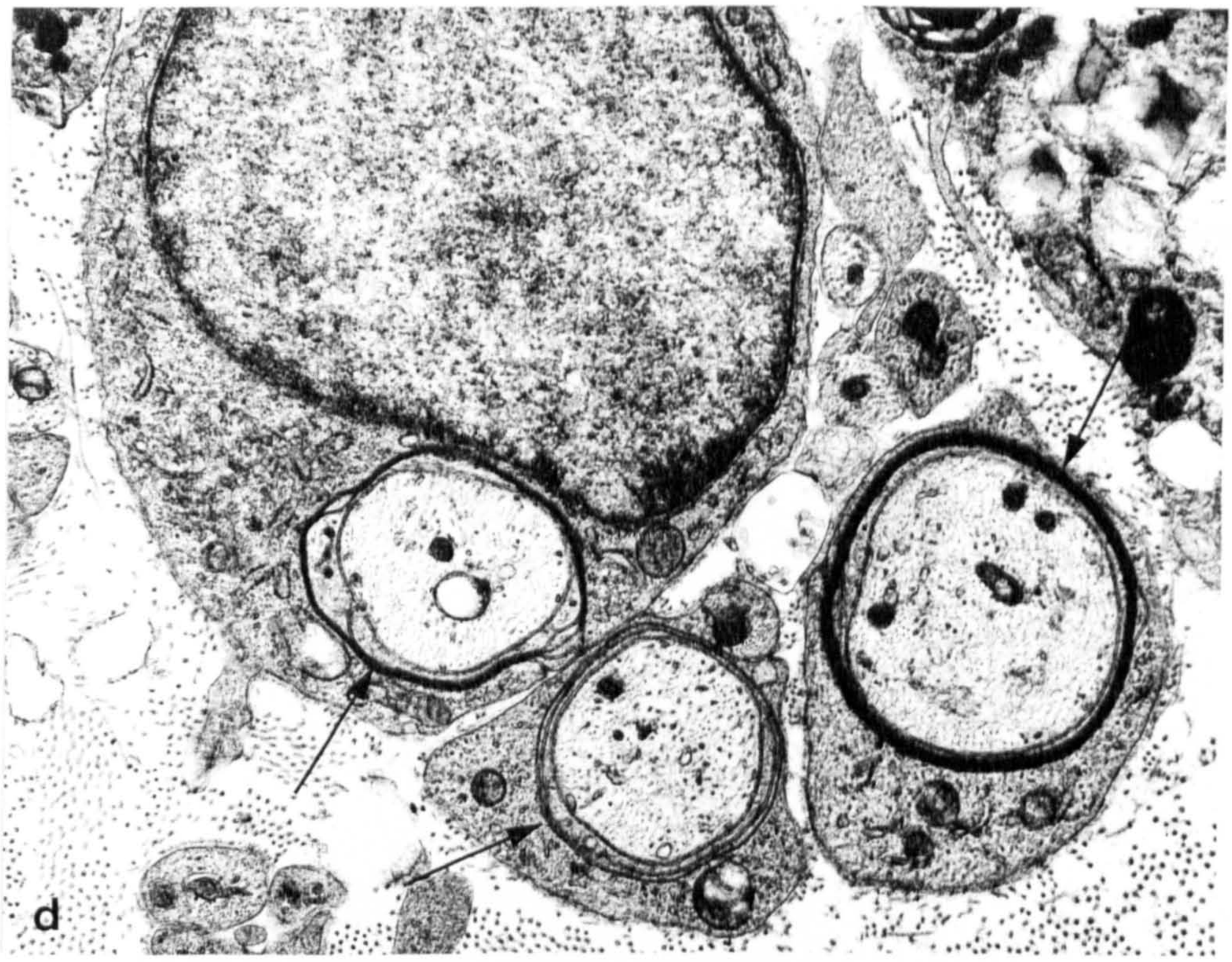
d

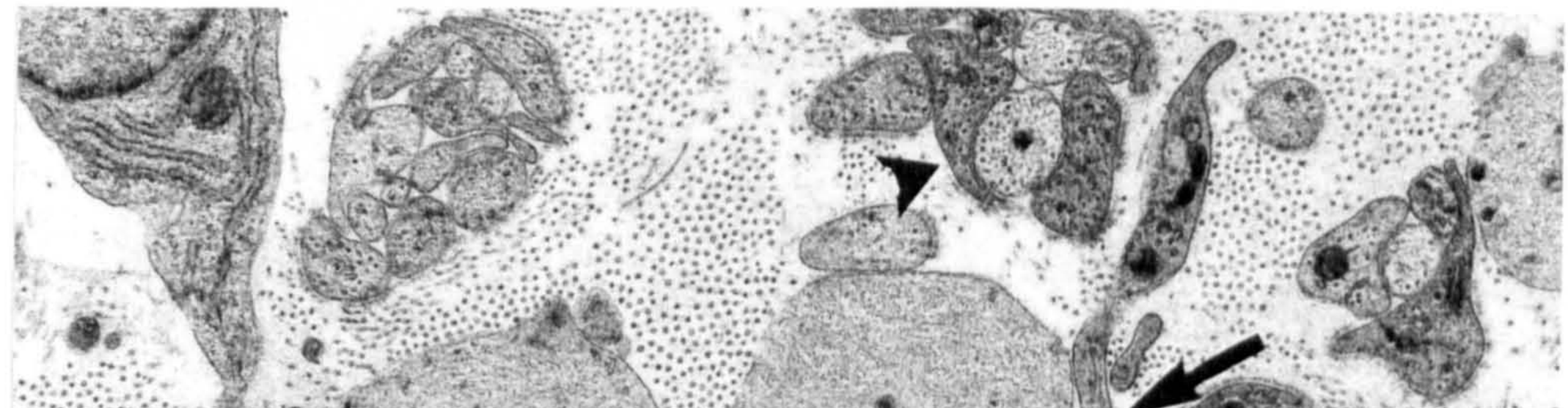
e

The deficit in *dy/dy* sciatic nerves also appears to have long-term consequences for nerve regeneration following crush injury. The proportion of myelinated axons in the distal stump relative to the proximal stump increased in *dy/dy* nerves but a substantial difference persisted in the number of remyelinated axons relative to unaffected mice for four (unaffected mice = 61.3% and *dy/dy* mice = 47.9% remyelinated) and six weeks (unaffected mice = 85.1%, *dy/dy* mice = 52.7% remyelinated) post-crush (fig. 4.3b, c; fig 4.6). In addition axon-Schwann cell relationships in regenerating *dy/dy* sciatic nerves were still clearly abnormal. Those axons that were ensheathed by Schwann cells could often be seen to form uncompacted myelin sheaths (fig. 4.7). At the six week timepoint many of the abnormalities observed in uninjured *dy/dy* nerves had become apparent in the regenerated nerves including patchy, discontinuous basal lamina around the axon-Schwann cell units, unensheathed axons and an abnormally high proportion of axons remained unmyelinated.

Figure 4.6: Semi-thin sections show that remyelination is still less extensive in *dy/dy* sciatic nerves 4 to 6 weeks post-crush Light micrographs of toluidine blue-stained transverse 1 μm resin sections of the distal stumps of sciatic nerves, 0.4 cm distal to the crush, 4 and 6 weeks post-crush. **(a)** In unaffected nerves, remyelination is extensive 4 weeks post-crush (thin arrow). **(b)** 4 weeks post-crush the distal stump of *dy/dy* nerves has begun to undergo some remyelination (thin arrow), but this is very limited. **(c)** 6 weeks post-crush remyelination in the unaffected nerves appears to be almost complete (thin arrow). **(d)** 6 weeks post-crush remyelination (thin arrow) in *dy/dy* sciatic nerves is more extensive than at 4 weeks but is still less widespread than at 4 weeks (b). Magnification x40. Scale bar = 40 μm.

Sciatic nerves were crushed by Professor Susan Standring, processed, stained and sectioned into semi-thin sections by the Electron Microscopy unit at Guy's hospital and photographed by Yael Uziyel.

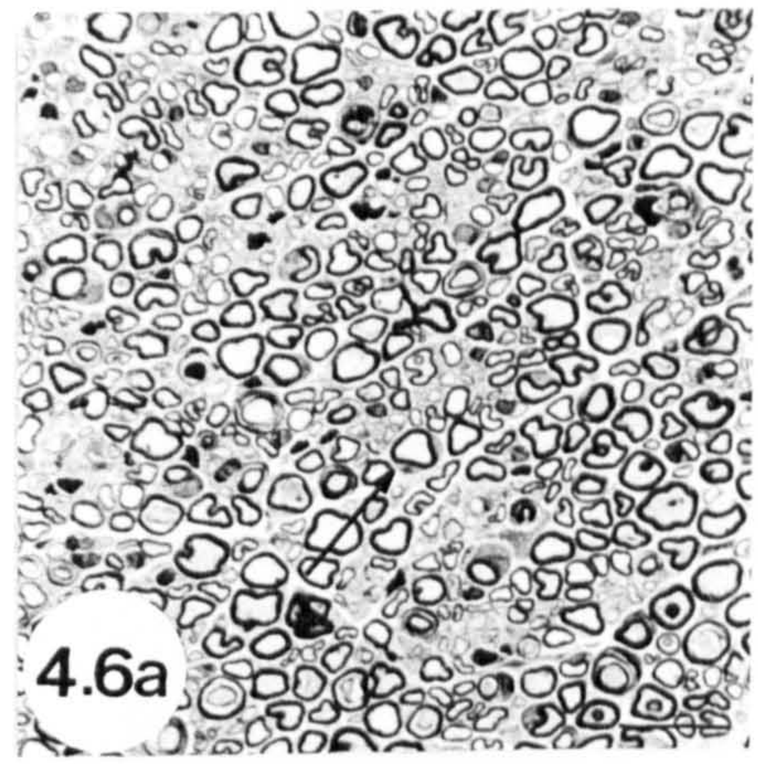
4.6a

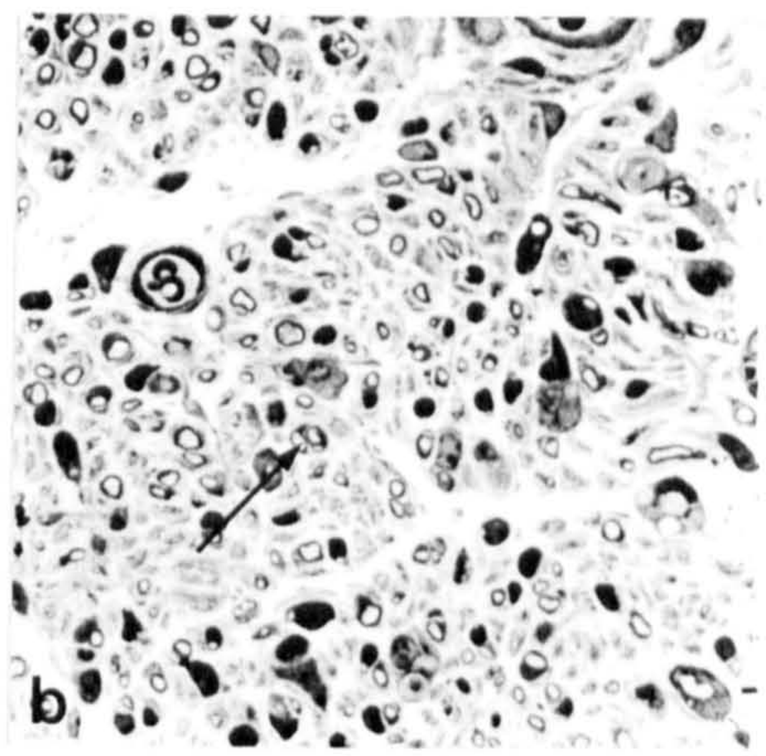
b

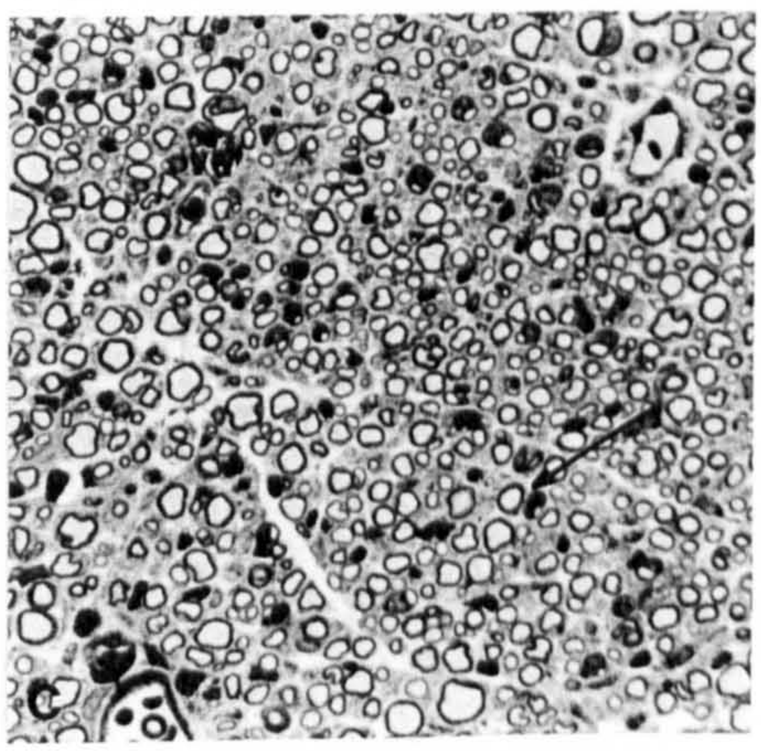
c

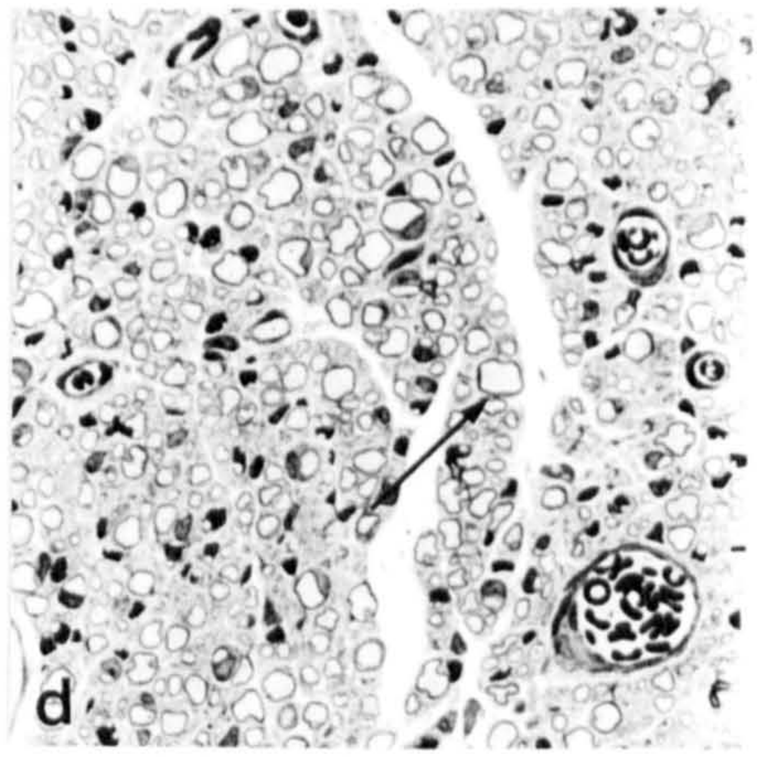
d

Figure 4.7: Electron micrographs show that remyelination is still less extensive and abnormal in *dy/dy* sciatic nerves 4 weeks post-crush. Electron micrographs of transverse sections of distal stumps of *dy/dy* sciatic nerves, 0.4 cm distal to the crush site, 4 weeks post-crush. (a) Some axons remain unmyelinated in regenerating *dy/dy* nerves. The basal lamina is patchy (arrowhead) and axons are incompletely ensheathed by Schwann cells that extend processes towards more than one axon, exposing some axons directly to basal lamina. (b) In remyelinated axons, the myelin sheath remains uncompacted (thin arrow). Magnification: (a) x25000, (b) x17500. Scale bar: (a) = 8 μm, (b) = 5.6 μm.

Sciatic nerves were crushed by Professor Susan Standring, processed for electron microscopy by the Electron Microscopy unit at Guy's hospital and photographed by Professor Susan Standring.

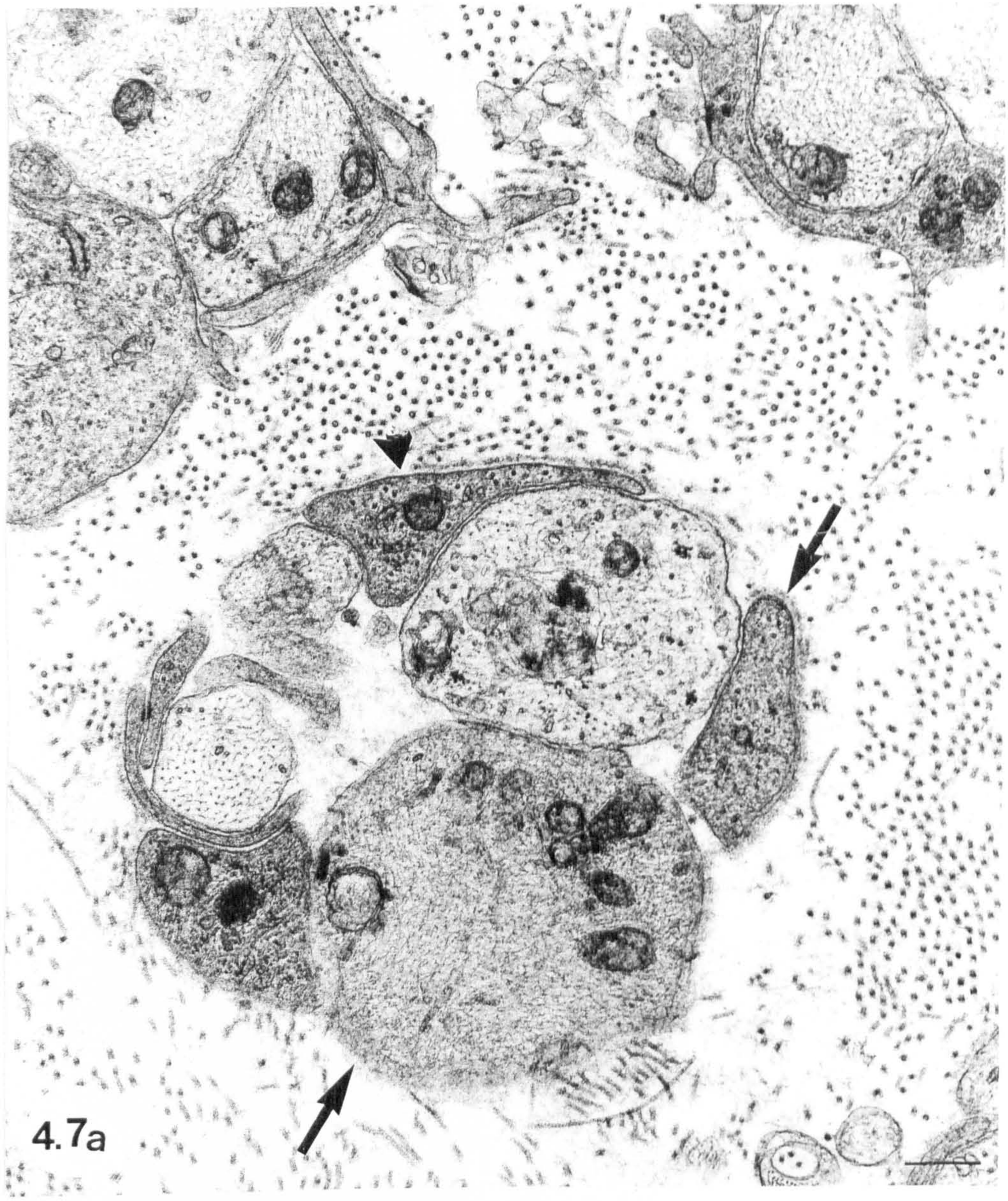
4.7a

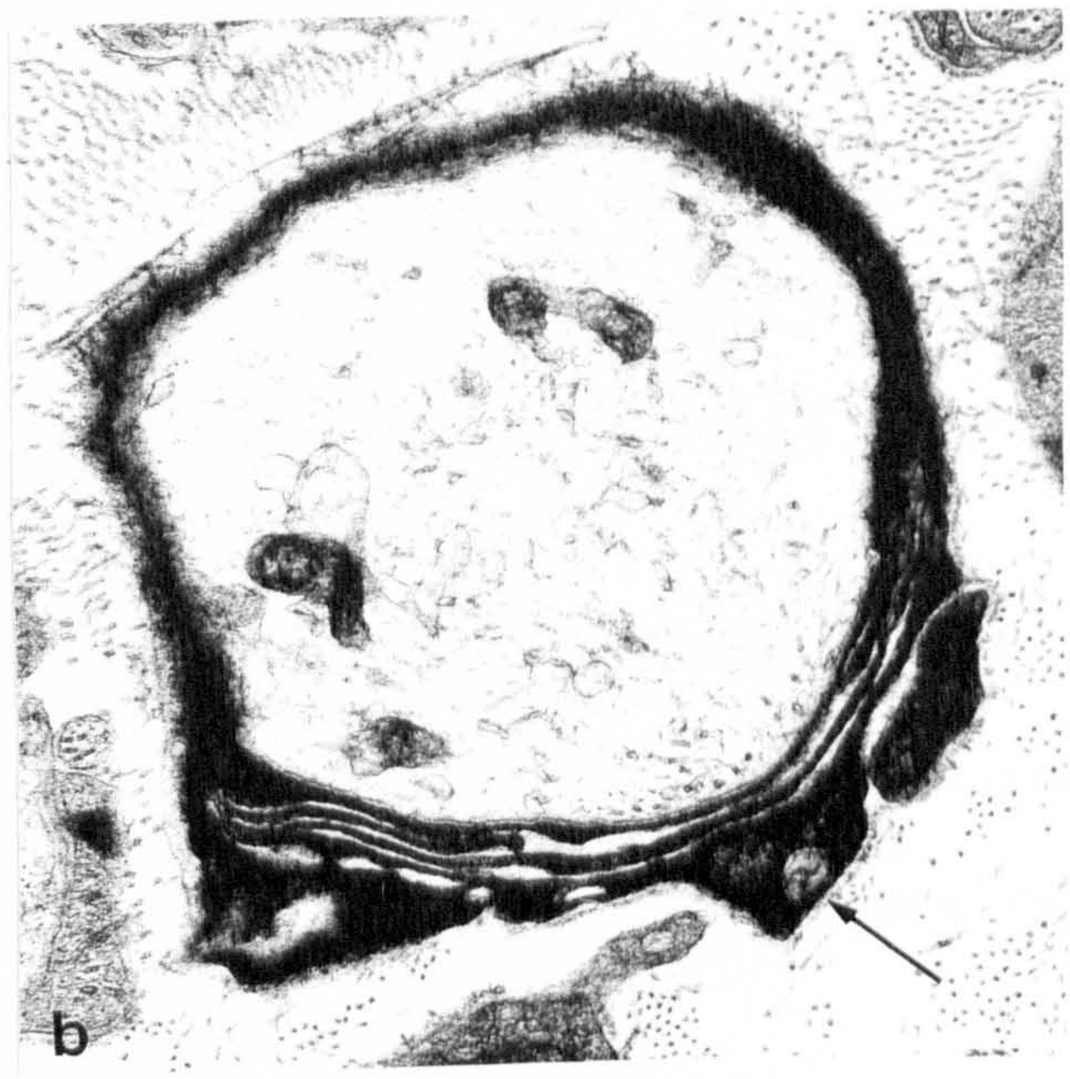
b

4.3: Discussion

4.3.1: Axon sprouting following transection is less extensive in the *dy/dy* mouse

Two weeks after a transection injury, the distal stumps of the cut sciatic nerves in both unaffected and *dy/dy* mice were immunopositive for the axonal marker PGP 9.5 meaning that axons had bridged the gap in both. However it was clear that axonal sprouting was far less extensive in the *dy/dy* sciatic nerves than in the unaffected nerves. This suggests that axons in the proximal stump of *dy/dy* nerves were surrounded by an environment less conducive to axonal sprouting.

Under normal circumstances, nerve regeneration following transection in the PNS is successful, as long as the gap between the two cut ends of the nerve is not too great. In this case the gap was only 0.5mm which was sufficiently small for the transected nerves in unaffected mice to successfully bridge the gap. Regenerating axons use the bands of Büngner and the Schwann cells aligned along these endoneurial basal lamina tubes to help guide them from the proximal to the distal stump. The severe deficit of laminin α2 chain in *dy/dy* mice means that they are incapable of forming a structurally intact endoneurial basal lamina and consequently Schwann cells are not able to interact normally with axons (Arahata, 1993; Bradley and Jenkison, 1973; Bradley and Jenkison, 1975; Madrid et al., 1975; Sunada et al., 1994; Xu et al., 1994a). This would most likely impair their ability to form bands of Büngner to use as conduits for the growing axons during regeneration.

Northern blot analysis of mRNA levels has shown that during regeneration proliferating Schwann cells in contact with axons produce increased quantities of the gene transcripts encoding lamin β1 and γ1 chains but not α1 chain (Doyu et al.,

1993). Schwann cells are however capable of producing the laminin α2 chain (Hsiao et al., 1993). Recent evidence suggests that the laminin α2 chain protein is induced and maintained by Schwann cell contact with regenerating axons, thus immunoreactivity was down-regulated during degeneration but was progressively upregulated during the process of regeneration (Masaki et al., 2000). Intense laminin immunoreactivity is detectable in the bands of Büngner 7-10 days after nerve crush or transection when axons have begun to extend towards the distal stump (Kuecherer-Ehret et al., 1990; Tona et al., 1993).

The migrating and proliferating Schwann cells help to create the bands of Büngner by the induction of laminin chain production during regeneration. The laminin chains detected so far during regeneration, the α2, β1 and γ1 chains, constitute the laminin-2 heterotrimer and it is therefore likely that the predominant or exclusive heterotrimer found in the bands of Büngner is laminin-2 (Doyu et al., 1993; Masaki et al., 2000). Blockade of laminin-2 activity both *in vivo* and *in vitro* has been shown to inhibit neurite outgrowth following Wallerian degeneration (Agius and Cochard, 1998; Anton et al., 1994a). Axonal regeneration in the PNS of *dy/dy* mice is most probably directly restricted by poorly formed bands of Büngner. Vacated endoneurial basal lamina tubes are discontinuous in *dy/dy* nerves and Schwann cell contact with axons during regeneration would not be able to induce adequate production and deposition of the laminin α2 chain by Schwann cells.

It is also likely that the activity of Schwann cells distally and in the bands of Büngner affects axon outgrowth. Transection of the sciatic nerve results in increased expression of the low affinity neurotrophin receptor, p75, in Schwann cells in the bands of Büngner (Taniuchi et al., 1986; Taniuchi et al., 1988). Once

the axons had extended through the bands of Büngner towards the distal stump, expression of the receptor was down- regulated. In DRG's neuronal expression of the p75 receptor is down-regulated while glial expression is upregulated following sciatic nerve transection (Zhou et al., 1996). When Schwann cells loose axonal contact, for instance following transection, they begin to dedifferentiate; immature and non-myelin-forming Schwann cells are known to express the p75 receptor, whereas mature myelin-forming Schwann cells do not (Jessen and Mirsky, 1991). *In vitro* Schwann cells migrate more rapidly on denervated NGF-rich sciatic nerve substrates than on NGF-poor intact substrates and blocking antibodies to both NGF and the p75 receptor partially inhibit Schwann cell migration (Anton et al., 1994b). Thus both the Schwann cell and its surrounding environment are in a state conducive to Schwann cell migration during regeneration. Moreover laminin-2 may play a role in regulating Schwann cell migration. Blockade of laminin-2 activity on denervated sciatic nerve substrates *in vitro* almost halves the rate of Schwann cell migration (Anton et al., 1994a). The lack of laminin-2 in the bands of Büngner of regenerating *dy/dy* nerves means that Schwann cell migration is probably compromised.

A deficit in Schwann cell migration may be a factor in the poor axonal sprouting observed in the transected nerves of *dy/dy* mice. During regeneration axons are always accompanied by migrating Schwann cells and axon outgrowth appears to be dependent on the active participation of proliferating and migrating Schwann cells (Feneley et al., 1991; Hall, 1986a; Hall, 1986b). In fact there is some evidence that Schwann cells may be leading axons during regeneration. When the cut end of a nerve was transplanted onto a soleus muscle, the axons and Schwann cells emerged

together from the cut end of the nerve and the axons were associated with Schwann cells along their entire lengths (Son and Thompson, 1995b). Usually the axons and Schwann cells were co-extensive but in some cases the tips of the Schwann cell processes were seen to be ahead while the axons appeared to be navigating along the Schwann cell processes. Moreover Schwann cell extension limits the rate of axonal regeneration; axons grew faster along pre-established Schwann cell processes than when Schwann cells accompanied them in their growth (Son and Thompson, 1995b). It is less clear whether this is the case during development, when neural crest is ablated in stage 13 chick embryos, thereby removing Schwann cells or Schwann cell precursors, motor axons will not grow into the forelimb (Noakes et al., 1988). If this is true then it would suggest that the motor axons were guided by the Schwann cells. However the HNK-1 antibody marker used by Noakes does not reliably distinguish between axons and Schwann cells and at this developmental stage it would be difficult to distinguish their leading processes morphologically.

Following transection the existing basal lamina tubes are destroyed. Even if the gap between the two cut ends of the nerve is relatively short, this presents a major obstacle to axonal regeneration and especially so in the *dy/dy* mice that are unable to produce one of the major constituents of the endoneurial basal lamina tubes. Laminin-2 has been shown to promote both neurite outgrowth *in vitro* and *in vivo* during regeneration and Schwann cell migration (Anton et al., 1994a; Cho et al., 1998; Cohen and Johnson, 1991; Engvall et al., 1992). The deficiency of a molecule capable of promoting two aspects of the regenerative process, axonal outgrowth and Schwann cell migration, means that axonal sprouting is poor in

transected *dy/dy* peripheral nerves.

4.3.2: Regeneration and remyelination is delayed and abnormal in *dy/dy* sciatic nerves following crush injury

As in transection, crush injury results in Wallerian degeneration but subsequent regeneration is usually more successful as the basal lamina tubes remain intact and Schwann cells are not required to migrate as extensively. Thus crushing the sciatic nerves of *dy/dy* mice resulted in more extensive axonal regeneration and allowed us to investigate in more detail axon-Schwann cell interactions in the absence of laminin-2. In previous studies, crush injuries to the peripheral nerves of *dy/dy* or dy^{2j}/dy^{2j} were shown to result in improvements in the extent of Schwann cell ensheathment, myelination and basal lamina coverage compared to the intact nerve (Bray et al., 1983; Stirling, 1975b). Our findings show that in fact the morphological abnormalities observed in intact *dy/dy* peripheral nerves are recapitulated in regenerating nerves. Although the degenerative process appeared to proceed normally in *dy/dy* nerves, mutant mice were unable to remyelinate the axons at a comparable rate and as efficiently. The electron micrographs showed that although axons were present in the distal stumps of *dy/dy* nerves at two weeks post-crush, only 14.9% of the axons in the bands of Büngner were myelinated compared to 63.6% in unaffected nerves. Differences in the extent of remyelination persisted up to the last time point examined, at 6 weeks post-crush 85.1% of axons were remyelinated in unaffected nerves compared with 52.7% in mutant nerves. In addition, axonal ensheathment by *dy/dy* Schwann cells was abnormal and in many cases incomplete (Uziyel et al., 2000), allowing frequent direct apposition of axons. Also myelination in the *dy/dy* nerves was abnormal; the myelin sheath was often

uncompacted and frequently extended to neighbouring axons.

Despite the establishment of some axonal contact by Schwann cells in regenerating *dy/dy* peripheral nerves following crush injury *dy/dy* Schwann cells cannot be induced to produce the α2 chain. Unaffected Schwann cells in regenerating nerves are induced to produce the α2, β1 and γ1 chains necessary to form the laminin-2 heterotrimer (Doyu et al., 1993; Masaki et al., 2000). The production of basal lamina is a requirement for Schwann cell-axon interactions prior to Schwann cell differentiation and myelination (Carey et al., 1986; Eldridge et al., 1989). Schwann cell contact with the basal lamina causes the Schwann cells to cease proliferating; the Schwann cells then differentiate and undergo a change in morphology, elongating and ensheathing and aligning themselves along the axon and eventually producing myelin (Carey et al., 1986; Obremski and Bunge, 1995; Obremski et al., 1993a; Obremski et al., 1993b). Suspended nerve fascicles sometimes form in long-term cultures of sensory ganglia explants. When Schwann cells in these cultures are deprived of contact with the ECM these fascicles begin to exhibit Schwann cell abnormalities resembling those seen in *dy/dy* mice including instances of incomplete ensheathment of axons (Bunge and Bunge, 1978). Recently, myelination was shown to occur *in vitro* in co-cultures of Schwann cells and DRG neurons in the absence of a basal lamina (Podratz et al., 1998), but at a much reduced rate and extent, reminiscent of the *dy/dy* mouse *in vivo*.

In the regenerating nerves of *dy/dy* mice some axons grew along the outer aspects of the Schwann cells in the bands of Büngner in direct contact with the basal lamina (fig. 4.5, 4.7). Without direct contact with the basal lamina or exposure only to patchy, laminin-2 deficient basal lamina Schwann cells in the *dy/dy* mice were not

able to differentiate fully and ensheathe the axons adequately. In fact the bundles of completely unensheathed axons and the loose ensheathment of other axons by Schwann cells in regenerating *dy/dy* nerves sometimes resembled an embryonic phenotype and recapitulated the abnormalities seen in the intact nerves (Bradley and Jenkison, 1973; Uziyel et al., 2000).

These findings are consistent with a specific role for laminin-2 in determining the polarity of differentiated Schwann cells *in vivo*. It has been clear for some time that basal lamina induces Schwann cell differentiation and elongation *in vitro* (Carey et al., 1986; Obremski and Bunge, 1995; Obremski et al., 1993a; Obremski et al., 1993b). The abnormal morphology of *dy/dy* Schwann cells both *in vivo* and *in vitro* (Uziyel et al., 2000) (see chapter 6.2.6) suggests that it is the laminin α2 chain component of the endoneurial basal lamina that specifically regulates this aspect of their morphology. This is also true of terminal Schwann cells; abnormal Schwann cell process extension into the synaptic cleft has been observed at the NMJ of *dy/dy* mice (Banker et al., 1979). The synaptic basal lamina normally contains laminin-4, an α2 chain-containing laminin. Its absence in the synaptic basal lamina of *dy/dy* mice may account for the abnormal polarity of *dy/dy* terminal Schwann cells. Regulation of Schwann cell polarity is not exclusive to α2 chain laminins as inappropriate extension of terminal Schwann cell processes into the synaptic cleft has also been observed in mice deficient in the synaptic laminin, laminin-11 (Patton et al., 1998). Thus it appears that specific laminin heterotrimers actively control the polarity of Schwann cells and constrain process extension.

Chapter 5: The role of laminin-2 in Schwann cell migration

5.1: Introduction

During both development and regeneration Schwann cell migration is an important process in establishing a normally functioning peripheral nerve. Schwann cell precursors are generated from neural crest cells at around E14-15 in rats and E12-13 in mice (Jessen and Mirsky, 1999). During development these precursors co-migrate with the growth cones extended by embryonic peripheral axons. As they begin to differentiate into immature Schwann cells at around E17 in rats and E15 in mice, they migrate further along the nerve bundles, extend cytoplasmic processes and begin to subdivide the nerve into smaller bundles (Ziskind-Conhaim, 1988). This results in each axon being individually enwrapped by a Schwann cell, prior to myelination during the first few postnatal weeks. Whilst it has been claimed that during development Schwann cells appear to precede the axonal growth cones, the antibody marker used was not Schwann cell-specific (Noakes and Bennett, 1987; Noakes et al., 1988). There is stronger *in vivo* evidence that Schwann cells can migrate and extend processes ahead of growth cones during regeneration (Son and Thompson, 1995b).

Schwann cell migration following injury to peripheral nerves is of particular importance in establishing a conduit for regenerating axons. Regenerating axons extending from the proximal stump of the injured nerve along the bands of Büngner are always accompanied by migrating Schwann cells (Feneley et al., 1991). Thus basal lamina tubes alone are not sufficient to support axonal regeneration, neurites are rarely seen to extend towards the distal stump in regenerating nerves if Schwann cells are not present or are prevented from proliferating and migrating

(Feneley et al., 1991; Hall, 1986a; Hall, 1986b).

Schwann cell migration *in vitro* has been shown to be promoted by a variety of ECM molecules and by molecules expressed by the Schwann cells themselves. Fibronectin, laminin-1 and laminin-2 have been shown to promote integrin-mediated Schwann cell migration (Milner et al., 1997). Migrating Schwann cells in regenerating nerves align themselves along the bands of Büngner. These endoneurial basal lamina tubes are rich in laminin-2. Blocking of laminin-2 activity *in vitro* on denervated sciatic nerve substrates inhibits both neurite outgrowth and Schwann cell migration (Anton et al., 1994a). Other ECM molecules influence migration of CNS cells *in vitro* too; vitronectin promotes astrocyte migration and both fibronectin and laminin-2 promote the migration of oligodendrocyte precursor cells whereas tenascin-C inhibits the migration of these precursors (Frost et al., 1996; Kiernan et al., 1996; Milner et al., 1999). The Schwann cell surface membrane protein CD9 promotes Schwann cell migration on intact nerve substrates in cryoculture (Anton et al., 1995).

Schwann cell migration has been studied long-term *in vivo* following injury to the nerve but *in vitro* techniques such as those used to study molecules involved in Schwann cell, oligodendrocyte and astrocyte migration provide a more accessible method to assay migration. Cryoculture involves the use of unfixed tissue sections such as peripheral nerves, as substrates for cell migration. In sections of intact peripheral nerves the basal lamina is exposed as well as the cell membranes of Schwann cells and of axons. It has been widely used to assay both Schwann cell migration and neurite outgrowth on intact and denervated peripheral nerve substrates and usually involves the use of blocking antibodies to determine the role

of specific molecules in these processes (Agius and Cochard, 1998; Anton et al., 1995; Anton et al., 1994a; Anton et al., 1994b). Sections of intact sciatic nerve provide a substrate that includes Schwann cells and axons and the molecules they express as well as the basal lamina and its molecular components. Sections of intact *dy/dy* peripheral nerves are lacking in the laminin-2 component of the endoneurial basal lamina and as such provide a means to investigate the extent to which laminin-2 is involved as a substrate for Schwann cell migration (see chapter 6.2.4 for its role in regulating the intrinsic motility of Schwann cells).

Neonatal rat DRG explants were plated onto cryosections of sciatic nerve and the extent of Schwann cell migration was visualised by labelling DRG explants with the CMFDA cell tracker dye. CMFDA is taken up by growing neurites but predominately by migrating Schwann cells; it is membrane permeable and diffuses into living cells where the chloromethyl moieties react with intracellular thiols and the acetate groups are cleaved by cytoplasmic esterases to produce a fluorescent product. This fluorescence could then be visualised on an Axioskop microscope with epifluorescence optics. I firstly determined that the rate of Schwann cell migration in the cryoculture assay was linear over an extended period of time *in vitro* and that it compared favourably with rates of Schwann cell migration measured *in vivo*. The cyroculture migration assay showed that intact laminin-2-deficient *dy/dy* sciatic nerves are significantly less efficient as a substrate for Schwann cell migration. Moreover a normal rate of migration could be restored by pre-treating *dy/dy* sciatic nerve substrates with exogenous laminin-2.

5.2: Results

5.2.1: Measurement of rat Schwann cell migration *in vitro*

The rate of Schwann cell migration from rat neonatal DRG explants in cryoculture for periods up to 65 hours was initially determined using sections of homologous normal adult rat sciatic nerve as a substrate (fig. 5.1a). These experiments allowed me to validate the cryoculture system and to determine:

a) Whether the rate of Schwann cell migration remained constant over extended periods *in vitro*.

b) Whether the rate of Schwann cell migration in cryoculture and *in vivo* were comparable.

The distance migrated by CMFDA-labelled rat Schwann cells was measured from digitised images and defined as the distance from the central point of the explant to fluorescent-labelled cells at the leading edge of the outgrowth zone (fig. 5.1a). Schwann cells were distinguishable by their morphology and in some of the cryoculture experiments axons were counterstained with an antibody to GAP-43 to help distinguish between neurites and Schwann cells (not shown). The rate of Schwann cell migration in these cryoculture experiments measured at three time points was found to be linear (correlation coefficient = 0.996) (fig. 5.1b). The average rate of Schwann cell migration of 22 μm/hour in homologous rat cryoculture experiments, compared well with reported rates of migration in regenerating nerves *in vivo* of approximately 10-30 μm/hour (Anderson et al., 1991; Daniloff, 1991; Feneley et al., 1991). However some component of the Schwann cell migration measured in these and consequent Schwann cell migration assays in chapters 5 and 6.2.4 may be due to Schwann cell division as well.

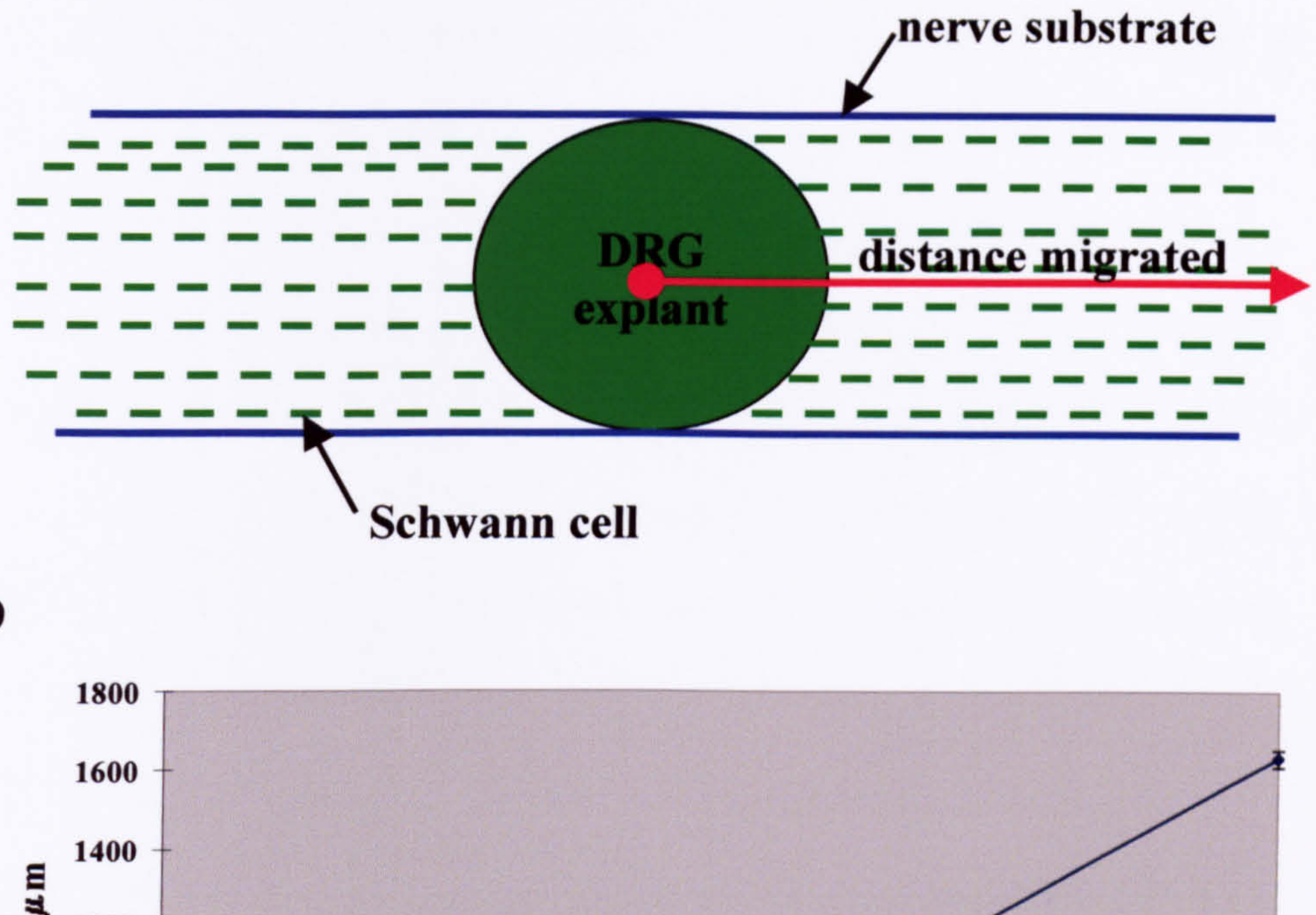

Figure 5.1: Rat Schwann cells migrate from DRG explants for up to 65 hours at a linear rate on cryosections of rat sciatic nerve. (a) Neonatal rat DRG's were plated onto sections of rat sciatic nerve. After 24, 40 and 60 hours the living Schwann cells were labelled with a cell tracker dye, CMFDA. The explants were fixed and the distance migrated determined as the distance from the centre of the explant to the leading edge of the migrating Schwann cells. **(b)** Graph of the distance the Schwann cells migrated at 24 hours (n = 74), 40 hours (n = 120) and 65 hours (n = 99). The correlation coefficient of 0.996 is consistent with a linear rate of migration over 65 hours of 22 µm/hour. Mean ± s.e.m. This experimental paradigm was carried out at least 10 times.

5.2.2: Rat Schwann cell migration is slower on *dy/dy* sciatic nerve substrates

A heterologous cryoculture system allows for species-specific labelling or manipulation of cells and molecules in the cryoculture. Modification of the cryoculture technique to a heterologous system such that P3 rat DRG explants were plated onto sections of normal mouse sciatic nerve resulted in a rate of migration comparable to that seen in homologous cryoculture experiments. P3 rat DRG explants were plated onto sections of sciatic nerve from either unaffected or *dy/dy* mice. In previous experiments where the effect of laminin-2 on Schwann cell migration has been measured using blocking antibodies, the activity of other laminin chains or heterotrimers may also have been blocked (Anton et al., 1994a). It was found that Schwann cell migration was significantly reduced ($p<0.01$) on the *dy/dy* sciatic nerve substrates (fig. 5.2, 5.3a). Schwann cells migrated 1148.1 μm over a 40 hour time period (28.7 μm/hour) on unaffected nerve substrates and 961.5 μm on *dy/dy* nerve substrates (24 μm/hr), a reduction in the rate of migration of 16.4%.

The myelination abnormality in *dy/dy* mice is more severe proximal to the spinal cord. The reasons for this are unclear but may be due to a greater deficit of laminin-2 in proximal nerves. I therefore investigated whether the rate of Schwann cell migration was more affected on sections of *dy/dy* sciatic nerve proximal to the spinal cord. Although the average rate of migration on sections of *dy/dy* sciatic nerve proximal to the spinal cord (21.33 μm/hr) was marginally less than the rate

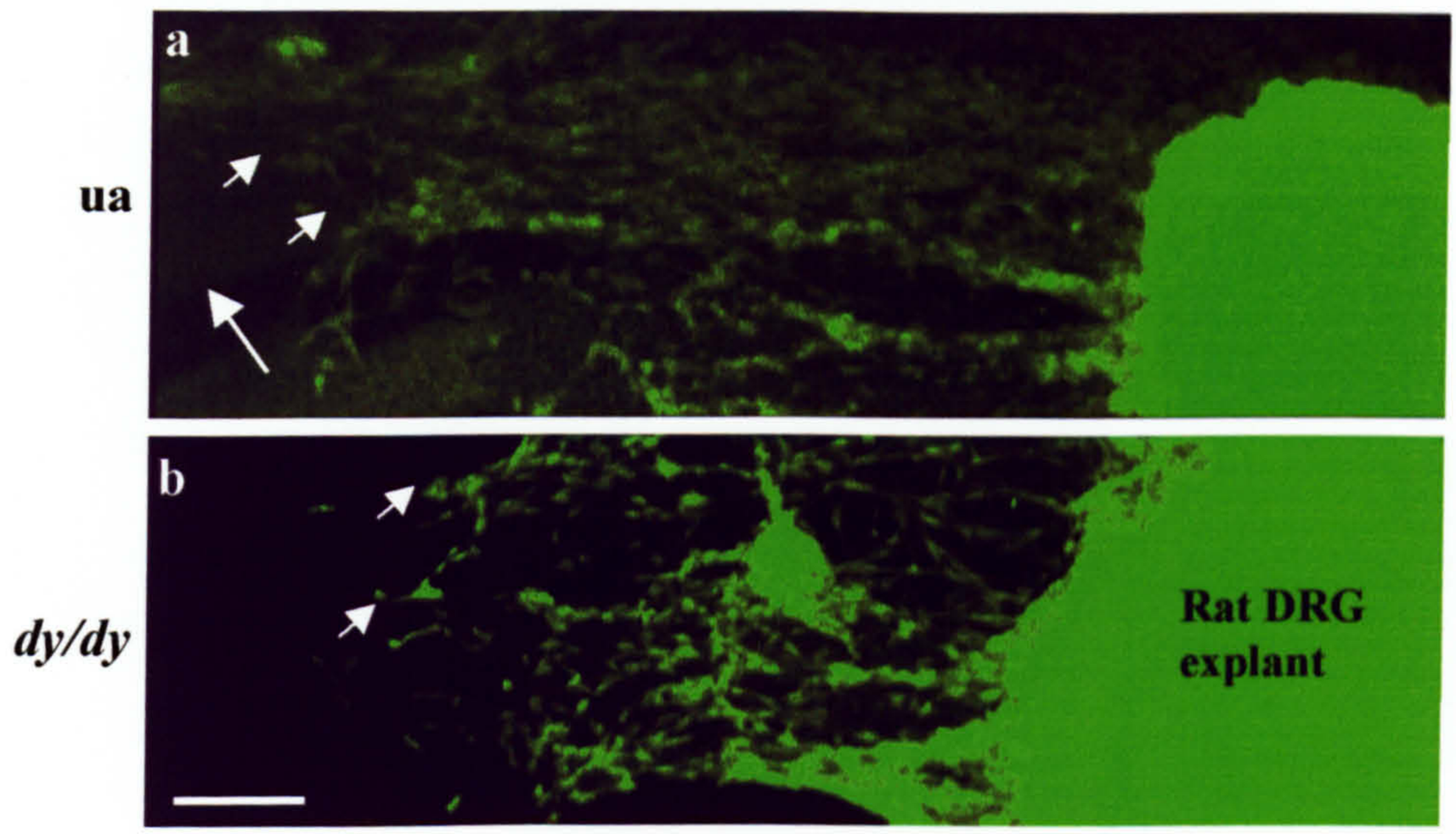

Figure 5.2: Rat Schwann cells migrated at a reduced rate on *dy/dy* sciatic nerve substrates. Neonatal rat DRG explants were placed on sections of unaffected (ua) and *dy/dy* sciatic nerves. After 40 hours they were stained with the cell tracker dye CMFDA, fixed and the distance migrated measured at the leading edge of the Schwann cells (arrowheads). **(a)** Schwann cells mig -rating on an unaffected mouse sciatic nerve substrate. The underlying nerve is just visible (arrow). **(b)** Schwann cell migration on a *dy/dy* mouse sciatic nerve substrate is substantially less than on unaffected nerve substrates. Magnification x10. Scale bar = 250 μm.

Figure 5.3: The rate of Schwann cell migration is significantly reduced on *dy/dy* mouse sciatic nerve substrates from portions of sciatic nerve both distal and proximal to the spinal cord. Neonatal rat DRG explants were initially plated on random portions of *dy/dy* or unaffected (ua) sciatic nerve (a), then in subsequent experiments on cryosections cut from portions of sciatic nerve either distal or proximal to the spinal cord (b). The explants were stained with the cell tracker dye CMFDA and fixed after 40 hours *in vitro*. The distance migrated by Schwann cells was assessed using digitised images. **(a)** Schwann cell migration was significantly reduced on random portions of *dy/dy* sciatic nerve (*, $p<0.01$). Schwann cells migrated 961.5 ± 15.5 μm on *dy/dy* sciatic nerve substrates, a 16.4% reduction compared to migration on unaffected sciatic nerve substrates, which averaged 1148.1 ± 21 μm. **(b)** Schwann cell migration was significantly reduced on proximal portions (**, $p<0.01$) of *dy/dy* sciatic nerve compared to unaffected nerve. Migration was 853.2 ± 25.7 μm on proximal *dy/dy* sciatic nerves and 985.9 ± 25.7 μm, a reduction of 13.5%. Migration was also significantly reduced on distal portions of *dy/dy* sciatic nerve (***, $p<0.01$) by 14.2% compared to Schwann cell migration on distal portions of unaffected sciatic nerve. Schwann cells migrated 1033 ± 16.6 μm on distal portions of unaffected nerve and 886.5 ± 18.3 μm on distal portions of *dy/dy* sciatic nerves. There was no significant difference between the reduction in Schwann cell migration on distal and on proximal portions of *dy/dy* sciatic nerve. Mean ± s.e.m. Schwann cell migration assay experiments were carried out at least 10 times on random sections of nerve and at least 4 times on using proximal/distal portions of sciatic nerve.

5.3a

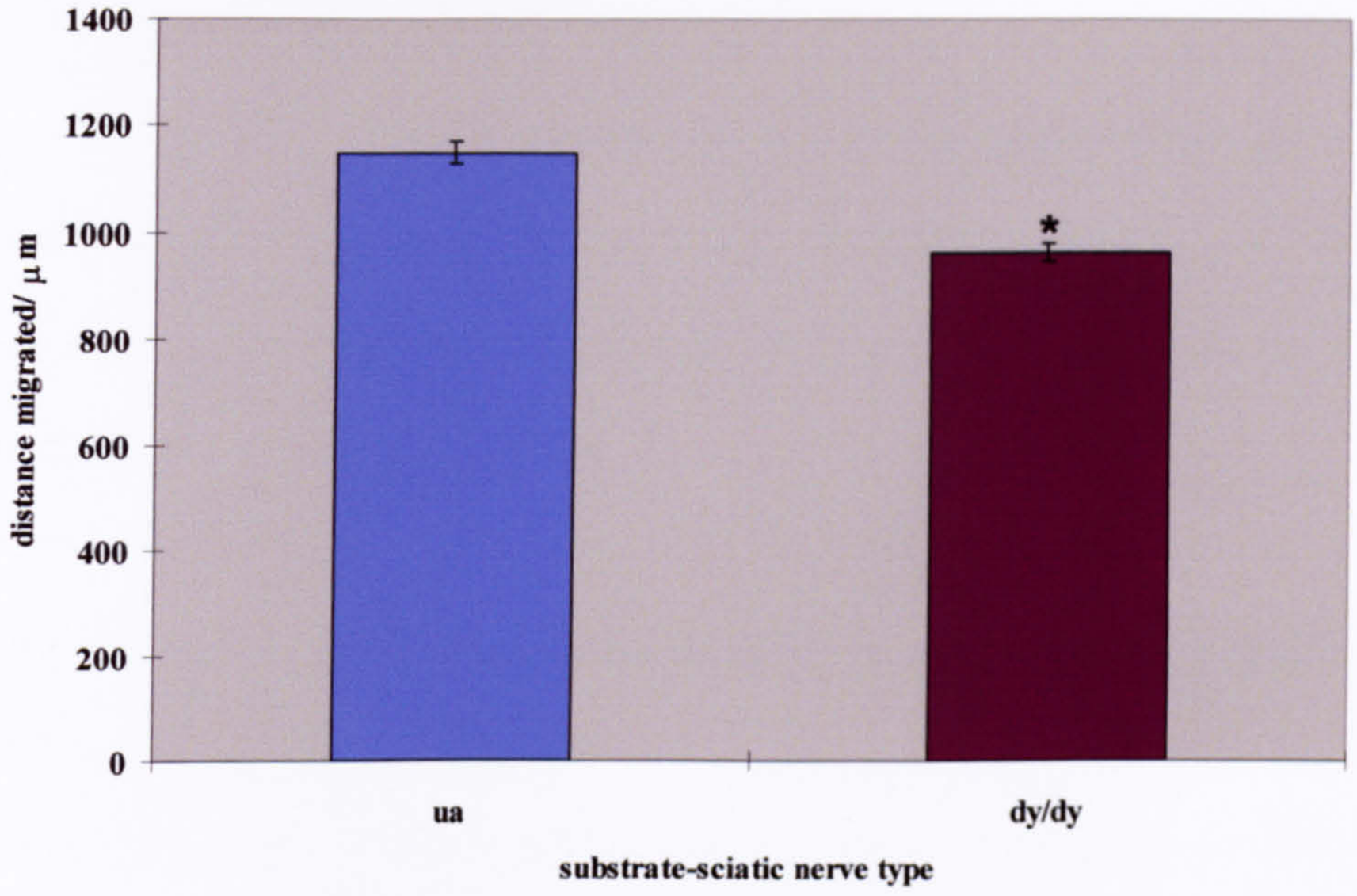
1400
1200
1000
800
600
400
200
0
distance migrated/ μ m
*
ua
dy/dy
substrate-sciatic nerve type

b

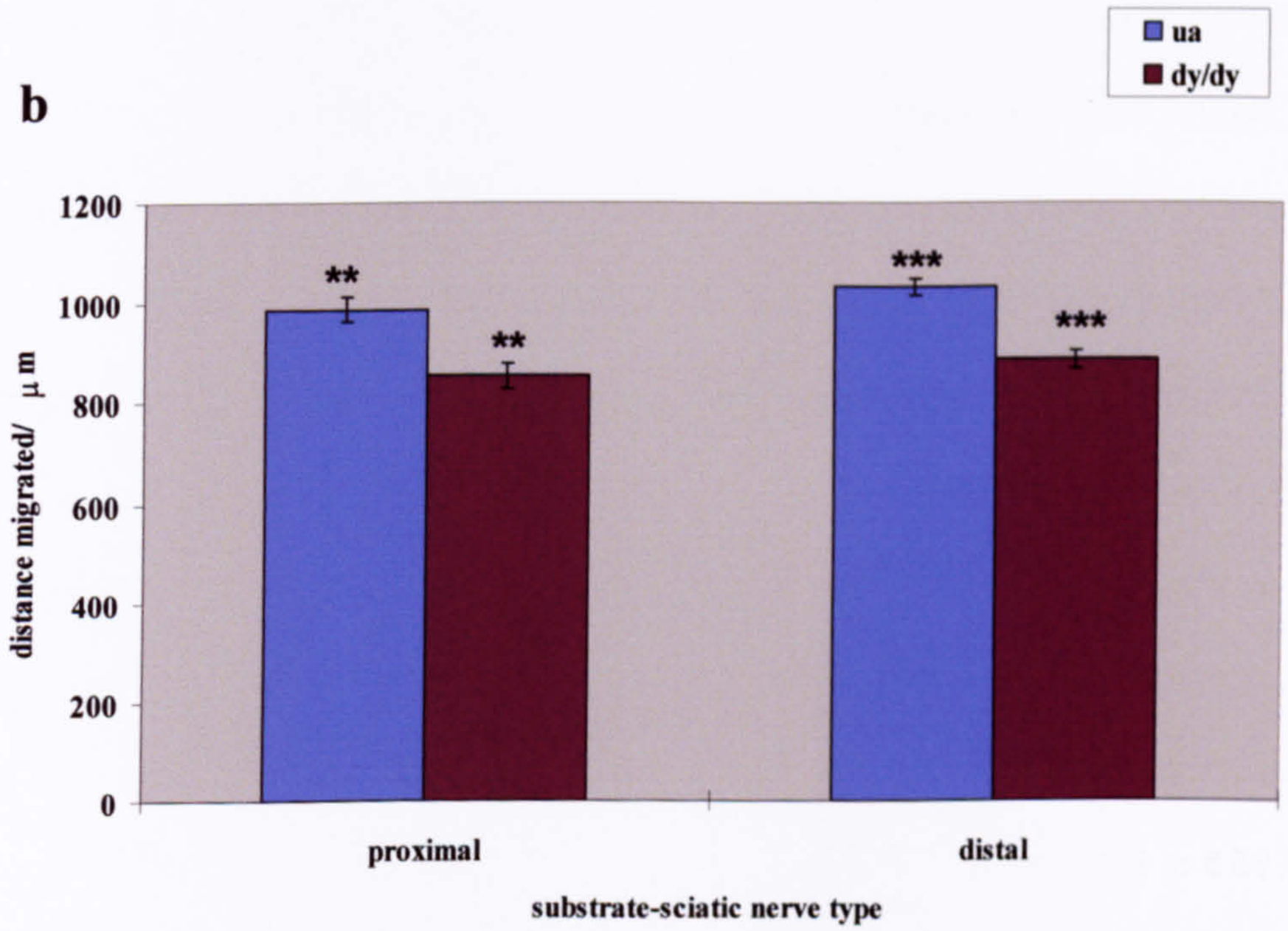
ua
dy/dy
1200
1000
800
600
400
200
0
distance migrated/ μ m
**
**
***
***
proximal
distal
substrate-sciatic nerve type

on sections of distal nerve (22.16 μm/hr), this difference was not statistically significant. In fact, Schwann cells also migrated marginally faster on distal (25.83 μm/hr) than on proximal unaffected nerves (24.65 μm/hr) (fig. 5.3b). Moreover the rate of Schwann cell migration on *dy/dy* nerves was significantly less on both distal and proximal sections of nerves ($p<0.01$).

5.2.3: The reduced rate of rat Schwann cell migration on *dy/dy* sciatic nerves is compensated by exogenous laminin-2

To determine whether the above reduction in the rate of migration is a direct consequence of the lack of laminin-2 in *dy/dy* sciatic nerves, Schwann cell migration from E19 rat DRG explants was compared on sections of *dy/dy* and unaffected nerves with and without the addition of exogenous laminin-2 (fig. 5.4, 5.5). Exogenous laminin-2 raised the rate of migration on *dy/dy* sciatic nerve substrates to 24.92 μm/hr, to the level of the unaffected nerve.

Figure 5.4: The deficit in the rate of Schwann cell migration on *dy/dy* sciatic nerve substrates is compensated by exogenous laminin-2. E19 rat DRG explants were plated onto cryosections of *dy/dy* or unaffected (ua) sciatic nerve, some of which had had exogenous laminin-2 added. Schwann cell migration was observed after 40 hours using CMFDA cell tracker dye. **(a)** Schwann cells migrating on an unaffected nerve substrate. The distance migrated by Schwann cells on the nerve substrate from the centre of the explant to the leading edge of the Schwann cells (arrowheads) was measured. **(b)** Schwann cells do not appear to migrate as far on *dy/dy* sciatic nerves as on unaffected nerves (arrowheads). **(c)** Addition of exogenous laminin-2 (ln-2) does not appear to affect the distance migrated on unaffected nerve substrates (arrowhead). **(d)** Addition of exogenous laminin-2 enhances Schwann cell migration on *dy/dy* sciatic nerves so that it appears that Schwann cells at the leading edge (arrowheads) have migrated as far as they would on an unaffected nerve substrate. Scale bar = 250 μm.

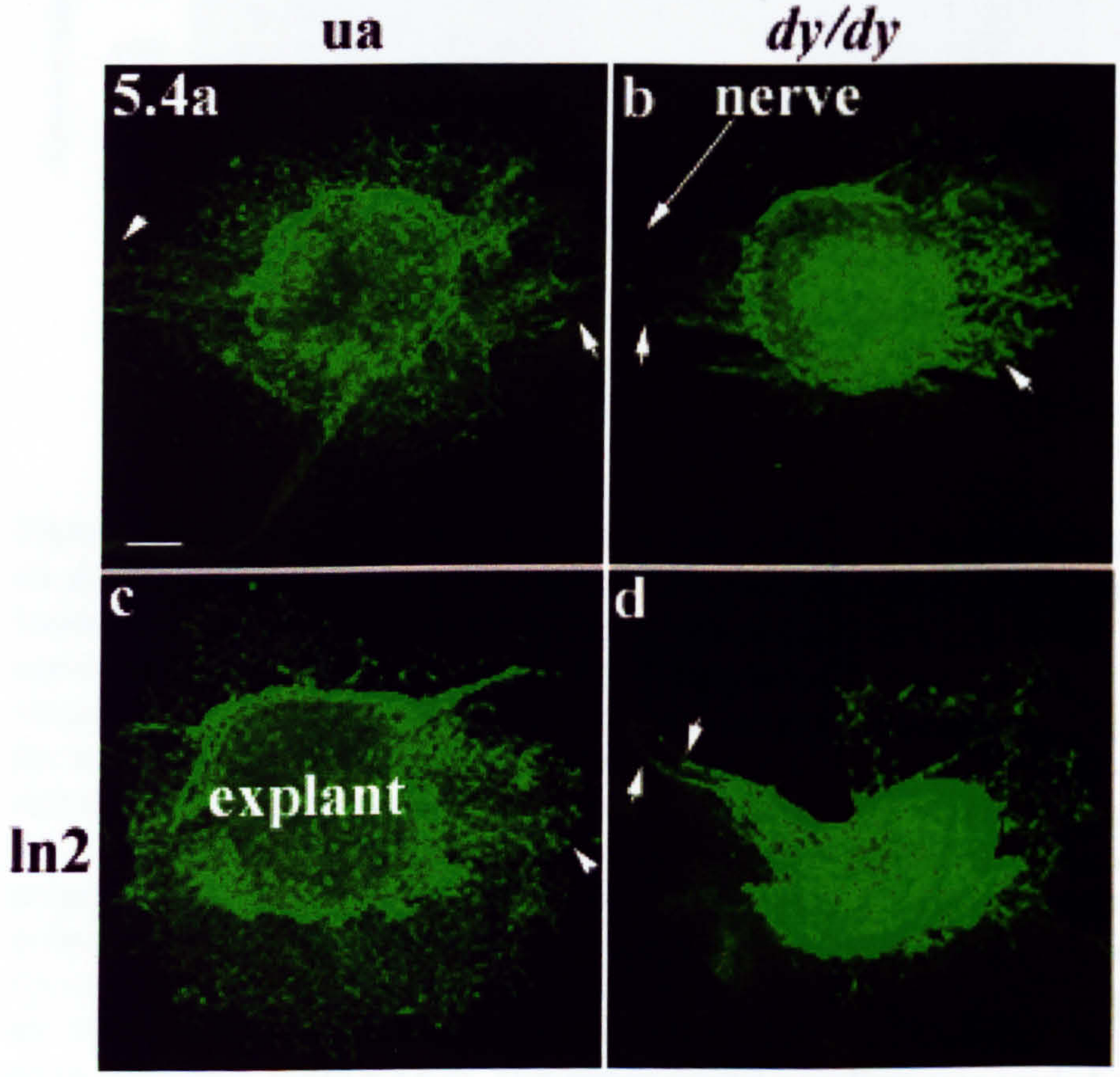
ua
dy/dy
5.4a
b nerve
c
explant
d
ln2

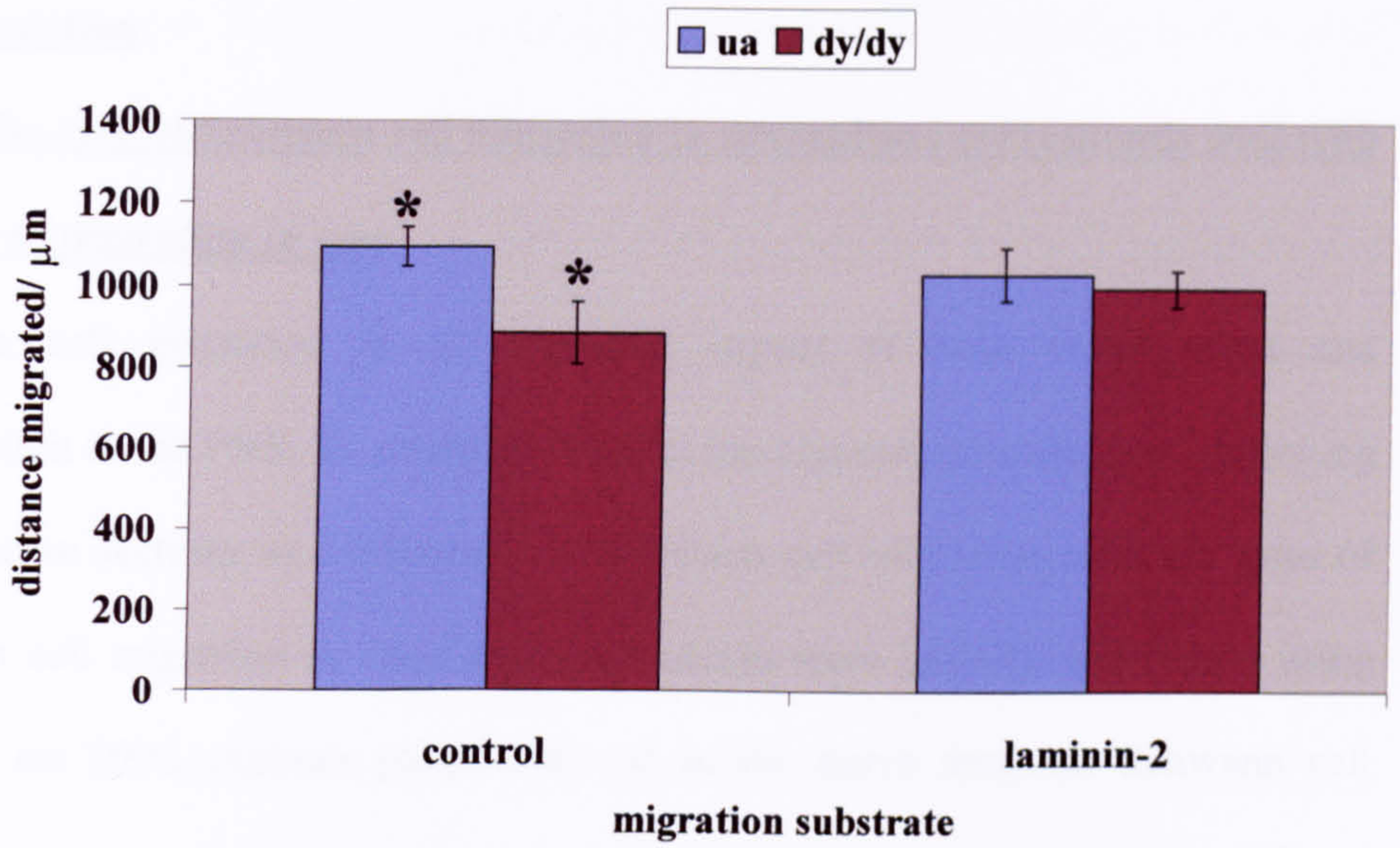

Figure 5.5: The significant deficit in the rate of Schwann cell migration on *dy/dy* sciatic nerves can be rectified with the addition of exogenous laminin-2. Schwann cells migrating on *dy/dy* and unaffected (ua) sciatic nerve substrates with or without additional exogenous laminin-2 were visualised with the cell tracker dye CMFDA and the distance migrated at the leading edge of the Schwann cells was measured. There was a significant (*, $p<0.05$) decrease in the distance migrated on *dy/dy* (n = 6) compared to unaffected (n = 7) sciatic nerve substrates in control conditions when no exogenous laminin-2 was present. Addition of exogenous laminin-2 resulted in increased Schwann cell migration on *dy/dy* (n = 14) sciatic nerve substrates but not on unaffected (n = 5) nerve substrates, such that there was no longer any significant difference in the distance migrated on the different sciatic nerve substrates. Mean ± s.e.m. This experimental paradigm was carried out 3 times.

5.3: Discussion

5.3.1: The rate of Schwann cell migration in cryoculture corresponds well with the rate of migration *in vivo*

Schwann cell migration is an important aspect of both development and regeneration in the PNS. To establish whether the cryoculture technique employing sciatic nerve sections as a substrate for Schwann cell migration reflected rates of Schwann cell migration *in vivo*, migration assays were initially undertaken using neonatal rat DRG explants plated onto rat sciatic nerve sections. Schwann cell migration in cryoculture was measured at three time points over 65 hours and found to maintain a constant rate of 22 μm/hour. This was comparable to rates observed in several studies of Schwann cell migration *in vivo* during regeneration, but in these migration assays Schwann cell division is probably a factor in the distance of Schwann cells from the explant.

Evacuated muscle grafts have been shown to provide as effective a substrate as nerve grafts for bridging substantial gaps between nerve stumps following transection (Feneley et al., 1991). The skeletal muscle provides a basal lamina substrate rich in the laminin-2 heterotrimer (Leivo and Engvall, 1988) to support Schwann cell migration and axonal outgrowth in regenerating nerves. Schwann cells migrated mostly along the basal lamina tubes left by the evacuated myofibrils at a rate equivalent to approximately 20 μm/hour over a period of 20 days (Feneley et al., 1991). In another *in vivo* assay, Fluoro-Gold labelled rat sciatic nerve Schwann cells were transplanted into severed rat sciatic nerves and were found to have migrated up to 30mm in 120 days, a rate of approximately 10 μm/hour (Daniloff, 1991). Schwann cells free to migrate along tibial nerve grafts without

accompanying axons migrated mostly along the inside of the existing basal lamina tubes and formed columns resembling the bands of Büngner. These Schwann cells migrated about 8.5mm in 6 to 8 weeks, corresponding to a rate of 8 μm/hour, half the rate observed when accompanied by axons (Anderson et al., 1991). Thus the rates of Schwann cell migration I observed *in vitro* using cryoculture appeared to closely reflect rates measured *in vivo*.

5.3.2: The rate of Schwann cell migration *in vitro* is reduced on laminin-2 deficient *dy/dy* sciatic nerve substrates but can be restored using exogenous laminin-2

The endoneurial basal lamina is particularly important for guiding Schwann cell migration during regeneration. Using the laminin-2-deficient sciatic nerves of *dy/dy* mice as a substrate in cryoculture provided a useful means to assess its specific contribution to Schwann cell migration. The severe deficiency of laminin-2 and the patchy basal lamina covering found in the peripheral nerves of *dy/dy* mice did not lead to a substantial deficit of Schwann cell migration *in vitro*. However there was a significant (16.4%) reduction in the distance migrated by the Schwann cells from the neonatal rat DRG explants on *dy/dy* nerves relative to unaffected nerves. The fact that addition of exogenous laminin-2 corrects the deficit in Schwann cell migration on *dy/dy* sciatic nerves is consistent with the lack of laminin-2 in the endoneurial basal lamina of *dy/dy* mice being primarily responsible for the deficit. Although the PNS abnormalities in the *dy/dy* mouse are more severe proximal to the spinal cord, in the spinal nerve roots and proximal portions of the sciatic nerve (Bradley and Jenkison, 1973; Bradley and Jenkison, 1975), it is not clear whether

this is due to a more severe deficiency of the laminin α2 chain. The reduction in Schwann cell migration was marginally greater on proximal portions of *dy/dy* sciatic nerve than distal portions in cryoculture, but not significantly so.

In a previous cryoculture study, Schwann cell migration was assayed from DRG explants plated onto untreated denervated nerve substrates and denervated nerve substrates treated with laminin-2 function-blocking antibodies (Anton et al., 1994a). Migration on nerve substrates treated with the antibody was substantially reduced by almost 40%. This reduction is considerably more than the reduction in the rate of migration I observed on *dy/dy* nerves and could be accounted for in several ways. Firstly, it is possible that there is a low amount of laminin-2 expressed in *dy/dy* endoneurial basal lamina, whereas the antibody would globally block all laminin-2. Secondly, exogenous expression of other laminin chains such as the α4 chain in the endoneurium of *dy/dy* mice may partially compensate for the absence of the α2 chain (Patton et al., 1997). Thirdly, whereas laminin α2 is specifically absent in *dy/dy* nerves, the ARM-1 antibody may inhibit other associated laminin chains and consequently inhibit the ability of other laminins such as laminin-1 in the perineurial basal lamina to promote Schwann cell migration in cryoculture. Finally and probably most importantly, the sciatic nerves used by Anton and her colleagues (1994a) in their study were taken from predegenerated nerves whereas *dy/dy* nerves were not. Intact nerve sections contain axons and Schwann cells but denervated sections do not. DRG neurons extend neurites preferentially onto denervated adult nerve substrates in cryoculture (Bedi et al., 1992) and it seems that denervated substrates are also more conducive to Schwann cell migration. In intact nerves CSPG's mask the activity of laminin-2 in

the endoneurial basal lamina but in regenerating nerves this masking is removed, probably as a result of the activity of matrix metalloproteinases (MMPs) such as MMP-2 and 9 (Ferguson and Muir, 2000). The greater acess to laminin-2 combined the acellular nature of predegenerated nerves may allow laminin-2 to play a greater role in Schwann cell migration during regeneration.

It is certainly clear that neither the ARM-1 treated denervated nerves nor the use of *dy/dy* nerves as substratum *in vitro* resulted in complete blockade of Schwann cell migration. Although laminin-2 is an important factor in Schwann cell migration, it must work in conjunction with other molecules. When silicon chambers used to bridge a 5 mm gap in severed rat sciatic nerves were filled with solutions of NGF, fibronectin, laminin or a combination of laminin and fibronectin, it was found that all these factors promoted Schwann cell migration, but that the synergistic activity of the fibronectin/laminin combination was particularly effective (Bailey et al., 1993). The effectiveness of a combination of ECM molecules in promoting Schwann cell migration is most likely related to their ability to activate different Schwann cell integrin receptors. Laminins mediate Schwann cell migration through β1 heterodimers, laminin-1 through α6β1 and laminin-2 through α1β1 or α2β1, whereas Schwann cell migration on fibronectin is mediated primarily through αvβ8 integrin (Milner et al., 1997). Thus it is likely that *in vivo*, different combinations of ECM molecules and growth factors may act to promote Schwann cell migration by activating different receptor combinations.

Blocking NGF activity with antibodies in cryoculture on sections of denervated sciatic nerve also partially inhibits Schwann cell migration and NGF pre-treatment of denervated sections promotes Schwann cell migration (Anton et al., 1994b).

Expression of both NGF and its receptors is raised in Schwann cells during development and regeneration (Bandtlow et al., 1987; DiStefano and Johnson, 1988; Heumann et al., 1987; Taniuchi et al., 1988), which is consistent with NGF being one of several contributory factors that promote Schwann cell migration during these processes. Another possible factor may be CD9, a Schwann cell surface membrane glycoprotein that is also found on embryonic sensory, motor and sympathetic neurons. CD9 is a tetraspan protein that is co-localised with and can associate with the α3, α6 and β1 Schwann cell integrins (Hadjiargyrou et al., 1996). In the adult, Schwann cell CD9 mRNA is down-regulated in degenerating nerves and then subsequently re-expressed in regenerating nerves upon axonal contact (Banerjee and Patterson, 1995). In a cryoculture assay in which migrating Schwann cells were exposed to an antibody against CD9, Schwann cell migration was promoted (Anton et al., 1995), consistent with a role for CD9 in negative regulation of Schwann cell migration.

Chapter 6: The influence of laminin-2 on Schwann cell properties *in vitro*

6.1: Introduction

In this chapter I have used *in vitro* techniques to examine the effect of laminin-2 on intrinsic Schwann cell properties. In development, Schwann cells are derived from pluripotent neural crest cells (Le Douarin and Smith, 1988) and induced towards the glial lineage by GGF (Shah et al., 1994) when crest cells first encounter growing axons (Loring and Erickson, 1987; Rickmann et al., 1985). Schwann cell precursors are first generated at around E12-13 in mice (E14-15 in rats) (Dong et al., 1999). These precursors differ substantially from mature Schwann cells in several respects. Precursors die by apoptosis in the absence of axonal support *in vitro* whereas immature and mature Schwann cells are self-supporting and survive through autocrine loops (Dong et al., 1999; Jessen et al., 1994). In addition there are morphological differences between precursors and Schwann cells *in vitro*; precursors have a flattened, multipolar morphology and extensive cell-cell contacts whereas Schwann cells are normally bi- or tripolar. Precursors are also far more motile than Schwann cells (Dong et al., 1999; Jessen et al., 1994). Rat Schwann cells show a mitogenic response to FGF's whereas their precursors do not (Jessen et al., 1994). In contrast FGF-2 is mitogenic for mouse Schwann cell precursors, this may be due to FGF-2 playing a role in the generation of immature Schwann cells (Dong et al., 1999).

Immature Schwann cells are generated from Schwann cell precursors at around E14-15 in mice (E16-17 in rats) and display some of the characteristics of mature Schwann cells. Immature Schwann cells can generate three Schwann cell

phenotypes; myelin forming Schwann cells that ensheath and myelinate larger diameter axons in a one to one manner (Webster, 1971; Windebank et al., 1985), non-myelin forming Schwann cells that ensheath several smaller diameter axons within their grooves but do not myelinate and terminal Schwann cells that ensheath the axon at the motor endplate. The morphology and mitogenic response to FGF's of immature Schwann cells is the same as that of mature Schwann cells (Dong et al., 1999; Jessen et al., 1994). In addition, the Schwann cell cytoplasmic protein, S100, expressed at very low levels or not all in Schwann cell precursors becomes strongly expressed in immature and all mature Schwann cells. Immature rat Schwann cells express many of the same molecular markers as those expressed by mature non-myelin forming Schwann cells, this includes the low affinity neurotrophin receptor, p75, GFAP, N-CAM and L1 (Jessen and Mirsky, 1991).

The final stage of differentiation to non-myelin-forming or myelin-forming Schwann cells occurs in the first postnatal weeks in rodents and is thought to be regulated by axonal signalling but the exact mechanism is not clear. Non-myelin forming Schwann cells express the same molecular markers as immature Schwann cells but myelin forming Schwann cells begin to express myelin proteins such as P_0, MAG, PLP, MBP, CNPase and PLP instead and proceed to myelinate the axon (Jessen and Mirsky, 1991). When axonal contact is lost, for instance following nerve transection, Schwann cells are able to dedifferentiate to an immature Schwann cell phenotype.

Cultures of dissociated sciatic nerve cells were carried out in order to compare the intrinsic properties of isolated *dy/dy* and unaffected Schwann cells and to investigate how the abnormalities observed *in vivo* may have arisen. The number of

Schwann cells extracted per unit length of *dy/dy* sciatic nerves was far greater than in unaffected nerves and after 40 hours *in vitro* a far higher proportion of *dy/dy* Schwann cells were found to have survived. The increased rate of survival suggested that *dy/dy* Schwann cells were either proliferating more or undergoing apoptotic death less than unaffected Schwann cells *in vitro*. Previous studies had found that in adult *dy/dy* peripheral nerves, many undifferentiated Schwann cells continued to proliferate (Perkins et al., 1981; Perkins et al., 1980). Observations of living cultures showed that while *dy/dy* Schwann cells extend processes within 2 hours *in vitro* unaffected Schwann cells are much slower to do so. Increased Schwann cell migration from *dy/dy* DRG explants on laminin-1 *in vitro* showed that laminin-2 has an effect on intrinsic Schwann cell motility as well as promoting Schwann cell migration as a substratum (chapter 5.2.2).

6.2: Results

6.2.1: *dy/dy* Schwann cells do not express the laminin α2 chain in sciatic nerve cultures

Cultures of sciatic nerve cells consisting predominately of Schwann cells were fixed after 40 hours *in vitro*. Double immunostaining was carried out using antibodies against the Schwann cell cytoplasmic protein, S100 and against the laminin α2 chain to determine whether *dy/dy* Schwann cells were capable of expressing laminin α2 *in vitro*. Schwann cells from both unaffected and *dy/dy* mice expressed the S100 protein intracellularly (fig. 6.1). The laminin α2 chain was expressed in a punctate pattern on the surface of unaffected S100 immunoreactive Schwann cells and was also found to be deposited on the laminin-1-coated glass coverslips (fig. 6.1a). Expression of the laminin α2 chain on the surface of *dy/dy* Schwann cells was not observed, nor did there appear to be any deposition on the glass coverslips (fig. 6.1b). Thus it appears that cultured *dy/dy* Schwann cells, like their *in vivo* counterparts, are unable to synthesise laminin α2 chain protein.

6.2.2: Dissociation of *dy/dy* sciatic nerves results in increased numbers of Schwann cells *in vitro* that rapidly extend cytoplasmic processes

Cultures of sciatic nerve cells from P15-20 mice were examined 2-3 hours after plating under a phase contrast microscope and following immunostaining with the antibody to S100, to determine any differences in the morphology of *dy/dy* and unaffected Schwann cells when initially dissociated. Each coverslip was plated with cells from an 1cm length of sciatic nerve (this was considered to be "half a sciatic nerve" from the vertebral column to the point of bifurcation in the hind- limbs).

Figure 6.1: *dy/dy* Schwann cells do not express the laminin α2 chain *in vitro*. After 40 hours *in vitro dy/dy* and unaffected (ua) Schwann cells were double-labelled with antibodies against the laminin α2 chain (green) and S100 (red), a Schwann cell marker. **(a)** In cultures of unaffected sciatic nerves cells, the laminin α2 chain is strongly expressed on the surface of Schwann cells and is deposited on to the coverslip as well (arrows). The cultures are immunoreactive for both S100 and the α2 chain. **(b)** The Schwann cells in cultures of *dy/dy* sciatic nerve cells do not appear to express any laminin α2 chain at all, and cultures of *dy/dy* sciatic nerve cells are immunoreactive for S100 only. Magnification = x40. Scale bar = 50 μm.

Dissociated Schwann cells were double immunostained in this manner in at least 10 experiments.

Laminin α2 chain and S100

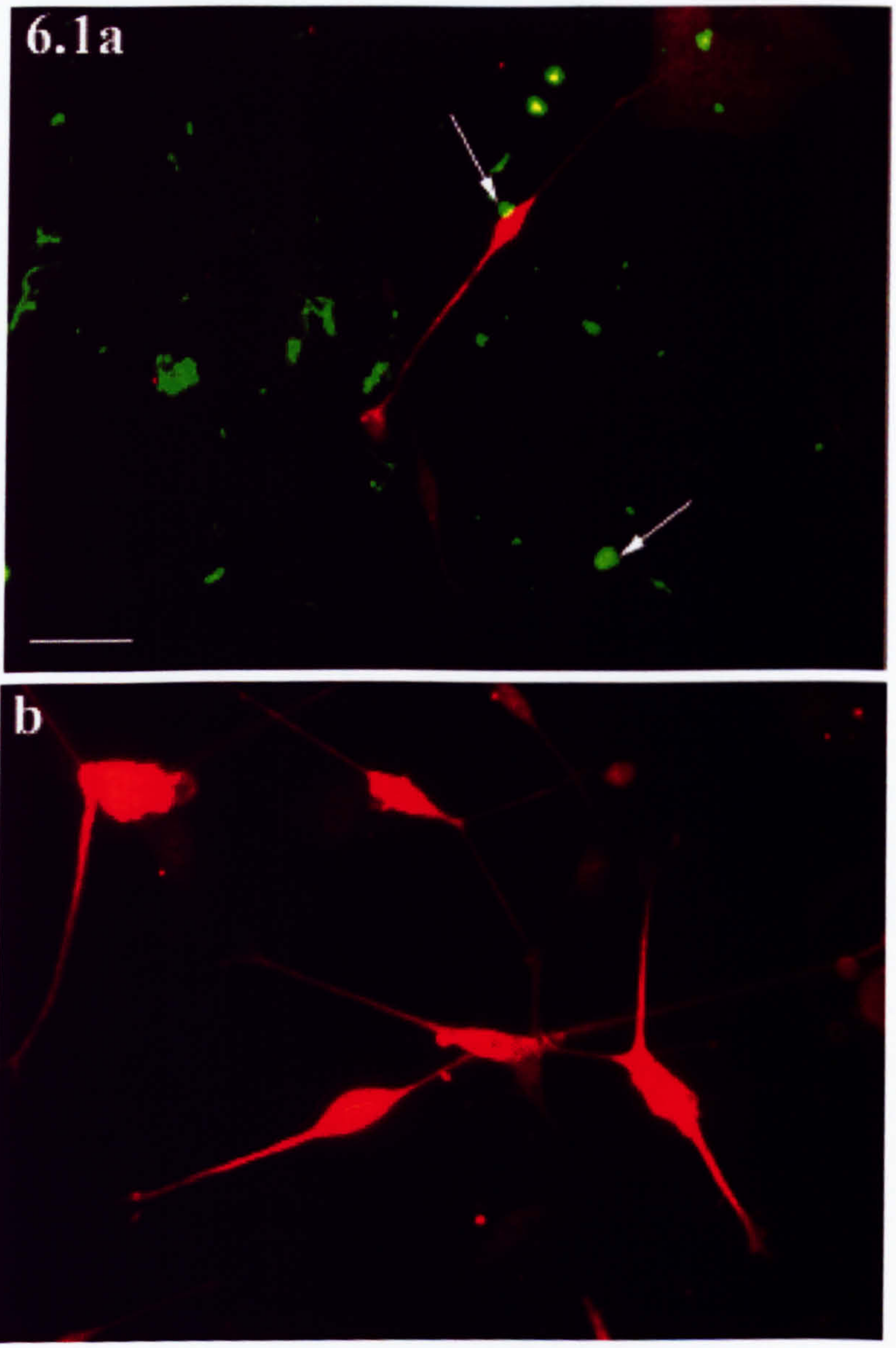

ua

dy/dy

Schwann cells from unaffected and *dy/dy* mice were plated onto laminin-1 pre-coated coverslips, fixed after 3 hours *in vitro* and immunostained with the S100 antibody. There was a significant difference ($p<0.05$) in the yield of Schwann cells from unaffected sciatic nerves and *dy/dy* nerves. Whilst each coverslip was plated with cells derived from the same length of nerve, almost twice as many S100 immunoreactive Schwann cells were obtained from *dy/dy* sciatic nerve (4434 ± 864) as from nerves of unaffected mice (2657 ± 695) (fig. 6.2). Thus, it appears that *dy/dy* sciatic nerves either contain a greater number of Schwann cells per unit length or they are better able to survive the dissociation process.

In addition, when observed after acute isolation both *dy/dy* and unaffected sciatic nerve cells appeared rounded and without residual processes and were indistinguishable. However examination of sciatic nerve cultures 3 hours post plating under phase contrast microscopy revealed that while *dy/dy* Schwann cells had extended processes unaffected Schwann cells were still lacking any processes (fig. 6.3a, b). This implies that *dy/dy* Schwann cells may be in a more "activated" state than unaffected Schwann cells.

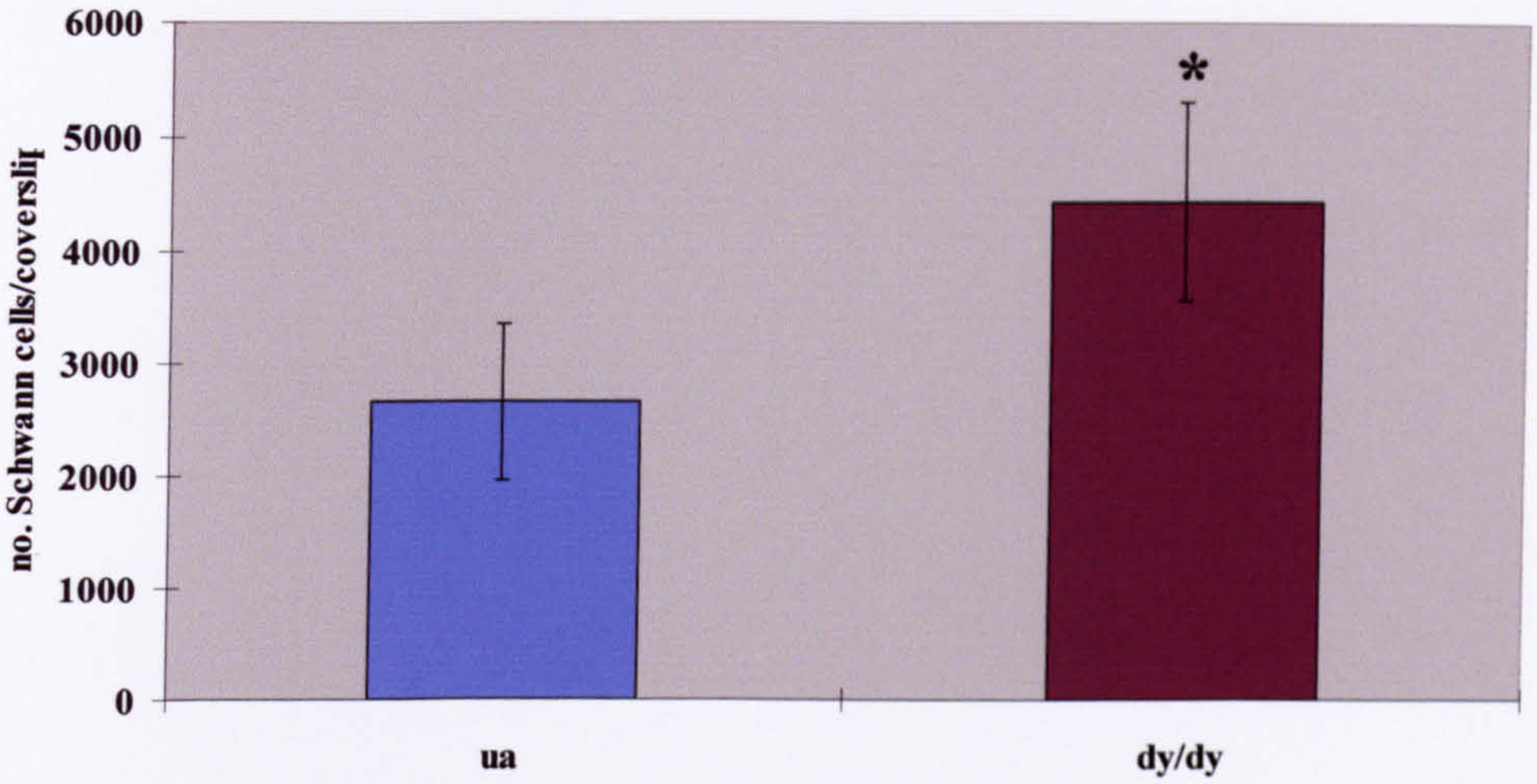

Figure 6.2: *dy/dy* sciatic nerves yields a greater number of dissociated Schwann cells than unaffected sciatic nerves. Graph showing the average number of S100 immunoreactive Schwann cells counted on each laminin-1-coated coverslip 3 hours after plating. Each coverslip contained Schwann cells yielded from 1cm of sciatic nerve. An average of 2656.5 ± 695.3 (n = 4) Schwann cells were counted in cultures of unaffected (ua) sciatic nerve cells and 4433.8 ± 864.3 (n = 4) Schwann cells were counted in cultures of *dy/dy* sciatic nerve cells. The difference in the number of Schwann cells yielded from *dy/dy* sciatic nerves was found to be significant (*, $p<0.05$). Mean ± s.e.m. This experimental paradigm was carried out 3 times.

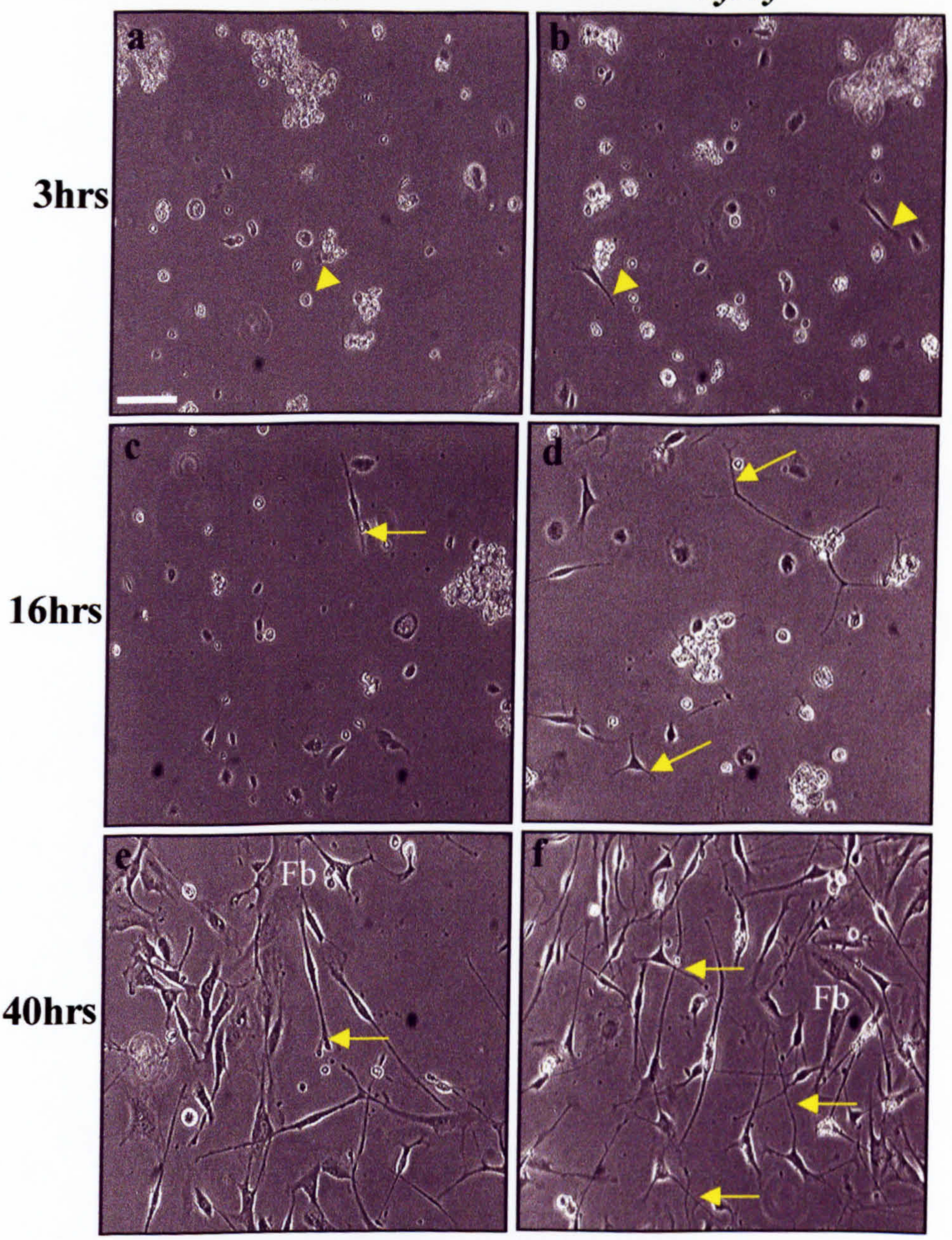

Figure 6.3:Morphological differences in *dy/dy* Schwann cells are revealed in living cultures of unaffected and *dy/dy* sciatic nerve. Sciatic nerve cells were dissociated from P15-20 *dy/dy* or unaffected (ua) mice and observed under a phase contrast microscope at various timepoints following plating. **(a,b)** 3 hours after plating *dy/dy* Schwann cells (b) have extended processes, whereas unaffected Schwann cells (a) have yet to do so (arrowheads). **(c,d)** 16 hours after plating, some unaffected Schwann cells (c) have started to extend processes, *dy/dy* Schwann cell (d) process extension is more widespread and some Schwann cells are multipolar (arrows). **(e, f)** 40 hours after plating, unaffected Schwann cells (e) have extended processes and the majority have a bipolar morphology (arrow). *dy/dy* Schwann cells (f) appear to be more numerous and many are multipolar in morphology (arrows). A few fibroblasts (Fb) are also visible after 40 hours *in vitro*. Magnification x40. Scale bar = 50μm. Live cultures were observed during the course of 3 . Live cultures were observed during the course of 3 experiments.

6.2.3: *dy/dy* Schwann cells survive better *in vitro* than unaffected Schwann cells on a variety of ECM substrates

Poly-L-lysine pre-coated glass coverslips were incubated with either laminin-1, laminin-2 or fibronectin to provide a variety of different ECM substrates for dissociated sciatic nerve cells from P15-20 unaffected and *dy/dy* mice. As before, each coverslip was plated with cells from 1cm lengths of sciatic nerve. Examination of living sciatic nerve cell cultures using phase contrast microscopy, showed that after 16 hours *in vitro* the number of Schwann cells which had extended processes still appeared to be greater in cultures of *dy/dy* sciatic nerve cells (fig. 6.3c, d). After 40 hours *in vitro* sciatic nerve cell cultures were fixed and stained with an antibody to S100. Approximately twice as many Schwann cells were found in cultures of *dy/dy* sciatic nerve cells after 40 hours *in vitro* than in cultures of unaffected sciatic nerve cells on all ECM substrates tested (fig. 6.4). Laminins-1 and 2 were preferred substrates relative to fibronectin for both *dy/dy* and unaffected Schwann cells *in vitro*. The "survival rate" of Schwann cells *in vitro* was calculated by comparing the number of Schwann cells 2-3 hours after plating with the number of Schwann cells at the final 40 hour time-point (Dong et al., 1995; Dong et al., 1999; Gavrilovic et al., 1995; Jessen et al., 1994). It was found that irrespective of substrate, a substantially greater proportion of *dy/dy* Schwann cells (41%) were able to survive *in vitro* than unaffected Schwann cells (30.5%). Preliminary experiments using 5-Bromo-2'-deoxyuridine (BrdU) labelling *in vitro* showed that a higher proportion of *dy/dy* Schwann cells were proliferating than unaffected Schwann cells.

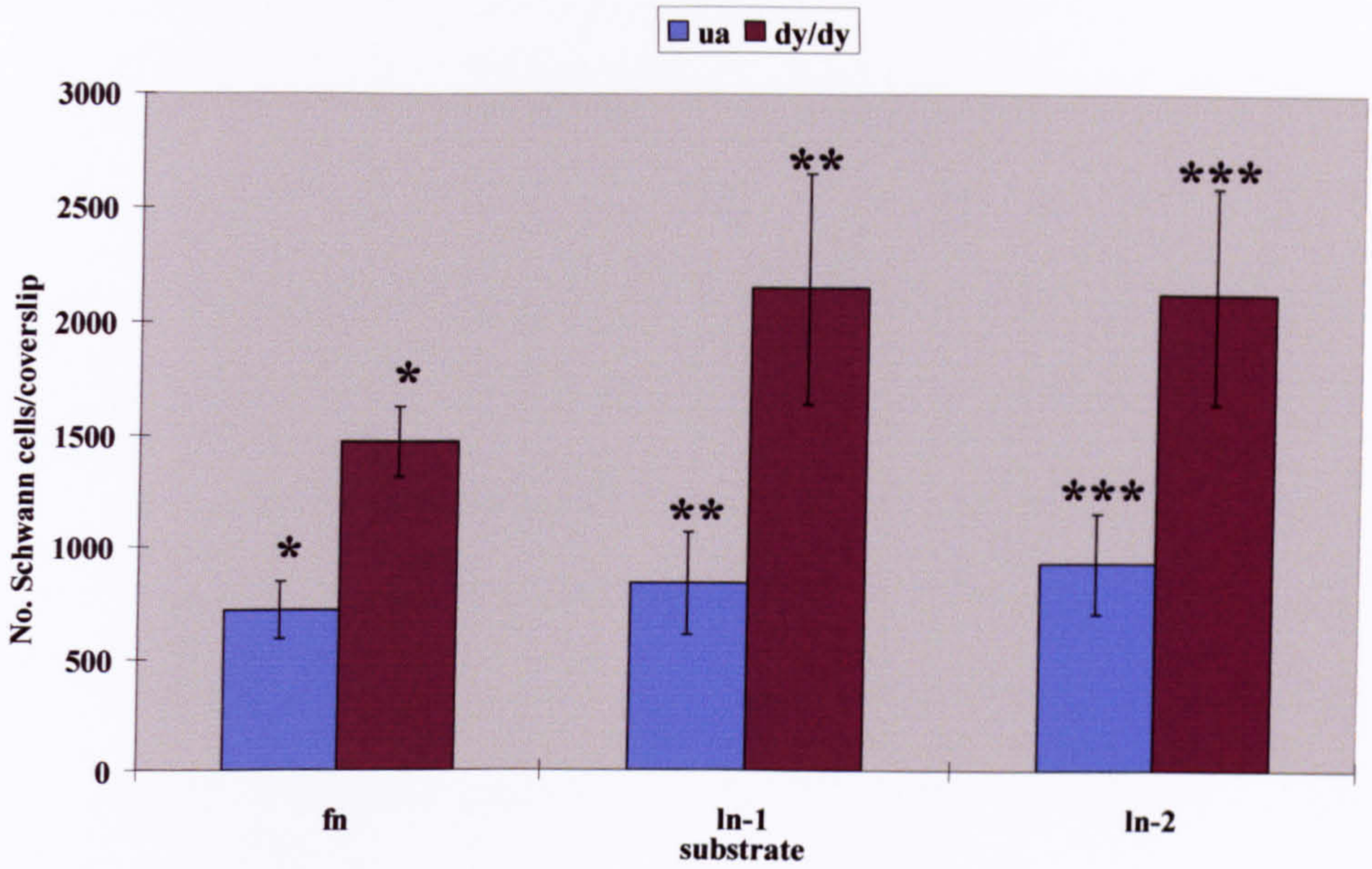

Figure 6.4: *dy/dy* Schwann cells survive better *in vitro* than unaffected Schwann cells on a variety of ECM substrates. Graph showing the aver -age number of S100 immunoreactive Schwann cells counted per coverslip after 40 hours *in vitro* on fibronectin (fn), laminin-1 (ln-1) and laminin-2 (ln-2) substrates. Sciatic nerve cells from 1cm of sciatic nerve were plated onto each coverslip. On fibronectin substrates an average of 714.8 ± 128 unaffected (ua, n = 19) and 1467.3 ± 156.8 *dy/dy* (n = 21) Schwann cells were counted. On a laminin-1 substrate, an average of 837 ± 227.2 unaff -ected (n = 11) and 2141.2 ± 507.4 *dy/dy* (n = 11) Schwann cells were counted per coverslip. On a laminin-2 substrate, an average of 927.1 ± 225 unaffected (n = 13) and 2110.8 ± 473.6 *dy/dy* (n = 13) Schwann cells were counted. The increase in the number of Schwann cells in cultures of *dy/dy* sciatic nerve was significant at $p < 0.005$, on fibronectin (*), laminin-1 (**) and laminin-2 (***). Mean ± s.e.m. This experimental paradigm was carried out at least 5 times.

6.2.4: *dy/dy* Schwann cells migrate faster than unaffected Schwann cells *in vitro*

DRG explants from P15-20 unaffected or *dy/dy* DRG's were placed on laminin-coated glass coverslips to compare the rate of migration of *dy/dy* and unaffected Schwann cells. After 40 hours *in vitro* the explants were stained with a fluorescent cell tracker dye, CMFDA, which was taken up by both DRG neurons and Schwann cells in the explant but more avidly by the latter. The cultures were immediately fixed and the distance migrated by the fluorescently-labelled Schwann cells from the DRG explants assessed. There was a significant difference ($p<0.001$) in the rate of migration of *dy/dy* Schwann cells (fig. 6.5). While unaffected Schwann cells migrated at 17.17 μm/hr, the rate of *dy/dy* Schwann cell migration was 23.2% greater at 21.16 μm/hr. Both these rates of migration are comparable to previously published estimates of rat Schwann cell migration *in vivo* during regeneration (Anderson et al., 1991; Daniloff, 1991; Feneley et al., 1991) and to rat Schwann cell migration in cryoculture (chapter 5.2.1). Again, Schwann cell division may be a factor in the distance migrated by Schwann cells from DRG explants.

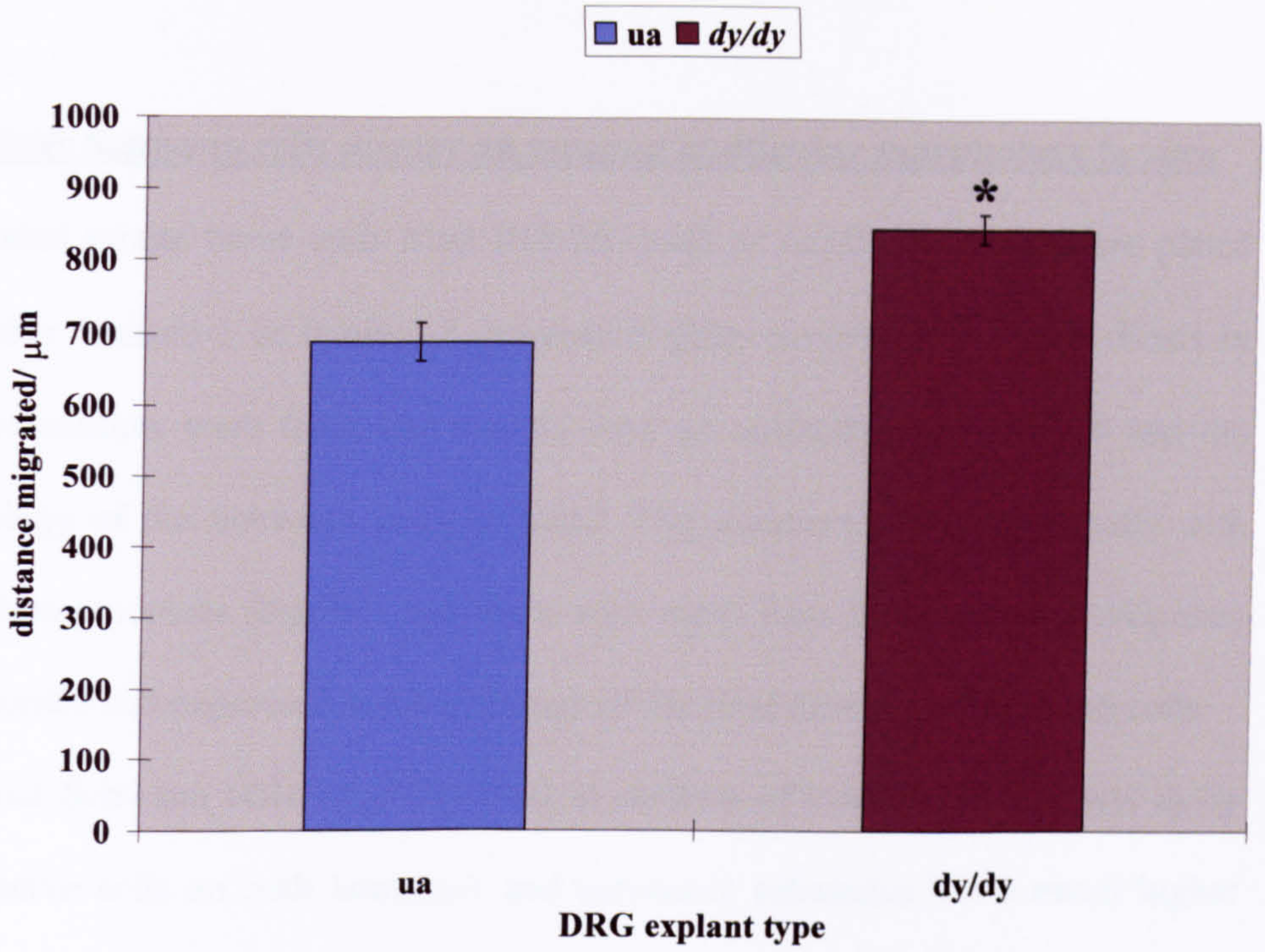

Figure 6.5: *dy/dy* Schwann cells migrate at a faster rate on laminin-1 than unaffected Schwann cells *in vitro*. DRG explants from P15-20 *dy/dy* and unaffected (ua) mice were placed on to coverslips coated with laminin -1. After 40 hours *in vitro*, the explants were stained with the cell tracker dye CMFDA and fixed, the distance migrated was assessed from digitised images. *dy/dy* Schwann cells were found to have migrated a distance of 846.5 ± 20.2 μm (n = 7), significantly further (*, p,0.001) than the 686.8 ± 26.1 μm (n = 8) migrated by unaffected Schwann cells. Mean ± s.e.m. This experimental para -digm was carried out 4 times.

6.2.5: *dy/dy* Schwann cells display an unusual multipolar morphology *in vitro*

Dissociated sciatic nerve cells from P15-20 *dy/dy* or unaffected mice were plated onto either laminin-1 or laminin-2 pre-coated glass coverslips. After 40 hours *in vitro* the cultures were fixed and stained with an antibody against S100 and the morphology of the Schwann cells assessed. The numbers of Schwann cells with two or less processes (bipolar) and those with more than 2 processes (multipolar) were counted and expressed as a percentage of the total number of Schwann cells. Multipolar Schwann cells were observed in cultures of both unaffected and *dy/dy* sciatic nerve cells on both laminin-1 and laminin-2 substrates but a much higher proportion of *dy/dy* Schwann cells were multipolar (fig. 6.6 b, d, f, 6.7) compared with unaffected Schwann cells (fig. 6.6a, c, e, 6.7). On either a laminin-1 or laminin-2 substrate approximately 12% of unaffected Schwann cells were multipolar. In contrast 64% of *dy/dy* Schwann cells were multipolar on a laminin-1 substrate and 48% on a laminin-2 substrate (fig. 6.7).

Figure 6.6: *dy/dy* Schwann cells display a multipolar morphology *in vitro*. Dissociated Schwann cells from the sciatic nerves of P15-20 unaffected (ua) and *dy/dy* mice were plated onto laminin-1 (ln-1) and laminin-2 (ln-2) coated coverslips. After 40 hours *in vitro* the Schwann cells were fixed and stained with an S100 antibody to distinguish the Schwann cells. **(a)** At low power it can be seen that in cultures of unaffected sciatic nerve cells on a laminin-1 substrate, the Schwann cells appear to be largely bipolar in morphology. **(b)** At low power magnification it can be seen that there is a wide distribution of multipolar Schwann cells in cultures of *dy/dy* sciatic nerve cells plated onto laminin-1 substrates. **(c)** The bipolar morphology of unaffected Schwann cells can be clearly seen on laminin-1 substrates (arrows). **(d)** A *dy/dy* Schwann cell on a laminin-1 substrate is clearly multipolar, extending several primary processes and exhibiting some branching of processes too (arrowheads). **(e)** Unaffected Schwann cells are bipolar on laminin-2 substrates too (arrows). **(f)** Even in the presence of laminin-2, many *dy/dy* Schwann cells are still multipolar with several primary processes and branching (arrowheads). Magnification: (a, b) x20, (c-f) x40. Scale bar: (a, b) 100 μm, (c-f) 50 μm.

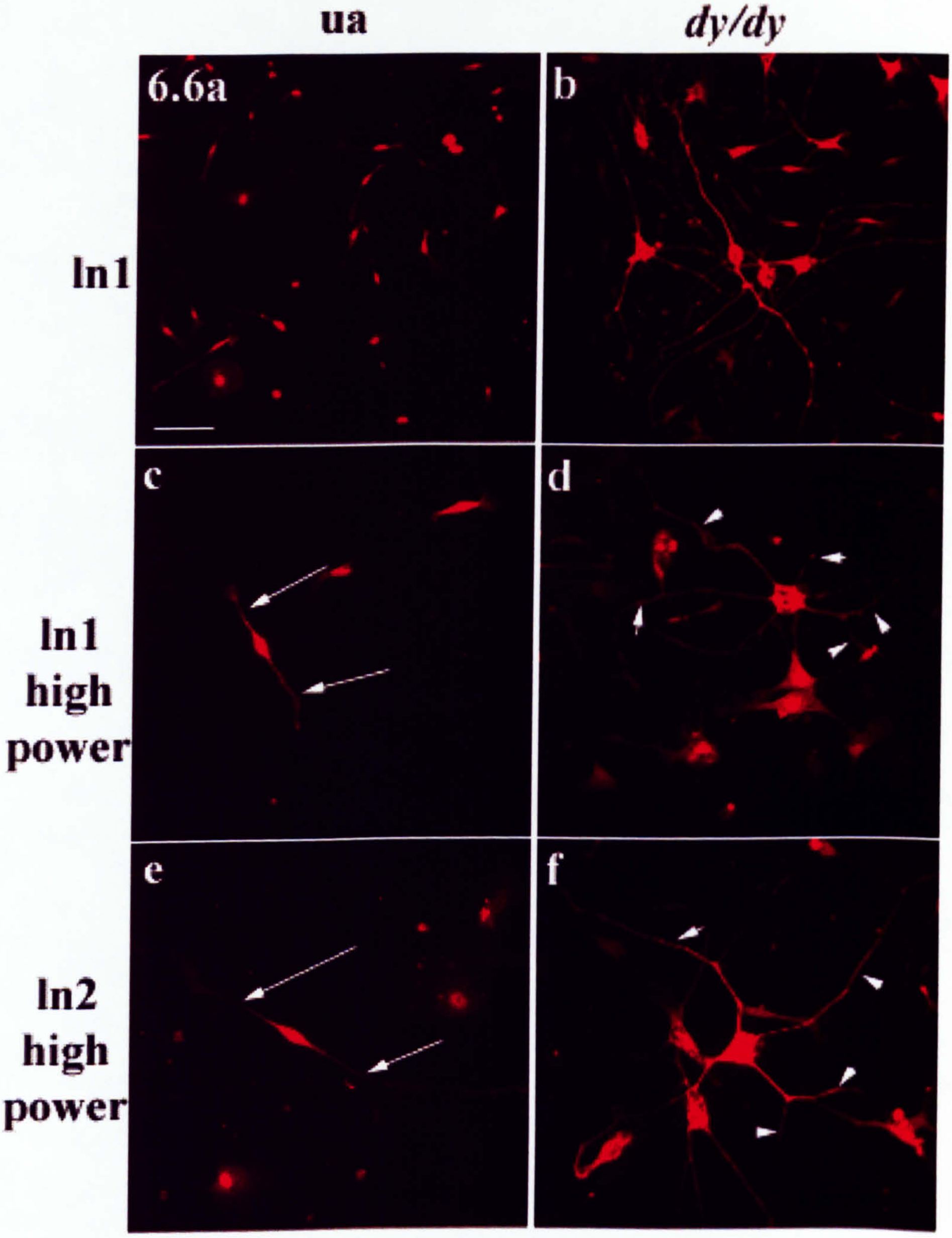
ua
dy/dy
6.6a
b
ln1
c
d
ln1
high
power
e
f
ln2
high
power

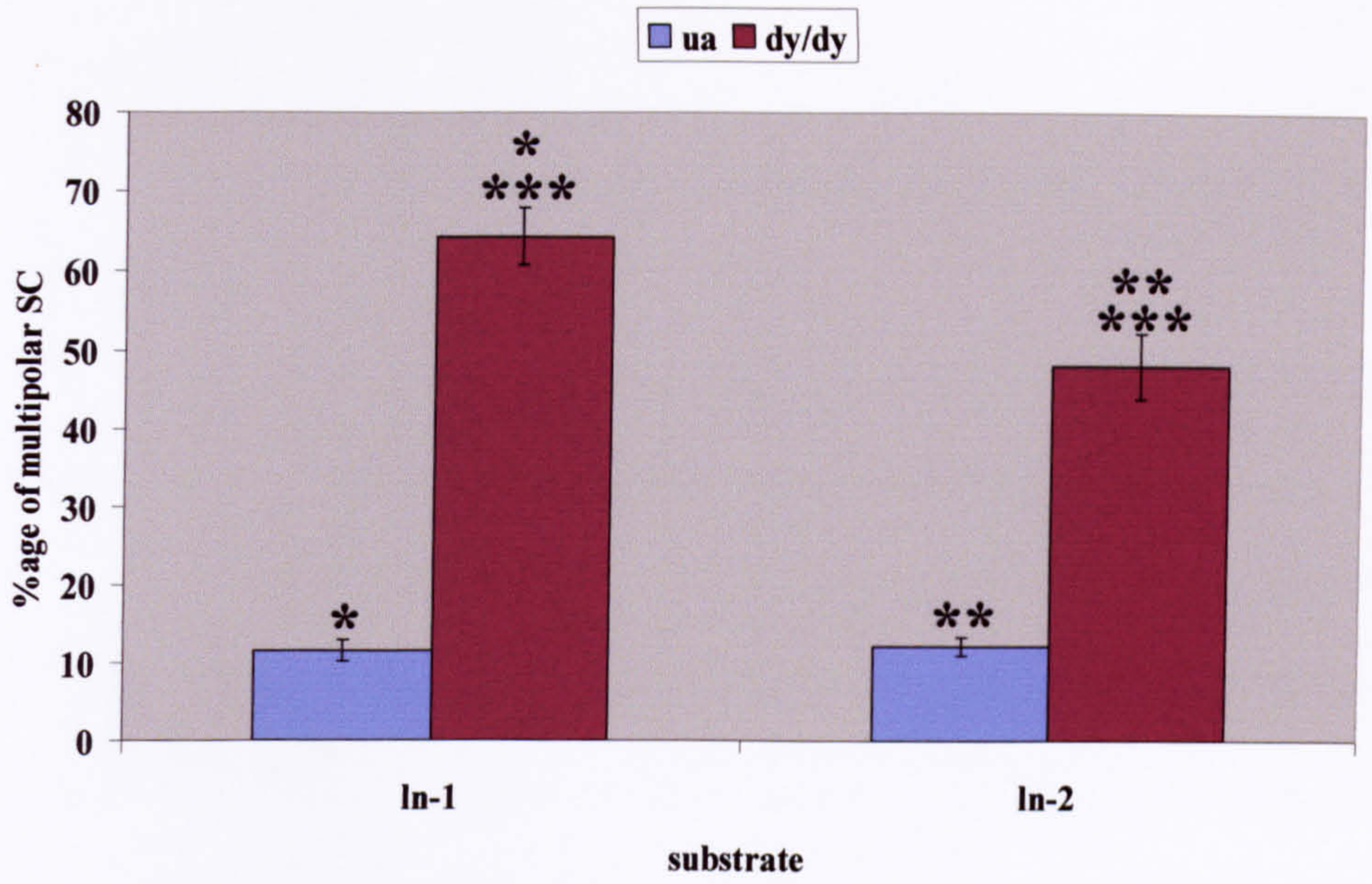

Figure 6.7: *dy/dy* Schwann cells have a multipolar morphology *in vitro* which is partially compensated on a laminin-2 substratum. Unaffected (ua) and *dy/dy* Schwann cells were plated onto coverslips coated with laminin -1 (ln-1) or laminin-2 (ln-2). After 40 hours *in vitro* cultures were fixed and stained with an antibody to the Schwann cell marker S100 and the percentage of bipolar and multipolar Schwann cells determined. 11.52% ± 1.38% of un -affected Schwann cells on the laminin-1 substrate were multipolar, signific -antly less (*, $p<0.001$) than the 64.2% ± 3.71% of *dy/dy* Schwann cells on the laminin-1 substrate which were multipolar. There were significantly fewer (**, $p<0.001$) multipolar Schwann cells in cultures of unaffected Schwann cells on laminin-2 than in cultures of *dy/dy* Schwann cells. On a laminin-2 substrate, 12.21 ± 1.15% of Schwann cells were multipolar whereas 47.99 ± 4.12% of *dy/dy* Schwann cells were multipolar. There was a significant dec -rease (***, $p<0.05$) in the number of multipolar Schwann cells in cultures of *dy/dy* Schwann cells on laminin-2 compared to laminin-1 substrates. Mean ± s.e.m. This experimental paradigm was repeated at least 3 times.

6.3: Discussion

dy/dy Schwann cells have distinct survival, migratory and morphological properties *in vitro*

Isolated *dy/dy* Schwann cells are unable to produce laminin α2 chain and I have shown in this chapter that this has a number of consequences for Schwann cell behaviour *in vitro*. Normal isolated Schwann cells and fibroblasts are capable of expressing the α1 (weakly), α2, β1, β2 and γ1 laminin chains (Hsiao et al., 1993). The α2 chain immunoreactivity I observed in cultures of unaffected sciatic nerve cells was punctate in the absence of the axonal contact required for Schwann cells to incorporate a continuous basal lamina (Clark and Bunge, 1989). In co-cultures of unaffected Schwann cells with either unaffected or *dy/dy* DRG neurons basal lamina coverage was almost 100% whereas in co-cultures of *dy/dy* Schwann cells with either unaffected or *dy/dy* neurons basal lamina coverage was this fell to 55-60% but was restored to complete coverage with the addition of normal fibroblasts (Cornbrooks et al., 1982). Thus α2 chain production by Schwann cells and fibroblasts is essential for basal lamina incoroporation *in vitro*. The inability of *dy/dy* Schwann cells to produce α2 chain protein not only prevents the incorporation of a continuous basal lamina but also results in Schwann cells with distinctly different phenotypes.

The ability of isolated P20 *dy/dy* Schwann cells to extend processes earlier than unaffected Schwann cells of the same age was reminiscent of the properties that normal neonatal Schwann cells display in culture (data not shown). Like *dy/dy* Schwann cells, these were often seen to extend processes within 2-3 hours of plating, whereas almost no process extension was observed in cells plated from

adult sciatic nerves. This is consistent with the Schwann cells dissociated from *dy/dy* sciatic nerve displaying properties characteristic of immature Schwann cells. *dy/dy* Schwann cells survive dissociation better in the short-term than unaffected Schwann cells, possibly because *in situ* they are less tightly associated with axons. Mutant Schwann cells also have a higher rate of survival in the long-term. The rate of survival was independent of the culture substratum, implying that the ability of the *dy/dy* Schwann cells to survive *in vitro* was linked to some intrinsic properties. Survival in the long term may also be linked to the loose association of *dy/dy* Schwann cells with axons *in vivo*, which may mean that mutant Schwann cells are less traumatised during trituration and dissociation. The higher rate of survival may also be a consequence of either a higher rate of proliferation or a lower rate of apoptosis or both. 5-Bromo-2'-deoxyuridine (BrdU) labelling *in vivo*, by intraperitoneal injection for example, may have determined if adult *dy/dy* do have large numbers of Schwann cells that more actively proliferate.

In *vitro* Schwann cells proliferate and continue differentiating in the absence of ECM (Carey et al., 1986). Previous evidence suggests that there may be a population of "uncommitted cells", most probably immature Schwann cells, in adult *dy/dy* nerves that remain at the margins of axons bundles and do not ensheath the axons normally (Perkins et al., 1980). These "uncommitted cells" resemble Schwann cells in developing nerves and are blocked from differentiating fully or normally and are thus still able to proliferate unless grafted into the sciatic nerves of normal mice where they differentiate, ensheath and myelinate the axon (Perkins et al., 1981; Perkins et al., 1980). Thus *in vivo dy/dy* Schwann cells can be induced to differentiate normally and associate with axons in normal nerves and in contact

with intact endoneurial basal laminae, it is possible that in *dy/dy* nerves this contact is either lost or never achieved with the patchy basal lamina.

Further evidence that *dy/dy* Schwann cells are not as fully differentiated and in a rather more "activated" state stems from their increased motility. The fact that *dy/dy* Schwann cells extend processes earlier than unaffected Schwann cells gave an indication that they may be more motile. This was supported by results from an assay of *in vitro* Schwann cell migration in which *dy/dy* Schwann cells migrated at a faster rate than unaffected Schwann cells. Time-lapse microscopy in a previous study showed that Schwann cell precursors are approximately ten times more motile than neonatal Schwann cells *in vitro* (Jessen et al., 1994). This is also true of CNS oligodendrocytes, where undifferentiated progenitors are more motile than their mature counterparts (Noble et al., 1988).

One of the most striking differences between isolated *dy/dy* and unaffected Schwann cells was in their morphology. Whereas the majority of unaffected Schwann cells assumed a bipolar morphology *in vitro*, *dy/dy* Schwann cells were largely multipolar. Addition of exogenous laminin-2 as a substrate for *dy/dy* Schwann cells significantly lowered the proportion of multipolar Schwann cells although this remained greater than in cultures of unaffected Schwann cells on laminin-2. These morphological differences manifested *in vitro* may reflect the differences seen *in vivo* following nerve crush injury (chapter 4.2.2), with Schwann cell processes interacting with several axons. In addition the multipolarity of *dy/dy* Schwann cells may reflect their increased motility *in vitro*.

The ability of the laminin α2 chain to influence Schwann cell morphology means that it is likely to have a role in polarising Schwann cells during both development

and regeneration and in the normally functioning PNS. Ectopic extension of Schwann cell processes into the synaptic cleft in *dy/dy* mice (Banker et al., 1979) and in mice lacking the laminin-11 heterotrimer (Patton et al., 1998) is consistent with a role for specific laminins in controlling the polarity of Schwann cells. It seems likely that both the α2 and α5 chains are capable of inhibiting Schwann cell process extension. Thus laminin-2 in endoneurial basal lamina could constrain myelin-forming Schwann cells from extending processes to more than one axon and enable myelin forming Schwann cells to form the one-to-one relationship between axon and Schwann cell that is a prerequisite for myelination in the PNS. At the NMJ the α2 chain containing laminin-4 and the α5 chain-containing laminin-11 ensure that terminal Schwann cells extend processes only around the axon shaft but excludes them from the synaptic cleft.

The morphological differences between *dy/dy* and unaffected Schwann cells *in vitro* are also likely to be linked to differences in their relative stages of maturity. As has been described previously, Schwann cell precursors are normally multipolar with extensive cell-cell contacts (Dong et al., 1999; Jessen et al., 1994). As Schwann cells mature they adopt more simple tri- or bipolar shapes *in vitro*. When Schwann cells come into contact with the basal lamina they cease proliferating, differentiate and undergo morphological changes as they elongate and align themselves along axons (Carey et al., 1986; Obremski and Bunge, 1995; Obremski et al., 1993a; Obremski et al., 1993b). Thus the Schwann cell basal lamina clearly has a role in regulating Schwann cell morphology, either directly in the case of glial processes in the synaptic cleft or as a result of controlling the differentiation of Schwann cells. The specific deficiency of the laminin α2 chain in *dy/dy* Schwann cells results in

distinct differences *in vitro* in the properties of *dy/dy* and unaffected Schwann cells, consistent with a significant role for the α2 chain/laminin-2 heterotrimer in regulating Schwann cell maturation, motility and polarity *in vivo*.

Chapter 7: The role of laminin-2 in the interaction of Schwann cells with neurons

7.1: Introduction

Laminin-2 has been shown to promote neurite outgrowth *in vitro* by a variety of types of neurons (Agius and Cochard, 1998; Anton et al., 1994a; Cho et al., 1998; Cohen and Johnson, 1991; Engvall et al., 1992) and has been implicated in the regulation of axon growth and guidance *in vivo*. However, the absence of overt axon targeting errors in *dy/dy* mice suggests that whatever its role may be in axonal guidance, there is evidently compensation by the intervention of alternative molecules in development. However, in vitro studies with *dy/dy* Schwann cells and neurons offer the possibility to explore the impact of laminin-2 deficiency on the specific interactions between axons and Schwann cells. A quantitative assessment of primary and terminal branches showed that neurite branching by DRG neurons was less complex on laminin-2-deficient *dy/dy* Schwann cell substrates. The findings here are consistent with a role for laminin-2 in regulating the extent of neurite branching.

7.2: Results

7.2.1: *dy/dy* Schwann cells provide a poor substrate for neurite outgrowth

The ability of laminin-2 to influence neurite outgrowth and branching was investigated by culturing DRG neurons isolated from both *dy/dy* and unaffected mice on a layer of cultured sciatic nerve cells, derived from either *dy/dy* or unaffected mouse sciatic nerves. The sciatic nerve cultures were prepared 48 hours prior to plating with neurons to provide a cell coverage close to confluence, to act as a uniform substrate for neurite growth. DRG neurons were distinguished from Schwann cells in these co-cultures using a GAP-43 immunoreactivity. Whilst GAP-43 is strongly expressed by growing neurons it is also found in non-myelin forming Schwann cells both *in vivo* and *in vitro*, and by denervated myelin forming Schwann cells (Curtis et al., 1992; Scherer et al., 1994b; Woolf et al., 1992). However at the antibody dilution used in this study, Schwann cells were only ever weakly immunopositive and clearly distinguishable from intensively labelled neurons. In addition Schwann cells and neurons displayed very different sizes and morphologies.

Several characteristics of the cultured DRG neurons were analysed to determine differences in patterns of neurite outgrowth: the numbers of primary processes which extended from each neuronal cell body (a measure of the *initiation* of neurite outgrowth); the number of terminal neurite branches (a measure of the *extent* of subsequent neurite growth); and the number of terminal neurite branches per primary process (a measure of *branching frequency*) were evaluated in each case. Firstly, it was found that the number of primary processes extended by neurons was largely independent of the source of Schwann cells with which *dy/dy* and

unaffected DRG neurons were co-cultured (fig. 7.2a).

The source of the Schwann cells was the key factor in determining subsequent neurite outgrowth and branching (fig. 7.1a, c, e, g). Both the number of terminal branches (fig. 7.2b) and, consequently, the branching frequency (fig. 7.2c) was significantly reduced ($p<0.01$) in co-cultures with *dy/dy* Schwann cells. Thus the source of the Schwann cells rather than of the DRG neurons was the instrumental factor in patterning neurite outgrowth.

7.2.2: Exogenous laminin-2 restores a normal pattern of neurite outgrowth in co-cultures of DRG neurons and *dy/dy* Schwann cells

To determine whether the reduction in complexity of DRG neurite outgrowth patterns in co-cultures with *dy/dy* Schwann cells was a consequence of the laminin-2 deficiency, we compared the morphology of DRG neurons in co-cultures with or without pre-treatment with exogenous laminin-2 (10 μg/ml). Whilst addition of exogenous laminin-2 had no significant effect on the number of primary processes extended in DRG neuron-*dy/dy* Schwann cell co-cultures (fig. 7.2a), it did affect the branching complexity of neurites extended on *dy/dy* Schwann cells, but not on unaffected Schwann cells (fig. 7.1). Addition of exogenous laminin-2 produced significant increases ($p<0.01$) in both the number of terminal branches and the branching frequency (fig. 7.2b, c) of DRG neurons co-cultured with *dy/dy* Schwann cells. Thus neurite outgrowth patterns of DRG neurons co-cultured with *dy/dy* Schwann cells in the presence of exogenous laminin-2 resembled those growing on unaffected Schwann cells (fig. 7.1b, d, f, h).

Figure 7.1: Neurite branching is diminished in DRG neuron-*dy/dy* Schwann cell co-cultures. DRG neurons from unaffected (uan) and *dy/dy* (*dyn)* mice were co-cultured with Schwann cells from unaffected (uas) and *dy/dy* (*dys)* mice on laminin-1 (a, c, e, g) and with cultured Schwann cells pre-treated with exogenous laminin-2 before addition of DRG neurons (b, d, f, h). 18 hours after the DRG neurons had been plated onto the Schwann cells, the cultures were fixed and stained with a rabbit anti-GAP-43 antibody. **(a)** Unaffected DRG neurons cultured with unaffected Schwann cells display profuse and highly branched neurite outgrowth. **(b)** Addition of exogenous laminin-2 to co-cultures of unaffected Schwann cells and DRG neurons does not appear to affect the morphology of the DRG neurons. **(c)** *dy/dy* DRG neurons co-cultured unaffected Schwann cells also have profuse and highly branched neurite outgrowth. **(d)** Addition of exogenous laminin-2 does not alter the morphology of the co-cultures in (c). **(e)** In co-cultures of unaffected DRG neurons with *dy/dy* Schwann cells the branching pattern of the neurites is less complex than those co-cultured with unaffected Schwann cells. **(f)** This lack of complexity appears to be corrected by treating *dy/dy* Schwann cells with laminin-2, which restores the branching complexity of the neurites. **(g)** *dy/dy* DRG neurons co-cultured with *dy/dy* Schwann cells also lack complexity in their branching pattern. **(h)** Addition of exogenous laminin-2 appears to correct the deficit in branching frequency of the neurites observed in co-cultures of *dy/dy* DRG neurons with *dy/dy* Schwann cells. Magnification x20. Scale bar = 100μm

+laminin-2

uas/
uan

7.1a

b

uas/
dyn

c

d

dys/
uan

e

f

dys/
dyn

g

h

Figure 7.2: Exogenous laminin-2 converts the neurite branching pattern of DRG neurons to a normal appearance on *dy/dy* Schwann cells. Unaffected and *dy/dy* DRG neurons were plated onto confluent cultures of unaffected and *dy/dy* sciatic nerve cells. After 18 hours *in vitro* the co-cultures were fixed and immunostained with a rabbit anti-GAP-43 antibody. The number of primary neurite processes (a), terminal neurite processes (b), and the complexity of neurite branching (the number of terminal processes per primary process) (c) was assessed from digitised images. **(a)** There is a significant difference in the number of primary processes extended by both *dy/dy* (*) and unaffected (**) neurons on *dy/dy* and unaffected Schwann cells ($p<0.01$) which is not significantly altered by addition of laminin-2 to the Schwann cells. **(b)** There is a large and significant decrease ($p<0.01$) in the number of terminal processes extending from both unaffected (*) and *dy/dy* (***) neurons cultured on *dy/dy* Schwann cells. The numbers of terminal processes extending from both unaffected (**) and *dy/dy* (****) neurons when co-cultured with *dy/dy* Schwann cells which had been treated with exogenous laminin-2 were significantly increased when compared to those plated on untreated Schwann cells ($p<0.01$). **(c)** Branching frequency of either unaffected (*) or *dy/dy* neurons (***) was significantly reduced in co-cultures with *dy/dy* Schwann cells ($p<0.01$), and significantly increased when either unaffected (**) or *dy/dy* (****) neurons were co-cultured with laminin-2 pre-treated *dy/dy* Schwann cells ($p< 0.01$). Experimental conditions: uasuan = unaffected neurons plated on unaffected Schwann cells (control, n = 100; exogenous laminin-2 treatment, n =54). uas*dyn* = *dy/dy* neurons on unaffected Schwann cells (control, n = 72; exogenous laminin-2 treatment, n =33). *dys*uan = unaffected neurons on *dy/dy* Schwann cells (control, n= 142; exogenous laminin-2 treatment, n = 60). *dysdyn* = *dy/dy* neurons on *dy/dy* Schwann cells (control, n = 131; exogenous laminin-2 treatment, n =26). Mean ± s.e.m. This experimental paradigm was repeated at least 5 times.

7.2a

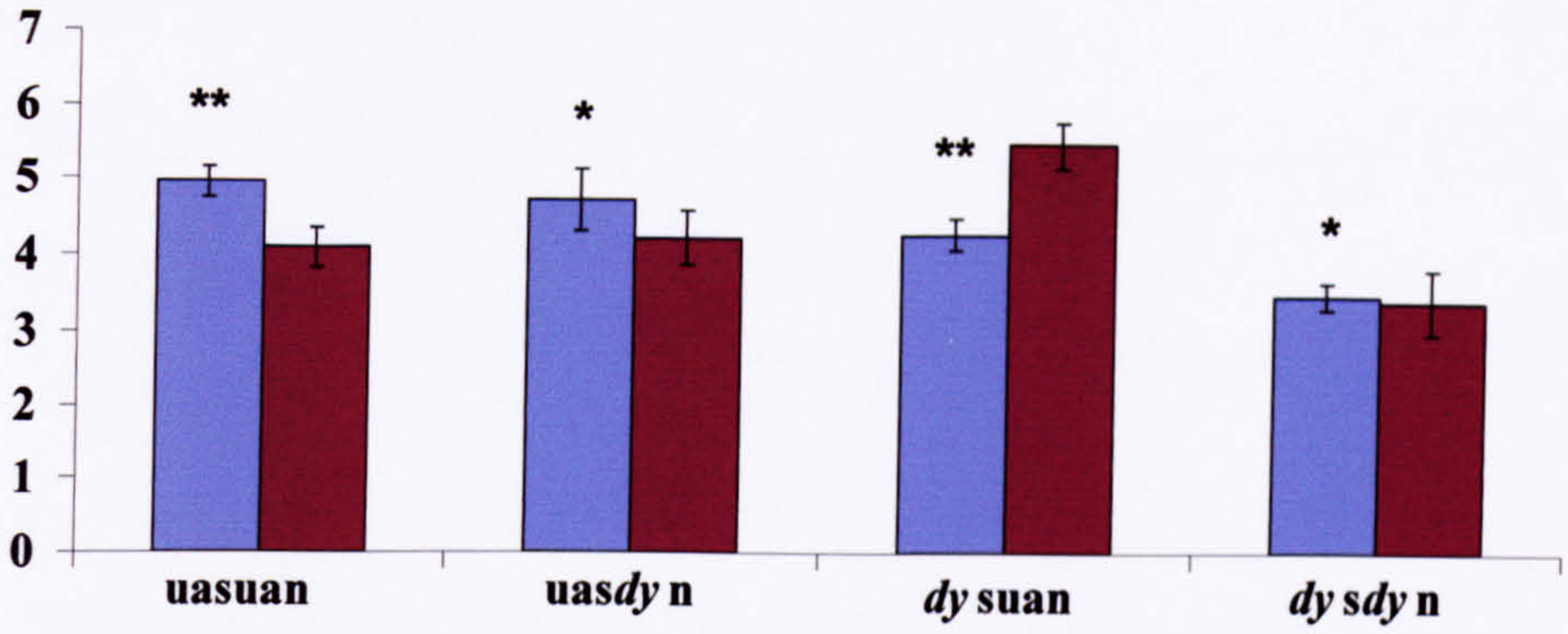
primary processes
7
6
5
4
3
2
1
0
**
*
**
*
uasuan
uasdy n
dy suan
dy sdy n

b

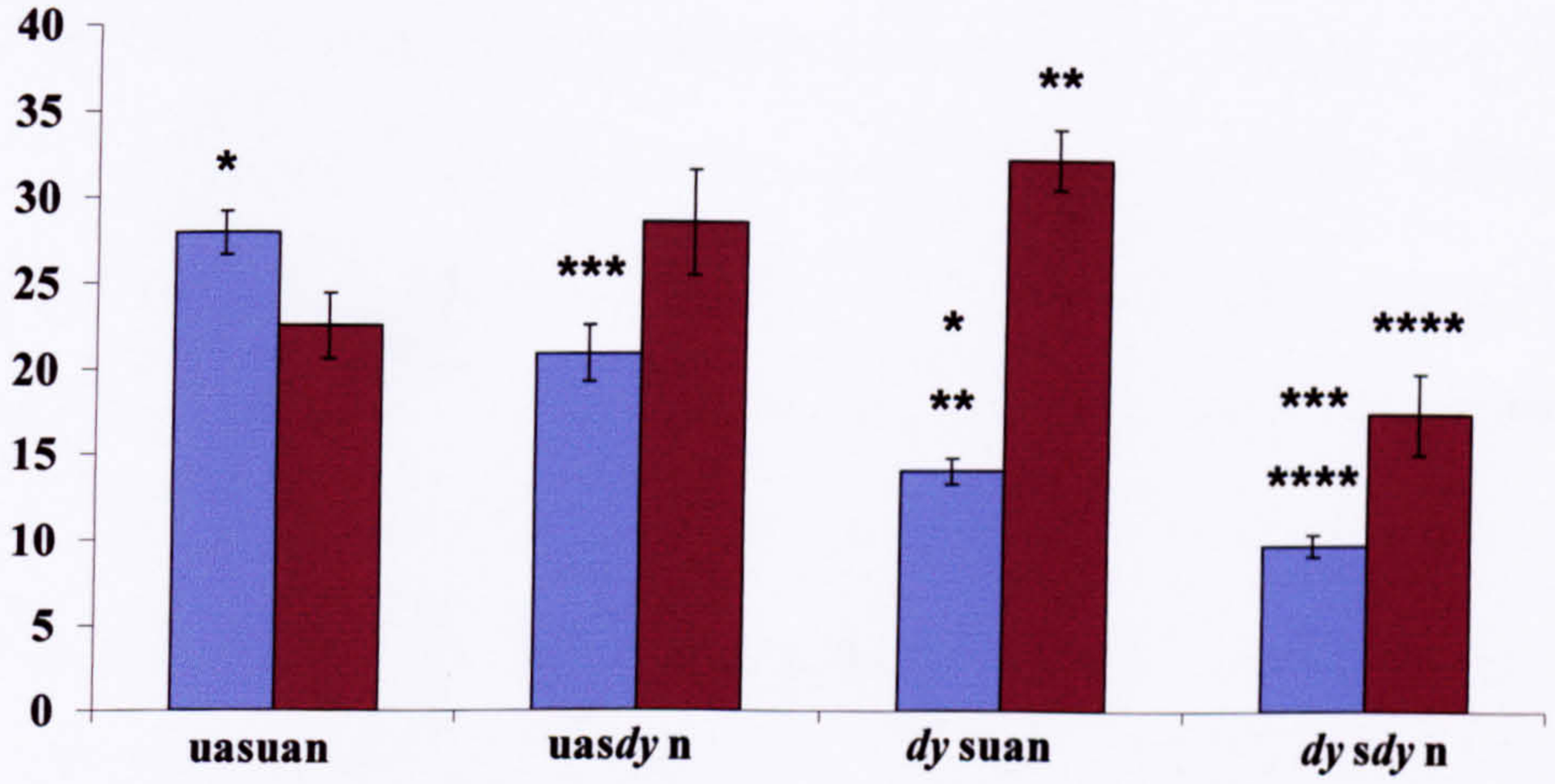
terminal processes
40
35
30
25
20
15
10
5
0
*
***
**
*
**
***
****
***
****
uasuan
uasdy n
dy suan
dy sdy n

c

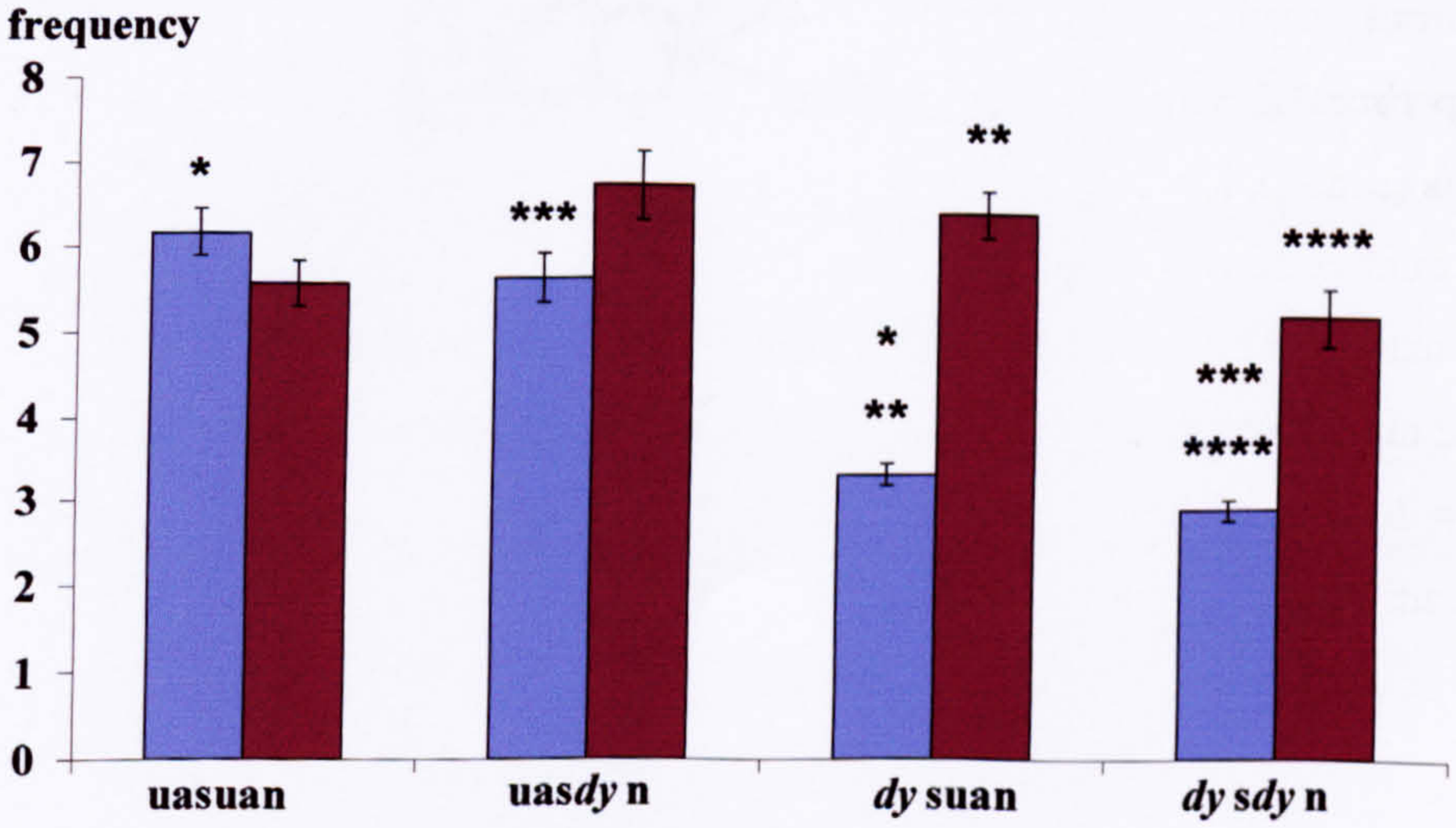
branching frequency
8
7
6
5
4
3
2
1
0
*
***
**
*
**
***
****
***
****
uasuan
uasdy n
dy suan
dy sdy n
Co-culture type
control
exogenous laminin-2

7.3: Discussion

dy/dy Schwann cells, lacking the laminin α2 chain, are a poor substrate for neurite branching *in vitro*

The work described in this chapter shows that the deficiency of laminin-2 in *dy/dy* Schwann cells affects not only the properties of Schwann cells themselves but also exerts an effect on their interactions with axons. Both *dy/dy* and unaffected DRG neurons cultured on a substrate of *dy/dy* Schwann cells displayed morphological differences from those cultured on unaffected sciatic nerve Schwann cells. Analysis of the pattern of neurite branching confirmed that there was a significant decrease in the number of terminal branches and hence the branching frequency of neurites on laminin-α2 chain-deficient *dy/dy* sciatic nerve cells. The ability of exogenous laminin-2 to remedy this deficiency is consistent with the lack of the α2 chain being the primary cause of this branching abnormality on *dy/dy* Schwann cells. As DRG neurons from mutant or unaffected mice responded identically in co-cultures with unaffected Schwann cells, it is evident that the neural abnormalities observed in the PNS of *dy/dy* mice are a consequence of abnormalities in Schwann cells (and possibly of other sciatic nerve cells, such as fibroblasts). This is consistent with the findings in an earlier study in which the extent of basal lamina formation was found to be diminished in co-cultures of *dy/dy* Schwann cells with either unaffected or *dy/dy* neurons but not in co-cultures of *dy/dy* neurons with unaffected Schwann cells (Cornbrooks et al., 1982). It is possible to rescue this basal lamina deficiency *in vitro* with the addition of normal mouse sciatic nerve fibroblasts.

Partial inhibition of neuritic branching has also been observed when laminin-2 activity is blocked on sciatic nerve sections used as a substrate for neurite

outgrowth and Schwann cell migration from DRG explants (Anton et al., 1994a). Whilst the ability of laminins such as laminin-2 to promote neurite outgrowth *in vitro* is well studied (Anton et al., 1994a; Cho et al., 1998; Cohen and Johnson, 1991; Engvall et al., 1992), there are no descriptions of axon pathfinding defects in the *dy/dy* mouse. However appropriate regulation of axonal branching is critical during regeneration since the greater the number of axons sprouting along the bands of Büngner the more successful and precise will be the resulting regeneration. Recent work has shown that laminin-2 may exert a greater influence on axon outgrowth during regeneration. Thus in cryoculture, specific antibody blockade of laminin-2 function reduced neurite outgrowth from dissociated DRG neurons to a much greater extent on denervated sciatic nerve substrates than on intact sciatic nerve substrates (Agius and Cochard, 1998). These *in vitro* experiments are consistent with an important role for laminin-2 *in vivo* during regeneration in the PNS. It seems likely that as axons sprout along bands of Büngner, laminin-2 produced by Schwann cells not only fosters axonal sprouting but also the elaboration of terminal branches. In *dy/dy* mice with transected sciatic nerves axon sprouting in the distal stump is meagre (chapter 4.3.1). These data from Schwann cell-neuron co-cultures suggest that even if initial axonal sprouting is not inhibited in the regenerating nerves of *dy/dy* mice, the deficit in laminin-2 leads to a reduced extent of branching and consequently less efficient axon regeneration in the distal stump.

Chapter 8: General Discussion

8.1: Neural abnormalities in the *dy/dy* mouse

The *dy/dy* mouse suffers from a form of muscular dystrophy that affects both the skeletal muscle and the PNS (Bradley and Jenkison, 1973; Michelson et al., 1955). This dystrophy is caused by a deficiency of the laminin α2 chain in skeletal muscle and in the endoneurial basal lamina of peripheral nerves (Arahata, 1993; Sunada et al., 1994; Xu et al., 1994a). The most prominent phenotype in peripheral nerves of *dy/dy* mice is the presence of many axons that are either unensheathed by Schwann cells and directly apposed or incompletely ensheathed with patchy myelination and elongated nodes of Ranvier (Bradley et al., 1977; Bradley and Jenkison, 1973; Bradley and Jenkison, 1975; Jaros and Bradley, 1979; Madrid et al., 1975; Okada et al., 1975; Okada et al., 1976). The abnormalities observed suggest that laminin α2 chain-containing laminins play an important role in regulating appropriate Schwann cell-axon interactions *in vivo*. In this thesis I have therefore used the *dy/dy* mouse to further investigate the role of laminin-2 in different aspects of Schwann cell behaviour and in their interactions with axons both *in vivo* and *in vitro*.

I firstly examined expression of α2 chain protein in myogenic and neural tissues and I have provided preliminary evidence from Western blotting and immunohistochemistry for the existence of a laminin α2 chain variant that is much reduced in the peripheral nerves of *dy/dy* mice but continues to be expressed in myogenic tissues. Although the level of laminin α2 chain protein and mRNA detected in the skeletal muscle of *dy/dy* mice appears to be dependent on the antibodies or probes used, it is clear that the expression of this chain is negligible in the PNS of *dy/dy* mice (Ringelmann et al., 1999; Sewry et al., 1998; Sorokin et al.,

2000).

In the intact PNS of *dy/dy* mice I confirmed the findings of previous studies showing that Schwann cells failed to ensheath axons fully or extended processes to and ensheathed both myelinated and unmyelinated axons and that many axons remained completely unensheathed. I showed that these abnormalities were re-established in regenerating nerves and moreover, remyelination was both delayed and less extensive in regenerating mutant nerves. Immunohistochemical analysis of sciatic nerves revealed morphological differences in the associations of Schwann cells with axons that could explain these differences. Immunostaining of cryosections with an antibody to S100 showed that *dy/dy* Schwann cell morphology differed *in vivo* where many mutant Schwann cells were rounded rather than ellipsoid. In cultures of dissociated sciatic nerve, a large proportion of mutant Schwann cells displayed a multipolar rather than a bipolar morphology. Moreover, *dy/dy* Schwann cells were more motile than unaffected Schwann cells. In co-cultures of Schwann cells and DRG neurons, *dy/dy* Schwann cells acted as a poor substrate for promoting neurite branching of both unaffected and mutant DRG neurons. Complex neurite branching patterns of DRG neurons could be restored on mutant Schwann cells by preincubation with exogenous laminin-2.

The pleiotropic nature of laminin-2 expression and the extensive neural abnormalities observed in the *dy/dy* mouse, especially when compared to other forms of muscular dystrophy raises the possibility that there is a substantial neurogenic component to this dystrophy. In a recent study, insertion of a human transgene under the control of a myogenic promoter alleviated some of the symptoms in mice with a targeted deletion of the laminin α2 chain and allowed

them to regenerate skeletal muscle (Kuang et al., 1999). However they still showed some characteristic symptoms of *dy/dy* and $\alpha 2^{-/-}$ mice including hind-limb flexion to the trunk when lifted up by the tail and progressive hind-limb paralysis. Thus some symptoms in *dy/dy* mice cannot be alleviated by restoring α2 chain expression only in skeletal muscle, supporting the idea of a significant neurogenic component

8.2: Involvement of Schwann cell laminins in Schwann cell migration and axonal outgrowth

Previous studies have not revealed any abnormalities in axonal pathfinding in the PNS of *dy/dy* mice. However poor axonal sprouting into the distal stump following transection of mutant sciatic nerves (chapter 4.2.1) and a lower branching frequency of DRG neurons extending neurites in co-cultures with *dy/dy* Schwann cells (chapter 7.2.1) indicate a role for laminin-2 in promoting neurite branching, at least during regeneration. I have compared Schwann cell migration on intact unaffected and *dy/dy* mouse sciatic nerve substrates (chapter 5.2) and shown that laminin-2 plays a significant role in promoting Schwann cell migration. Interactions with migrating Schwann cells are essential for axonal outgrowth during both development and regeneration. Thus axonal re-growth is poor in the distal stump of regenerating axons in the bands of Büngner of *dy/dy* nerves, as both the interaction with migrating Schwann cells and the promotion of neurite branching by laminin-2 of sprouting axons in the distal stump is compromised (fig. 8.1).

Figure 8.1: The possible roles of laminin-2 in Schwann cell development and differentiation and in Schwann cell-axon interactions. Neural crest cells differentiate into a variety of cells including neuronal cells and Schwann cell precursors. Differentiation towards the neuronal lineage is driven by BMP's and towards the Schwann cell lineage by GGF's and Delta-Notch signalling. The cells in cultures of *dy/dy* sciatic nerve cells differ in their morphology and in their motility and ability to survive and proliferate, this may be due to the continued presence of large numbers of multipotent neural crest cells. This would imply that laminin-2 (Ln-2) may be able to regulate BMP, GGF or Delta-Notch signalling.

There is stronger evidence that laminin-2 is involved in regulating glial development once neural crest cells have differentiated towards the Schwann cell lineage. Autocrine survival loops regulated by growth factors ensure the survival of immature Schwann cells. Binding of laminins to integrins promotes the formation of complexes with growth factors that share the same signalling pathway, leading to growth factor receptor aggregation. A deficiency in laminin-2 could up or down-regulate the level of integrin receptors expressed and the number of ocupied integrin receptors, this could have downstream affects on the growth factors involved in Schwann cell autocrine survival loops.

Motility of Schwann cells may also be regulated by levels of laminin-2 expression. Differentiating Schwann cells express specific integrin receptors that are able to promote laminin-2-mediated Schwann cell migration. Up or down-regulation of integrin receptor expression, continued expression of integrins that mediate migration by Schwann cells that fail to differentiate and a lack of laminin-2 substrate for migrating Schwann cells to bind to, may all alter the motility of *dy/dy* Schwann cells.

Laminin-2 regulates Schwann cell morphology, constraining the Schwann cells to the bipolar morphology necessary for myelin forming Schwann cells to align themselves along individual axons before ensheathing and myelinating them. Laminin-2 expressed by migrating Schwann cells can also promote neurite branching as well as neurite outgrowth. This property is particularly important in the bands of Büngner of regenerating nerves.

Figure 8.1: The role of laminin-2 in Schwann cell maturation and Schwann cell-axon interactions

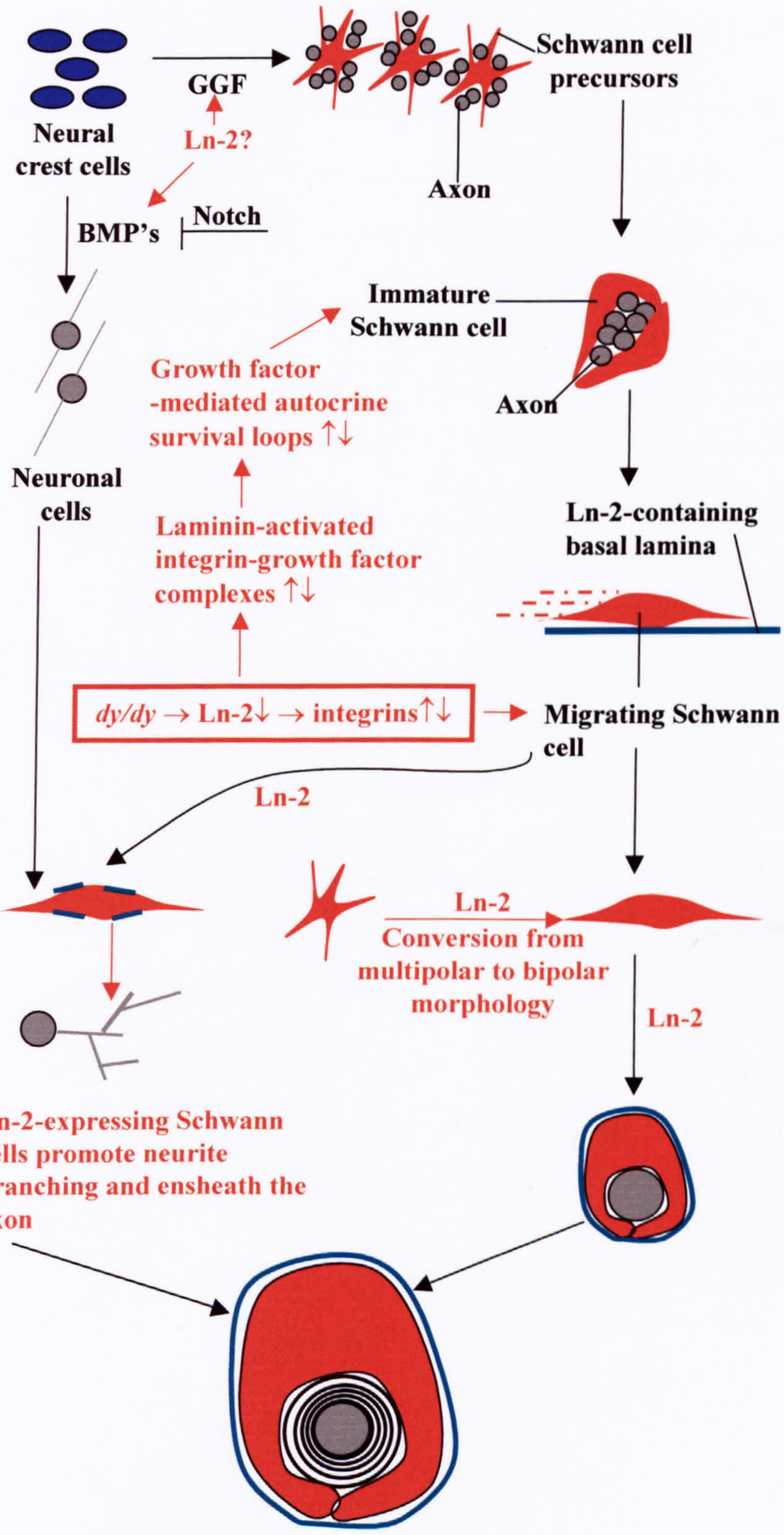

Previous studies have indicated the importance of Schwann cells in regulating axonal outgrowth both during development and regeneration. Mice with a targeted deletion of either the ErbB2 or the ErbB3 neuregulin receptors lose the majority of their Schwann cells in early development. Consequently, the vast majority of both sensory and motor neurons die through apoptosis during development and surviving axons are extensively defasciculated (Morris et al., 1999; Riethmacher et al., 1997; Woldeyesus et al., 1999). This suggests a role for Schwann cells in guiding and possibly also leading axons to their peripheral targets during development. It has been claimed that columns of Schwann cells have extend up to 100 μm ahead of motor axons into the chick forelimb bud from stages 24 to 27, but the antibody marker used could not reliably distinguish between Schwann cells and growth cones (Noakes and Bennett, 1987).

During regeneration the presence of migrating Schwann cells is essential for axonal outgrowth. When Schwann cells are prevented from migrating within the bands of Büngner axonal regeneration is delayed and less extensive (Feneley et al., 1991; Hall, 1986a; Rodriguez et al., 2000). Regenerating axons are always associated with Schwann cells throughout the length of the axon and it is thought that the rate of Schwann cell migration may limit the extent of axonal sprouting in regenerating nerves. In axotomised nerves transplanted to a skeletal muscle substrate Schwann cell processes were seen extending ahead of associated axons (Son and Thompson, 1995b). This is consistent with a possible guidance role for Schwann cells during regeneration.

Laminin-2 has been shown to have neurite-promoting properties in intact and regenerating neurons *in vitro* (Anton et al., 1994a; Cho et al., 1998; Cohen and

Johnson, 1991; Engvall et al., 1992) and is produced by and expressed on Schwann cells (Hsiao et al., 1993; Leivo and Engvall, 1988). Blocking the activity of the laminin-2 heterotrimer inhibited neurite branching on denervated nerve substrates in cryoculture (Anton et al., 1994a). In an *in vitro* assay neurite outgrowth from motor neurons was also promoted on a laminin-1 substrate and on a combined substrate of laminins-2, 4 ($\alpha2\beta1\gamma1$) and 8 ($\alpha4\beta1\gamma1$). Ectopic postnatal expression of laminin $\alpha4$ chain has been detected in both endoneurial basal lamina and skeletal muscle of *dy/dy* mice (Patton et al., 1997; Ringelmann et al., 1999). Laminin $\alpha4$ chain-containing heterotrimers include laminins-8 and 9; laminin-8 is normally expressed in the endoneurial basal lamina only during development and is restricted to mesenchymal cells postnatally and the laminin-9 heterotrimer is normally restricted to synaptic and perineurial basal lamina (Miner et al., 1997). It may be that in *dy/dy* nerves the presence of a large number of Schwann cells that are not terminally differentiated results in the continued deposition of the laminin $\alpha4$ chain in the endoneurium. However ectopic expression of the laminin $\alpha4$ chain is clearly not sufficient to compensate structurally in the basal lamina or functionally in promoting axonal re-growth during regeneration and neurite branching *in vitro*. Whilst laminin-8 promotes neurite outgrowth in combination with laminins-2 and 4, there is no evidence that it can alone support neurite outgrowth (Cho et al., 1998).

In the developing and regenerating nerve, complex interactions between various ECM molecules regulate axonal outgrowth and Schwann cell migration. For instance fibronectins are upregulated during development and regeneration (Lefcort et al., 1992) and can promote Schwann cell migration (Bailey et al., 1993; Milner et

al., 1997). Tenascin-C is also expressed in developing and regenerating peripheral nerves (Scholze et al., 1996; Zhang et al., 1995) and has both adhesive and anti-adhesive properties for Schwann cells and axons depending on which functional domain is activated (Gotz et al., 1996). CSPGs mask the activity of laminin-2 in intact nerves. Expression of MMPs-2 and 9, enzymes that degrade CSPGs, are increased during regeneration and addition of these enzymes to intact nerve substrates in cryoculture increases neurite outgrowth (Ferguson and Muir, 2000). Thus MMP-2 and 9 may remove the masking activity of CSPGs in regenerating nerves, enabling endoneurial laminin-2 in the bands of Büngner to promote neurite outgrowth and branching of sprouting axons. Specific laminin heterotrimers are also involved in inhibitory interactions with Schwann cells and motor axons. The laminin-11 heterotrimer found at the synaptic basal lamina is inhibitory to motor axons (Cho et al., 1998) and to Schwann cell process extension (Patton et al., 1998), thereby preventing axons from extending beyond the motor end-plate once they have reached their target and terminal Schwann cells from extending processes into the synaptic cleft.

8.3: Laminin-2 and Schwann cell maturation and myelination

The appearance of both intact (chapter 3.2.1) and regenerated *dy/dy* peripheral nerve fibres (chapter 4.2) and the properties of *dy/dy* Schwann cells *in vitro* such as increased motility and multipolar morphology (chapter 6.2) suggests that the deficit in laminin-2 affects the maturation of Schwann cells and their association with axons. The presence of basal lamina induces Schwann cells to differentiate, elongate, ensheath and myelinate axons (Carey et al., 1986; Clark and Bunge, 1989;

Obremski and Bunge, 1995; Obremski et al., 1993a; Obremski et al., 1993b). Loss of contact with axons following injury leads to dedifferentiation of myelin-forming Schwann cells to a premyelinating phenotype, downregulation of myelin proteins and proliferation (Bunge, 1993; Lemke and Chao, 1988; Mirsky and Jessen, 1996). In mutant nerves, the absence or incompleteness of the basal lamina means that many Schwann cells do not interact with axons appropriately and consequently Schwann cells either never contact an axon and mature fully or lose axonal contact and dedifferentiate.

The inability of *dy/dy* Schwann cells to ensheath axons suggests a role for laminin-2 in regulating the adoption of the bipolar morphology necessary for Schwann cell ensheathment as a prelude to myelination. We observed aberrant *dy/dy* Schwann cell morphology in both ultrastructural and immunohistochemical analyses of sciatic nerves and in cultures of Schwann cells. Plating *dy/dy* Schwann cells onto a laminin-2 rather than laminin-1 substrate resulted in a switch from an aberrant multipolar morphology to a bipolar morphology in a significant proportion of *dy/dy* Schwann cells, consistent with laminin-2 regulating this process. The ability of specific laminin heterotrimers to determine cell morphology may be related to their spatial expression pattern *in vivo*. Thus laminin-2 expressed in the endoneurial basal lamina can induce a bipolar morphology in Schwann cells and laminin-11, enriched at the NMJ, is able to regulate terminal Schwann cell morphology (Patton et al., 1998; Sewry et al., 1998). Laminin-11 appears to act as a "stop signal" to terminal Schwann cells, preventing process extension into the synaptic cleft. By analogy laminin-2 may act as a constraining influence, also preventing the extension of multiple processes and restricting Schwann cells to a bipolar

morphology. Consistent with this, I found that laminin-1, restricted to the perineurial basal lamina and therefore not in contact with Schwann cells, fails to promote the acquisition by *dy/dy* Schwann cells of a bipolar morphology *in vitro*. Skeletal muscle basal lamina is also rich in laminin-2 and may in a similar fashion regulate the morphology of skeletal muscle fibres. Thus cultures of control myoblasts adopted a bipolar morphology, whereas a substantial proportion (approximately 15-20%) of *dy/dy* myoblasts were multipolar, extending several "wispy" processes (Sorokin et al., 2000). Aberrant multipolar morphology may be less extensive in cultures of *dy/dy* myoblasts than Schwann cells as myogenic cells continue to express reduced but clearly detectable levels of the laminin α2 chain in *dy/dy* mice (Ringelmann et al., 1999; Sewry et al., 1998; Sorokin et al., 2000). The high number of phenotypically immature Schwann cells that may be present in *dy/dy* peripheral nerves could arise both as a direct consequence of the loss of continuous basal lamina and axon-Schwann cell interactions, but also indirectly as a result of changes in laminin receptor activity. The presence of a large number of abnormally differentiated Schwann cells and the deficiency of laminin-2 could contribute to changes in integrin receptor expression in *dy/dy* mice. Thus DRG neurons cultured on low concentrations of laminin-1 increased surface expression of the α6β1 integrin (Condic and Letourneau, 1997). Regulation of integrin expression levels by laminins has also been observed *in vivo*. Patients with merosin-deficient CMD, *dy/dy* mice and laminin $\beta 2^{-/-}$ mice all display corresponding decreases in the levels of their cognate integrin subunits (Cohn et al., 1999; Hodges et al., 1997; Martin et al., 1996; Vachon et al., 1997). The α6 integrin is upregulated in *dy/dy* mouse skeletal muscle following injury (Sorokin et

al., 2000) but in this study I was unable to detect corresponding changes in the expression of the α6 integrin subunit on cultured *dy/dy* Schwann cells (data not shown).

It is likely, however, that integrin receptor expression is affected in the PNS of *dy/dy* mice and this may have an impact on several aspects of Schwann cell development. For instance, complexes formed between laminin-bound integrins and growth factors sharing the same signalling pathways (Mainiero et al., 1996; Miyamoto et al., 1996; Plopper et al., 1995; Sundberg and Rubin, 1996) may be affected in *dy/dy* mice. This may consequently affect the activity of growth factors involved in the autocrine survival loops of immature Schwann cells (Meier et al., 1999).

Integrin dimers involved in laminin-2-mediated migration such as α1β1 and α6β1, are expressed on undifferentiated Schwann cells (Milner et al., 1997) but substantially down-regulated in differentiated myelin forming Schwann cells and upregulated in these Schwann cells following nerve injury after loss of axonal contact (Fernandez-Valle et al., 1994; Stewart et al., 1997). Widespread expression of the α1β1 receptor in mature peripheral nerves is mainly detectable on non-myelin forming Schwann cells, whereas myelin forming Schwann cells show increased expression of α6β4. Increased numbers of undifferentiated or abnormally differentiated Schwann cells that are not in contact with axons in *dy/dy* nerves may result in their upregulation of the α1β1 and α6β1 receptors that mediate Schwann cell migration on laminin. This could account for the increased motility I observed of *dy/dy* Schwann cells migrating from DRG explants on a laminin-1 substrate. Blocking the activity of β1 integrins inhibits laminin-mediated myelination in both

Schwann cells and oligodendrocytes, probably by weakening Schwann cell adhesion to the basal lamina (Buttery and ffrench-Constant, 1999; Fernandez-Valle et al., 1994) (fig. 8.1).

The "aberrant" cells in *dy/dy* nerves are all S100 immunoreactive, suggesting that they most closely resemble immature Schwann or non-myelin forming Schwann cells. However there may be a more complex explanation for the presence of "aberrant" cells in *dy/dy* peripheral nerves. Recently evidence has emerged that multipotent neural crest stem cells persist into late gestation; a sub-population of cells isolated from E14.5 rat sciatic nerve was able to generate both neurons and glia, well after neural crest cells have begun migrating (Morrison et al., 1999). It is thought that neural crest stem cells are directed first towards a neurogenic fate by the strong instructive signals of BMP-2 and that activation of the Notch receptor then causes the loss of neurogenic capacity in neural crest cells, resulting in glial differentiation (Morrison et al., 2000). Glial differentiation in the PNS is apparently irreversible. However, in the CNS oligodendrocyte precursors can be induced to revert back to multipotential neural stem cells through exposure to FCS and BMPs followed by bFGF (Kondo and Raff, 2000; Morrison et al., 2000). These CNS neural stem cells can then generate oligodendrocytes, astrocytes and neurons. Cultured neuroepithelial cells from the spinal cords of E10.5 to E13.5 rats are able to generate both CNS cell types and PNS neural crest stem cells and PNS cells such as Schwann cells and peripheral neurons (Mujtaba et al., 1998). An alternative explanation for the presence of cells with abnormal morphology and activity in cultures of *dy/dy* sciatic nerve cells may be linked to the persistence of neural crest stem cells in the PNS as a consequence of the laminin-2 deficiency (fig 8.1).

8.4: Conclusion

This thesis has highlighted the different aspects of Schwann cell maturation and of Schwann cell-axon interactions that laminin-2 may be involved in. Laminin-2 is clearly a vital factor in conferring the appropriate morphology for myelin forming Schwann cells as a prerequisite to axonal ensheathment and myelination. Adoption of a bipolar morphology is part of the process of differentiation in Schwann cells as they mature from precursors and defines the relationship between a terminally differentiated myelin-forming Schwann cell and the individual axon it ensheaths. One study detected laminin α2 chain immunoreactivity in the basal lamina of myelinated axons in human peripheral nerves, but found that α2 chain immunoreactivity was barely detectable in the basal lamina surrounding non-myelin forming Schwann cells and the axons that they ensheath (Malandrini et al., 1997). Oligodendrocytes that myelinate CNS axons are not surrounded by a laminin-2 rich basal lamina and extend several processes in order to myelinate many axons. The Schwann cell-axon interaction in *dy/dy* peripheral nerves has been compared to the pattern of myelination in the CNS (Jaros and Bradley, 1979). It seems likely that laminin-2 is required in the basal lamina of the PNS to confer an appropriate morphology on myelin forming Schwann cells, enabling them to interact with individual axons and to differentiate towards a myelin forming phenotype (fig. 8.1). Myelination is possible in the absence of basal lamina in Schwann cell-neuron co-cultures, but it is substantially delayed and reduced, just as it is during development and regeneration in *dy/dy* mice lacking a continuous Schwann cell basal lamina (Podratz et al., 1998; Uziyel et al., 2000).

I have shown that laminin-2 not only influences Schwann cell properties but also regulates the interactions between Schwann cells and axons both *in vitro* and *in vivo*. Promotion of neurite branching appears to be laminin-2-mediated and this is probably an important aspect of axonal re-growth in regenerating nerves. The many facets of PNS development and regeneration that the laminin-2 heterotrimer is involved in, lends weight to the evidence that the dystrophy in *dy/dy* mice has a major neurogenic as well as a myogenic component.

References

Aberdam, D., Galliano, M. F., Mattei, M. G., Pisani-Spadafora, A., Ortonne, J. P., and Meneguzzi, G. (1994). Assignment of mouse nicein genes to chromosomes 1 and 18. Mamm Genome *5*, 229-33.

Agius, E., and Cochard, P. (1998). Comparison of neurite outgrowth induced by intact and injured sciatic nerves: a confocal and functional analysis. J Neurosci *18*, 328-38.

Agrawal, H. C., and Agrawal, D. (1991). Proteolipid protein and DM-20 are synthesized by Schwann cells, present in myelin membrane, but they are not fatty acylated. Neurochem Res *16*, 855-8.

Ahn, A. H., and Kunkel, L. M. (1995). Syntrophin binds to an alternatively spliced exon of dystrophin. J Cell Biol *128*, 363-71.

Airenne, T., Haakana, H., Sainio, K., Kallunki, T., Kallunki, P., Sariola, H., and Tryggvason, K. (1996). Structure of the human laminin gamma 2 chain gene (LAMC2): Alternative splicing with different tissue distribution of two transcripts. Genomics *32*, 54-64.

Allamand, V., Sunada, Y., Salih, M. A. M., Straub, V., Ozo, C. O., AlTuraiki, M. H. S., Akbar, M., Kolo, T., Colognato, H., Zhang, X., Sorokin, L. M., Yurchenco, P. D., Tryggvason, K., and Campbell, K. P. (1997). Mild congenital muscular dystrophy in two patients with an internally deleted laminin alpha 2-chain. Human Molecular Genetics *6*, 747-752.

Anderson, P. N., Nadim, W., and Turmaine, M. (1991). Schwann cell migration through freeze-killed peripheral nerve grafts without accompanying axons. Acta Neuropathol *82*, 193-9.

Anton, E. S., Hadjiargyrou, M., Patterson, P. H., and Matthew, W. D. (1995). CD9 plays a role in Schwann cell migration in vitro. J Neurosci *15*, 584-95.

Anton, E. S., Sandrock, A. W., Jr., and Matthew, W. D. (1994a). Merosin promotes neurite growth and Schwann cell migration in vitro and nerve regeneration in vivo: evidence using an antibody to merosin, ARM-1. Dev Biol *164*, 133-46.

Anton, E. S., Weskamp, G., Reichardt, L. F., and Matthew, W. D. (1994b). Nerve growth factor and its low-affinity receptor promote Schwann cell migration.

Proc Natl Acad Sci U S A *91*, 2795-9.

Apel, E. D., Roberds, S. L., Campbell, K. P., and Merlie, J. P. (1995). Rapsyn may function as a link between the acetylcholine receptor and the agrin-binding dystrophin-associated glycoprotein complex. Neuron *15*, 115-26.

Arahata, K., Hayashi, Y.K., Koga, R., Goto, K., Lee, J.H., Miyagoe, Y., Ishii, H., Tsukahara, T., Takeda, S., Woo, M., Nonaka, I., Matsuzaki, T. and Sugita, H. (1993). Laminin in animal models for muscular dystrophy: Defect of laminin M in skeletal and cardiac muscles and peripheral nerve of the homozygous dystrophic *dy/dy* mice. Proc. Japan Acad. *69*, 259-264.

Arnaout, M. A. (1990). Structure and function of the leukocyte adhesion molecules CD11/CD18. Blood *75*, 1037-50.

Arroyo, E. J., Bermingham, J. R., Jr., Rosenfeld, M. G., and Scherer, S. S. (1998). Promyelinating Schwann cells express Tst-1/SCIP/Oct-6. J Neurosci *18*, 7891-902.

Aumailley, M., Pesch, M., Tunggal, L., Gaill, F., and Fassler, R. (2000). Altered synthesis of laminin 1 and absence of basement membrane component deposition in beta 1 integrin-deficient embryoid bodies. Journal of Cell Science *113*, 259-268.

Baichwal, R. R., Bigbee, J. W., and DeVries, G. H. (1988). Macrophage-mediated myelin-related mitogenic factor for cultured Schwann cells. Proc Natl Acad Sci U S A *85*, 1701-5.

Bailey, S. B., Eichler, M. E., Villadiego, A., and Rich, K. M. (1993). The influence of fibronectin and laminin during Schwann cell migration and peripheral nerve regeneration through silicon chambers. J Neurocytol *22*, 176-84.

Bandtlow, C. E., Heumann, R., Schwab, M. E., and Thoenen, H. (1987). Cellular localization of nerve growth factor synthesis by in situ hybridization. Embo J *6*, 891-9.

Banerjee, S. A., and Patterson, P. H. (1995). Schwann cell CD9 expression is regulated by axons. Mol Cell Neurosci *6*, 462-73.

Banker, B. Q., Hirst, N. S., Chester, C. S., and Fok, R. Y. (1979). Histometric and electron cytochemical study of muscle in the dystrophic mouse. Ann N Y Acad Sci *317*, 115-31.

Bedi, K. S., Winter, J., Berry, M., and Cohen, J. (1992). Adult dorsal root ganglion neurons extend neurites on predegenerated but not on normal peripheral

nerves in vitro. European Journal of Neuroscience *4*, 193-200.

Benjamins, J. A., and Morell, P. (1978). Proteins of myelin and their metabolism. Neurochem Res *3*, 137-74.

Bernier, S. M., Utani, A., Sugiyama, S., Doi, T., Polistina, C., and Yamada, Y. (1995). Cloning and expression of laminin alpha 2 chain (M-chain) in the mouse. Matrix Biol *14*, 447-55.

Beuche, W., and Friede, R. L. (1984). The role of non-resident cells in Wallerian degeneration. J Neurocytol *13*, 767-96.

Biscoe, T. J., Caddy, K. W., Pallot, D. J., Pehrson, U. M., and Stirling, C. A. (1974). The neurological lesion in the dystrophic mouse. Brain Res *76*, 534-6.

Biscoe, T. J., Headley, P. M., Martin, M. R., and Stirling, C. A. (1977). Electrophysiological observations on the spinal cord of the normal and dystrophic mouse. J Neurol Sci *31*, 51-61.

Bitgood, M. J., and McMahon, A. P. (1995). Hedgehog and Bmp genes are coexpressed at many diverse sites of cell-cell interaction in the mouse embryo. Dev Biol *172*, 126-38.

Blanchard, A. D., Sinanan, A., Parmantier, E., Zwart, R., Broos, L., Meijer, D., Meier, C., Jessen, K. R., and Mirsky, R. (1996). Oct-6 (SCIP/Tst-1) is expressed in Schwann cell precursors, embryonic Schwann cells, and postnatal myelinating Schwann cells: comparison with Oct-1, Krox-20, and Pax-3. J Neurosci Res *46*, 630-40.

Boison, D., Bussow, H., D'Urso, D., Muller, H. W., and Stoffel, W. (1995). Adhesive properties of proteolipid protein are responsible for the compaction of CNS myelin sheaths. J Neurosci *15*, 5502-13.

Bradley, W. G., and Jaros, E. (1973). Axoplasmic flow in axonal neuropathies. II. Axoplasmic flow in mice with motor neuron disease and muscular dystrophy. Brain *96*, 247-58.

Bradley, W. G., and Jaros, E. (1979). Involvement of peripheral and central nerves in murine dystrophy. Ann N Y Acad Sci *317*, 132-42.

Bradley, W. G., Jaros, E., and Jenkison, M. (1977). The nodes of Ranvier in the nerves of mice with muscular dystrophy. J Neuropathol Exp Neurol *36*, 797-806.

Bradley, W. G., and Jenkison, M. (1973). Abnormalities of peripheral nerves in murine muscular dystrophy. J Neurol Sci *18*, 227-47.

Bradley, W. G., and Jenkison, M. (1975). Neural abnormalities in the dystrophic mouse. J Neurol Sci *25*, 249-55.

Bray, G. M., and Aguayo, A. J. (1975). Quantitative ultrastructural studies of the axon Schwann cell abnormality in spinal nerve roots from dystrophic mice. J Neuropathol Exp Neurol *34*, 517-30.

Bray, G. M., David, S., Carlstedt, T., and Aguayo, A. J. (1983). Effects of crush injury on the abnormalities in the spinal roots of and peripheral nerves of dystrophic mice. Muscle and Nerve *6*, 497-503.

Bronner-Fraser, M. (1993). Mechanisms of neural crest cell migration. Bioessays *15*, 221-30.

Bronner-Fraser, M., and Fraser, S. (1989). Developmental potential of avian trunk neural crest cells in situ. Neuron *3*, 755-66.

Bronner-Fraser, M., and Fraser, S. E. (1988). Cell lineage analysis reveals multipotency of some avian neural crest cells. Nature *335*, 161-4.

Brown, M. J., and Radich, S. J. (1979). Polyaxonal myelination in developing dystrophic and normal mouse nerves. Muscle Nerve *2*, 217-22.

Brown, S. C., Fassati, A., Popplewell, L., Page, A. M., Henry, M. D., Campbell, K. P., and Dickson, G. (1999). Dystrophic phenotype induced in vitro by antibody blockade of muscle alpha-dystroglycan-laminin interaction. Journal of Cell Science *112*, 209-216.

Bunge, R. P. (1993). Expanding roles for the Schwann cell: ensheathment, myelination, trophism and regeneration. Curr Opin Neurobiol *3*, 805-9.

Bunge, R. P., and Bunge, M. B. (1978). Evidence that contact with connective tissue matrix is required for normal interaction between Schwann cells and nerve fibers. J Cell Biol *78*, 943-50.

Bunge, R. P., Bunge, M. B., and Eldridge, C. F. (1986). Linkage between axonal ensheathment and basal lamina production by Schwann cells. Annu Rev Neurosci *9*, 305-28.

Burden-Gulley, S. M., Pendergast, M., and Lemmon, V. (1997). The role of cell adhesion molecule L1 in axonal extension, growth cone motility, and signal transduction. Cell Tissue Res *290*, 415-22.

Burgeson, R. E., Chiquet, M., Deutzmann, R., Ekblom, P., Engel, J., Kleinman, H., Martin, G. R., Meneguzzi, G., Paulsson, M., Sanes, J., and et al.

(1994). A new nomenclature for the laminins. Matrix Biol *14*, 209-11.

Burstyn-Cohen, T., Frumkin, A., Xu, Y. T., Scherer, S. S., and Klar, A. (1998). Accumulation of F-spondin in injured peripheral nerve promotes the outgrowth of sensory axons. J Neurosci *18*, 8875-85.

Butt, A. M., Colquhoun, K., Tutton, M., and Berry, M. (1994). Three-dimensional morphology of astrocytes and oligodendrocytes in the intact mouse optic nerve. J Neurocytol *23*, 469-85.

Buttery, P. C., and ffrench-Constant, C. (1999). Laminin-2/integrin interactions enhance myelin membrane formation by oligodendrocytes. Molecular and Cellular Neuroscience *14*, 199-212.

Carbonetto, S. (1977). Neuromuscular transmission in dystrophic mice. J Neurophysiol *40*, 836-43.

Carey, D. J., Todd, M. S., and Rafferty, C. M. (1986). Schwann cell myelination: induction by exogenous basement membrane-like extracellular matrix. J Cell Biol *102*, 2254-63.

Caro, P. A., Scavina, M., Hoffman, E., Pegoraro, E., and Marks, H. G. (1999). MR imaging findings in children with merosin-deficient congenital muscular dystrophy. AJNR Am J Neuroradiol *20*, 324-6.

Cartaud, A., Coutant, S., Petrucci, T. C., and Cartaud, J. (1998). Evidence for in situ and in vitro association between beta-dystroglycan and the subsynaptic 43K rapsyn protein. Consequence for acetylcholine receptor clustering at the synapse. J Biol Chem *273*, 11321-6.

Carter, W. G., Ryan, M. C., and Gahr, P. J. (1991). Epiligrin, a new cell adhesion ligand for integrin alpha 3 beta 1 in epithelial basement membranes. Cell *65*, 599-610.

Champliaud, M. F., Lunstrum, G. P., Rousselle, P., Nishiyama, T., Keene, D. R., and Burgeson, R. E. (1996). Human amnion contains a novel laminin variant, laminin 7, which like laminin 6, covalently associates with laminin 5 to promote stable epithelial-stromal attachment. Journal of Cell Biology *132*, 1189-1198.

Cheng, Y. S., Champliaud, M. F., Burgeson, R. E., Marinkovich, M. P., and Yurchenco, P. D. (1997). Self-assembly of laminin isoforms. J Biol Chem *272*, 31525-32.

Cho, S. I., Ko, J., Patton, B. L., Sanes, J. R., and Chiu, A. Y. (1998). Motor

neurons and Schwann cells distinguish between synaptic and extrasynaptic isoforms of laminin. J Neurobiol *37*, 339-58.

Chung, A. E., Jaffe, R., Freeman, I. L., Vergnes, J. P., Braginski, J. E., and Carlin, B. (1979). Properties of a basement membrane-related glycoprotein synthesized in culture by a mouse embryonal carcinoma-derived cell line. Cell *16*, 277-87.

Church, R. L., Tanzer, M. L., and Pfeiffer, S. E. (1973). Collagen and procollagen production by a clonal line of Schwann cells. Proc Natl Acad Sci U S A *70*, 1943-6.

Clark, M. B., and Bunge, M. B. (1989). Cultured Schwann cells assemble normal-appearing basal lamina only when they ensheathe axons. Dev Biol *133*, 393-404.

Clemence, A., Mirsky, R., and Jessen, K. R. (1989). Non-myelin-forming Schwann cells proliferate rapidly during Wallerian degeneration in the rat sciatic nerve. J Neurocytol *18*, 185-92.

Cohen, J., and Johnson, A. R. (1991). Differential effects of laminin and merosin on neurite outgrowth by developing retinal ganglion cells. J Cell Sci Suppl *15*, 1-7.

Cohen, M. W., Hoffstrom, B. G., and DeSimone, D. W. (2000). Active zones on motor nerve terminals contain alpha 3beta 1 integrin. J Neurosci *20*, 4912-21.

Cohn, R. D., Mayer, U., Saher, G., Herrmann, R., vanderFlier, A., Sonnenberg, A., Sorokin, L., and Voit, T. (1999). Secondary reduction of alpha 7B integrin in laminin alpha 2 deficient congenital muscular dystrophy supports an additional transmembrane link in skeletal muscle. Journal of the Neurological Sciences *163*, 140-152.

Collo, G., Starr, L., and Quaranta, V. (1993). A new isoform of the laminin receptor integrin alpha 7 beta 1 is developmentally regulated in skeletal muscle. J Biol Chem *268*, 19019-24.

Colognato, H., MacCarrick, M., Orear, J. J., and Yurchenco, P. D. (1997). The laminin alpha 2-chain short arm mediates cell adhesion through both the alpha 1 beta 1 and alpha 2 beta 1 integrins. Journal of Biological Chemistry *272*, 29330-29336.

Colognato, H., Winkelmann, D. A., and Yurchenco, P. D. (1999). Laminin polymerization induces a receptor-cytoskeleton network. Journal of Cell Biology *145*, 619-631.

Colognato, H., and Yurchenco, P. D. (2000). Form and function: the laminin family of heterotrimers. Dev Dyn *218*, 213-34.

Colognato, H., and Yurchenco, P. D. (1999). The laminin alpha 2 expressed by dystrophic dy(2J) mice is defective in its ability to form polymers. Current Biology *9*, 1327-1330.

Condic, M. L., and Letourneau, P. C. (1997). Ligand-induced changes in integrin expression regulate neuronal adhesion and neurite outgrowth. Nature *389*, 852-6.

Cooper, A. R., Kurkinen, M., Taylor, A., and Hogan, B. L. (1981). Studies on the biosynthesis of laminin by murine parietal endoderm cells. Eur J Biochem *119*, 189-97.

Cornbrooks, C. J., Mithen, F., Cochran, J. M., and Bunge, R. P. (1982). Factors affecting Schwann cell basal lamina formation in cultures of dorsal root ganglia from mice with muscular dystrophy. Brain Res *282*, 57-67.

Curtis, R., Stewart, H. J., Hall, S. M., Wilkin, G. P., Mirsky, R., and Jessen, K. R. (1992). GAP-43 is expressed by nonmyelin-forming Schwann cells of the peripheral nervous system. J Cell Biol *116*, 1455-64.

Daniloff, J. K. (1991). A novel assay for the in vivo study of Schwann cells. Exp Neurol *114*, 140-3.

Davies, A. M. (1998). Neuronal survival: early dependence on Schwann cells. Curr Biol *8*, R15-8.

Davies, J. A., Cook, G. M., Stern, C. D., and Keynes, R. J. (1990). Isolation from chick somites of a glycoprotein fraction that causes collapse of dorsal root ganglion growth cones. Neuron *4*, 11-20.

De Angelis, D. A., and Braun, P. E. (1996). 2',3'-Cyclic nucleotide 3'-phosphodiesterase binds to actin-based cytoskeletal elements in an isoprenylation-independent manner. J Neurochem *67*, 943-51.

de Ferra, F., Engh, H., Hudson, L., Kamholz, J., Puckett, C., Molineaux, S., and Lazzarini, R. A. (1985). Alternative splicing accounts for the four forms of myelin basic protein. Cell *43*, 721-7.

Debby-Brafman, A., Burstyn-Cohen, T., Klar, A., and Kalcheim, C. (1999). F-Spondin, expressed in somite regions avoided by neural crest cells, mediates inhibition of distinct somite domains to neural crest migration. Neuron *22*, 475-88.

Delwel, G. O., de Melker, A. A., Hogervorst, F., Jaspars, L. H., Fles, D. L.,

Kuikman, I., Lindblom, A., Paulsson, M., Timpl, R., and Sonnenberg, A. (1994). Distinct and overlapping ligand specificities of the alpha 3A beta 1 and alpha 6A beta 1 integrins: recognition of laminin isoforms. Mol Biol Cell *5*, 203-15.

Delwel, G. O., Hogervorst, F., Kuikman, I., Paulsson, M., Timpl, R., and Sonnenberg, A. (1993). Expression and function of the cytoplasmic variants of the integrin alpha 6 subunit in transfected K562 cells. Activation-dependent adhesion and interaction with isoforms of laminin. J Biol Chem *268*, 25865-75.

Desaki, J., Matsuda, S., and Sakanaka, M. (1995). Morphological changes of neuromuscular junctions in the dystrophic (dy) mouse: a scanning and transmission electron microscopic study. J Electron Microsc (Tokyo) *44*, 59-65.

Desban, N., and Duband, J. L. (1997). Avian neural crest cell migration on laminin: interaction of the alpha1beta1 integrin with distinct laminin-1 domains mediates different adhesive responses. J Cell Sci *110*, 2729-44.

Dickinson, M. E., Selleck, M. A., McMahon, A. P., and Bronner-Fraser, M. (1995). Dorsalization of the neural tube by the non-neural ectoderm. Development *121*, 2099-106.

DiStefano, P. S., and Johnson, E. M., Jr. (1988). Nerve growth factor receptors on cultured rat Schwann cells. J Neurosci *8*, 231-41.

Dong, Z., Brennan, A., Liu, N., Yarden, Y., Lefkowitz, G., Mirsky, R., and Jessen, K. R. (1995). Neu differentiation factor is a neuron-glia signal and regulates survival, proliferation, and maturation of rat Schwann cell precursors. Neuron *15*, 585-96.

Dong, Z., Sinanan, A., Parkinson, D., Parmantier, E., Mirsky, R., and Jessen, K. R. (1999). Schwann cell development in embryonic mouse nerves. J Neurosci Res *56*, 334-48.

Douglas, A. J., and Thompson, R. J. (1993). Structure of the myelin membrane enzyme 2',3'-cyclic nucleotide 3'- phosphodiesterase: evidence for two human mRNAs. Biochem Soc Trans *21*, 295-7.

Doyu, M., Sobue, G., Ken, E., Kimata, K., Shinomura, T., Yamada, Y., Mitsuma, T., and Takahashi, A. (1993). Laminin A, B1, and B2 chain gene expression in transected and regenerating nerves: regulation by axonal signals. J Neurochem *60*, 543-51.

D'Souza, S. E., Haas, T. A., Piotrowicz, R. S., Byers-Ward, V., McGrath, D. E., Soule, H. R., Cierniewski, C., Plow, E. F., and Smith, J. W. (1994). Ligand and cation binding are dual functions of a discrete segment of the integrin beta 3 subunit: cation displacement is involved in ligand binding. Cell *79*, 659-67.

Duband, J. L., Belkin, A. M., Syfrig, J., Thiery, J. P., and Koteliansky, V. E. (1992). Expression of alpha 1 integrin, a laminin-collagen receptor, during myogenesis and neurogenesis in the avian embryo. Development *116*, 585-600.

Duncan, I. D., Hammang, J. P., and Trapp, B. D. (1987). Abnormal compact myelin in the myelin-deficient rat: absence of proteolipid protein correlates with a defect in the intraperiod line. Proc Natl Acad Sci U S A *84*, 6287-91.

Durbec, P. L., Larsson-Blomberg, L. B., Schuchardt, A., Costantini, F., and Pachnis, V. (1996). Common origin and developmental dependence on c-ret of subsets of enteric and sympathetic neuroblasts. Development *122*, 349-58.

Durbeej, M., Henry, M. D., and Campbell, K. P. (1998). Dystroglycan in development and disease. Current Opinion in Cell Biology *10*, 594-601.

Dytrych, L., Sherman, D. L., Gillespie, C. S., and Brophy, P. J. (1998). Two PDZ domain proteins encoded by the murine periaxin gene are the result of alternative intron retention and are differentially targeted in Schwann cells. J Biol Chem *273*, 5794-800.

Eccleston, P. A., Collarini, E. J., R., J. K., Mirsky, R., and Richardson, W. D. (1990). Schwann cells secrete a PDGF-like factor:evidence for an autocrine growth mechanism involving PDGF. Eur J Neurosci *2*, 985-992.

Ehrig, K., Leivo, I., Argraves, W. S., Ruoslahti, E., and Engvall, E. (1990). Merosin, a tissue-specific basement membrane protein, is a laminin-like protein. Proc Natl Acad Sci U S A *87*, 3264-8.

Eickholt, B. J., Mackenzie, S. L., Graham, A., Walsh, F. S., and Doherty, P. (1999). Evidence for collapsin-1 functioning in the control of neural crest migration in both trunk and hindbrain regions. Development *126*, 2181-9.

Einheber, S., Milner, T. A., Giancotti, F., and Salzer, J. L. (1993). Axonal regulation of Schwann cell integrin expression suggests a role for alpha 6 beta 4 in myelination. J Cell Biol *123*, 1223-36.

Einheber, S., Zanazzi, G., Ching, W., Scherer, S., Milner, T. A., Peles, E., and Salzer, J. L. (1997). The axonal membrane protein Caspr, a homologue of neurexin

IV, is a component of the septate-like paranodal junctions that assemble during myelination. J Cell Biol *139*, 1495-506.

Eldridge, C. F., Bunge, M. B., and Bunge, R. P. (1989). Differentiation of axon-related Schwann cells in vitro: II. Control of myelin formation by basal lamina. J Neurosci *9*, 625-38.

Eldridge, C. F., Bunge, M. B., Bunge, R. P., and Wood, P. M. (1987). Differentiation of axon-related Schwann cells in vitro. I. Ascorbic acid regulates basal lamina assembly and myelin formation. J Cell Biol *105*, 1023-34.

Engel, J., Odermatt, E., Engel, A., Madri, J. A., Furthmayr, H., Rohde, H., and Timpl, R. (1981). Shapes, domain organizations and flexibility of laminin and fibronectin, two multifunctional proteins of the extracellular matrix. J Mol Biol *150*, 97-120.

Engvall, E., Earwicker, D., Day, A., Muir, D., Manthorpe, M., and Paulsson, M. (1992). Merosin promotes cell attachment and neurite outgrowth and is a component of the neurite-promoting factor of RN22 schwannoma cells. Exp Cell Res *198*, 115-23.

Engvall, E., Earwicker, D., Haaparanta, T., Ruoslahti, E., and Sanes, J. R. (1990). Distribution and isolation of four laminin variants; tissue restricted distribution of heterotrimers assembled from five different subunits. Cell Regul *1*, 731-40.

Ervasti, J. M., and Campbell, K. P. (1991). Membrane organization of the dystrophin-glycoprotein complex. Cell *66*, 1121-31.

Falls, D. L., Rosen, K. M., Corfas, G., Lane, W. S., and Fischbach, G. D. (1993). ARIA, a protein that stimulates acetylcholine receptor synthesis, is a member of the neu ligand family. Cell *72*, 801-15.

Fannon, A. M., Sherman, D. L., Ilyina-Gragerova, G., Brophy, P. J., Friedrich, V. L., Jr., and Colman, D. R. (1995). Novel E-cadherin-mediated adhesion in peripheral nerve: Schwann cell architecture is stabilized by autotypic adherens junctions [published erratum appears in J Cell Biol 1995 Jun;129(6):1721]. J Cell Biol *129*, 189-202.

Feltri, M. L., Scherer, S. S., Nemni, R., Kamholz, J., Vogelbacker, H., Scott, M. O., Canal, N., Quaranta, V., and Wrabetz, L. (1994). Beta 4 integrin expression in myelinating Schwann cells is polarized, developmentally regulated

and axonally dependent. Development *120*, 1287-301.

Feneley, M. R., Fawcett, J. W., and Keynes, R. J. (1991). The role of Schwann cells in the regeneration of peripheral nerve axons through muscle basal lamina grafts. Exp Neurol *114*, 275-85.

Ferguson, T. A., and Muir, D. (2000). MMP-2 and MMP-9 Increase the Neurite-Promoting Potential of Schwann Cell Basal Laminae and Are Upregulated in Degenerated Nerve. Mol Cell Neurosci *16*, 157-167.

Fernandez-Valle, C., Bunge, R. P., and Bunge, M. B. (1995). Schwann cells degrade myelin and proliferate in the absence of macrophages: evidence from in vitro studies of Wallerian degeneration. J Neurocytol *24*, 667-79.

Fernandez-Valle, C., Gwynn, L., Wood, P. M., Carbonetto, S., and Bunge, M. B. (1994). Anti-beta 1 integrin antibody inhibits Schwann cell myelination. J Neurobiol *25*, 1207-26.

Figlewicz, D. A., Quarles, R. H., Johnson, D., Barbarash, G. R., and Sternberger, N. H. (1981). Biochemical demonstration of the myelin-associated glycoprotein in the peripheral nervous system. J Neurochem *37*, 749-58.

Filbin, M. T., Walsh, F. S., Trapp, B. D., Pizzey, J. A., and Tennekoon, G. I. (1990). Role of myelin P0 protein as a homophilic adhesion molecule. Nature *344*, 871-2.

Frail, D. E., and Braun, P. E. (1984). Two developmentally regulated messenger RNAs differing in their coding region may exist for the myelin-associated glycoprotein. J Biol Chem *259*, 14857-62.

Franco-Obregon, A., Jr., and Lansman, J. B. (1995). Spontaneous opening of the acetylcholine receptor channel in developing muscle cells from normal and dystrophic mice. J Neurosci Res *42*, 452-8.

Franzen, R., Schoenen, J., Leprince, P., Joosten, E., Moonen, G., and Martin, D. (1998). Effects of macrophage transplantation in the injured adult rat spinal cord: A combined immunocytochemical and biochemical study. Journal of Neuroscience Research *51*, 316-327.

Friedman, B., Scherer, S. S., Rudge, J. S., Helgren, M., Morrisey, D., McClain, J., Wang, D. Y., Wiegand, S. J., Furth, M. E., Lindsay, R. M., and et al. (1992). Regulation of ciliary neurotrophic factor expression in myelin-related Schwann cells in vivo. Neuron *9*, 295-305.

Froehner, S. C., Murnane, A. A., Tobler, M., Peng, H. B., and Sealock, R. (1987). A postsynaptic Mr 58,000 (58K) protein concentrated at acetylcholine receptor-rich sites in Torpedo electroplaques and skeletal muscle. J Cell Biol *104*, 1633-46.

Frost, E., Kiernan, B. W., Faissner, A., and ffrench-Constant, C. (1996). Regulation of oligodendrocyte precursor migration by extracellular matrix: evidence for substrate-specific inhibition of migration by tenascin-C. Dev Neurosci *18*, 266-73.

Fu, S. Y., and Gordon, T. (1997). The cellular and molecular basis of peripheral nerve regeneration. Mol Neurobiol *14*, 67-116.

Funakoshi, H., Frisen, J., Barbany, G., Timmusk, T., Zachrisson, O., Verge, V. M., and Persson, H. (1993). Differential expression of mRNAs for neurotrophins and their receptors after axotomy of the sciatic nerve. J Cell Biol *123*, 455-65.

Gaese, F., Kolbeck, R., and Barde, Y. A. (1994). Sensory ganglia require neurotrophin-3 early in development. Development *120*, 1613-9.

Garbay, B., Heape, A. M., Sargueil, F., and Cassagne, C. (2000). Myelin synthesis in the peripheral nervous system. Prog Neurobiol *61*, 267-304.

Garbern, J. Y., Cambi, F., Tang, X. M., Sima, A. A., Vallat, J. M., Bosch, E. P., Lewis, R., Shy, M., Sohi, J., Kraft, G., Chen, K. L., Joshi, I., Leonard, D. G., Johnson, W., Raskind, W., Dlouhy, S. R., Pratt, V., Hodes, M. E., Bird, T., and Kamholz, J. (1997). Proteolipid protein is necessary in peripheral as well as central myelin. Neuron *19*, 205-18.

Gavazzi, I., Kumar, R. D., McMahon, S. B., and Cohen, J. (1999). Growth responses of different subpopulations of adult sensory neurons to neurotrophic factors in vitro. Eur J Neurosci *11*, 3405-14.

Gavrilovic, J., Brennan, A., Mirsky, R., and Jessen, K. R. (1995). Fibroblast growth factors and insulin growth factors combine to promote survival of rat Schwann cell precursors without induction of DNA synthesis. Eur J Neurosci *7*, 77-85.

Gee, S. H., Blacher, R. W., Douville, P. J., Provost, P. R., Yurchenco, P. D., and Carbonetto, S. (1993). Laminin-binding protein 120 from brain is closely related to the dystrophin-associated glycoprotein, dystroglycan, and binds with high affinity to the major heparin binding domain of laminin. J Biol Chem *268*, 14972-

80.

Gehlsen, K. R., Dickerson, K., Argraves, W. S., Engvall, E., and Ruoslahti, E. (1989). Subunit structure of a laminin-binding integrin and localization of its binding site on laminin. J Biol Chem *264*, 19034-8.

Giancotti, F. G., and Ruoslahti, E. (1999). Integrin signaling. Science *285*, 1028-32.

Giger, R. J., Cloutier, J. F., Sahay, A., Prinjha, R. K., Levengood, D. V., Moore, S. E., Pickering, S., Simmons, D., Rastan, S., Walsh, F. S., Kolodkin, A. L., Ginty, D. D., and Geppert, M. (2000). Neuropilin-2 is required in vivo for selective axon guidance responses to secreted semaphorins. Neuron *25*, 29-41.

Gilbert, W. R., Garwood, M. M., Agrawal, D., Schmidt, R. E., and Agrawal, H. C. (1982). Immunoblot identification of phosphorylated basic proteins of rat and rabbit CNS and PNS myelin: evidence for four phosphorylated basic proteins and P2 in rat PNS myelin. Neurochem Res *7*, 1495-506.

Gillespie, C. S., Sherman, D. L., Blair, G. E., and Brophy, P. J. (1994). Periaxin, a novel protein of myelinating Schwann cells with a possible role in axonal ensheathment. Neuron *12*, 497-508.

Gotz, B., Scholze, A., Clement, A., Joester, A., Schutte, K., Wigger, F., Frank, R., Spiess, E., Ekblom, P., and Faissner, A. (1996). Tenascin-C contains distinct adhesive, anti-adhesive, and neurite outgrowth promoting sites for neurons. J Cell Biol *132*, 681-99.

Gravel, M., DeAngelis, D., and Braun, P. E. (1994). Molecular cloning and characterization of rat brain 2',3'-cyclic nucleotide 3'-phosphodiesterase isoform 2. J Neurosci Res *38*, 243-7.

Gravel, M., Peterson, J., Yong, V. W., Kottis, V., Trapp, B., and Braun, P. E. (1996). Overexpression of 2',3'-cyclic nucleotide 3'-phosphodiesterase in transgenic mice alters oligodendrocyte development and produces aberrant myelination. Mol Cell Neurosci *7*, 453-66.

Greenfield, S., Brostoff, S., Eylar, E. H., and Morell, P. (1973). Protein composition of myelin of the peripheral nervous system. J Neurochem *20*, 1207-16.

Greenfield, S., Brostoff, S. W., and Hogan, E. L. (1980). Characterization of the basic proteins from rodent peripheral nervous system myelin. J Neurochem *34*, 453-5.

Greenfield, S., Weise, M. J., Gantt, G., Hogan, E. L., and Brostoff, S. W. (1982). Basic proteins of rodent peripheral nerve myelin: immunochemical identification of the 21.5K, 18.5K, 17K, 14K, and P2 proteins. J Neurochem *39*, 1278-82.

Griffiths, I., Klugmann, M., Anderson, T., Yool, D., Thomson, C., Schwab, M. H., Schneider, A., Zimmermann, F., McCulloch, M., Nadon, N., and Nave, K. A. (1998). Axonal swellings and degeneration in mice lacking the major proteolipid of myelin. Science *280*, 1610-3.

Griffiths, I. R., Mitchell, L. S., McPhilemy, K., Morrison, S., Kyriakides, E., and Barrie, J. A. (1989). Expression of myelin protein genes in Schwann cells. J Neurocytol *18*, 345-52.

Griffiths, I. R., Schneider, A., Anderson, J., and Nave, K. A. (1995). Transgenic and natural mouse models of proteolipid protein (PLP)- related dysmyelination and demyelination. Brain Pathol *5*, 275-81.

Grinspan, J. B., Marchionni, M. A., Reeves, M., Coulaloglou, M., and Scherer, S. S. (1996). Axonal interactions regulate Schwann cell apoptosis in developing peripheral nerve: neuregulin receptors and the role of neuregulins. J Neurosci *16*, 6107-18.

Gu, Y., Sorokin, L., Durbeej, M., Hjalt, T., Jonsson, J. I., and Ekblom, M. (1999). Characterization of bone marrow laminins and identification of alpha5-containing laminins as adhesive proteins for multipotent hematopoietic FDCP-Mix cells [see comments]. Blood *93*, 2533-42.

Guicheney, P., Vignier, N., Helbling-Leclerc, A., Nissinen, M., Zhang, X., Cruaud, C., Lambert, J. C., Richelme, C., Topaloglu, H., Merlini, L., Barois, A., Schwartz, K., Tome, F. M., Tryggvason, K., and Fardeau, M. (1997). Genetics of laminin alpha 2 chain (or merosin) deficient congenital muscular dystrophy: from identification of mutations to prenatal diagnosis. Neuromuscul Disord *7*, 180-6.

Hadjiargyrou, M., Kaprielian, Z., Kato, N., and Patterson, P. H. (1996). Association of the tetraspan protein CD9 with integrins on the surface of S-16 Schwann cells. J Neurochem *67*, 2505-13.

Hagedorn, L., Suter, U., and Sommer, L. (1999). P0 and PMP22 mark a multipotent neural crest-derived cell type that displays community effects in

response to TGF-beta family factors. Development *126*, 3781-94.

Hahn, A. F., Whitaker, J. N., Kachar, B., and Webster, H. D. (1987). P2, P1, and P0 myelin protein expression in developing rat sixth nerve: a quantitative immunocytochemical study. J Comp Neurol *260*, 501-12.

Hall, D. E., Reichardt, L. F., Crowley, E., Holley, B., Moezzi, H., Sonnenberg, A., and Damsky, C. H. (1990). The alpha 1/beta 1 and alpha 6/beta 1 integrin heterodimers mediate cell attachment to distinct sites on laminin. J Cell Biol *110*, 2175-84.

Hall, S. M. (1986a). The effect of inhibiting Schwann cell mitosis on the re-innervation of acellular autografts in the peripheral nervous system of the mouse. Neuropathol Appl Neurobiol *12*, 401-14.

Hall, S. M. (1986b). Regeneration in cellular and acellular autografts in the peripheral nervous system. Neuropathol Appl Neurobiol *12*, 27-46.

Hall, S. M. (1989). Regeneration in the peripheral nervous system. Neuropathol Appl Neurobiol *15*, 513-29.

Harris, J., and Wilson, P. (1971). Denervation in murine dystrophy. Nature *229*, 61-2.

Hayashi, Y. K., Chou, F. L., Engvall, E., Ogawa, M., Matsuda, C., Hirabayashi, S., Yokochi, K., Ziober, B. L., Kramer, R. H., Kaufman, S. J., Ozawa, E., Goto, Y., Nonaka, I., Tsukahara, T., Wang, J. Z., Hoffman, E. P., and Arahata, K. (1998). Mutations in the integrin alpha 7 gene cause congenital myopathy. Nature Genetics *19*, 94-97.

Helbling-Leclerc, A., Zhang, X., Topaloglu, H., Cruaud, C., Tesson, F., Weissenbach, J., Tome, F. M., Schwartz, K., Fardeau, M., Tryggvason, K., and et al. (1995). Mutations in the laminin alpha 2-chain gene (LAMA2) cause merosin-deficient congenital muscular dystrophy. Nat Genet *11*, 216-8.

Hemler, M. E. (1999). Dystroglycan versatility. Cell *97*, 543-546.

Henderson, C. E., Phillips, H. S., Pollock, R. A., Davies, A. M., Lemeulle, C., Armanini, M., Simmons, L., Moffet, B., Vandlen, R. A., Simpson, L. C., and et al. (1994). GDNF: a potent survival factor for motoneurons present in peripheral nerve and muscle [see comments] [published erratum appears in Science 1995 Feb 10;267(5199):777]. Science *266*, 1062-4.

Henkemeyer, M., Marengere, L. E., McGlade, J., Olivier, J. P., Conlon, R. A.,

Holmyard, D. P., Letwin, K., and Pawson, T. (1994). Immunolocalization of the Nuk receptor tyrosine kinase suggests roles in segmental patterning of the brain and axonogenesis. Oncogene *9*, 1001-14.

Herrmann, R., Straub, V., Meyer, K., Kahn, T., Wagner, M., and Voit, T. (1996). Congenital muscular dystrophy with laminin alpha 2 chain deficiency: Identification of a new intermediate phenotype and correlation of clinical findings to muscle immunohistochemistry. European Journal of Pediatrics *155*, 968-976.

Heumann, R., Korsching, S., Bandtlow, C., and Thoenen, H. (1987). Changes of nerve growth factor synthesis in nonneuronal cells in response to sciatic nerve transection. J Cell Biol *104*, 1623-31.

Hodges, B. L., Hayashi, Y. K., Nonaka, I., Wang, W., Arahata, K., and Kaufman, S. J. (1997). Altered expression of the alpha 7 beta 1 integrin in human and murine muscular dystrophies. Journal of Cell Science *110*, 2873-2881.

Hoffman, E. P., Brown, R. H., Jr., and Kunkel, L. M. (1987). Dystrophin: the protein product of the Duchenne muscular dystrophy locus. Cell *51*, 919-28.

Hohenester, E., Tisi, D., Talts, J. F., and Timpl, R. (1999). The crystal structure of a laminin G-like module reveals the molecular basis of alpha-dystroglycan binding to laminins, perlecan, and agrin. Molecular Cell *4*, 783-792.

Hsiao, L. L., Engvall, E., Peltonen, J., and Uitto, J. (1993). Expression of laminin isoforms by peripheral nerve-derived connective tissue cells in culture. Comparison with epitope distribution in normal human nerve and neural tumors in vivo. Lab Invest *68*, 100-8.

Huizar, P., Kuno, M., and Miyata, Y. (1975). Electrophysiological properties of spinal motoneurones of normal and dystrophic mice. J Physiol (Lond) *248*, 231-46.

Hunter, D. D., Porter, B. E., Bulock, J. W., Adams, S. P., Merlie, J. P., and Sanes, J. R. (1989a). Primary sequence of a motor neuron-selective adhesive site in the synaptic basal lamina protein S-laminin. Cell *59*, 905-13.

Hunter, D. D., Shah, V., Merlie, J. P., and Sanes, J. R. (1989b). A laminin-like adhesive protein concentrated in the synaptic cleft of the neuromuscular junction. Nature *338*, 229-34.

Hynes, R. O. (1992). Integrins: versatility, modulation, and signaling in cell adhesion. Cell *69*, 11-25.

Ibraghimov-Beskrovnaya, O., Ervasti, J. M., Leveille, C. J., Slaughter, C. A.,

Sernett, S. W., and Campbell, K. P. (1992). Primary structure of dystrophin-associated glycoproteins linking dystrophin to the extracellular matrix. Nature *355*, 696-702.

Iivanainen, A., Morita, T., and Tryggvason, K. (1999). Molecular cloning and tissue-specific expression of a novel murine laminin gamma 3 chain. Journal of Biological Chemistry *274*, 14107-14111.

Iivanainen, A., Sainio, K., Sariola, H., and Tryggvason, K. (1995). Primary structure and expression of a novel human laminin alpha 4 chain. FEBS Lett *365*, 183-8.

Jaakkola, S., Savunen, O., Halme, T., Uitto, J., and Peltonen, J. (1993). Basement membranes during development of human nerve: Schwann cells and perineurial cells display marked changes in their expression profiles for laminin subunits and beta 1 and beta 4 integrins. J Neurocytol *22*, 215-30.

Jablecki, C., and Brimijoin, S. (1974). Reduced axoplasmic transport of choline acetyltransferase activity in dystrophic mice. Nature *250*, 151-4.

Jaegle, M., Mandemakers, W., Broos, L., Zwart, R., Karis, A., Visser, P., Grosveld, F., and Meijer, D. (1996). The POU factor Oct-6 and Schwann cell differentiation. Science *273*, 507-10.

Jaros, E., and Bradley, W. G. (1979). Atypical axon-Schwann cell relationships in the common peroneal nerve of the dystrophic mouse: an ultrastructural study. Neuropathol Appl Neurobiol *5*, 133-47.

Jessen, K. R., Brennan, A., Morgan, L., Mirsky, R., Kent, A., Hashimoto, Y., and Gavrilovic, J. (1994). The Schwann cell precursor and its fate: a study of cell death and differentiation during gliogenesis in rat embryonic nerves. Neuron *12*, 509-27.

Jessen, K. R., and Mirsky, R. (1991). Schwann cell precursors and their development. Glia *4*, 185-94.

Jessen, K. R., and Mirsky, R. (1999). Schwann cells and their precursors emerge as major regulators of nerve development. Trends in Neurosciences *22*, 402-410.

Jessen, K. R., Morgan, L., Stewart, H. J., and Mirsky, R. (1990). Three markers of adult non-myelin-forming Schwann cells, 217c(Ran-1), A5E3 and GFAP: development and regulation by neuron-Schwann cell interactions. Development *109*, 91-103.

Keynes, R., Tannahill, D., Morgenstern, D. A., Johnson, A. R., Cook, G. M., and Pini, A. (1997). Surround repulsion of spinal sensory axons in higher vertebrate embryos. Neuron *18*, 889-97.

Keynes, R. J., and Stern, C. D. (1984). Segmentation in the vertebrate nervous system. Nature *310*, 786-9.

Kiernan, B. W., Gotz, B., Faissner, A., and ffrench-Constant, C. (1996). Tenascin-C inhibits oligodendrocyte precursor cell migration by both adhesion-dependent and adhesion-independent mechanisms. Mol Cell Neurosci *7*, 322-35.

Kioussi, C., Gross, M. K., and Gruss, P. (1995). Pax3: a paired domain gene as a regulator in PNS myelination. Neuron *15*, 553-62.

Kitamura, K., Suzuki, M., and Uyemura, K. (1976). Purification and partial characterization of two glycoproteins in bovine peripheral nerve myelin membrane. Biochim Biophys Acta *455*, 806-16.

Klar, A., Baldassare, M., and Jessell, T. M. (1992). F-spondin: a gene expressed at high levels in the floor plate encodes a secreted protein that promotes neural cell adhesion and neurite extension. Cell *69*, 95-110.

Kleitman, N., Simon, D. K., Schachner, M., and Bunge, R. P. (1988). Growth of embryonic retinal neurites elicited by contact with Schwann cell surfaces is blocked by antibodies to L1. Exp Neurol *102*, 298-306.

Koch, M., Olson, P. F., Albus, A., Jin, W., Hunter, D. D., Brunken, W. J., Burgeson, R. E., and Champliaud, M. F. (1999). Characterization and expression of the laminin gamma 3 chain: A novel, non-basement membrane-associated, laminin chain. Journal of Cell Biology *145*, 605-617.

Koenig, M., Monaco, A. P., and Kunkel, L. M. (1988). The complete sequence of dystrophin predicts a rod-shaped cytoskeletal protein. Cell *53*, 219-26.

Kolodkin, A. L., Matthes, D. J., and Goodman, C. S. (1993). The semaphorin genes encode a family of transmembrane and secreted growth cone guidance molecules. Cell *75*, 1389-99.

Komiya, Y., and Austin, L. (1974). Axoplasmic flow of protein in the sciatic nerve of normal and dystrophic mice. Exp Neurol *43*, 1-12.

Kondo, T., and Raff, M. (2000). Oligodendrocyte precursor cells reprogrammed to become multipotential CNS stem cells [see comments]. Science *289*, 1754-7.

Kornberg, L. J., Earp, H. S., Turner, C. E., Prockop, C., and Juliano, R. L.

(1991). Signal transduction by integrins: increased protein tyrosine phosphorylation caused by clustering of beta 1 integrins. Proc Natl Acad Sci U S A *88*, 8392-6.

Kramer, R. H., Vu, M. P., Cheng, Y. F., Ramos, D. M., Timpl, R., and Waleh, N. (1991). Laminin-binding integrin alpha 7 beta 1: functional characterization and expression in normal and malignant melanocytes. Cell Regul *2*, 805-17.

Kuang, W., Xu, H., Vachon, P. H., and Engvall, E. (1998a). Disruption of the lama2 gene in embryonic stem cells: laminin alpha 2 is necessary for sustenance of mature muscle cells. Exp Cell Res *241*, 117-25.

Kuang, W., Xu, H., Vachon, P. H., Liu, L., Loechel, F., Wewer, U. M., and Engvall, E. (1998b). Merosin-deficient congenital muscular dystrophy - Partial genetic correction in two mouse models. Journal of Clinical Investigation *102*, 844-852.

Kuang, W., Xu, H., Vilquin, J. T., and Engvall, E. (1999). Activation of the lama2 gene in muscle regeneration: abortive regeneration in laminin alpha2-deficiency. Lab Invest *79*, 1601-13.

Kuecherer-Ehret, A., Graeber, M. B., Edgar, D., Thoenen, H., and Kreutzberg, G. W. (1990). Immunoelectron microscopic localization of laminin in normal and regenerating mouse sciatic nerve. J Neurocytol *19*, 101-9.

Kwon, Y. K., Bhattacharyya, A., Alberta, J. A., Giannobile, W. V., Cheon, K., Stiles, C. D., and Pomeroy, S. L. (1997). Activation of ErbB2 during wallerian degeneration of sciatic nerve. J Neurosci *17*, 8293-9.

Laemmli, U. K. (1970). Cleavage of structural proteins during the assembly of the head of bacteriophage T4. Nature *227*, 680-5.

Law, P. K., Saito, A., and Fleischer, S. (1983). Ultrastructural changes in muscle and motor end-plate of the dystrophic mouse. Exp Neurol *80*, 361-82.

Le Beau, J. M., LaCorbiere, M., Powell, H. C., Ellisman, M. H., and Schubert, D. (1988). Extracellular fluid conditioned during peripheral nerve regeneration stimulates Schwann cell adhesion, migration and proliferation. Brain Res *459*, 93-104.

Le Douarin, N. M., and Smith, J. (1988). Development of the peripheral nervous system from the neural crest. Annu Rev Cell Biol *4*, 375-404.

Lee, M., Brennan, A., Blanchard, A., Zoidl, G., Dong, Z., Tabernero, A., Zoidl, C., Dent, M. A., Jessen, K. R., and Mirsky, R. (1997). P0 is constitutively

expressed in the rat neural crest and embryonic nerves and is negatively and positively regulated by axons to generate non-myelin-forming and myelin-forming Schwann cells, respectively. Mol Cell Neurosci *8*, 336-50.

Lefcort, F., Venstrom, K., McDonald, J. A., and Reichardt, L. F. (1992). Regulation of expression of fibronectin and its receptor, alpha 5 beta 1, during development and regeneration of peripheral nerve. Development *116*, 767-82.

Leivo, I., and Engvall, E. (1988). Merosin, a protein specific for basement membranes of Schwann cells, striated muscle, and trophoblast, is expressed late in nerve and muscle development. Proc Natl Acad Sci U S A *85*, 1544-8.

Leivo, I., Laurila, P., Wahlstrom, T., and Engvall, E. (1989). Expression of merosin, a tissue-specific basement membrane protein, in the intermediate trophoblast cells of choriocarcinoma and placenta. Lab Invest *60*, 783-90.

Leivo, I., Vaheri, A., Timpl, R., and Wartiovaara, J. (1980). Appearance and distribution of collagens and laminin in the early mouse embryo. Dev Biol *76*, 100-14.

Lemke, G. (1993). The molecular genetics of myelination: an update. Glia *7*, 263-71.

Lemke, G. (1996). Neuregulins in development. Mol Cell Neurosci *7*, 247-62.

Lemke, G., and Chao, M. (1988). Axons regulate Schwann cell expression of the major myelin and NGF receptor genes. Development *102*, 499-504.

Lemke, G., Lamar, E., and Patterson, J. (1988). Isolation and analysis of the gene encoding peripheral myelin protein zero. Neuron *1*, 73-83.

Lemke, G. E., and Brockes, J. P. (1984). Identification and purification of glial growth factor. J Neurosci *4*, 75-83.

Lentz, S. I., Miner, J. H., Sanes, J. R., and Snider, W. D. (1997). Distribution of the ten known laminin chains in the pathways and targets of developing sensory axons. Journal of Comparative Neurology *378*, 547-561.

Letourneau, P. C., Roche, F. K., Shattuck, T. A., Lemmon, V., and Takeichi, M. (1991). Interactions of Schwann cells with neurites and with other Schwann cells involve the calcium-dependent adhesion molecule, N-cadherin. J Neurobiol *22*, 707-20.

Letourneau, P. C., Shattuck, T. A., Roche, F. K., Takeichi, M., and Lemmon, V. (1990). Nerve growth cone migration onto Schwann cells involves the calcium-

dependent adhesion molecule, N-cadherin. Dev Biol *138*, 430-42.

Levi, A. D., Bunge, R. P., Lofgren, J. A., Meima, L., Hefti, F., Nikolics, K., and Sliwkowski, M. X. (1995). The influence of heregulins on human Schwann cell proliferation. J Neurosci *15*, 1329-40.

Liem, K. F., Jr., Tremml, G., Roelink, H., and Jessell, T. M. (1995). Dorsal differentiation of neural plate cells induced by BMP-mediated signals from epidermal ectoderm. Cell *82*, 969-79.

Lin, W., Sanchez, H. B., Deerinck, T., Morris, J. K., Ellisman, M., and Lee, K. F. (2000). Aberrant development of motor axons and neuromuscular synapses in erbB2-deficient mice. Proc Natl Acad Sci U S A *97*, 1299-304.

Loftus, J. C., O'Toole, T. E., Plow, E. F., Glass, A., Frelinger, A. L. d., and Ginsberg, M. H. (1990). A beta 3 integrin mutation abolishes ligand binding and alters divalent cation-dependent conformation. Science *249*, 915-8.

London, Y. (1971). Ox peripheral nerve myelin membrane. Purification and partial characterization of two basic proteins. Biochim Biophys Acta *249*, 188-96.

Loring, J. F., and Erickson, C. A. (1987). Neural crest cell migratory pathways in the trunk of the chick embryo. Dev Biol *121*, 220-36.

Love, D. R., Hill, D. F., Dickson, G., Spurr, N. K., Byth, B. C., Marsden, R. F., Walsh, F. S., Edwards, Y. H., and Davies, K. E. (1989). An autosomal transcript in skeletal muscle with homology to dystrophin. Nature *339*, 55-8.

Love, F. M., and Thompson, W. J. (1998). Schwann cells proliferate at rat neuromuscular junctions during development and regeneration. J Neurosci *18*, 9376-85.

Lowenstein, E. J., Daly, R. J., Batzer, A. G., Li, W., Margolis, B., Lammers, R., Ullrich, A., Skolnik, E. Y., Bar-Sagi, D., and Schlessinger, J. (1992). The SH2 and SH3 domain-containing protein GRB2 links receptor tyrosine kinases to ras signaling. Cell *70*, 431-42.

Lunn, E. R., Perry, V. H., Brown, M. C., Rosen, H., and Gordon, S. (1989). Absence of Wallerian degeneration does not hinder regeneration in peripheral nerve. Eur J Neurosci *1*, 27-33.

Luo, Y., Raible, D., and Raper, J. A. (1993). Collapsin: a protein in brain that induces the collapse and paralysis of neuronal growth cones. Cell *75*, 217-27.

Lyons, K. M., Hogan, B. L., and Robertson, E. J. (1995). Colocalization of BMP

7 and BMP 2 RNAs suggests that these factors cooperatively mediate tissue interactions during murine development. Mech Dev *50*, 71-83.

Madrid, R. E., Jaros, E., Cullen, M. J., and Bradley, W. G. (1975). Genetically determined defect of Schwann cell basement membrane in dystrophic mice. Nature *257*, 319-321.

Mainiero, F., Pepe, A., Yeon, M., Ren, Y., and Giancotti, F. G. (1996). The intracellular functions of alpha6beta4 integrin are regulated by EGF. J Cell Biol *134*, 241-53.

Malandrini, A., Villanova, M., Sabatelli, P., Squarzoni, S., Six, J., Toti, P., Guazzi, G., and Maraldi, N. M. (1997). Localization of the laminin alpha 2 chain in normal human skeletal muscle and peripheral nerve: An ultrastructural immunolabeling study. Acta Neuropathologica *93*, 166-172.

Manfioletti, G., Ruaro, M. E., Del Sal, G., Philipson, L., and Schneider, C. (1990). A growth arrest-specific (gas) gene codes for a membrane protein. Mol Cell Biol *10*, 2924-30.

Marchionni, M. A., Goodearl, A. D., Chen, M. S., Bermingham-McDonogh, O., Kirk, C., Hendricks, M., Danehy, F., Misumi, D., Sudhalter, J., Kobayashi, K., and et al. (1993). Glial growth factors are alternatively spliced erbB2 ligands expressed in the nervous system [see comments]. Nature *362*, 312-8.

Marinkovich, M. P., Lunstrum, G. P., and Burgeson, R. E. (1992a). The anchoring filament protein kalinin is synthesized and secreted as a high molecular weight precursor. J Biol Chem *267*, 17900-6.

Marinkovich, M. P., Lunstrum, G. P., Keene, D. R., and Burgeson, R. E. (1992b). The dermal-epidermal junction of human skin contains a novel laminin variant. J Cell Biol *119*, 695-703.

Martin, G. R., and Timpl, R. (1987). Laminin and other basement membrane components. Annu Rev Cell Biol *3*, 57-85.

Martin, P. T., Kaufman, S. J., Kramer, R. H., and Sanes, J. R. (1996). Synaptic integrins in developing, adult, and mutant muscle: Selective association of alpha 1, alpha 7A, and alpha 7B integrins with the neuromuscular junction. Developmental Biology *174*, 125-139.

Martini, R., Mohajeri, M. H., Kasper, S., Giese, K. P., and Schachner, M. (1995). Mice doubly deficient in the genes for P0 and myelin basic protein show

that both proteins contribute to the formation of the major dense line in peripheral nerve myelin. J Neurosci *15*, 4488-95.

Martini, R., and Schachner, M. (1988). Immunoelectron microscopic localization of neural cell adhesion molecules (L1, N-CAM, and myelin-associated glycoprotein) in regenerating adult mouse sciatic nerve. J Cell Biol *106*, 1735-46.

Masaki, T., Matsumura, K., Saito, F., Sunada, Y., Shimizu, T., Yorifuji, H., Motoyoshi, K., and Kamakura, K. (2000). Expression of dystroglycan and laminin-2 in peripheral nerve under axonal degeneration and regeneration. Acta Neuropathologica *99*, 289-295.

Masu, Y., Wolf, E., Holtmann, B., Sendtner, M., Brem, G., and Thoenen, H. (1993). Disruption of the CNTF gene results in motor neuron degeneration. Nature *365*, 27-32.

Matsumura, K., Ervasti, J. M., Ohlendieck, K., Kahl, S. D., and Campbell, K. P. (1992). Association of dystrophin-related protein with dystrophin-associated proteins in mdx mouse muscle. Nature *360*, 588-91.

Matsumura, K., Yamada, H., Shimizu, T., and Campbell, K. P. (1993). Differential expression of dystrophin, utrophin and dystrophin-associated proteins in peripheral nerve. FEBS Lett *334*, 281-5.

Maurel, P., and Salzer, J. L. (2000). Axonal regulation of Schwann cell proliferation and survival and the initial events of myelination requires PI 3-kinase activity. J Neurosci *20*, 4635-45.

McKerracher, L., David, S., Jackson, D. L., Kottis, V., Dunn, R. J., and Braun, P. E. (1994). Identification of myelin-associated glycoprotein as a major myelin-derived inhibitor of neurite growth. Neuron *13*, 805-11.

Meier, C., Parmantier, E., Brennan, A., Mirsky, R., and Jessen, K. R. (1999). Developing Schwann cells acquire the ability to survive without axons by establishing an autocrine circuit involving insulin-like growth factor, neurotrophin-3, and platelet-derived growth factor-BB. J Neurosci *19*, 3847-59.

Menegoz, M., Gaspar, P., Le Bert, M., Galvez, T., Burgaya, F., Palfrey, C., Ezan, P., Arnos, F., and Girault, J. A. (1997). Paranodin, a glycoprotein of neuronal paranodal membranes. Neuron *19*, 319-31.

Mentaberry, A., Adesnik, M., Atchison, M., Norgard, E. M., Alvarez, F., Sabatini, D. D., and Colman, D. R. (1986). Small basic proteins of myelin from

central and peripheral nervous systems are encoded by the same gene. Proc Natl Acad Sci U S A *83*, 1111-4.

Messersmith, E. K., Leonardo, E. D., Shatz, C. J., Tessier-Lavigne, M., Goodman, C. S., and Kolodkin, A. L. (1995). Semaphorin III can function as a selective chemorepellent to pattern sensory projections in the spinal cord. Neuron *14*, 949-59.

Meyer, D., and Birchmeier, C. (1994). Distinct isoforms of neuregulin are expressed in mesenchymal and neuronal cells during mouse development. Proc Natl Acad Sci U S A *91*, 1064-8.

Meyer, D., and Birchmeier, C. (1995). Multiple essential functions of neuregulin in development [published erratum appears in Nature 1995 Dec 14;378(6558):753]. Nature *378*, 386-90.

Michelson, A. M., Russel, E. S., and Harman, P. J. (1955). Dystrophia muscularis:a hereditary primary myopathy in the house mouse. Proceeds of the National Academy of Sciences (Washington) *61*, 1079-1084.

Milner, R., Huang, X., Wu, J., Nishimura, S., Pytela, R., Sheppard, D., and ffrench-Constant, C. (1999). Distinct roles for astrocyte alphavbeta5 and alphavbeta8 integrins in adhesion and migration. J Cell Sci *112*, 4271-9.

Milner, R., Wilby, M., Nishimura, S., Boylen, K., Edwards, G., Fawcett, J., Streuli, C., Pytela, R., and ffrench-Constant, C. (1997). Division of labor of Schwann cell integrins during migration on peripheral nerve extracellular matrix ligands. Dev Biol *185*, 215-28.

Miner, J. H., Patton, B. L., Lentz, S. I., Gilbert, D. J., Jenkins, N. A., Copeland, N. G., and Sanes, J. R. (1997). The laminin alpha chains: Expression, developmental transitions, and chromosomal locations of alpha 1-5, identification of heterotrimeric laminins 8-11, and cloning of a novel alpha 3 isoform. Journal of Cell Biology *137*, 685-701.

Mirsky, R., and Jessen, K. R. (1996). Schwann cell development, differentiation and myelination. Curr Opin Neurobiol *6*, 89-96.

Mirsky, R., Parmantier, E., McMahon, A. P., and Jessen, K. R. (1999). Schwann cell-derived desert hedgehog signals nerve sheath formation. Ann N Y Acad Sci *883*, 196-202.

Miyagoe, Y., Hanaoka, K., Nonaka, I., Hayasaka, M., Nabeshima, Y., Arahata,

K., and Takeda, S. (1997). Laminin alpha 2 chain-null mutant mice by targeted disruption of the Lama2gene: a new model of merosin (laminin 2)-deficient congenital muscular dystrophy. Febs Letters *415*, 33-39.

Miyamoto, S., Teramoto, H., Gutkind, J. S., and Yamada, K. M. (1996). Integrins can collaborate with growth factors for phosphorylation of receptor tyrosine kinases and MAP kinase activation: roles of integrin aggregation and occupancy of receptors. J Cell Biol *135*, 1633-42.

Monuki, E. S., Kuhn, R., and Lemke, G. (1993). Repression of the myelin P0 gene by the POU transcription factor SCIP. Mech Dev *42*, 15-32.

Monuki, E. S., Kuhn, R., Weinmaster, G., Trapp, B. D., and Lemke, G. (1990). Expression and activity of the POU transcription factor SCIP. Science *249*, 1300-3.

Monuki, E. S., Weinmaster, G., Kuhn, R., and Lemke, G. (1989). SCIP: a glial POU domain gene regulated by cyclic AMP. Neuron *3*, 783-93.

Moore, M. W., Klein, R. D., Farinas, I., Sauer, H., Armanini, M., Phillips, H., Reichardt, L. F., Ryan, A. M., Carver-Moore, K., and Rosenthal, A. (1996). Renal and neuronal abnormalities in mice lacking GDNF. Nature *382*, 76-9.

Morandi, L., Di Blasi, C., Farina, L., Sorokin, L., Uziel, G., Azan, G., Pini, A., Toscano, A., Lanfossi, M., Galbiati, S., Cornelio, F., and Mora, M. (1999). Clinical correlations in 16 patients with total or partial laminin alpha2 deficiency characterized using antibodies against 2 fragments of the protein. Arch Neurol *56*, 209-15.

Morris, J. K., Lin, W., Hauser, C., Marchuk, Y., Getman, D., and Lee, K. F. (1999). Rescue of the cardiac defect in ErbB2 mutant mice reveals essential roles of ErbB2 in peripheral nervous system development. Neuron *23*, 273-83.

Morrison, S. J., Perez, S. E., Qiao, Z., Verdi, J. M., Hicks, C., Weinmaster, G., and Anderson, D. J. (2000). Transient Notch activation initiates an irreversible switch from neurogenesis to gliogenesis by neural crest stem cells. Cell *101*, 499-510.

Morrison, S. J., White, P. M., Zock, C., and Anderson, D. J. (1999). Prospective identification, isolation by flow cytometry, and in vivo self-renewal of multipotent mammalian neural crest stem cells. Cell *96*, 737-49.

Mujtaba, T., Mayer-Proschel, M., and Rao, M. S. (1998). A common neural progenitor for the CNS and PNS. Dev Biol *200*, 1-15.

Mukhopadhyay, G., Doherty, P., Walsh, F. S., Crocker, P. R., and Filbin, M. T. (1994). A novel role for myelin-associated glycoprotein as an inhibitor of axonal regeneration. Neuron *13*, 757-67.

Murphy, P., Topilko, P., Schneider-Maunoury, S., Seitanidou, T., Baron-Van Evercooren, A., and Charnay, P. (1996). The regulation of Krox-20 expression reveals important steps in the control of peripheral glial cell development. Development *122*, 2847-57.

Naef, R., and Suter, U. (1998). Many facets of the peripheral myelin protein PMP22 in myelination and disease. Microsc Res Tech *41*, 359-71.

Nakao, J., Shinoda, J., Nakai, Y., Murase, S., and Uyemura, K. (1997). Apoptosis regulates the number of Schwann cells at the premyelinating stage. J Neurochem *68*, 1853-62.

Nathaniel, E. J., and Pease, D. C. (1963). Regenerative changes in rat dorsal roots following Wallerian degeneration. J Ultrastruct Res *9*, 533-549.

Nave, K. A., Lai, C., Bloom, F. E., and Milner, R. J. (1987). Splice site selection in the proteolipid protein (PLP) gene transcript and primary structure of the DM-20 protein of central nervous system myelin. Proc Natl Acad Sci U S A *84*, 5665-9.

Nikam, S. S., Tennekoon, G. I., Christy, B. A., Yoshino, J. E., and Rutkowski, J. L. (1995). The zinc finger transcription factor Zif268/Egr-1 is essential for Schwann cell expression of the p75 NGF receptor. Mol Cell Neurosci *6*, 337-48.

Noakes, P. G., and Bennett, M. R. (1987). Growth of axons into developing muscles of the chick forelimb is preceded by cells that stain with Schwann cell antibodies. J Comp Neurol *259*, 330-47.

Noakes, P. G., Bennett, M. R., and Stratford, J. (1988). Migration of Schwann cells and axons into developing chick forelimb muscles following removal of either the neural tube or the neural crest. J Comp Neurol *277*, 214-33.

Noakes, P. G., Gautam, M., Mudd, J., Sanes, J. R., and Merlie, J. P. (1995). Aberrant differentiation of neuromuscular junctions in mice lacking s-laminin/laminin beta 2. Nature *374*, 258-62.

Noble, M., Murray, K., Stroobant, P., Waterfield, M. D., and Riddle, P. (1988). Platelet-derived growth factor promotes division and motility and inhibits premature differentiation of the oligodendrocyte/type-2 astrocyte progenitor cell. Nature *333*, 560-2.

Nomizu, M., Otaka, A., Utani, A., Roller, P. P., and Yamada, Y. (1994). Assembly of synthetic laminin peptides into a triple-stranded coiled- coil structure. J Biol Chem *269*, 30386-92.

Obremski, V. J., and Bunge, M. B. (1995). Addition of purified basal lamina molecules enables Schwann cell ensheathment of sympathetic neurites in culture. Dev Biol *168*, 124-37.

Obremski, V. J., Johnson, M. I., and Bunge, M. B. (1993a). Fibroblasts are required for Schwann cell basal lamina deposition and ensheathment of unmyelinated sympathetic neurites in culture. J Neurocytol *22*, 102-17.

Obremski, V. J., Wood, P. M., and Bunge, M. B. (1993b). Fibroblasts promote Schwann cell basal lamina deposition and elongation in the absence of neurons in culture. Dev Biol *160*, 119-34.

Ohlendieck, K., and Campbell, K. P. (1991). Dystrophin-associated proteins are greatly reduced in skeletal muscle from mdx mice. J Cell Biol *115*, 1685-94.

Ohlendieck, K., Ervasti, J. M., Matsumura, K., Kahl, S. D., Leveille, C. J., and Campbell, K. P. (1991a). Dystrophin-related protein is localized to neuromuscular junctions of adult skeletal muscle. Neuron *7*, 499-508.

Ohlendieck, K., Ervasti, J. M., Snook, J. B., and Campbell, K. P. (1991b). Dystrophin-glycoprotein complex is highly enriched in isolated skeletal muscle sarcolemma. J Cell Biol *112*, 135-48.

Okada, E., Mizuhira, V., and Nakamura, H. (1975). Abnormalities of the sciatic nerves of dystrophic mice, with reference to nerve counts and mean area of axons. Bull Tokyo Med Dent Univ *22*, 25-43.

Okada, E., Mizuhira, V., and Nakamura, H. (1977). Abnormally combined myelinated and unmyelinated nerves in dystrophic mice. J Neurol Sci *33*, 243-9.

Okada, E., Mizuhira, V., and Nakamura, H. (1976). Dysmyelination in the sciatic nerves of dystrophic mice. J Neurol Sci *28*, 505-20.

Omlin, F. X., Webster, H. D., Palkovits, C. G., and Cohen, S. R. (1982). Immunocytochemical localization of basic protein in major dense line regions of central and peripheral myelin. J Cell Biol *95*, 242-8.

Opdecamp, K., Nakayama, A., Nguyen, M. T., Hodgkinson, C. A., Pavan, W. J., and Arnheiter, H. (1997). Melanocyte development in vivo and in neural crest cell cultures: crucial dependence on the Mitf basic-helix-loop-helix-zipper

transcription factor. Development *124*, 2377-86.

Orr-Urtreger, A., Trakhtenbrot, L., Ben-Levy, R., Wen, D., Rechavi, G., Lonai, P., and Yarden, Y. (1993). Neural expression and chromosomal mapping of Neu differentiation factor to 8p12-p21. Proc Natl Acad Sci U S A *90*, 1867-71.

Ott, U., Odermatt, E., Engel, J., Furthmayr, H., and Timpl, R. (1982). Protease resistance and conformation of laminin. Eur J Biochem *123*, 63-72.

Pall, E. A., Bolton, K. M., and Ervasti, J. M. (1996). Differential heparin inhibition of skeletal muscle alpha-dystroglycan binding to laminins. Journal of Biological Chemistry *271*, 3817-3821.

Pareek, S., Suter, U., Snipes, G. J., Welcher, A. A., Shooter, E. M., and Murphy, R. A. (1993). Detection and processing of peripheral myelin protein PMP22 in cultured Schwann cells. J Biol Chem *268*, 10372-9.

Parmantier, E., Cabon, F., Braun, C., D'Urso, D., Muller, H. W., and Zalc, B. (1995). Peripheral myelin protein-22 is expressed in rat and mouse brain and spinal cord motoneurons. Eur J Neurosci *7*, 1080-8.

Parmantier, E., Lynn, B., Lawson, D., Turmaine, M., Namini, S. S., Chakrabarti, L., McMahon, A. P., Jessen, K. R., and Mirsky, R. (1999). Schwann cell-derived desert hedgehog controls the development of peripheral nerve sheaths. Neuron *23*, 713-724.

Parsons, J. T. (1996). Integrin-mediated signalling: regulation by protein tyrosine kinases and small GTP-binding proteins. Curr Opin Cell Biol *8*, 146-52.

Patton, B. L., Chiu, A. Y., and Sanes, J. R. (1998). Synaptic laminin prevents glial entry into the synaptic cleft. Nature *393*, 698-701.

Patton, B. L., Connoll, A. M., Martin, P. T., Cunningham, J. M., Mehta, S., Pestronk, A., Miner, J. H., and Sanes, J. R. (1999). Distribution of ten laminin chains in dystrophic and regenerating muscles. Neuromuscul Disord *9*, 423-33.

Patton, B. L., Miner, J. H., Chiu, A. Y., and Sanes, J. R. (1997). Distribution and function of laminins in the neuromuscular system of developing, adult, and mutant mice. Journal of Cell Biology *139*, 1507-1521.

Pattyn, A., Morin, X., Cremer, H., Goridis, C., and Brunet, J. F. (1999). The homeobox gene Phox2b is essential for the development of autonomic neural crest derivatives. Nature *399*, 366-70.

Paulsson, M., Deutzmann, R., Timpl, R., Dalzoppo, D., Odermatt, E., and

Engel, J. (1985). Evidence for coiled-coil alpha-helical regions in the long arm of laminin. Embo J *4*, 309-16.

Paulsson, M., and Saladin, K. (1989). Mouse heart laminin. Purification of the native protein and structural comparison with Engelbreth-Holm-Swarm tumour laminin. J Biol Chem *264*, 18726-18732.

Paulsson, M., Saladin, K., and Engvall, E. (1991). Structure of laminin variants. The 300kDa chains of merosin and bovine heart laminin are related to the human placenta merosin heavy chain and replace the a chain in some laminin variants. J Biol Chem *266*, 17545-17551.

Pegoraro, E., Fanin, M., Trevisan, C. P., Watkins, S. C., Angelini, C., and Hoffman, E. P. (1998). Identification of a novel laminin alpha 2 isoform expressed in muscle, and identification of a severe congenital muscular dystrophy (CMD) patient who uniqually accumulates this isoform. Neurology *50*, 4121.

Pegoraro, E., Fanin, P. M., Trevisan, C. P., Angelini, C., and Hoffman, E. P. (2000). A novel laminin alpha2 isoform in severe laminin alpha2 deficient congenital muscular dystrophy [In Process Citation]. Neurology *55*, 1128-34.

Peles, E., Nativ, M., Lustig, M., Grumet, M., Schilling, J., Martinez, R.,

Plowman, G. D., and Schlessinger, J. (1997). Identification of a novel contactin-associated transmembrane receptor with multiple domains implicated in protein-protein interactions. Embo J *16*, 978-88.

Perez, S. E., Rebelo, S., and Anderson, D. J. (1999). Early specification of sensory neuron fate revealed by expression and function of neurogenins in the chick embryo. Development *126*, 1715-28.

Perkins, C. S., Bray, G. M., and Aguayo, A. J. (1981). Ongoing block of Schwann cell differentiation and deployment in dystrophic mouse spinal roots. Brain Res *227*, 213-20.

Perkins, C. S., Bray, G. M., and Aguayo, A. J. (1980). Persistent multiplication of axon-associated cells in the spinal roots of dystrophic mice. Neuropathol Appl Neurobiol *6*, 83-91.

Plopper, G. E., McNamee, H. P., Dike, L. E., Bojanowski, K., and Ingber, D. E. (1995). Convergence of integrin and growth factor receptor signaling pathways within the focal adhesion complex. Mol Biol Cell *6*, 1349-65.

Plow, E. F., Haas, T. A., Zhang, L., Loftus, J., and Smith, J. W. (2000). Ligand

binding to integrins. J Biol Chem *275*, 21785-8.

Podratz, J. L., Rodriguez, E. H., DiNonno, E. S., and Windebank, A. J. (1998). Myelination by Schwann cells in the absence of extracellular matrix assembly. Glia *23*, 383-8.

Poliak, S., Gollan, L., Martinez, R., Custer, A., Einheber, S., Salzer, J. L., Trimmer, J. S., Shrager, P., and Peles, E. (1999). Caspr2, a new member of the neurexin superfamily, is localized at the juxtaparanodes of myelinated axons and associates with K+ channels. Neuron *24*, 1037-47.

Polinsky, M., Balazovich, K., and Tosney, K. W. (2000). Identification of an invariant response: Stable contact with Schwann cells induces veil extension in sensory growth cones. Journal of Neuroscience *20*, 1044-1055.

Porter, B. E., Justice, M. J., Copeland, N. G., Jenkins, N. A., Hunter, D. D., Merlie, J. P., and Sanes, J. R. (1993). S-laminin: mapping to mouse chromosome 9 and expression in the linked mutants tippy and ducky. Genomics *16*, 278-81.

Privat, A., Jacque, C., Bourre, J. M., Dupouey, P., and Baumann, N. (1979). Absence of the major dense line in myelin of the mutant mouse "shiverer". Neurosci Lett *12*, 107-12.

Puckett, C., Hudson, L., Ono, K., Friedrich, V., Benecke, J., Dubois-Dalcq, M., and Lazzarini, R. A. (1987). Myelin-specific proteolipid protein is expressed in myelinating Schwann cells but is not incorporated into myelin sheaths. J Neurosci Res *18*, 511-8.

Pulkkinen, L., Christiano, A. M., Airenne, T., Haakana, H., Tryggvason, K., and Uitto, J. (1994). Mutations in the gamma 2 chain gene (LAMC2) of kalinin/laminin 5 in the junctional forms of epidermolysis bullosa. Nat Genet *6*, 293-7.

Pulkkinen, L., Gerecke, D. R., Christiano, A. M., Wagman, D. W., Burgeson, R. E., and Uitto, J. (1995). Cloning of the beta 3 chain gene (LAMB3) of human laminin 5, a candidate gene in junctional epidermolysis bullosa. Genomics *25*, 192-8.

Qu, Z., Apel, E. D., Doherty, C. A., Hoffman, P. W., Merlie, J. P., and Huganir, R. L. (1996). The synapse-associated protein rapsyn regulates tyrosine phosphorylation of proteins colocalized at nicotinic acetylcholine receptor clusters. Mol Cell Neurosci *8*, 171-84.

Rambukkana, A., Salzer, J. L., Yurchenco, P. D., and Tuomanen, E. I. (1997). Neural targeting of Mycobacterium leprae mediated by the G domain of the laminin-alpha2 chain. Cell *88*, 811-21.

Rambukkana, A., Yamada, H., Zanazzi, G., Mathus, T., Salzer, J. L., Yurchenco, P. D., Campbell, K. P., and Fischetti, V. A. (1998). Role of alpha-dystroglycan as a Schwann cell receptor for Mycobacterium leprae [see comments]. Science *282*, 2076-9.

Rasminsky, M. (1978). Ectopic generation of impulses and cross-talk in spinal nerve roots of "dystrophic" mice. Ann Neurol *3*, 351-7.

Rasminsky, M., Kearney, R. E., Aguayo, A. J., and Bray, G. M. (1978). Conduction of nervous impulses in spinal roots and peripheral nerves of dystrophic mice. Brain Res *143*, 71-85.

Richards, A., AlImara, L., and Pope, F. M. (1996). The complete cDNA sequence of laminin alpha 4 and its relationship to the other human laminin alpha chains. European Journal of Biochemistry *238*, 813-821.

Richards, A. J., al-Imara, L., Carter, N. P., Lloyd, J. C., Leversha, M. A., and Pope, F. M. (1994). Localization of the gene (LAMA4) to chromosome 6q21 and isolation of a partial cDNA encoding a variant laminin A chain. Genomics *22*, 237-9.

Rickmann, M., Fawcett, J. W., and Keynes, R. J. (1985). The migration of neural crest cells and the growth of motor axons through the rostral half of the chick somite. J Embryol Exp Morphol *90*, 437-55.

Riethmacher, D., Sonnenberg-Riethmacher, E., Brinkmann, V., Yamaai, T., Lewin, G. R., and Birchmeier, C. (1997). Severe neuropathies in mice with targeted mutations in the ErbB3 receptor. Nature *389*, 725-30.

Ringelmann, B., Roder, C., Hallmann, R., Maley, M., Davies, M., Grounds, M., and Sorokin, L. (1999). Expression of laminin alpha1, alpha2, alpha4, and alpha5 chains, fibronectin, and tenascin-C in skeletal muscle of dystrophic 129ReJ dy/dy mice. Exp Cell Res *246*, 165-82.

Rios, J. C., Melendez-Vasquez, C. V., Einheber, S., Lustig, M., Grumet, M., Hemperly, J., Peles, E., and Salzer, J. L. (2000). Contactin-associated protein (Caspr) and contactin form a complex that is targeted to the paranodal junctions during myelination. J Neurosci *20*, 8354-64.

Rodriguez, F. J., Verdu, E., Ceballos, D., and Navarro, X. (2000). Nerve guides seeded with autologous schwann cells improve nerve regeneration. Exp Neurol *161*, 571-84.

Roomi, M. W., Ishaque, A., Khan, N. R., and Eylar, E. H. (1978). The PO protein. The major glycoprotein of peripheral nerve myelin. Biochim Biophys Acta *536*, 112-21.

Rosales, C., O'Brien, V., Kornberg, L., and Juliano, R. (1995). Signal transduction by cell adhesion receptors. Biochim Biophys Acta *1242*, 77-98.

Rousselle, P., and Aumailley, M. (1994). Kalinin is more efficient than laminin in promoting adhesion of primary keratinocytes and some other epithelial cells and has a different requirement for integrin receptors. J Cell Biol *125*, 205-14.

Rousselle, P., Lunstrum, G. P., Keene, D. R., and Burgeson, R. E. (1991). Kalinin: an epithelium-specific basement membrane adhesion molecule that is a component of anchoring filaments. J Cell Biol *114*, 567-76.

Russo, K., Di Stasio, E., Macchia, G., Rosa, G., Brancaccio, A., and Petrucci, T. C. (2000). Characterization of the beta-dystroglycan-growth factor receptor 2 (Grb2) interaction. Biochem Biophys Res Commun *274*, 93-8.

Ryan, M. C., Tizard, R., VanDevanter, D. R., and Carter, W. G. (1994). Cloning of the LamA3 gene encoding the alpha 3 chain of the adhesive ligand epiligrin. Expression in wound repair. J Biol Chem *269*, 22779-87.

Saito, F., Masaki, T., Kamakura, K., Anderson, L. V., Fujita, S., Fukuta-Ohi, H., Sunada, Y., Shimizu, T., and Matsumura, K. (1999). Characterization of the transmembrane molecular architecture of the dystroglycan complex in schwann cells. J Biol Chem *274*, 8240-6.

Salzer, J. L., Holmes, W. P., and Colman, D. R. (1987). The amino acid sequences of the myelin-associated glycoproteins: homology to the immunoglobulin gene superfamily. J Cell Biol *104*, 957-65.

Sanchez, M. P., Silos-Santiago, I., Frisen, J., He, B., Lira, S. A., and Barbacid, M. (1996). Renal agenesis and the absence of enteric neurons in mice lacking GDNF. Nature *382*, 70-3.

Sasaki, M., Kleinman, H. K., Huber, H., Deutzmann, R., and Yamada, Y. (1988). Laminin, a multidomain protein. The A chain has a unique globular domain and homology with the basement membrane proteoglycan and the laminin B

chains. J Biol Chem *263*, 16536-44.

Schaller, M. D., Otey, C. A., Hildebrand, J. D., and Parsons, J. T. (1995). Focal adhesion kinase and paxillin bind to peptides mimicking beta integrin cytoplasmic domains. J Cell Biol *130*, 1181-7.

Schaller, M. D., and Parsons, J. T. (1994). Focal adhesion kinase and associated proteins. Curr Opin Cell Biol *6*, 705-10.

Scherer, S. S. (1997). The biology and pathobiology of Schwann cells. Curr Opin Neurol *10*, 386-97.

Scherer, S. S., Wang, D. Y., Kuhn, R., Lemke, G., Wrabetz, L., and Kamholz, J. (1994a). Axons regulate Schwann cell expression of the POU transcription factor SCIP. J Neurosci *14*, 1930-42.

Scherer, S. S., Xu, Y. T., Bannerman, P. G., Sherman, D. L., and Brophy, P. J. (1995). Periaxin expression in myelinating Schwann cells: modulation by axon-glial interactions and polarized localization during development. Development *121*, *4265-73*.

Scherer, S. S., Xu, Y. T., Roling, D., Wrabetz, L., Feltri, M. L., and Kamholz, J. (1994b). Expression of growth-associated protein-43 kD in Schwann cells is regulated by axon-Schwann cell interactions and cAMP. J Neurosci Res *38*, 575-89.

Schlaepfer, D. D., and Hunter, T. (1996a). Evidence for in vivo phosphorylation of the Grb2 SH2-domain binding site on focal adhesion kinase by Src-family protein-tyrosine kinases [published erratum appears in Mol Cell Biol 1996 Dec;16(12):7182-4]. Mol Cell Biol *16*, 5623-33.

Schlaepfer, D. D., and Hunter, T. (1996b). Signal transduction from the extracellular matrix--a role for the focal adhesion protein-tyrosine kinase FAK. Cell Struct Funct *21*, 445-50.

Schober, S., Mielenz, D., Echtermeyer, F., Hapke, S., Poschl, E., von der Mark, H., Moch, H., and von der Mark, K. (2000). The role of extracellular and cytoplasmic splice domains of alpha7- integrin in cell adhesion and migration on laminins. Exp Cell Res *255*, 303-13.

Scholze, A., Gotz, B., and Faissner, A. (1996). Glial cell interactions with tenascin-C: adhesion and repulsion to different tenascin-C domains is cell type related. Int J Dev Neurosci *14*, 315-29.

Schuler, F., and Sorokin, L. M. (1995). Expression of laminin isoforms in mouse myogenic cells in vitro and in vivo. J Cell Sci *108*, 3795-3804.

Schumacher, M., Jung-Testas, I., Robel, P., and Baulieu, E. E. (1993). Insulin-like growth factor I: a mitogen for rat Schwann cells in the presence of elevated levels of cyclic AMP. Glia *8*, 232-40.

Selleck, M. A., and Bronner-Fraser, M. (2000). Avian neural crest cell fate decisions: a diffusible signal mediates induction of neural crest by the ectoderm. Int J Dev Neurosci *18*, 621-7.

Selleck, M. A., and Bronner-Fraser, M. (1996). The genesis of avian neural crest cells: a classic embryonic induction. Proc Natl Acad Sci U S A *93*, 9352-7.

Selleck, M. A., and Bronner-Fraser, M. (1995). Origins of the avian neural crest: the role of neural plate-epidermal interactions. Development *121*, 525-38.

Sendtner, M., Schmalbruch, H., Stockli, K. A., Carroll, P., Kreutzberg, G. W., and Thoenen, H. (1992). Ciliary neurotrophic factor prevents degeneration of motor neurons in mouse mutant progressive motor neuronopathy [see comments]. Nature *358*, 502-4.

Sereda, M., Griffiths, I., Puhlhofer, A., Stewart, H., Rossner, M. J., Zimmerman, F., Magyar, J. P., Schneider, A., Hund, E., Meinck, H. M., Suter, U., and Nave, K. A. (1996). A transgenic rat model of Charcot-Marie-Tooth disease. Neuron *16*, 1049-60.

Sewry, C. A., Naom, I., D'Alessandro, M., Sorokin, L., Bruno, S., Wilson, L. A., Dubowitz, V., and Muntoni, F. (1997). Variable clinical phenotype in merosin-deficient congenital muscular dystrophy associated with differential immunolabelling of two fragments of the laminin alpha 2 chain. Neuromuscul Disord *7*, 169-75.

Sewry, C. A., Uziyel, Y., Torelli, S., Buchanan, S., Sorokin, L., Cohen, J., and Watt, D. J. (1998). Differential labelling of laminin alpha 2 in muscle and neural tissue of dy/dy mice: are there isoforms of the laminin alpha 2 chain? [published erratum appears in Neuropathol Appl Neurobiol 1998 Apr;24(2):166]. Neuropathol Appl Neurobiol *24*, 66-72.

Shah, N. M., and Anderson, D. J. (1997). Integration of multiple instructive cues by neural crest stem cells reveals cell-intrinsic biases in relative growth factor responsiveness. Proc Natl Acad Sci U S A *94*, 11369-74.

Shah, N. M., Groves, A. K., and Anderson, D. J. (1996). Alternative neural crest cell fates are instructively promoted by TGFbeta superfamily members. Cell *85*, 331-43.

Shah, N. M., Marchionni, M. A., Isaacs, I., Stroobant, P., and Anderson, D. J. (1994). Glial growth factor restricts mammalian neural crest stem cells to a glial fate. Cell *77*, 349-60.

Shewan, D., Berry, M., and Cohen, J. (1995). Extensive regeneration in vitro by early embryonic neurons on immature and adult CNS tissue. J Neurosci *15*, 2057-62.

Shimoji, Y., Ng, V., Matsumura, K., Fischetti, V. A., and Rambukkana, A. (1999). A 21-kDa surface protein of Mycobacterium leprae binds peripheral nerve laminin-2 and mediates Schwann cell invasion. Proceedings of the National Academy of Sciences of the United States of America *96*, 9857-9862.

Shorer, Z., Philpot, J., Muntoni, F., Sewry, C., and Dubowitz, V. (1995). Demyelinating peripheral neuropathy in merosin-deficient congenital muscular dystrophy. J Child Neurol *10*, 472-5.

Smith, J. W., and Cheresh, D. A. (1990). Integrin (alpha v beta 3)-ligand interaction. Identification of a heterodimeric RGD binding site on the vitronectin receptor. J Biol Chem *265*, 2168-72.

Smith, M. E., and Curtis, B. M. (1979). Frog sciatic nerve myelin: a chemical characterization. J Neurochem *33*, 447-52.

Smyth, N., Vatansever, H. S., Murray, P., Meyer, M., Frie, C., Paulsson, M., and Edgar, D. (1999). Absence of basement membranes after targeting the LAMC1 gene results in embryonic lethality due to failure of endoderm differentiation. Journal of Cell Biology *144*, 151-160.

Snipes, G. J., Suter, U., Welcher, A. A., and Shooter, E. M. (1992). Characterization of a novel peripheral nervous system myelin protein (PMP-22/SR13). J Cell Biol *117*, 225-38.

Sommer, L., Shah, N., Rao, M., and Anderson, D. J. (1995). The cellular function of MASH1 in autonomic neurogenesis. Neuron *15*, 1245-58.

Son, Y. J., and Thompson, W. J. (1995a). Nerve sprouting in muscle is induced and guided by processes extended by Schwann cells. Neuron *14*, 133-41.

Son, Y. J., and Thompson, W. J. (1995b). Schwann cell processes guide

regeneration of peripheral axons. Neuron *14*, 125-32.

Son, Y. J., Trachtenberg, J. T., and Thompson, W. J. (1996). Schwann cells induce and guide sprouting and reinnervation of neuromuscular junctions. Trends Neurosci *19*, 280-5.

Sorokin, L. M., Maley, M. A., Moch, H., von der Mark, H., von der Mark, K., Cadalbert, L., Karosi, S., Davies, M. J., McGeachie, J. K., and Grounds, M. D. (2000). Laminin alpha4 and integrin alpha6 are upregulated in regenerating dy/dy skeletal muscle: comparative expression of laminin and integrin isoforms in muscles regenerating after crush injury. Exp Cell Res *256*, 500-14.

Spinardi, L., Einheber, S., Cullen, T., Milner, T. A., and Giancotti, F. G. (1995). A recombinant tail-less integrin beta 4 subunit disrupts hemidesmosomes, but does not suppress alpha 6 beta 4-mediated cell adhesion to laminins. J Cell Biol *129*, 473-87.

Sternberger, N. H., Quarles, R. H., Itoyama, Y., and Webster, H. D. (1979). Myelin-associated glycoprotein demonstrated immunocytochemically in myelin and myelin-forming cells of developing rat. Proc Natl Acad Sci U S A *76*, 1510-4.

Stewart, H. J., Eccleston, P. A., Jessen, K. R., and Mirsky, R. (1991). Interaction between cAMP elevation, identified growth factors, and serum components in regulating Schwann cell growth. J Neurosci Res *30*, 346-52.

Stewart, H. J., Turner, D., Jessen, K. R., and Mirsky, R. (1997). Expression and regulation of alpha1beta1 integrin in Schwann cells. J Neurobiol *33*, 914-28.

Stirling, C. A. (1975a). Abnormalities in Schwann cell sheaths in spinal nerve roots of dystrophic mice. J Anat *119*, 169-80.

Stirling, C. A. (1975b). Experimentally induced myelination of amyelinated axons in dystrophic mice. Brain Research *87*, 130-135.

Sunada, Y., Edgar, T.S., Lotz, B.P., Rust, R.S. and Campbell, K.P. (1995a). Merosin-negative congenital muscular dystrophy associated with extensive brain abnormalities. Neurology *45*, 22084-2089.

Sunada, Y., Bernier, S. M., Kozak, C. A., Yamada, Y., and Campbell, K. P. (1994). Deficiency of merosin in dystrophic dy mice and genetic linkage of laminin M chain gene to dy locus. J Biol Chem *269*, 13729-32.

Sunada, Y., Bernier, S. M., Utani, A., Yamada, Y., and Campbell, K. P. (1995b). Identification of a novel mutant transcript of laminin α2 chain gene

responsible for muscular dystrophy and dysmyelination in *dy^{2J}* mice. Human Molecular Genetics *4*, 1055-1061.

Sundberg, C., and Rubin, K. (1996). Stimulation of beta1 integrins on fibroblasts induces PDGF independent tyrosine phosphorylation of PDGF beta-receptors. J Cell Biol *132*, 741-52.

Suter, U., Moskow, J. J., Welcher, A. A., Snipes, G. J., Kosaras, B., Sidman, R. L., Buchberg, A. M., and Shooter, E. M. (1992a). A leucine-to-proline mutation in the putative first transmembrane domain of the 22-kDa peripheral myelin protein in the trembler-J mouse. Proc Natl Acad Sci U S A *89*, 4382-6.

Suter, U., Welcher, A. A., Ozcelik, T., Snipes, G. J., Kosaras, B., Francke, U., Billings-Gagliardi, S., Sidman, R. L., and Shooter, E. M. (1992b). Trembler mouse carries a point mutation in a myelin gene. Nature *356*, 241-4.

Suzuki, A., Yoshida, M., and Ozawa, E. (1995). Mammalian alpha 1- and beta 1-syntrophin bind to the alternative splice- prone region of the dystrophin COOH terminus. J Cell Biol *128*, 373-81.

Syroid, D. E., Maycox, P. J., Soilu-Hanninen, M., Petratos, S., Bucci, T., Burrola, P., Murray, S., Cheema, S., Lee, K. F., Lemke, G., and Kilpatrick, T. J. (2000). Induction of postnatal Schwann cell death by the low-affinity neurotrophin receptor in vitro and after axotomy. J Neurosci *20*, 5741-7.

Syroid, D. E., Maycox, P. R., Burrola, P. G., Liu, N., Wen, D., Lee, K. F., Lemke, G., and Kilpatrick, T. J. (1996). Cell death in the Schwann cell lineage and its regulation by neuregulin. Proc Natl Acad Sci U S A *93*, 9229-34.

Tait, S., Gunn-Moore, F., Collinson, J. M., Huang, J., Lubetzki, C., Pedraza, L., Sherman, D. L., Colman, D. R., and Brophy, P. J. (2000). An oligodendrocyte cell adhesion molecule at the site of assembly of the paranodal axo-glial junction [see comments]. J Cell Biol *150*, 657-66.

Takahashi, N., Roach, A., Teplow, D. B., Prusiner, S. B., and Hood, L. (1985). Cloning and characterization of the myelin basic protein gene from mouse: one gene can encode both 14 kd and 18.5 kd MBPs by alternate use of exons. Cell *42*, 139-48.

Tan, E., Topaloglu, H., Sewry, C., Zorlu, Y., Naom, I., Erdem, S., D'Alessandro, M., Muntoni, F., and Dubowitz, V. (1997). Late onset muscular dystrophy with cerebral white matter changes due to partial merosin deficiency.

Neuromuscul Disord *7*, 85-9.

Taniuchi, M., Clark, H. B., and Johnson, E. M., Jr. (1986). Induction of nerve growth factor receptor in Schwann cells after axotomy. Proc Natl Acad Sci U S A *83*, 4094-8.

Taniuchi, M., Clark, H. B., Schweitzer, J. B., and Johnson, E. M., Jr. (1988). Expression of nerve growth factor receptors by Schwann cells of axotomized peripheral nerves: ultrastructural location, suppression by axonal contact, and binding properties. J Neurosci *8*, 664-81.

Terranova, V. P., Rohrbach, D. H., and Martin, G. R. (1980). Role of laminin in the attachment of PAM 212 (epithelial) cells to basement membrane collagen. Cell *22*, 719-26.

Timpl, R. (1989). Structure and biological activity of basement membrane proteins. Eur J Biochem *180*, 487-502.

Timpl, R., and Brown, J. C. (1996). Supramolecular assembly of basement membranes. Bioessays *18*, 123-132.

Timpl, R., Rohde, H., Robey, P. G., Rennard, S. I., Foidart, J. M., and Martin, G. R. (1979). Laminin--a glycoprotein from basement membranes. J Biol Chem *254*, 9933-7.

Tisi, D., Talts, J. F., Timpl, R., and Hohenester, E. (2000). Structure of the C-terminal laminin G-like domain pair of the laminin alpha2 chain harbouring binding sites for alpha-dystroglycan and heparin. Embo J *19*, 1432-40.

Tomaselli, K. J., Doherty, P., Emmett, C. J., Damsky, C. H., Walsh, F. S., and Reichardt, L. F. (1993). Expression of beta 1 integrins in sensory neurons of the dorsal root ganglion and their functions in neurite outgrowth on two laminin isoforms. J Neurosci *13*, 4880-8.

Tomaselli, K. J., Hall, D. E., Flier, L. A., Gehlsen, K. R., Turner, D. C., Carbonetto, S., and Reichardt, L. F. (1990). A neuronal cell line (PC12) expresses two beta 1-class integrins-alpha 1 beta 1 and alpha 3 beta 1-that recognize different neurite outgrowth- promoting domains in laminin. Neuron *5*, 651-62.

Tome, F. M., Evangelista, T., Leclerc, A., Sunada, Y., Manole, E., Estournet, B., Barois, A., Campbell, K. P., and Fardeau, M. (1994). Congenital muscular dystrophy with merosin deficiency. C R Acad Sci III *317*, 351-7.

Tona, A., Perides, G., Rahemtulla, F., and Dahl, D. (1993). Extracellular matrix in regenerating rat sciatic nerve: a comparative study on the localization of laminin, hyaluronic acid, and chondroitin sulfate proteoglycans, including versican. J Histochem Cytochem *41*, 593-9.

Topilko, P., Schneider-Maunoury, S., Levi, G., Baron-Van Evercooren, A., Chennoufi, A. B., Seitanidou, T., Babinet, C., and Charnay, P. (1994). Krox-20 controls myelination in the peripheral nervous system. Nature *371*, 796-9.

Trachtenberg, J. T., and Thompson, W. J. (1997). Nerve terminal withdrawal from rat neuromuscular junctions induced by neuregulin and Schwann cells. J Neurosci *17*, 6243-55.

Trachtenberg, J. T., and Thompson, W. J. (1996). Schwann cell apoptosis at developing neuromuscular junctions is regulated by glial growth factor. Nature *379*, 174-7.

Trapp, B. D., Andrews, S. B., Cootauco, C., and Quarles, R. (1989). The myelin-associated glycoprotein is enriched in multivesicular bodies and periaxonal membranes of actively myelinating oligodendrocytes. J Cell Biol *109*, 2417-26.

Trapp, B. D., Bernier, L., Andrews, S. B., and Colman, D. R. (1988a). Cellular and subcellular distribution of 2',3'-cyclic nucleotide 3'- phosphodiesterase and its mRNA in the rat central nervous system. J Neurochem *51*, 859-68.

Trapp, B. D., Dubois-Dalcq, M., and Quarles, R. H. (1984a). Ultrastructural localization of P2 protein in actively myelinating rat Schwann cells. J Neurochem *43*, 944-8.

Trapp, B. D., Hauer, P., and Lemke, G. (1988b). Axonal regulation of myelin protein mRNA levels in actively myelinating Schwann cells. J Neurosci *8*, 3515-21.

Trapp, B. D., and Quarles, R. H. (1984). Immunocytochemical localization of the myelin-associated glycoprotein. Fact or artifact? J Neuroimmunol *6*, 231-49.

Trapp, B. D., and Quarles, R. H. (1982). Presence of the myelin-associated glycoprotein correlates with alterations in the periodicity of peripheral myelin. J Cell Biol *92*, 877-82.

Trapp, B. D., Quarles, R. H., and Griffin, J. W. (1984b). Myelin-associated glycoprotein and myelinating Schwann cell-axon interaction in chronic B,B'-iminodipropionitrile neuropathy. J Cell Biol *98*, 1272-8.

Utani, A., Nomizu, M., Sugiyama, S., Miyamoto, S., Roller, P. P., and Yamada,

Y. (1995). A specific sequence of the laminin alpha 2 chain critical for the initiation of heterotrimer assembly. J Biol Chem *270*, 3292-8.

Utani, A., Nomizu, M., Timpl, R., Roller, P. P., and Yamada, Y. (1994). Laminin chain assembly. Specific sequences at the C terminus of the long arm are required for the formation of specific double- and triple- stranded coiled-coil structures. J Biol Chem *269*, 19167-75.

Uyemura, K., Tobari, C., Hirano, S., and Tsukada, Y. (1972). Comparative studies on the myelin proteins of bovine peripheral nerve and spinal cord. J Neurochem *19*, 2607-14.

Uziyel, Y., Hall, S., and Cohen, J. (2000). Influence of laminin-2 on Schwann cell-axon interactions. Glia *32*, 109-121.

Vachon, P. H., Loechel, F., Xu, H., Wewer, U. M., and Engvall, E. (1996). Merosin and laminin in myogenesis; Specific requirement for merosin in myotube stability and survival. Journal of Cell Biology *134*, 1483-1497.

Vachon, P. H., Xu, H., Liu, L., Loechel, F., Hayashi, Y., Arahata, K., Reed, J. C., Wewer, U. M., and Engvall, E. (1997). Integrins (alpha7beta1) in muscle function and survival. Disrupted expression in merosin-deficient congenital muscular dystrophy. J Clin Invest *100*, 1870-81.

Valentijn, L. J., Baas, F., Wolterman, R. A., Hoogendijk, J. E., van den Bosch, N. H., Zorn, I., Gabreels-Festen, A. W., de Visser, M., and Bolhuis, P. A. (1992). Identical point mutations of PMP-22 in Trembler-J mouse and Charcot-Marie-Tooth disease type 1A. Nat Genet *2*, 288-91.

Vilquin, J. T., Guerette, B., Puymirat, J., Yaffe, D., Tome, F. M. S., Fardeau, M., Fiszman, M., Schwartz, K., and Tremblay, J. P. (1999). Myoblast transplantations lead to the expression of the laminin alpha 2 chain in normal and dystrophic (dy/dy) mouse muscles. Gene Therapy *6*, 792-800.

Vilquin, J. T., Kinoshita, I., Roy, B., Goulet, M., Engvall, E., Tome, F., Fardeau, M., and Tremblay, J. P. (1996). Partial laminin alpha 2 chain restoration in alpha 2 chain-deficient dy/dy mouse by primary muscle cell culture transplantation. Journal of Cell Biology *133*, 185-197.

Vogelezang, M. G., Scherer, S. S., Fawcett, J. W., and ffrench-Constant, C. (1999). Regulation of fibronectin alternative splicing during peripheral nerve repair. J Neurosci Res *56*, 323-33.

Vuolteenaho, R., Nissinen, M., Sainio, K., Byers, M., Eddy, R., Hirvonen, H., Shows, T. B., Sariola, H., Engvall, E., and Tryggvason, K. (1994). Human laminin M chain (merosin): complete primary structure, chromosomal assignment, and expression of the M and A chain in human fetal tissues. J Cell Biol *124*, 381-94.

Wakamatsu, Y., Maynard, T. M., and Weston, J. A. (2000). Fate determination of neural crest cells by NOTCH-mediated lateral inhibition and asymmetrical cell division during gangliogenesis. Development *127*, 2811-21.

Wang, H. U., and Anderson, D. J. (1997). Eph family transmembrane ligands can mediate repulsive guidance of trunk neural crest migration and motor axon outgrowth. Neuron *18*, 383-96.

Wardlaw, A. J., Hibbs, M. L., Stacker, S. A., and Springer, T. A. (1990). Distinct mutations in two patients with leukocyte adhesion deficiency and their functional correlates. J Exp Med *172*, 335-45.

Weaver, C. D., Yoshida, C. K., de Curtis, I., and Reichardt, L. F. (1995). Expression and in vitro function of beta 1-integrin laminin receptors in the developing avian ciliary ganglion [published erratum appears in J Neurosci 1996 Nov 1;16(21):7097-8]. J Neurosci *15*, 5275-85.

Webster, H. D. (1971). The geometry of peripheral myelin sheaths during their formation and growth in rat sciatic nerves. J Cell Biol *48*, 348-67.

Weinberg, H. J., and Spencer, P. S. (1978). The fate of Schwann cells isolated from axonal contact. J Neurocytol *7*, 555-69.

Weinberg, H. J., Spencer, P. S., and Raine, C. S. (1975). Aberrant PNS development in dystrophic mice. Brain Res *88*, 532-7.

West, W. T., and Murphy, E. D. (1960). Histopathology of hereditary, progressive muscular dystrophy in inbred strain 129 mice. Anat Rec *137*, 279-95.

Wewer, U. M., and Engvall, E. (1996). Merosin/laminin-2 and muscular dystrophy. Neuromuscul Disord *6*, 409-18.

Wiggins, R. C., Benjamins, J. A., and Morell, P. (1975). Appearance of myelin proteins in rat sciatic nerve during development. Brain Res *89*, 99-106.

Williams, L. R., Longo, F. M., Powell, H. C., Lundborg, G., and Varon, S. (1983). Spatial-temporal progress of peripheral nerve regeneration within a silicone chamber: parameters for a bioassay. J Comp Neurol *218*, 460-70.

Williamson, R. A., Henry, M. D., Daniels, K. J., Hrstka, R. F., Lee, J. C., Sunada, Y., Ibraghimov-Beskrovnaya, O., and Campbell, K. P. (1997). Dystroglycan is essential for early embryonic development: disruption of Reichert's membrane in Dag1-null mice. Hum Mol Genet *6*, 831-41.

Willison, H. J., Trapp, B. D., Bacher, J. D., and Quarles, R. H. (1988). The expression of myelin-associated glycoprotein in regenerating cat sciatic nerve. Brain Res *444*, 10-6.

Windebank, A. J., Wood, P., Bunge, R. P., and Dyck, P. J. (1985). Myelination determines the caliber of dorsal root ganglion neurons in culture. J Neurosci *5*, 1563-9.

Woldeyesus, M. T., Britsch, S., Riethmacher, D., Xu, L., SonnenbergRiethmacher, E., AbouRebyeh, F., Harvey, R., Caroni, P., and Birchmeier, C. (1999). Peripheral nervous system defects in erbB2 mutants following genetic rescue of heart development. Genes & Development *13*, 2538-2548.

Woolf, C. J., Reynolds, M. L., Chong, M. S., Emson, P., Irwin, N., and Benowitz, L. I. (1992). Denervation of the motor endplate results in the rapid expression by terminal Schwann cells of the growth-associated protein GAP-43. J Neurosci *12*, 3999-4010.

Wright, D. E., and Snider, W. D. (1996). Focal expression of glial cell line-derived neurotrophic factor in developing mouse limb bud. Cell Tissue Res *286*, 209-17.

Xu, H., Christmas, P., Wu, X. R., Wewer, U. M., and Engvall, E. (1994a). Defective muscle basement membrane and lack of M-laminin in the dystrophic dy/dy mouse. Proc Natl Acad Sci U S A *91*, 5572-6.

Xu, H., Wu, X. R., Wewer, U. M., and Engvall, E. (1994b). Murine muscular dystrophy caused by a mutation in the laminin alpha 2 (Lama2) gene. Nat Genet *8*, 297-302.

Yamada, H., Chiba, A., Endo, T., Kobata, A., Anderson, V. B., Hori, H., FukutaOhi, H., Kanazawa, I., Campbell, K. P., Shimizu, T., and Matsumura, K. (1996). Characterization of dystroglycan - Laminin interaction in peripheral nerve. Journal of Neurochemistry *66*, 1518-1524.

Yamada, H., Shimizu, T., Tanaka, T., Campbell, K. P., and Matsumura, K.

(1994). Dystroglycan is a binding protein of laminin and merosin in peripheral nerve. FEBS Lett *352*, 49-53.

Yang, B., Jung, D., Motto, D., Meyer, J., Koretzky, G., and Campbell, K. P. (1995). SH3 domain-mediated interaction of dystroglycan and Grb2. J Biol Chem *270*, 11711-4.

Yao, C. C., Ziober, B. L., Squillace, R. M., and Kramer, R. H. (1996). alpha 7 integrin mediates cell adhesion and migration on specific laminin isoforms. Journal of Biological Chemistry *271*, 25598-25603.

Yin, X., Crawford, T. O., Griffin, J. W., Tu, P., Lee, V. M., Li, C., Roder, J., and Trapp, B. D. (1998). Myelin-associated glycoprotein is a myelin signal that modulates the caliber of myelinated axons. J Neurosci *18*, 1953-62.

Yoshino, J. E., Dinneen, M. P., Sprinkle, T. J., and DeVries, G. H. (1985). Localization of 2',3'-cyclic nucleotide 3'-phosphodiesterase on cultured Schwann cells. Brain Res *325*, 199-203.

Yotsumoto, S., Fujiwara, H., Horton, J. H., Mosby, T. A., Wang, X. Q., Cui, Y. S., and Ko, M. S. H. (1996). Cloning and expression analyses of mouse dystroglycan gene: Specific expression in maternal decidua at the peri-implantation stage. Human Molecular Genetics *5*, 1259-1267.

Yurchenco, P. D., and Cheng, Y. S. (1993). Self-assembly and calcium-binding sites in laminin. A three-arm interaction model. J Biol Chem *268*, 17286-99.

Yurchenco, P. D., Cheng, Y. S., and Colognato, H. (1992). Laminin forms an independent network in basement membranes [published erratum appears in J Cell Biol 1992 Jun;118(2):493]. J Cell Biol *117*, 1119-33.

Yurchenco, P. D., and Schittny, J. C. (1990). Molecular architecture of basement membranes. Faseb J *4*, 1577-90.

Zeman, R. J., and Sandow, A. (1979). Denervation effects on dystrophic and normal muscles and the etiology of dystrophy. Ann N Y Acad Sci *317*, 171-86.

Zhang, X., Vuolteenaho, R., and Tryggvason, K. (1996). Structure of the human laminin alpha 2-chain gene (LAMA2), which is affected in congenital muscular dystrophy. Journal of Biological Chemistry *271*, 27664-27669.

Zhang, Y., Campbell, G., Anderson, P. N., Martini, R., Schachner, M., and Lieberman, A. R. (1995). Molecular basis of interactions between regenerating adult rat thalamic axons and Schwann cells in peripheral nerve grafts. II. Tenascin-

C. J Comp Neurol *361*, 210-24.

Zhou, X. F., Rush, R. A., and McLachlan, E. M. (1996). Differential expression of the p75 nerve growth factor receptor in glia and neurons of the rat dorsal root ganglia after peripheral nerve transection. J Neurosci *16*, 2901-11.

Ziskind-Conhaim, L. (1988). Physiological and morphological changes in developing peripheral nerves of rat embryos. Brain Res *470*, 15-28.

Zorick, T. S., and Lemke, G. (1996). Schwann cell differentiation. Curr Opin Cell Biol *8*, 870-6.

Zorick, T. S., Syroid, D. E., Arroyo, E., Scherer, S. S., and Lemke, G. (1996). The transcription factors SCIP and Krox-20 mark distinct stages and cell fates in Schwann cell differentiation. Mol Cell Neurosci *8*, 129-45.

Zorick, T. S., Syroid, D. E., Brown, A., Gridley, T., and Lemke, G. (1999). Krox-20 controls SCIP expression, cell cycle exit and susceptibility to apoptosis in developing myelinating Schwann cells. Development *126*, 1397-406.